VOL. 107 NO. EY1. MAY 1981

JOURNAL OF THE ENERGY DIVISION

PROCEEDINGS OF
THE AMERICAN SOCIETY
OF CIVIL ENGINEERS

VOL.107 NO.EY1. MAY 1981

JOURNAL OF THE ENERGY DIVISION

PROCEEDINGS OF THE AMERICAN SOCIETY OF CIVIL ENGINEERS

Copyright© 1981 by
American Society
of Civil Engineers
All Rights Reserved
ISSN 0190-8294

AMERICAN SOCIETY OF CIVIL ENGINEERS

BOARD OF DIRECTION

President
Irvan F. Mendenhall

Past President
Joseph S. Ward

President Elect
James R. Sims

Vice Presidents
Robert D. Bay
Francis J. Connell
Lyman R. Gillis
Albert A. Grant

Directors
Martin G. Abegg
Floyd A. Bishop
L. Gary Byrd
Larry J. Feeser
John A. Focht, Jr.
Sergio Gonzalez-Karg
James E. Humphrey, Jr.
Richard W. Karn
Leon D. Luck
Arthur R. McDaniel
Paul R. Munger
William R. Neuman
Leonard S. Oberman
John D. Parkhurst
Celestino R. Pennoni
Robert B. Rhode
S. Russell Stearns
William H. Taylor
Stafford E. Thornton
Robert E. Whiteside
Richard S. Woodruff

EXECUTIVE OFFICERS

Eugene Zwoyer, *Executive Director*
Julie E. Gibouleau, *Assistant to the Executive Director*
Louis L. Meier, *Washington Counsel/Assistant Secretary*
William H. Wisely, *Executive Director Emeritus*
Michael N. Salgo, *Treasurer*
Elmer B. Isaak, *Assistant Treasurer*

STAFF DIRECTORS

Donald A. Buzzell, *Managing Director for Education and Professional Affairs*
Robert A. Crist, Jr., *Managing Director for Publications and Technical Affairs*
Alexander Korwek, *Managing Director for Finance and Administrative Services*
Alexandra Bellow, *Director, Human Resources*
David Dresia, *Director, Publications Production and Marketing*
Barker D. Herr, *Director, Membership*
Richard A. Jeffers, *Controller*
Carl E. Nelson, *Director, Field Services*
Don P. Reynolds, *Director, Policy, Planning and Public Affairs*
Bruce Rickerson, *Director, Legislative Services*
James M. Shea, *Director, Public Communications*
Albert W. Turchick, *Director, Technical Services*
George K. Wadlin, *Director, Education Services*
R. Lawrence Whipple, *Director, Engineering Management Services*

COMMITTEE ON PUBLICATIONS

Stafford E. Thornton, *Chairman*
Martin G. Abegg
John A. Focht, Jr.
Richard W. Karn
Paul R. Munger
William R. Neuman

ENERGY DIVISION

Executive Committee
Jerry M. Hart, *Chairman*
Sidney O. Steinborn, *Vice Chairman*
Richard S. McGinnis
Jerry P. Schneider, *Secretary*
James D. Calvert, *Management Group B Contact Member*
Francis J. Patti

Publications Committee
S. L. Chu, ***Chairman***
K. P. Buchert
Richard W. Keenan
Francis J. Patti
William Y. T. Shieh
K. H. Yang

PUBLICATION SERVICES DEPARTMENT

David Dresia, *Director, Publications Production and Marketing*

Technical and Professional Publications

Richard R. Torrens, *Manager*
Linda Ellington, *Copy Editor*
Thea C. Feldman, *Copy Editor*
Meryl Mandle, *Copy Editor*
Joshua R. Spieler, *Copy Editor*
Shiela Menaker, *Production Co-ordinator*
Richard C. Scheblein, *Draftsman*

Information Services

Elan Garonzik, *Editor*

PERMISSION TO PHOTOCOPY JOURNAL PAPERS

Permission to photocopy for personal or internal reference beyond the limits in Sections 107 and 108 of the U.S. Copyright Law is granted by the American Society of Civil Engineers for libraries and other users registered with the Copyright Clearance Center, 21 Congress Street, Salem, Mass. 01970, provided the appropriate fee is paid to the CCC for all articles bearing the CCC code. Requests for special permission or bulk copying should be addressed to the Manager of Technical and Professional Publications, American Society of Civil Engineers.

CONTENTS

Refuse-to-Energy Wastewater Treatment
by Gordon P. Treweek 1

Leachates from Solid Waste Recovery Operations
by A. Douglas Rademaker and James C. Young 17

Small-Scale Hydro in New England: 1960–1976
by Paul H. Kirshen 31

Optimization of Pump Turbines
by Joachim Raabe 41

River Thermal Standards Costs in Upper Midwest
by Thomas E. Croley II, Arthur R. Giaquinta, and Robert A. Woodhouse 65

Louvered Offshore Intake for Diverting Fish
by Yusuf G. Mussalli, Edward P. Taft, Johannes Larsen, and J. M. Toennies 79

This Journal is published aperiodically by the American Society of Civil Engineers. Publications office is at 345 East 47th Street, New York, N.Y. 10017. Address all ASCE correspondence to the Editorial and General Offices at 345 East 47th Street, New York, N.Y. 10017. Allow six weeks for change of address to become effective. Subscription price to members is $6.50. Nonmember subscriptions available; prices obtainable on request. EY, TC.

The most recent issues of this journal, previously the Journal of the Power Division, were published in January 1979, August 1979, April 1980, and October 1980.

The Society is not responsible for any statement made or opinion expressed in its publications.

Methane Gas Utilization from Landfill Site
by Anthony J. Crutcher, Frank A. Rovers, and Edward A. McBean 95

Effects of Clamps on Fatigue of ACSR Conductors
by George E. Ramey and John S. Townsend 103

Optimization of Integrated Energy Systems
by Theodore A. Shugar, Michael D. Jackson, and Steven J. Anderson 121

Equipment Qualification: Special Considerations
by Anil K. Kar 141

Domestic Water Supplies for Power Plant Cooling
by Gideon Sinai, William A. Jury, and Lewis H. Stolzy 149

Occurrence and Prediction of Acid Drainages
by Frank T. Caruccio, Gwendelyn Geidel, and Mike Pelletier 167

DISCUSSION

Proc. Paper 16215

Hybrid Cooling System Thermodynamics and Economics, by Arthur R. Giaquinta, Thomas E. Croley II, and Tai-Dan Hsu (Apr., 1980).
errata 181

Feasibility of Five Low-Head Hydro Projects, by James V. Williamson and Anthony Wayne Pietz (Apr., 1980).
errata 181

INFORMATION RETRIEVAL

The key words, abstract, and reference "cards" for each article in this Journal represent part of the ASCE participation in the EJC information retrieval plan. The retrieval data are placed herein so that each can be cut out, placed on a 3 × 5 card and given an accession number for the user's file. The accession number is then entered on key word cards so that the user can subsequently match key words to choose the articles he wishes. Details of this program were given in an August, 1962 article in CIVIL ENGINEERING, reprints of which are available on request to ASCE headquarters.

16225 REFUSE-TO-ENERGY WASTEWATER TREATMENT

KEY WORDS: **Energy;** Organic matter; Pollutants; **Pollution control; Refuse;** Technology assessment; **Waste recycling; Wastewater (pollution); Wastewater treatment;** Water pollution; **Water pollution effects;** Water treatment plants

ABSTRACT: Wastewater treatment technologies are evaluated for their potential utilization at waste-as-fuel (WAF) and refuse-derived-fuel (RDF) facilities to treat waterborne pollutants. The principal WAF/RDF wastestreams contain the following: organic pollutants (BOD_5, COD, and TSS) in concentrations up to 100,000 mg/L at pyrolysis units; organic priority pollutants in concentrations up to 100 mg/L at pyrolysis and digester units; and trace metals in concentrations up to 1,000 mg/L in incinerator scrubbers. The efficacy of aerobic, anaerobic, and physical-chemical facilities to treat the wastestreams from incinerators, hydrapulping facilities, pyrolysis units, and digesters is projected from documented experiences. Based on this analysis, potential treatment trains are recommended to render the wastestreams acceptable for discharge to publicly owned treatment works or ambient waterways.

REFERENCE: Treweek, Gordon P., "Refuse-to-Energy Wastewater Treatment," *Journal of the Energy Division,* ASCE, Vol. 107, No. EY1, **Proc. Paper 16225**, May, 1981, pp. 1-16

16231 LEACHATES FROM SOLID WASTE RECOVERY

KEY WORDS: Ash content; Environmental effects; **Environmental engineering; Groundwater quality; Leaching; Pollutants; Sanitary landfill;** Solid waste disposal; **Waste disposal;** Waste recycling; **Water pollution**

ABSTRACT: Conversion of urban solid waste to energy often produces solid residues that require subsequent disposal. Generally they are placed in ash ponds, spread on land, or placed in sanitary landfills. These residues were studied, and the potential environmental problems associated with their disposal were assessed. Peak concentrations of various leachate constituents exceed permissible discharge standards. These materials leach rapidly from the residues so that the total leached mass per unit of residue is quite small. Therefore, some type of treatment of ash pond overflow may be required if controlled discharge will not keep constitutent concentrations below permissible discharge levels.

REFERENCE: Rademaker, A. Douglas, and Young, James C., "Leachates from Solid Waste Recovery Operations," *Journal of the Energy Division,* ASCE, Vol. 107, No. EY1, **Proc. Paper 16231**, May, 1981, pp. 17-29

16229 SMALL-SCALE HYDRO IN NEW ENGLAND: 1960-1976

KEY WORDS: Capacity; **Cost comparisons; Electric power costs;** Hydroelectric power generation; **Hydroelectric powerplants;** Hydroelectric resources; **Licensing; New England; Powerplants;** Size; Time factors

ABSTRACT: A review of the capacity and licensing data on small-scale hydro (SSH) in New England in the period 1960 to 1976 is presented and compared to national and regional hydropower data. Costs of electricity data are also reviewed. Major findings are that until recently New England has followed the past national trend of decreased interest in both large-scale hydro (LSH) and SSH and of retiring small, inefficient plants. Generally, LSH has been used for peaking, SSH for run-of-the-river. Most of the present capacity in New England is privately owned; little is state or municipally owned. Since the interest in hydropower is inversely related to the costs of alternatives for producing electricity, it appears that the recent interest in SSH will continue (municipal and rural coop interest seems particularly strong).

REFERENCE: Kirshen, Paul H., "Small-Scale Hydro in New England: 1960-1976," *Journal of the Energy Division,* ASCE, Vol. 107, No. EY1, **Proc. Paper 16229**, May, 1981, pp. 31-39

16228 OPTIMIZATION OF PUMP TURBINES

KEY WORDS: Aerodynamics; **Cavitation; Design; Excavation;** Impellers; Losses; **Optimization; Pumped storage; Pumping; Pump turbines;** Speed; Viscous flow

ABSTRACT: For the purpose of optimizing pump turbines installed in pumped storage plants with regard to efficiency, cavitation, and excavation costs, a method of computation has been devised which includes a new system of determining type number and impeller outside diameter. An example employing data applicable to a modern pump turbine—Rodund 2(Austria)—reveals computed results that are well in conformity with actual values as regards the impeller outside diameter and operating data. The method of computation makes use of coefficients pertaining to viscous flow, cavitation, aerodynamics, and the geometrical dimensions of the runner vanes. Furthermore, special operational features of pump turbines are presented, the latter requiring additional considerations in design.

REFERENCE: Raabe, Joachim, "Optimization of Pump Turbines," *Journal of the Energy Division,* ASCE, Vol. 107, No. EY1, **Proc. Paper 16228**, May, 1981, pp. 41-63

16261 RIVER THERMAL STANDARDS COSTS IN UPPER MIDWEST

KEY WORDS: Computer models; **Cooling; Design;** Economics; **Evaporation;** Mississippi River; Missouri River; **Powerplants; Rivers; Temperature;** Thermal factors; Thermal measurements; **Thermoelectric power generation;** Waste heat; **Water consumption**

ABSTRACT: Thermodynamic and economic models are combined to evaluate river thermal standards. Existing and hypothetical thermal regulations, including the extreme cases of no thermal standards and no allowable heated discharges, are examined to show the dependence of power-production-related cooling costs and water consumption on thermal standards. A critical appraisal of the cost of thermal standards in terms of water consumption and other expenses is thereby possible. This enables subjective assessments of the standards to proceed with full knowledge of the tradeoffs involved between the costs of power production and environmental impacts. Results are presented for existing and proposed power plants located along the Missouri and Upper Mississippi Rivers in the Midcontinent Area Power Pool (MAPP) geographical area.

REFERENCE: Croley, Thomas E., II, Giaquinta, Arthur R., and Woodhouse, Robert A., "River Thermal Standards Costs in Upper Midwest," *Journal of the Energy Division,* ASCE, Vol. 107, No. EY1, **Proc. Paper 16261**, May, 1981, pp. 65-77

16259 LOUVERED OFFSHORE INTAKE FOR DIVERTING FISH

KEY WORDS: **Environmental engineering;** Fish passages; **Fishways;** Flow distribution; **Inlets (waterways);** Louvers; Ocean engineering; **Offshore structures**

ABSTRACT: The developmental work on louvered offshore intakes is presented. The model studies included: (1) Preliminary studies in a test flume, capped with plexiglass, and equipped with 15 L-shaped louvers; (2) a 1:9 scale hydraulic model to study the flow distribution along various louver geometrics, louver array angles, and location of the base-wall; and (3) 1:1 (full) scale model testing with live fish. The biological test results were variable and ranged from about 91 to 23 percent. The concept is unique is unique and requires further development prior to being considered a practical solution for fish diversion. The study is presented to report on the developmental work done to date in order to guide researchers in the field.

REFERENCE: Mussalli, Yusuf G., Taft, Edward P., Larsen, Johannes, and Toennies, J. M., "Louvered Offshore Intake for Diverting Fish," *Journal of the Energy Division,* ASCE, Vol. 107, No. EY1, **Proc. Paper 16259**, May, 1981, pp. 79-94

16264 METHANE GAS UTILIZATION FROM LANDFILL SITE

KEY WORDS: **Economic analysis; Energy conservation; Gas recovery;** Gas wells; Greenhouses; **Methane;** Pumping; **Sanitary landfill;** Systems engineering

ABSTRACT: The results are described of a case study of a gas extraction and utilization system located on a sanitary landfill site. The system includes the following: a 0.9-m-diameter gas extraction well, gas monitoring probes installed radially from the well, a continuously operating gas pump, waste gas outlet, and an onsite greenhouse heated by a modified forced air gas furnace. The recovery of landfill gas is both feasible and economical, even in an unprocessed state. The system operating characteristics for a 5-month period in the winter of 1979 are provided.

REFERENCE: Crutcher, Anthony J., Rovers, Frank A., and McBeam, Edward A., "Methane Gas Utilization from Landfill Site," *Journal of the Energy Division,* ASCE, Vol. 107, No. EY1, **Proc. Paper 16264**, May, 1981, pp. 95-102

16233 CLAMPS AND FATIGUE OF CONDUCTORS

KEY WORDS: **Aeolian vibration; Clamps;** Dynamic stress measurement; Experimental data; **Fatigue (materials); Fatigue tests;** Laboratory tests; Static stress measurement; **Transmission lines; Vibration**

ABSTRACT: The results of an experimental testing program, aimed at evaluating the relative conductor fatigue damage mitigation performances of some overhead suspension clamps, are explored. Three different support clamps are examined: short-radius, medium-radius, and long-radius. Theoretical considerations and equations that define both static and dynamic conductor stresses are presented. Emphasis is placed on stresses at, and caused by, the suspension clamps. Aeolian vibrations were simulated in laboratory testing by mechanical vibrations induced at the natural frequency of the conductor. The testing was limited in scope to three identical test specimens per support hardware with the major vibration parameters held constant. The long-radius suspension clamp was substantially superior to the others tested at minimizing conductor fatigue damage.

REFERENCE: Ramey, George E., and Townsend, John S., "Effects of Clamps on Fatigue of ACSR Conductors," *Journal of the Energy Division,* ASCE, Vol. 107, No. EY1, **Proc. Paper 16233**, May, 1981, pp. 103-119

16257 OPTIMIZATION OF INTEGRATED ENERGY SYSTEMS

KEY WORDS: **Cost effectiveness; Economics; Energy conversion; Forecasting;** Fuel oil; Industrial plants; Linear programming; Nonlinear programming; **Optimization; Systems engineering**

ABSTRACT: Application of renewable and nonrenewable energy conversion technologies are forecast for medium and large industrial facilities. Data are obtained from an optimization model that determines the least, life-cycles cost energy supply system for an industrial facility. Optimal solutions were composed of integrated combinations of energy conversion technologies. Besides being more cost-effective than status quo systems fired exclusively on fuel oil, the optimal integrated systems displace a significant percentage of fuel oil. Energy conversion technologies that participate in the optimal solutions for medium and large industrial facilities include: fluidized-bed coal combustion, cogeneration, oil-fired systems, with smaller contributions from refuse derived fuel systems. Oil-fired systems participate only in a peaking capacity wherever coal combustion is permitted. Otherwise, the status quo systems are forecasted to prevail.

REFERENCE: Shugar, Theodore A., Jackson, Michael D., and Anderson, Steven J., "Optimization of Integrated Energy Systems," *Journal of the Energy Division,* ASCE, Vol. 107, No. EY1, **Proc. Paper 16257**, May, 1981, pp. 121-139

16226 EQUIPMENT QUALIFICATION: SPECIAL CONSIDERATIONS

KEY WORDS: **Dynamic characteristics; Equipment;** Nozzle flow; **Nuclear power plants;** Pressure; **Qualifications; Safety design;** Temperature; **Tests; Vibration**

ABSTRACT: Special requirements for the qualification of safety-related equipment are presented. The importance of the simultaneous application of all concurrent loads (e.g., vibratory motion, temperature, pressure, nozzle loads) is explained. In addition, reasons are given for the simultaneous application of the three components of the vibratory motion. Attention is drawn to the need for the test response spectra closely enveloping the required response spectra. The input motion should not have frequency contents higher than the frequency at the onset of the rigid response in the required response spectra.

REFERENCE: Kar, Anil K., "Equipment Qualification: Special Considerations," *Journal of the Energy Division,* ASCE, Vol. 107, No. EY1, **Proc. Paper 16226**, May, 1981, pp. 141-148

16258 DOMESTIC WATER TO COOL POWER PLANTS

KEY WORDS: Conveyors; Cooling system design; **Cooling systems; Cooling water; Domestic water;** Ecology; **Powerplants;** Thermal pollution; **Thermal power plants;** Thermal water; **Thermoelectric power generation; Water supply systems**

ABSTRACT: A new method, "Once Through Conveyor (OTC)" for cooling inland thermal power plants is proposed. It involves the diversion of water from an existing domestic supply network through the power plant condenser and back to the network. Since natural water sources are not being used, the problem of ecological disturbance, due to the increased temperature of the water, does not arise. Increased salinity in open reaches, due to greater evaporation caused by the higher temperature, is calculated to be insignificant, and no contamination by any toxic pollution is anticipated. This is well above the anticipated needs in the area by the year 2000. The OTC method is more energy efficient, cheaper, and less environmentally intrusive than other commonly used methods. This method may be highly suitable for the cooling of power plants built close to adequate water supply systems.

REFERENCE: Sinai, Gideon, Jury, William A., and Stolzy, Lewis H., "Domestic Water Supplies for Power Plant Cooling," *Journal of the Energy Division,* ASCE, Vol. 107, No. EY1, **Proc. Paper 16258**, May, 1981, pp. 149-165

16278 OCCURRENCE AND PREDICTION OF ACID DRAINAGE

KEY WORDS: **Acidic water;** Acid mine water; **Drainage;** Excavation; Leaching; Mines (excavations); Mining; **Monitoring;** Rock excavation; Sulphur; **Water pollution**

ABSTRACT: During some land excavations, sulfide minerals are exposed to the atmosphere, and they oxidize and subsequently produce acid drainages. A method to monitor rock characteristics and to identify potentially acid-producing strata has been developed. Samples of dark shales were exposed to simulated weathering tests and periodically leached with deionized water, simulated acid rain and acid mine drainage. The leachate quality was monitored and related to the whole rock analysis. Samples with low concentrations of calcareous material and low total sulfur contents produced mildly acidic leachates when leached with water and acid rain. Samples with high concentrations of calcareous material and high sulfur contents were found initially to neutralize the simulated acid drainage and generate acidity. A strong relationship was found to exist between the effluent quality and the carbonate-sulfur ratio.

REFERENCE: Caruccio, Frank T., Geidel, Gwendelyn, and Pelletier, Mike, "Occurrence and Prediction of Acid Drainages," *Journal of the Energy Division,* ASCE, Vol. 107, No. EY1, **Proc. Paper 16278**, May, 1981, pp. 167-178

REFUSE-TO-ENERGY WASTEWATER TREATMENT[a]

By Gordon P. Treweek,[1] M. ASCE

INTRODUCTION

The fuel shortage of late 1973 and the subsequent dramatic increases in fuel prices have resulted in a major effort to find alternative sources of energy. One possible source of energy is the solid waste generated from municipal, agricultural, and forestry operations. Although the composition of these wastes varies widely with the type of enterprise, consumer habits, geographical location, time of year, and numerous other factors, the waste streams invariably contain a high organic content which can be either combusted directly or converted to conventional fuels. During the conversion/combustion process, air and water pollutants are generated, and must be treated prior to release from the waste-as-fuel (WAF) site. This paper presents concentration ranges for the major waterborne pollutants, and considers available treatment steps to remove them. Hopefully, WAF facilities can be designed and operated to minimize pollutant discharges and to effectively treat any residual wastestreams.

WASTESTREAM IDENTIFICATION

A two-step procedure is followed in processing refuse into useable fuel: (1) Preprocessing; and (2) conversion. Preprocessing consists of a series of physical operations which size, classify, and segregate the raw refuse into useable fractions. Conversion consists of one of the following four-unit operations: (1) Combustion (mass incineration or co-firing); (2) pyrolysis; (3) anaerobic digestion; or (4) methanation. From a water pollution control standpoint, filtrate from hydrapulping (preprocessing), incinerator scrubber washwaters, pyrolysis condensate, centrate from anaerobic digesters, and leachate from landfills (methanation) constitute the major sources of wastewater.

The extent of water use and wastewater production are primarily dependent upon the type of process utilized for preparing the municipal solid waste (MSW) and the actual combustion process itself. Wastewater streams range from very small quantities of high-organic demand wastewater, such as that associated

[a]Presented at the April 14–18, 1980, ASCE Annual Convention and Exposition, held at Portland, Oreg. (Preprint 80-025).

[1]Supervising Engr., James M. Montgomery Consulting Engrs., Inc., 555 East Walnut Street, Pasadena, Calif. 91101.

Note.—Discussion open until October 1, 1981. To extend the closing date one month, a written request must be filed with the Manager of Technical and Professional Publications, ASCE. Manuscript was submitted for review for possible publication on April 21, 1980. This paper is part of the Journal of the Energy Division, Proceedings of the American Society of Civil Engineers, ©ASCE, Vol. 107, No. EY1, May, 1981. ISSN 0190-8294/81/0001-0001/$01.00.

with the condensate of pyrolysis units, to relatively large volumes of low-organic demand wastewater, such as that utilized to sluice ash residue from mass burn combustors. Four major categories of pollutants were identified in the waste-streams at WAF facilities: (1) The organic surrogates, i.e., biochemical oxygen demand, carbonaceous oxygen demand, and total suspended solids (BOD_5, COD, and TSS), which measure the oxygen demand of the wastewater on the receiving water body; (2) the mineral quantity, specifically corrosive agents such as chlorides and sulfates, and the hydrogen ion concentration; (3) the organic priority pollutants including total organic carbon and total organic nitrogen; and (4) the heavy-metal priority pollutants. While in most cases, good data were available on the organic surrogates and the mineral quality of wastewater produced at refuse-derived-fuels (RDF) and WAF facilities, very little information was available on the organic and heavy-metal priority pollutants.

Preprocessing

The extent of wastewater production in preprocessing operations depends almost exclusively on whether wet or dry preprocessing steps are utilized. In dry preprocessing operations, wastewaters are produced in small quantities at only a few locations. Water is used rarely in the actual process since any moisture added to the RDF must be eventually evaporated in the conversion facility. The primary uses for water are dust control, fire fighting, and clean-up activities. Water is also used occasionally in some types of material separation units, such as those recovering aluminum and glass. Wastewaters primarily originate from washdown operations, drainage from storage pits, and the aforementioned materials recovery processes. Trash confined in the storage pit may leach compounds such as pesticides and organic solvents which can have adverse effects on wastewater treatment, but these conditions must be evaluated on an individual basis and treated accordingly. In most cases the wastewater from dry preprocessing operations can be discharged safely to sanitary sewers.

In contrast to dry preprocessing, wet preprocessing or pulping of MSW involves placing the material into a large hydrapulper, analogous in operation to a household garbage grinder. A thick slurry of MSW is formed with heavy particles of ferrous materials and other nonferrous materials separated by centrifugal action. The slurry, containing the organic fraction, glass, and small pieces of metal, is segregated into light and heavy fractions via liquid cyclone. The light organic fraction is dewatered by screening and pressing, and the liquid waste stream is recirculated to the pulper. The dewatered pulp can be cleaned and dried for use in paper products or burned for energy production.

Depending on the combination of energy recovery and materials separation, water is required for pulping, cleaning, equipment cooling, and resource recovery. In most cases the quality of water is not critical, which permits the use of nonpotable supplies such as sewage treatment plant effluents and sludges. By far the largest quantity of water is required by the hydrapulper. Water for the hydrapulper can be obtained from the dewatering and material recovery units through recirculation.

Two sources of wastewater exist in the hydrapulping system: (1) The blowdown from the recycling hydrapulper system; and (2) the filtrate from the sludge/slurry mixture which has been dewatered in the thickener and cone press. These

wastewaters are characterized by their large volume and high organic content (see Ref. 21 and Table 1).

Energy / Fuel Production

Following preprocessing, the MSW is either directly combusted or converted into fuels for combustion. Wastewaters are generated in the two principal combustion processes, i.e., the mass burn incinerator and the cofiring boiler; the anaerobic digestion process; and the pyrolysis process. The latter two processes produce fuels for subsequent combustion.

The wastewaters from combustion processes consist primarily of site drainage

TABLE 1.—Summary of Significant Pollutants Identified in Hydrapulping Waste Streams (21)

Parameter (1)	Concentration, in milligrams per liter	
	Blowdown (2)	Thickener wastewater (3)
Organic surrogates:		
BOD	2,840	2,660
COD	8,954	6,799
TSS	4,795	2,882
Oil and grease	—	—
Mineral quality:		
Na^+	—	—
Ca^{+2}	—	—
Total alkalinity:		
CL^-	—	—
SO_4^{-2}	—	—
NO_3^-	NH_3:N = 29	NH_3:N = 24
PO_4^{-3}	—	—
CN^-	—	—
pH units	5.78	4.8
DO	—	—
Priority pollutants: organics	—	—
Priority pollutants: metals	—	—
Total flow, in liters per minute	290	110

and washwaters, quench and sluice waters, boiler blowdown, and scrubber effluent. The first three categories of wastewater are generally small in quantity or of low strength and can be discharged directly into sanitary sewers. The largest quantity of water is used for scrubbing exhaust gases. Waterwall incinerator facilities help keep water use to a minimum by using electrostatic precipitators and dry handling systems for ash. While electrostatic precipitators are preferred from a water pollution control viewpoint, nevertheless wet scrubbers may be required for the removal of gaseous chlorides and SO_2 in order to meet air quality standards. The scrubber waters are generally acidic, with a pH in the range of 2.5–5.0. The total solids concentration varies from 500 mg/L–7,000 mg/L with about 80%–85% being dissolved solids. The chloride, hardness, sulfate,

and phosphate concentrations of the incoming raw water are significantly increased after passing through the scrubber. Furthermore, the scrubber wastewaters often contain high concentrations of trace metal priority pollutants which must be removed prior to discharge to either the sanitary sewer or the ambient receiving water (see Refs. 1, 3, 8, 10, 12, 13, 19 and Table 2).

Pyrolysis involves heating a preprocessed MSW to a sufficiently high tempera-

TABLE 2.—Summary of Significant Pollutants Identified in Incinerator Waste Streams (1,3,8,10,12,13,19)

Parameter (1)	Concentration, in milligrams per liter	
	Quench water (2)	Scrubber water (3)
Organic surrogates:		
BOD	—	15–400
COD	—	20–790
TSS	4–4,070	90–13,000
Oil and grease	—	—
Mineral quality:		
Na^{+}	3.36–1,306	14–1,621
Ca^{+2}	66–517	19–1,499
Total alkalinity:	0–835	0–2,630
CL^{-}	98–1,920	180–3,540
SO_4^{-2}	25–5,000	20–1,250
NO_3^{-}	35–100	10–710
PO_4^{-3}	1–21	1–51
CN^{-}	—	5.2
pH units	3.6–11.5	1.8–11.9
DO	—	—
Priority pollutants: organics	—	—
Priority pollutants: metals	—	
Hg		0.03–11
As		0.2–7
T-Cr		1–200
Cr^{6+}		0.06–7
Pb		13–500
Cd		1.2–20
Fe		40–3,600
Cu		1–52
Zn		30–1,050
Mn		5–65
Total flow	—[a]	—[a]

[a]Combined flows up to 2,000 L/min.

ture in a low-oxygen environment so that the organic components break down chemically. The heat for pyrolysis of MSW usually is obtained by totally oxidizing part of the refuse. The pyrolysis reaction produces three components: (1) A gas consisting primarily of hydrogen, methane, carbon monoxide, and carbon dioxide; (2) an oily or liquid fraction which contains organic chemicals such as acetic acid, acetone, and methanol plus water derived from hydrolysis or

organic compounds; and (3) a solid char fraction consisting of unburned carbon plus inert materials such as glass.

Water is used in pyrolysis plants for cooling, gas scrubbing, char quenching, and miscellaneous housekeeping. Wastewater streams of major concern are those collected from scrubbers, condensers, and other gas cleaning devices. These wastewaters usually are high strength and contain a variety of organic materials formed during the pyrolytic reaction or vaporized from the raw RDF. A BOD_5 in the range 50,000 ppm–100,000 ppm is caused by water-soluble organics such

TABLE 3.—Summary of Significant Pollutants Identified in Pyrolysis Waste Streams (2,6,20)

Variable (1)	Concentration, in milligrams per liter: Pyrolysis condensate and gas scrubber water (2)
Organic surrogates:	
BOD	50,000–77,000
COD	30,000–52,000
TSS	30–112
Oil and grease	500–1,000
Mineral quality:	
Na^+	89–170[a]
Ca^{+2}	84–135[a]
Total alkalinity:	
CL^-	360–690[a]
SO_4^{-2}	44–62[a]
NO_3^-	
PO_4^{-3}	
CN^-	2–8[a]
pH units	3.7[a]
DO	2.4–3.7[a]
Priority pollutants: organics	
Phenol	20–50[a]
2-4 dimethyl phenol	0.6–9[a]
Benzene	4[a]
Toluene	1[a]
Ethylbenzene	1[a]
Naphthalene	3[a]
Priority pollutants: metals	
Lead	0.3–0.8[a]
Zinc	2.8–15[a]
Flow, in liters per minute	Up to 250 liters/min: reports differ

[a]Data are based on "once through" use of scrubber water.

as alcohols, organic acids, and aldehydes. The BODs in this range are too high for conventional activated sludge and must be pretreated by other processes. In addition to the high organic strength, the pyrolysis condensate is characterized by high concentrations of organic priority pollutants such as phenol, benzene, and toluene; the gas scrubber waters are characterized by high concentrations of trace metal priority pollutants (see Refs. 2, 6, 20 and Table 3).

Anaerobic digestion of sewage sludge to produce methane gas has been a

common practice in sewage treatment, however, anaerobic digestion of MSW is only in the developmental stage at this time. A system for digesting the organic part of municipal trash in a mixture with sewage sludge is currently under shakedown testing in Pompano Beach, Fla. Two wastewater streams are anticipated: (1) Storage pit drainage; and (2) liquid effluent generated from dewatering the digested sludge. No data are available on the composition of these waste streams when MSW is digested with the sewage sludge. We anticipate that the dewatered filtrate from the digestion of combined MSW/sewage sludge will be similar to that which exists at normal sewage sludge digesters. Thus, the wastewaters will be characterized by high BODs, in the range 500 mg/L–10,000 mg/L and high concentrations of organic priority pollutants, in the range of 650 mg/L–3,800 mg/L (see Refs. 9 and 15 and Table 4).

TABLE 4.—Summary of Significant Pollutants Identified in Digester Supernatant/Filtrate (9,15)

Parameter (1)	Concentration, in milligrams per liter Digester supernatant/filtrate (2)
Organic surrogates:	
BOD	500–10,000
COD	1,000–30,000
TSS	200–15,000
Oil and grease	—
Mineral quality:	
Na^{+}	—
Ca^{+2}	—
Total alkalinity:	100–2,700
CL^{-}	—
SO_4^{-2}	—
NO_3^{-}	—
PO_4^{-3}	—
CN^{-}	—
pH units	6.4–7.2
DO	—
Priority pollutants: organics	Total volatile solids: 650–3,800
Priority pollutants: metals	—
Flow, in liters per minute	—

In summary, although many sources of wastewater exist at RDF and WAF facilities, the quantities and strengths of the wastewater are often small. Consequently, these wastes can usually be discharged directly into the sanitary sewer or held for a brief period in an oxidation pond before discharge to ambient receiving waters. In addition to these small insignificant sources, we found several major waste streams generated in RDF/WAF facilities. The exact quantities and strengths of these wastes are highly dependent upon the operating characteristics of the particular facility. Important considerations in the disposal of these wastes are: (1) The local ambient water quality standards; and (2) the availability of sanitary sewers.

The major waste streams of concern, associated with current RDF/WAF facilities, are:

1. Filtrate from the dewatered subsystem of the hydrapulping wet preprocessing facility.—This wastewater is characterized by moderate BOD_5/COD (less than 10,000 mg/L), moderate suspended solids (less than 10,000 mg/L), and acidic pH (pH less than 7.0).
2. Pyrolysis condensates and gas scrubber effluents.—These wastewaters are characterized by very high (greater than 10,000 mg/L) BOD_5/COD, low (less than 1,000 mg/L) suspended solids, and high organic content, especially phenols and benzene compounds.
3. Filtrate and supernatant from anaerobic digesters.—These wastewaters are characterized by high (greater than 10,000 mg/L) BOD_5/COD, high (greater than 10,000 mg/L) suspended solids, and neutral pHs.
4. Gas scrubber effluent from combustion facilities.—These wastewaters are characterized by low (less than 1,000 mg/L) BOD_5/COD, low (less than 1,000 mg/L) suspended solids, variable pH, and the presence of heavy metals.

Projected Treatment Efficiencies

The efficiencies of pollution control technologies applicable to the identified waste streams are considered in the following paragraphs.

As presented earlier, the principal waterborne emissions are the organic surrogates (BOD_5, COD, TSS), the organic priority pollutants, and trace metals. The first two are efficiently treated with biological processes, either aerobic or anaerobic, whereas the latter are successfully removed via physical-chemical processes. Physical-chemical methods are also effective in removing organic surrogates but the total cost is higher than with usual biological processes. Similarly, some adsorption and removal of trace metals occurs in biological processes, but this removal is incidental to the real purpose, i.e., the conversion of soluble organic material into microorganisms and gas.

Waste streams identified as quench water, sluice water, and ash pond effluent associated with mass burn and cofiring incinerators are readily treated with existing control technology. Other waste streams such as the scrubber waters at mass burn and incinerator facilities and digester supernatants at anaerobic digester facilities appear amenable to treatment via physical-chemical and aerobic biological processes, respectively. Which of the two control processes would be most successful in treating these wastes or whether the control processes may be required in tandem should be investigated in pilot studies. The remaining two waste streams, the pyrolysis gas scrubber water, and the thickener wastewater from the hydrapulping process have far greater strengths than normally associated with domestic wastewater. Pilot plant data (5,7,11,14,18,22) indicate that these wastewaters should be amenable to treatment by anaerobic processes; the pyrolysis gas scrubber water being especially adaptable to the anaerobic filter treatment process because of low suspended solids and elevated temperatures, the hydrapulping wastewater being amenable to the anaerobic biological contact process because of its high suspended solids. Both of these treatment processes are in the developmental stage and will require verification testing to determine operating parameters and applicability to particular waste streams.

Aerobic biological processes can be applied effectively to any of the organic

pollutants identified earlier. Under aerobic conditions, the soluble organic matter in a waste stream is converted into active biomass. Organic removal efficiencies of aerobic processes range between 80% and 90%. The removal efficiency of soluble organic material from the liquid phase is actually greater; however, enough solids escape the final clarification process to reduce the overall efficiency.

The efficiencies of the various treatment steps considered herein in removing significant pollutants from pertinent industrial discharges are presented in Table

TABLE 5.—Efficiency of Treatment Processes in Removing Significant Pollutants from Pertinent Industrial Discharges (4,16,17)

Industry/Level or Treatment (1)	Percent Removal							
	BOD (2)	COD (3)	SS (4)	Oil and grease (5)	Phenol (6)	Ammonia (7)	Sulfide (8)	Metals (9)
Petroleum:								
Primary	30–60	20–50	50–80	60–95	0–50			
Biological secondary	40–99	30–95	20–85	50–99	60–99	0–99	70–100	
Filtration	40–70	20–55	75–95	65–95	5–20			
Carbon adsorption	70–98	70–94	60–90	70–95	90–100			
Anaerobic filter		10–13						
Steam electric power:								
Biological secondary				50–70				
Secondary				70–90				
Anaerobic filter								50–95
Pulp and paper:								
Primary			95					
Biological secondary	85–99							
Anaerobic filter		73–94						
Steam supply and cooling:								
Precipitation and coagulation								90–100
Organic chemicals:								
Biological secondary	93	69–74						
Carbon adsorption	90	69						
Plastics and synthetics:								
Biological secondary	80–99	90–95						
Food Processing:								
Anaerobic filter		55–86						
Pharmaceutical:								
Anaerobic filter		94–98						
Wastewater treatment plant:								
Anaerobic filter	85	76	45					

5 and Refs. 4, 16, and 17. The listed industries produce wastestreams similar to those encountered in RDF-WAF facilities.

Recommended Pilot Plant Studies

Based on the strengths of wastewaters produced at RDF-WAF facilities, and the anticipated removal efficiencies of various treatment processes, pilot plant

studies are recommended to verify removal efficiencies and to determine whether linkage of processes in series is required to meet discharge standards. The pilot studies would investigate the effectiveness of aerobic, anaerobic, and physical-chemical processes in obtaining the desired effluent quality.

Two main aerobic processes are available: (1) Filters; and (2) activated sludge. In the biological filter, waste is applied continuously or intermittently to the top surface of the filter. Natural rocks or ceramic or plastic fill material have been successfully used as filter media. Air is circulated through the filter either by natural convection or forced draft to maintain aerobic conditions throughout the depth of the media. A diverse population of microbites and microlutes live on the surface of the media and utilize the waste either directly or as high food-chain consumers.

In the activated sludge process, the microbial population is dispersed in the liquid phase. The population is less diverse but more concentrated than in a biological filter. Air is introduced into the liquid phase to maintain aerobic conditions and to keep the microbial population in suspension. Organic removal in activated sludge can be improved by increasing the number of microorganisms in the mixed liquor or the period of contact of the waste with the microorganisms.

In order to provide flexibility in the operation of an aerobic pilot plant, both the biofilter and the activated sludge processes should be constructed. The biological filter can be selectively inserted into the treatment train in front of the aeration tank. In addition to overall increased efficiency, the diverse biota of the biological filter are resistant to shock loadings and toxic elements, thus affording a degree of protection against upset not available in an activated sludge process alone. The effective depth of the biological filter can be varied, as can the amount of flow path of recirculation within the filter. Waste streams with high COD will probably require the use of a biological filter as a first stage roughing filter prior to activated sludge treatment.

The activated sludge aeration stage should be designed as a completely mixed reactor; a configuration suitable for high organic loads and easy operation. The aeration tank should be divisible into four compartments to facilitate variation of aeration time. The aeration system can be converted from air to pure oxygen.

Anaerobic treatment is well adapted to target waste streams containing high concentrations of organic surrogates. An exception to this statement is the digester supernatant, where the efficacy of treating the effluent from an anaerobic treatment system with another anaerobic treatment system is dubious. The efficiency of anaerobic processes appears to increase with higher concentrations of organic surrogates and high temperatures in the anaerobic reaction vessel. Thus, an anaerobic treatment process is ideally suited for a warm, concentrated waste stream. The pyrolysis waste is the primary candidate for anaerobic treatment because of its concentration and elevated temperature. Another likely candidate is the hydrapulping waste stream.

Based on the available data for waste streams at WAF facilities, two anaerobic treatment processes are recommended for construction in the anaerobic pilot plant. These processes are the anaerobic filter and the anaerobic contact chamber. In the anaerobic contact process, the solids retention time is increased by recirculating sludge removed in the secondary sedimentation tank. The anaerobic filter, on the other hand, retains the sludge within the primary vessel; both on the media and between the voids of the media. In anaerobic processes the

conversion of soluble organics to gases is high; 80% gas (CH_4 + CO_2) to 20% sludge production is not uncommon. Because of this, anaerobic processes can treat large quantities of organic waste with only a moderate build up of sludge. Indeed, low sludge generation and methane production are the two major advantages of anaerobic treatment, as opposed to aerobic treatment, which

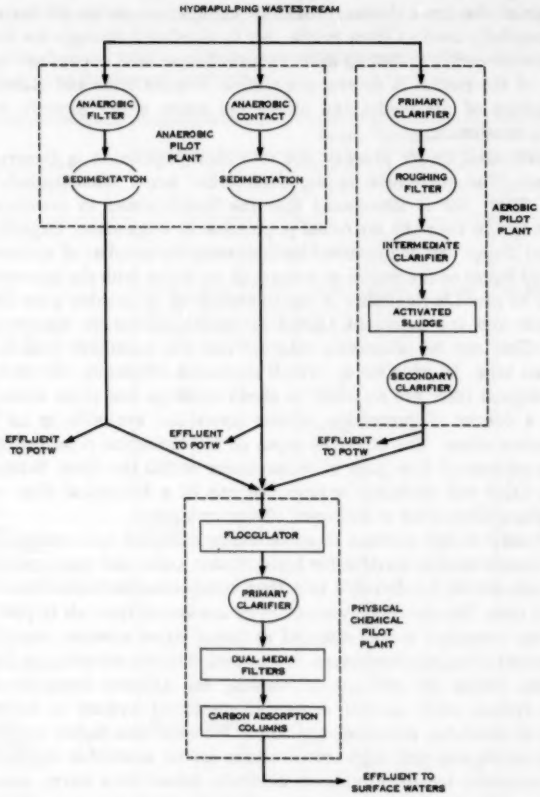

FIG. 1.—Aerobic and Anaerobic Treatment Processes followed by Physical Chemical Treatment [Should be Investigated in Treatment of Hydrapulping Wastestreams (Table 1)]

generates large quantities of sludge and requires continuous energy input.

Operating experience with both types of anaerobic processes is scant. Our literature review showed only one full-scale operation of the anaerobic filter and no full-scale operation of the anaerobic contact chamber. Despite these limited operations, both processes have significant advantages over aerobic

treatment. The anaerobic filter is simple to operate, does not require sludge recirculation, and requires construction of only one vessel. The anaerobic contact chamber can handle large suspended solids loadings with excellent methane production.

The physical-chemical treatment process is directly applicable to the treatment of wastes found in incinerator scrubber waters. Furthermore, the process may be combined with either the aerobic or anaerobic treatment processes to produce

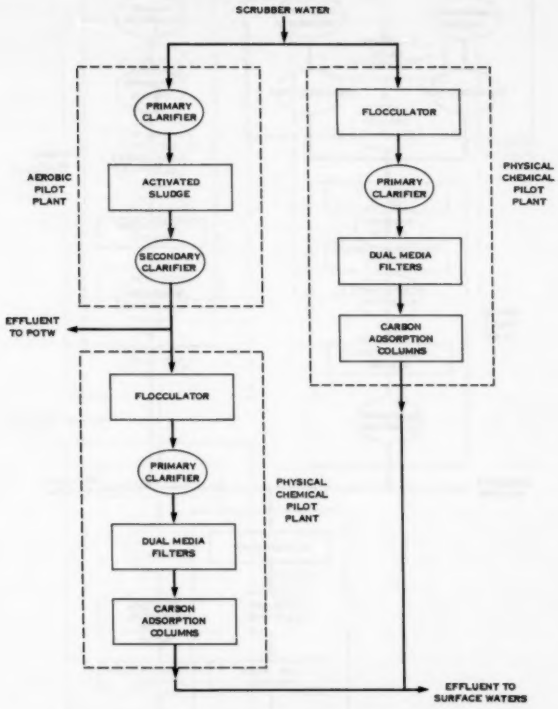

FIG. 2.—Both Aerobic and Physical Chemical Treatment Processes [Should be Investigated in Treatment of Scrubber Waters (Table 2)]

an effluent acceptable for discharge to ambient receiving waters.

Since a physical-chemical pilot plant may be used in a tertiary role as well as by itself, the flow must be compatible with the other pilot plants, particularly with the aerobic unit. Extensive bypass capability must be provided so that in the tertiary treatment mode, individual unit processes can be inserted or removed as desired. The unit processes of flocculation, sedimentation, filtration, and carbon adsorption should be provided in the physical-chemical pilot plant.

Operational variables that can be controlled for experimental purposes are: (1) The chemical dose—variation in amount and type of primary coagulant and filter aid; (2) flocculation—flocculation energy input, detention time, and sludge-

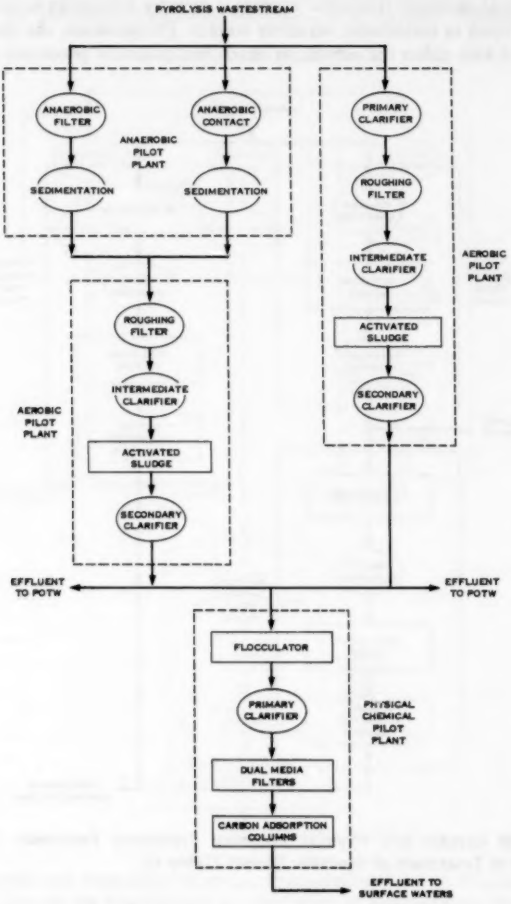

FIG. 3.—Aerobic and Anaerobic Treatment Processes, Operated in Series and in Parallel [Should be Investigated in Treatment of Pyrolysis Wastestreams (Table 3)]

solid content; (3) filtration—filter media design and filtration rate; and (4) carbon adsorption—contact time in the adsorption column.

Unlike the biological units, the physical-chemical pilot plant does not require

a period of cell growth and acclimation upon startup. Most modifications to the treatment process can be accomplished in a matter of minutes. Housing the physical-chemical processes in a separate trailer will provide additional flexibility in the sequential or concurrent operation of the different processes on the WAF wastestreams.

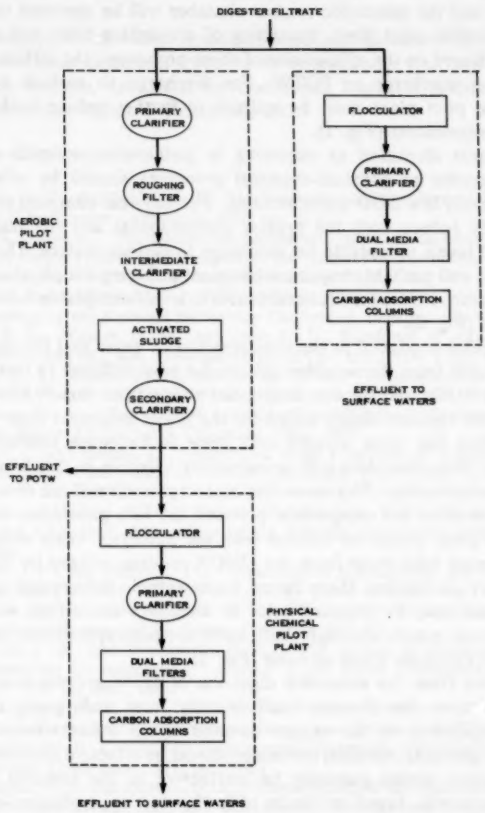

FIG. 4.—Aerobic and Physical Chemical Treatment Processes [Should be Investigated in Treatment of Digester Wastestreams (Table 4)]

Based on the wastestreams generated in WAF facilities, and the available wastewater treatment processes and efficiencies, combinations of treatment processes may be required to achieve the effluent limitations for discharge to ambient receiving waters. In most cases, the use of a single treatment process will produce an effluent acceptable for discharge to a publicly-owned treatment

works (POTW). However, in virtually all cases, a physical-chemical process following either an anaerobic or aerobic process will be required to polish the effluent and thereby meet discharge standards for surface waters.

For hydrapulping waste streams, either anaerobic or aerobic processes should be effective in producing a 90% reduction in the high BOD and COD of these wastewaters (16,17). For comparison purposes, two anaerobic processes, the anaerobic filter, and the anaerobic contact chamber will be operated in parallel along with the aerobic pilot plant, consisting of a roughing filter and activated sludge aeration. Based on the efficiencies of these processes, the effluent should be acceptable for discharge to POTW. For discharge to surface waters, a physical-chemical pilot plant must be utilized to further reduce both organic and inorganic contaminants (Fig. 1).

For contaminants identified as occurring in incinerator or boiler scrubber waters, either aerobic or physical-chemical processes should be effective in treating the relatively low BOD waste streams. The physical-chemical pilot plant should effectively reduce both the organic contaminants and the trace metal concentrations to levels acceptable for discharge to surface waters. The aerobic treatment process will probably require subsequent polishing via physical-chemical processes to remove trace metal contaminates to levels acceptable for discharge to surface waters (Fig. 2).

The waste streams produced in the condensation of gases and the separation of pyrolysis fuel oils from the scrubber oil are the most difficult to treat. Based on the very high BODs and the low suspended solids from this WAF process, the anaerobic filter appears ideally suited for the initial treatment step. To date, the anaerobic filter has been utilized only once in full-scale operations and consequently the pilot plant data will be especially valuable in the development of this innovative technology. The anaerobic contact process will run concurrently with the anaerobic filter for comparison between the two processes. Likewise, the aerobic pilot plant should be utilized with the pyrolysis waste streams and the results compared with those from the UNOX process utilized by the Union Carbide Company in treating their Purox wastewaters. Subsequent physical-chemical treatment may be required prior to discharge to surface waters for the removal of trace metals although these have not been specifically identified in the analysis of pyrolysis waste streams (Fig. 3).

The wastewaters from the anaerobic digestion of MSW are the most poorly characterized because the process itself is only now undergoing full-scale investigation. Depending on the oxygen demand of the waste streams, either the aerobic or the physical-chemical processes should be effective in its treatment. The aerobic process would generally be ineffective in the removal of trace metals and consequently, based on results of further testing, a physical-chemical process may be required to upgrade the effluent (Fig. 4).

In conclusion, based on the results of our investigation, we feel that three pilot plant trailers should be designed, constructed, and operated in the field at WAF facilities. These three pilot plants, anaerobic, aerobic, and physical-chemical, should be operated both in series and in parallel to obtain data on the relative efficiencies of the different processes. The operation of the anaerobic pilot plant should be especially valuable because of the innovative nature of the processes involved. In addition, the operation of the other pilot plants will provide valuable information on their respective removal efficiencies with respect

to organic and trace metal priority pollutants. The successful operation of the pilot plants at WAF facilities will provide valuable information on the wastewater streams generated and the applicability of various treatment schemes in reducing the pollutant levels in these waste streams to acceptable levels.

Acknowledgment

This study to characterize liquid pollutants produced at RDF-WAF facilities and to recommend treatment steps for these pollutants was funded by the Fuels Technology Branch, Industrial Environmental Research Laboratory, Environmental Protection Agency, Cincinnati, Ohio.

Appendix.—References

1. Achiger, W. C., and Daniels, L. E., "An Evaluation of Seven Incinerators," *Proceedings National Incinerator Conference,* 1970, pp. 32–61.
2. Ananth, C., et al., "Environmental Assessment of Waste-to-Energy Process: Union Carbide Purex System," MRI report to Environmental Protection Agency Industrial Environmental Research Laboratory, Cincinnati, Ohio, June, 1978.
3. Cross, F. L., and Ross, R. W., "Effluent Water From Incinerator Flue Gas Scrubbers," *Proceedings of the National Incinerator Conference,* 1968, pp. 69–72.
4. Culp, R. L., Wesner, G. M., and Culp, G. L., *Handbook of Advanced Wastewater Treatment,* 2nd ed., Van Nostrand-Reinhold Co., Inc., New York, N.Y., 1978.
5. Hang, R. T., Raksit, S. K., and Wong, G. G., "Anaerobic Filter Treated Waste Activated Sludge," *Water and Sewage Works Journal,* Vol. 124, No. 2, Feb., 1977.
6. Hoffman, D. A., "Pyrolysis of Solid Municipal Wastes," *Environmental Protection Agency Report 67012-73-039,* Cincinnati, Ohio, 1977.
7. Jennett, J., and Dennis, D., "Anaerobic Filter Treatment of Pharmaceutical Waste," *Journal of the Water Pollution Control Federation,* Vol. 47, No. 1, Jan., 1975.
8. Kaiser, E. R., and Carotti, "Municipal Incineration of Refuse with 2 Percent and 4 Percent Additions of Foam Plastics: Polyethylene, Polyurethane, Polystyrene, and Polyvinyl Chloride," *Proceedings of the National Incinerator Conference,* 1972, pp. 230–244.
9. Malina, J. F., and Felipo, J. D., "Treatment of Supernatants and Liquids Associated with Sludge Treatment," *Water and Sewage Works Journal,* Aug., 1971, pp. 32–38.
10. Matusky, F. E., and Hampton, R. K., "Incinerator Wastewater," *Proceedings of the National Incinerator Conference,* 1968, pp. 198–203.
11. Sanders, F. A., and Bloodgood, D. E., "The Effects of Nitrogen-to-Carbon Ratio on Anaerobic Decomposition," *Journal of the Water Pollution Control Federation,* Vol. 37, No. 12, Dec., 1965.
12. Schoenberger, R. J., et al., "Characterization and Treatment of Incinerator Process Waters," *Proceedings of the National Incinerator Conference,* 1970.
13. Schoenberger, R. J., "Studies of Incinerator Operation," *Proceedings of the National Incinerator Conference,* 1972, pp. 15–31.
14. Schoepfer, G. J., and Zeimke, N. R., "Development of the Anaerobic Contact Process, I, Pilot Plant Investigation and Economics," *Sewage and Industrial Wastes,* Vol. 31, No. 2, Feb., 1959.
15. "Sludge Treatment and Disposal," *Environmental Protection Agency Technology Transfer Manual,* 1974.
16. *State and Local Pretreatment Programs, Federal Guidelines, Appendices 1–7,* United States Environmental Protection Agency, Municipal Construction Division, Washington, D.C., Jan., 1977.
17. *State and Local Pretreatment Programs, Federal Guidelines, Volume I,* United States Environmental Protection Agency, Municipal Construction Division, Washington, D.C., Jan., 1977.
18. Taylor, W., "Full-Scale Anaerobic Trickling Filter Evaluation," Food Waste Research Section, United States Environmental Protection Agency, Cincinnati, Ohio.

19. Wilson, D. A., and Brown, R. E., "Characterization of Several Incinerator Process Waters," *Proceedings of the National Incinerator Conference,* 1970, pp. 196–203.
20. Wilson, E. M., et al. "Engineering and Economic Analysis of Waste to Energy Systems," Ralph M. Parsons Company report to the Environmental Protection Agency Industrial Environmental Research Laboratory, Cincinnati, Ohio, June, 1977.
21. Young, J. C., and Johnson, L., "Water Use and Wastewater Production at Solid Waste Processing/Energy Recovery Facilities," Engineering Research Institute, Iowa State University, Ames, Iowa, 1977.
22. Young, J. C., and McCarty, P. L., "The Anaerobic Filter for Waste Treatment," *Journal of the Water Pollution Control Federation,* Vol. 41, No. 5, May, 1969.

LEACHATES FROM SOLID WASTE RECOVERY OPERATIONS[a]

By A. Douglas Rademaker[1] and James C. Young,[2] M. ASCE

INTRODUCTION

The use of urban solid wastes for energy production recently has received a great deal of consideration. This interest stems from the fact that waste-to-energy conversion systems save valuable fuel resources and provide for disposal of wastes with reduced reliance on dumps and landfills. Residues from urban waste-to-energy conversion facilities include quenched ash, boiler sluice water, digested sludge, and soluble and particulate matter trapped in scrubber water. These residues generally are disposed of by means of land application, lagooning, or by sanitary landfilling. Studies of waste-to-energy conversion facilities to date have been concerned more with evaluating the mechanical aspects of the system elements for processing and burning the wastes, than with the possible environmental problems, such as ground-water contamination by disposal site leachates associated with the ultimate disposal of the residues produced.

Consequently, a study was conducted to determine the nature of residues produced at urban waste-to-energy conversion facilities and to evaluate leachates generated from the residues (2). The study program consisted of two phases. Phase A consisted of bench-scale tests in which solid residue samples from waste-to-energy conversion facilities were placed on gravel support media in glass columns and maintained at saturated conditions with distilled water. Leachate samples were collected daily from these columns. Phase B consisted of bench-scale tests in which solid residue samples from waste-to-energy conversion facilities were placed on a soil/sand mixture which was supported on a gravel medium in glass columns. The residue samples and soil/sand mixture were maintained at standard conditions, as in Phase A. Leachate samples were collected on a daily basis and composited and analyzed on a weekly basis.

The general objectives of these tests were: (1) To evaluate the quantity of materials that can be leached from residues of typical waste-to-energy conversion facilities; (2) to determine if heavy metals and organic priority pollutants leach

[a]Presented at the April 14–18, 1980, ASCE, Annual Convention and Exposition, held at Portland, Oreg. (Preprint 80-040).

[1]Environmental Engr., Brice, Petrides, and Assocs., Inc., Waterloo, Iowa.

[2]Prof., Dept. of Civ. Engrg., Iowa State Univ., Ames, Iowa 50011.

Note.—Discussion open until October 1, 1981. To extend the closing date one month, a written request must be filed with the Manager of Technical and Professional Publications, ASCE. Manuscript was submitted for review for possible publication on April 21, 1980. This paper is part of the Journal of the Energy Division, Proceedings of the American Society of Civil Engineers, ©ASCE, Vol. 107, No. EY1, May, 1981. ISSN 0190-8294/81/0001-0017/$01.00.

in sufficient quantities to pose a potential hazard when discharged to the environment; and (3) to determine the effects of soil on the character of leachate produced from the selected waste residues.

Experimental Study

Sample Collection.—To determine the potential water-related environmental impact of solid residues produced at urban waste-to-energy facilities, solid residue samples were collected from several operating plants, pilot plants, and laboratory scale units for subsequent use in laboratory-scale leachate generation tests. The following are descriptions of the sources of the solid residues.

Nashville Mass-Burning Ash.—Two quenched ash samples were collected at the Nashville Thermal Transfer Corporation mass-burning facility at Nashville,

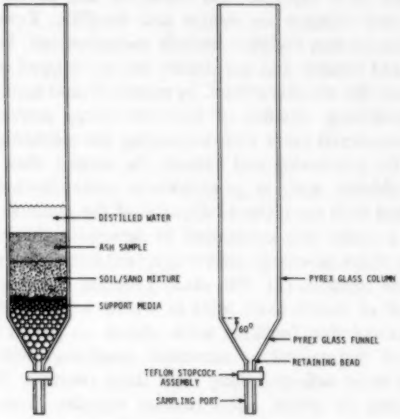

FIG. 1.—Schematic Diagram of Leaching Columns Showing Placement of Support Medium, Soil, and Ash

Tenn. Both samples were air-dried and hand-sieved through a 3/8-in. (10-mm) United States Standard Sieve to remove large particles of unburned wood, glass, wire, and concrete; the samples were then mixed thoroughly to provide homogeneous mixtures.

Ames Refuse-Derived Fuel (RDF)/Coal Ash.—In 1977 and 1978, tests were conducted at the Ames, Iowa power plant, at which various percentages of the fuel load consisted of shredded RDF provided by the Ames Solid Waste Recovery System. Ash was sluiced from the boilers and the electrostatic precipitators at the conclusion of each RDF/coal burn. Samples were collected during the bottom-ash sluicing period using a hand sampler, and were filtered through cloth filters to remove the water. The resulting ash solids were air-dried and hand-sieved through a 3/8-in. (10-mm) United States Standard Sieve.

Anaerobically-Digested Synthetic Solid Waste.—Waste sludge was collected from

pilot-scale anaerobic digesters which were in operation in the sanitary engineering research laboratories at Iowa State University at the time the leaching tests were conducted. The synthetic solid waste consisted of 40% kraft paper, 35% unprinted newprint, 13% Purina Dog Chow, and 12% dried grass by weight. The waste sludge samples were air-dried and pulverized to obtain a homogenous mixture.

Sludge from Biologically-Treated Pyrolysis Wastewater.—Sludge was collected from laboratory-scale biological treatment units receiving a mixture of a synthetic wastewater and wastewater from Union Carbide's PUROX™ waste-to-energy conversion facility located at South Charleston, W.Va. The synthetic waste feed consisted of bactopeptone, yeast extract, and dextrose, and made up 80% of the feed biochemical oxygen demand (BOD) load. Pyrolysis wastewater made up the other 20% of the feed BOD load. Ammonium chloride, ferric chloride, and magnesium chloride also were added to the units to serve as nutrients. Waste sludge from these units was dried and pulverized to obtain a homogenous mixture for the leaching tests.

TABLE 1.—Experimental Design for Leaching Tests Using Residues from Waste-to-Energy Conversion Facilities without Soil Contact

Column (1)	Material description (2)	Weight, in grams (3)
A	Nashville RDF ash	500
B	Ames coal/RDF ash (80% boiler load/10% solid waste[a])	500
C	Ames coal/RDF ash (100% boiler load/10% solid waste[a])	500
D	Ames coal/RDF ash (100% boiler load/20% solid waste[a])	500
E	Anaerobically-digested synthetic solid waste sludge	125
F	Distilled water (water blank)	—

[a]Percentage based on British thermal unit content.

Pompano Beach Filter Cake.—Filter cake from the anaerobic digestion bioconversion system at Pompano Beach, Fla. was air-dried, hand-sieved through a 3/8-in. (10-mm) United States Standard Sieve, and retained for analysis and testing.

Apparatus

Leaching Columns.—Leaching tests were conducted using pyrex glass columns having an inside diameter of 3.75 in. (95 mm), an outside diameter of 4.0 in. (0.1 m), and a height of 45 in. (1.14 m). Each column had a cross-sectional area of 0.077 sq ft (0.007 m^2) (see Fig. 1). The upper 38 in. (0.97 m) of the column consisted of the 4.0-in. (0.1-m) oxygen demand (OD) pyrex glass tubing. The lower 7 in. (0.18 m) consisted of a 4.0-in. (0.1-m) 60°, pyrex glass funnel which was fused to the glass column. A straight stop-cock assembly, with a 0.24-in. (6-mm) bore and Teflon stop cock was fused into the stem of the glass funnel. Three 1/4-in. (6.4-mm) beads were fused to the inside surface of the glass funnel 1 in. (25 mm) above the stop-cock assembly to prevent

media from falling into the stop-cock bore, which would cause it to become plugged. The Teflon stop-cock assembly provided flow regulation when opened partially, and a tight seal when closed.

Support Medium.—A gravel/sand base, consisting of four layers, was placed in the lower section of each column to retain the residue samples and to act as a filter to prevent the loss of solids when liquid samples were withdrawn. The bottom layer consisted of 3 in. (76 mm) of washed gravel, retained on a 1/2-in. (13-mm) United States Standard Sieve; the second layer consisted of 1 in. (25 mm) of washed gravel retained on a 3/8-in. (10-mm) United States Standard Sieve; the third layer consisted of 1 in. (25 mm) of washed gravel, retained on a #4 United States Standard Sieve; and the fourth and final layer consisted of washed silica sand retained on a #8 United States Standard Sieve.

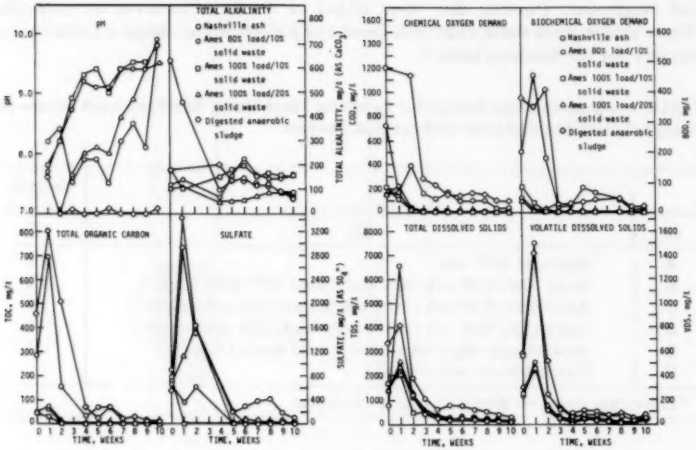

FIG. 2.—Leachate Quality Versus Leaching Time in Column Tests as Shown by Concentrations of Various Constituents

Soil/Sand Mixture.—Silty clay obtained from a soil bank in the Ames, Iowa area was hand-sieved through a #8 United States Sieve, and blended with an equivalent air dried weight of silica sand retained on a #25 United States Standard Sieve. The silica sand was blended with the topsoil to increase the permeability of the soil so that water would drain through it more rapidly.

Testing and Results

Phase A: Characterization of Leachates.—Phase A was initiated by thoroughly cleaning and acid washing the glass columns and gravel support media. Dry test materials, as listed in Table 1, were carefully weighed and placed on the top layer of support media. Five-hundred milliliters of distilled water were added carefully to each of the six columns, and the top of each column was covered

with a glass beaker to prevent foreign materials from falling into the columns. A black plastic tarp was used to cover the columns at all times, except when sampling, to discourage algae growth. The six columns were then allowed to stand for 24 h to saturate the test materials.

Twenty-four hours after initial residue wetting, the sampling program was initiated. Six dark bottles with Teflon-lined caps were cleaned thoroughly and labeled. Sample volumes of 250 ml were collected daily by opening the stop cocks and withdrawing the leachate at an approximate flow rate of 125 ml/min. After the pH was determined, each sample was transferred to the appropriate brown bottle for compositing, and stored at room temperature. Two-hundred and fifty milliliters of distilled water were then added to each of the six columns to replace the volume withdrawn as a sample. This sampling routine was followed on a daily basis. At the end of each week, the composite samples were analyzed for the following parameters: BOD (Ref. 3, p. 543); chloride (Ref. 1, p. 269); chemical oxygen demand (COD) (Ref. 3, p. 550); sulfate (Ref. 3, p. 628); total

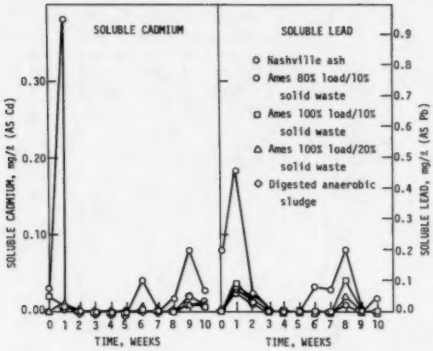

FIG. 3.—Cadmium and Lead Concentrations in Effluent from Leaching Columns

organic carbon (TOC) (Ref. 3, p. 532); total alkalinity (Ref. 3, p. 289); total dissolved solids (TDS) (Ref. 3, p. 91); total phosphorus (Ref. 3, p. 476); volatile dissolved solids (VDS) (Ref. 3, p. 95); fluoride (Ref. 3, p. 393); organic nitrogen (Ref. 3, p. 616); pH (Ref. 3, p. 460); ammonia nitrogen (Ref. 3, p. 616); soluble cadmium (Ref. 3, p. 179); nitrate nitrogen (Ref. 3, p. 620); soluble lead (Ref. 3, p. 179); nitrite nitrogen (Ref. 3, p. 620); and organic priority pollutants (Ref. 5). At the beginning of each week, a 250-ml grab sample also was collected and processed for acid/base-neutral extractions for organic compounds. Two similar test runs were made during Phase A as a check on test reproducibility.

The concentrations of many of the constituents characterizing the leachates peaked early during the testing period and then decreased consistently as illustrated by the data for selected parameters, as shown in Figs. 2 and 3. This decrease was primarily a function of the movement of water through the waste residue materials in the leaching columns. Movement of water through the residue material was expected to approximate plug flow. When the leachate samples were drawn

from the sampling port of the column there was a downward movement of water through the residue and filter media.

To estimate the flow regime present in the leaching columns, the chloride concentration of each waste residue leachate was plotted as the ordinate against time (abscissa) on semilog paper (see Fig. 4). If the actual washout process was of the first order, then the expected plot would be a straight line. Plots of chloride concentration in leachate from the Nashville ash and the anaerobically-digested synthetic solid waste residue approached straight lines, although those for the Ames ash did not. The sloping dashed lines show the expected concentration trends for each residue leachate under first-order washout conditions.

This deviation from first-order washout seems likely to have occurred because

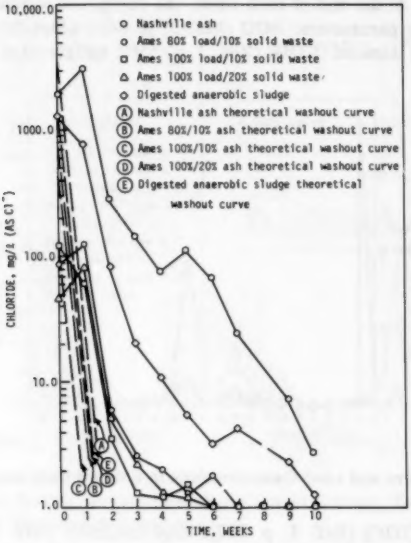
10,000.0
1000.0
100.0
10.0
1.0
CHLORIDE, mg/l (AS Cl⁻)
0 1 2 3 4 5 6 7 8 9 10
TIME, WEEKS
Nashville ash
Ames 80% load/10% solid waste
Ames 100% load/10% solid waste
Ames 100% load/20% solid waste
Digested anaerobic sludge
A Nashville ash theoretical washout curve
B Ames 80%/10% ash theoretical washout curve
C Ames 100%/10% ash theoretical washout curve
D Ames 100%/20% ash theoretical washout curve
E Digested anaerobic sludge theoretical washout curve

FIG. 4.—Chloride Washout Trends for Phase A Column Tests

of continued dissolving of soluble materials, thereby causing the measured washout curves to lie above the theoretical washout curve as was observed (see Fig. 4). The compositing of daily leachate samples may have contributed to initial deviations from the first-order washout trend. This would occur because the daily samples were averaged over a seven-day period, and peak concentrations occurring early in each week were diluted upon addition of subsequent daily samples to the composites.

Total Leachate Mass.—The total mass of each constituent leached from the residue samples over a seven-week period was calculated by multiplying the average concentration from two adjacent weekly measurements by the total volume of distilled water passed through each column during that time period.

This mass, divided by the original weight of waste residue in each column, is reported in Table 2, which lists the average for two separate tests from Phase A.

Organic Priority Pollutant Scan.—The acid and base-neutral extracts were analyzed by gas chromatography using a Perkin-Elmer Sigma I gas chromatograph system. This separated the organic compounds in each extract, and permitted identification of those compounds which are classified as "priority pollutants" by the Environmental Protection Agency (EPA) (5).

The number of organic compounds found in the acid and base-neutral extracts having peak areas of at least 5% of the peak area of the internal standard d_{10} anthracene are shown in Table 3. Only those compounds not detected in

TABLE 2.—Total Amount of Individual Constituents Leached from Solid Waste Residues

	Leached Mass, in milligrams per gram				
Parameter (1)	Nashville ash (2)	Ames ash, 80% load/ 10% solid waste (3)	Ames ash, 100% load/ 10% solid waste (4)	Ames ash, 100% load/ 20% solid waste (5)	Digested synthetic solid waste (6)
BOD	4.35	1.17	0.17	0.10	26.46
COD	3.29	1.07	0.56	0.72	33.18
TOC	2.48	0.26	0.17	0.28	16.86
TDS	30.12	12.98	12.14	13.29	73.95
VDS	5.99	3.06	2.62	2.78	28.35
KJEL-N	0.21	0.07	0.007	0.05	5.14
NH_4^+-N	0.05	0.02	0.002	0.02	2.63
NO_3^- + NO_2^--N	0.01	0.001	0.002	0.0	0.04
Cl^-	8.86	0.37	0.26	0.23	11.55
$SO_4^=$	16.69	5.05	9.42	11.88	48.55
Total alkalinity	4.34	2.69	2.97	1.32	20.90
Total PO_4	0.03	0.002	0.01	0.02	6.26
F^-	0.03	0.004	0.02	0.003	0.02
Cd	1.6×10^{-3}	2.2×10^{-5}	5.1×10^{-5}	1.2×10^{-5}	0.8×10^{-4}
Pb	1.8×10^{-3}	2.8×10^{-4}	4.2×10^{-4}	3.2×10^{-4}	13.6×10^{-4}

the control column effluent or in the solvent blank are reported. These data indicate that more organic compounds were present in the acid extracts than in the base-neutral extracts. No organic priority pollutants were detected.

As expected, TDS leaching was high. The organic constituents seemed to originate with pieces of unburned wood and compressed paper. Such materials were easily identified by eye in all ash residue samples.

Solvent Extraction For Organic Analysis.—A solvent extraction technique was used to remove organic materials from one 250-ml liquid sample collected each week. The extraction procedure yields a base-neutral extract and an acid extract using methylene chloride as the organic solvent (5). Base-neutral extracts contain

organics which remain unionized at a pH of 11 or higher, whereas acid extracts contain organics which remain unionized at a pH of 2 or lower. Extraction procedures were performed using a continuous extraction process with a 24-h reflux period. The methylene chloride extracts were passed through a column of anhydrous sodium sulfate to remove residual water. The extracts were then placed in Kuderna-Danish concentrators and condensed on a steam table until the final sample volume was approx 2 ml.

Condensed sample volumes were then adjusted to an exact volume using clean methylene chloride, and d_{10} anthracene was added to an internal standard in a sufficient quantity to produce a concentration of 20 mg/L in each concentrated extract.

TABLE 3.—Summary of Organic Analyses for Phase A Column Tests

Residue (1)	Number of Unidentified Organic Compounds	
	Acid extracts (2)	Base-neutral extracts (3)
Nashville ash	44	32
Ames ash, 80% load/10% solid waste	14	10
Ames ash, 100% load/10% solid waste	7	10
Ames ash, 100% load/20% solid waste	21	7
Digested anaerobic sludge residue	74	48

TABLE 4.—Experimental Design for Leaching Tests Using Residues from Waste-to-Energy Conversion Facilities Using Soil Contact

Column (1)	Solid waste residue (2)	Weight, in grams	
		Residue (3)	Sand/soil (4)
A	Nashville ash	500	500
B	Ames coal/RDF mixture	500	500
C	Biologically-treated pyrolysis waste sludge	6	—
D	Biologically-treated pyrolysis waste sludge	6	500
E	Sand/soil mixture (soil blank)	—	500
F	Distilled water (water blank)	—	—

Most low molecular weight organic compounds are removed by this methylene chloride extraction, including the organic priority pollutants. Some high molecular weight compounds, such as the soluble starches and proteins also may be removed.

Phase B: Effects of Soil Contact on Character of Leachates.—At the conclusion of Phase A, the leaching columns were cleaned thoroughly and a clean support medium was placed in each. Five-hundred grams of the sand/soil mixture were placed in columns A, B, C, and E. Table 4 lists the dry test materials placed in the columns. The daily sampling program used in Phase A was also used in Phase B. Sample volumes of 250 ml were collected weekly and processed for organic and inorganic analysis. Parameters evaluated in this phase were:

VDS, TDS, BOD, COD, chloride, and soluble heavy metals. Time series plots of the data for selected parameters are shown in Fig. 5. All data were corrected by subtracting the effects of the distilled water and soil column blanks where appropriate. As in Phase A, many of the constituents had concentration trends that peaked early and then decreased rapidly.

Total Leached Mass.—Priority pollutant metals were measured weekly, and the total leached mass of each constituent was calculated as in Phase A. A summary of the results is shown in Table 5.

A comparison of the cadmium and lead data for the ash samples with those in Table 2 shows that, with one exception, the soil contact reduced the total leachable mass. A comparison of the data for the pyrolysis sludge shows a

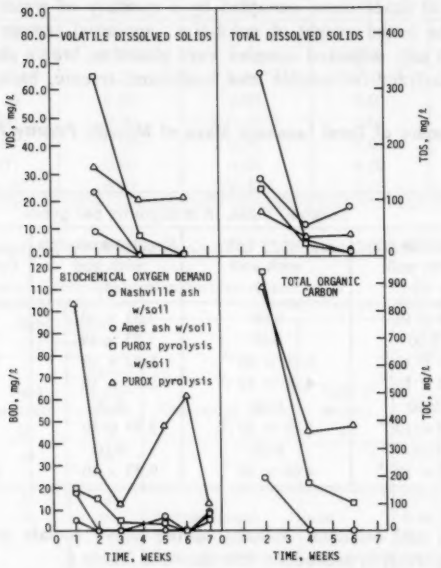

FIG. 5.—Washout Trends for Individual Constituents during Phase B Column Tests

mixed effect. Cadmium and lead did not seem to be attenuated, but other metals did seem to be reduced by soil column contact.

Leachate Test Comparison.—The EPA has proposed a procedure for measuring the total extractable mass of metallic priority pollutants from solid wastes (4). Tests were conducted during the writers' study to compare the EPA method with the column tests used in Phases A and B, and as a check to determine the recovery in the column tests.

The EPA extraction procedure was followed closely, but with some modifications to the equipment. The proposed agitator/extractor apparatus was replaced with a Phipps/Bird Stirrer equipped with 6-mm glass rods bent in an "L"

configuration to replace the metal paddles. Several waste residue samples therefore could be extracted simultaneously under controlled conditions.

Five representative 100-g ash or residue samples were placed in 2-L glass jars containing 1.6 L of distilled water. These mixtures were stirred with the glass paddles at 80 rpm for 24 h. The pH of each sample was maintained at 5 by adding 0.5 N acetic acid when needed.

The temperature was maintained at 20° C throughout the extraction process. At the end of the 24-h extraction period, the samples were allowed to stand under quiescent conditions to promote liquid and solid phase separation. The liquid was then decanted and the solid phase was discarded. The liquid phase samples were centrifuged and filtered through 0.45-μm filter pads. The filtered liquid sample volumes were then adjusted with deionized water so that the volumes were 20 times those occupied by a quantity of water at 4° C equal in weight to the initial weight of solid (i.e., an initial sample of 100 g was diluted to 2,000 ml). Adjusted samples were placed in brown glass bottles and subsequently analyzed for soluble lead, cadmium, arsenic, barium, chromium,

TABLE 5.—Summary of Total Leachate Mass of Metallic Priority Pollutants After Soil Contact

	Leached Mass, in milligrams per gram			
Soluble (1)	Nashville ash with soil (2)	Ames ash with soil (3)	Pyrolysis sludge with soil (4)	Pyrolysis sludge (5)
Pb	8.00×10^{-5}	0.00	3.33×10^{-3}	0.00
Cd	0.00	0.00	1.83×10^{-2}	1.83×10^{-3}
As	2.20×10^{-6}	5.20×10^{-6}	1.42×10^{-3}	1.15×10^{-3}
Ba	1.60×10^{-3}	4.00×10^{-4}	8.33×10^{-2}	0.21
Cr	0.00	0.00	0.00	3.33×10^{-3}
Hg	1.00×10^{-6}	1.60×10^{-6}	3.33×10^{-4}	8.0×10^{-4}
Ag	0.00	0.00	0.00	0.00
Se	1.90×10^{-5}	4.40×10^{-6}	9.83×10^{-4}	2.57×10^{-3}

mercury, silver, and selenium. Results of the heavy metals scan, using the modified EPA extraction procedure, are shown in Table 6.

Comparison of these data with those from column leaching shown in Tables 2 and 5 show that, in general, the column tests produced a greater total leached mass than did the EPA method. Too little data were collected, however, to determine the significance of this difference.

Organic Priority Pollutant Scan.—Leachate samples collected in Phase B were examined weekly for solvent extractable organic constituents. The number of compounds found in both acid and base-neutral extracts are tabulated in Table 7. These data show that more organic compounds were in the acid extract than in the base-neutral extracts. This is in agreement with the results of Phase A (see Table 4). Also as in Phase A, no priority pollutants were found in the ash residue samples.

A comparison of the number of compounds from soil-column tests reported in Table 6, with the comparable number in Table 3, where no soil was used,

shows that the soil reduced the number of base-neutral compounds appreciably, but acid extractable compounds did not seem to be adsorbed as readily.

Some organic priority pollutants were observed in the leachates from sludge

TABLE 6.—Heavy Metals Detected by Modified EPA Extraction Procedure

	Leached Mass, in milligrams per gram				
Soluble (1)	Nashville ash (2)	Ames ash, 80% load/ 10% solid waste (3)	Ames ash, 100% load/ 10% solid waste (4)	Ames ash, 100% load/ 20% solid waste (5)	Pompano Beach filter cake (6)
Pb	7×10^{-4}	0.00	4×10^{-4}	0.00	0.00
Cd	0.00	0.00	0.00	0.00	0.00
As	4×10^{-6}	0.00	2×10^{-6}	2×10^{-6}	0.00
Ba	2×10^{-3}	0.00	0.00	0.00	0.00
Cr	0.00	0.00	2×10^{-5}	0.00	0.00
Hg	0.00	0.00	0.00	0.00	0.00
Ag	0.00	0.00	0.00	0.00	0.00
Se	8×10^{-6}	0.00	0.00	0.00	3×10^{-5}

TABLE 7.—Summary of Organic Analysis of Leachates Collected during Phase B

	Number of Unidentified Organic Compounds		PRIORITY POLLUTANTS					
					Concentration, in milligrams per liter			
					Week			
Residue (1)	Acid extracts (2)	Base-neutral extracts (3)	Compound name (4)	Type of extract (5)	1 (6)	3 (7)	5 (8)	7 (9)
Nashville ash	49	19	—		—	—	—	—
Ames ash on soil	31	6	—		—	—	—	—
Pyrolysis waste sludge	72	34	0-chlorophenol	acid	0.24	—	0.16	0.14
			2,4-dimethylphenol	acid	0.01	0.03	0.02	0.02
			2-chloronaphthalene	base-neutral	0.11	0.01	0.04	0.02
			Naphthalene	base-neutral	0.20	0	0	0
			Acenaphthylene	base-neutral	0.03	0	0	0
			bis-(2-ethylhexyl) phthalate	base-neutral	0.49	0.08	—	0.09
Pyrolysis waste sludge on soil	70	2	0-chlorophenol	acid	0.81	0.41	0.09	0.16
			2,4-dimethylphenol	acid	0.04	0.21	0.16	0.15
			2-chloronaphthalene	base-neutral	0.03	0.02	0	0
			Naphthalene	base-neutral	0	0.04	0	0.02
			Acenaphthylene	base-neutral	0	0	0	0
			bis-(2-ethylhexyl) phthalate	base-neutral	0.11	0.21	—	—

produced upon biological treatment of pyrolysis wastewater. Those priority pollutants shown were known to exist in the untreated pyrolysis wastewater. As with the unidentified organic compounds, those in the base-neutral extracts

seemed to be more readily adsorbed on soil while the acid extractable compounds showed essentially no change upon contact with soil.

Leachate Composition and Environmental Standards

Organic and inorganic constituents, as summarized in Figs. 2, 3, and 5 and Table 7, can occur in concentrations considerably in excess of most state and Federal discharge standards to streams. Overflows from residue ponds receiving ash from facilities burning municipal solid waste conceivably can violate discharge standards. These concentrations peak rapidly upon contact of the ash with water so that total leached mass per unit of residue is quite low. Thus, some type of controlled release of ash pond overflow should permit most state standards to be met. Dry handling of ash residues can reduce the amount of water requiring discharge, but will not reduce the total amount of materials that could be leached upon disposal of these residues in landfills.

Unfortunately, there are no general standards for discharge or disposal of liquid wastes containing organic or inorganic priority pollutants. Proposed regulations presented by the EPA have, to date, not been promulgated.

Summary, Conclusions, and Recommendations

Phase A of the study consisted of bench-scale column tests in which leachates were generated from solid residues of the major categories of urban waste-to-energy conversion facilities. These leachates were analyzed to determine if organics and heavy metals were present in sufficient quantities to pose a potential hazard if discharged to the environment. Phase B involved bench-scale column tests in which leachates were generated and analyzed to determine the effects of soil on the character of the leachates, and to determine if organics and heavy metals leach through a typical soil in sufficient quantities to pose a potential environmental hazard.

The results of this study have shown the following:

1. The concentration of various constituents in effluents from leaching columns declined gradually from a peak early in the leaching period to essentially zero over a period of five weeks–seven weeks. The rate of washout could not be described as first-order, indicating that soluble materials were released from the solid phase as freshwater passed through the column.
2. Gas chromatographic analysis of column leachates revealed a number of unidentified organic compounds in ash samples. The source of these organic materials seemed to be unburned wood and compressed paper products not burned in the waste conversion unit. No organic priority pollutants were found in ash residues, but were present in sludges produced upon biological treatment of pyrolysis wastewaters.
3. Soil columns removed most base-neutral extractable organic compounds, but not acid extractable compounds. Metallic priority pollutants were removed, to some extent, upon contact with soil.

Considerable research and development work is needed to refine procedures for producing and analyzing leachates from solid residues. The EPA procedure,

while possibly giving the desired results, requires use of nonstandard equipment. Modifications of standard laboratory equipment seem to work equally as well. More work is also needed to model leaching of priority pollutants from landfills using column testing procedures. Standards for disposal of residues containing leachable priority pollutants may need to be expressed both in terms of total leachable mass and maximum concentration of undesirable constituents in the leachate.

Considerable research is needed to refine techniques for identification of organic pollutants. While gas chromatography/mass spectroscopy techniques are well-developed for tracing many common organic compounds through environmental pathways, techniques are not well-suited for identifying specific organic compounds in the presence of a large number of unknowns.

Techniques for removing compounds from solid residues need considerable refinement. A more complete evaluation of recovery efficiency when extracting these organics, and of the effects of concentration and storage of the extracts is also needed.

Acknowledgment

This project was supported in part by a grant from the United States Department of Energy, in association with the Ames Laboratory of Iowa State University, and in part by the Engineering Research Institute of Iowa State University. The first writer was a graduate research assistant in the Civil Engineering Department of Iowa State University at the time of this study.

Appendix.—References

1. *Annual Book of ASTM Standards,* Part 3, American Society for Testing and Materials, Philadelphia, Pa., 1975.
2. Rademaker, A. D., "Analysis of Leachates from Solid Residues Produced at Urban Waste-to-Energy Conversion Facilities," thesis presented to Iowa State University, at Ames, Iowa, in 1979, in partial fulfillment of the requirements for the degree of Master of Science.
3. *Standard Methods for the Examination of Water and Wastewater,* 14th ed., American Public Health Association, Washington, D.C., 1976.
4. "Hazardous Wastes: Proposed Guidelines and Regulation and Proposal on Identification and Listing," *Federal Register,* Part IV, United States Environmental Protection Agency, Dec. 18, 1978, pp. 58946–59028.
5. "Sampling and Analysis Procedures for Screening of Industrial Effluents for Priority Pollutants," United States Environmental Protection Agency, Environmental Monitoring and Support Laboratory, Cincinnati, Ohio, Mar., 1977.

SMALL-SCALE HYDRO IN NEW ENGLAND: 1960–1976

By Paul H. Kirshen,[1] A. M. ASCE

INTRODUCTION

As part of a project sponsored by the United States Department of Energy to study the obstacles and incentives to the development of small-scale hydropower (SSH) in the nineteen northeastern states and to recommend policies to increase the rate of development of SSH, a review of the historical hydropower statistics of New England has been made. The review was part of a process to attempt to understand the many factors that affect the development of SSH. (Other elements of this process included meetings with technical advisory committees, meetings with SSH developers, and interaction with other SSH researchers.) The review of historical data was also useful in evaluating the results of a computer simulation model of the SSH development process (HYDRO-I) (1,5).

Presented in this paper are time series data concerning conventional and small-scale hydropower in New England and the United States, analysis of the data, and then, finally, conclusions that can be drawn from the data. The definition of SSH used in this report is nameplate capacity less than or equal to 25 Mw.

TIME SERIES DATA

Shown in Table 1 are data from the period 1960–1976 on hydropower in each of the six New England states, in the region, and in the nation. Table 2 presents information on the patterns of SSH ownership in New England. For comparison purposes, some of the data in Table 1 are plotted in Fig. 1. Presented in Fig. 2 are costs of electricity in New England over the period 1960–1978 and the number of applications for minor projects (less than 1.5 Mw capacity) from throughout the United States submitted to the Federal Energy Regulatory Commission (FERC) over that period. All the data in Table 1 are from the Federal Power Commission (8). These reports describe the developed and potential hydroelectric power resources of the United States and have been

[1]Asst. Prof. of Engrg., Dept. of Civ. Engrg., Virginia Polytechnic Inst. and State Univ., Blacksburg, Va. 24060.

Note.—Discussion open until October 1, 1981. To extend the closing date one month, a written request must be filed with the Manager of Technical and Professional Publications, ASCE. Manuscript was submitted for review for possible publication on March 24, 1980. This paper is part of the Journal of the Energy Division, Proceedings of the American Society of Civil Engineers, ©ASCE, Vol. 107, No. EY1, May, 1981. ISSN 0190-8294/81/0001-0031/$01.00.

TABLE 1.—State and Regional Conventional Hydropower Data for New England

Variable (1)	1960 (2)	1964 (3)	1968 (4)	1972 (5)	1976 (6)
			(*a*) Maine		
Total SSH, in megawatts[a]	351.256	344.045	324.940	327.101	319.067
In thousands of kilowatt hours[b]	1,906,000	1,967,610	1,934,456	1,957,752	1,945,629
FPC licensed SSH, in megawatts	4.0	35.713	158.506	257.66	256.235
In thousands of kilowatt hours	20,000	213,600	1,017,550	1,631,721	1,651,079
Total SSH plants	91	80	78	76	68
FPC licensed SSH plants	1	6	22	41	41
			(*b*) New Hampshire		
Total SSH, in megawatts	149.369	145.040	131.942	127.417	120.992
In thousands of kilowatt hours	740,200	728,100	678,700	643,530	623,480
FPC licensed SSH, in megawatts	53.36	53.36	109.450	112.450	110.250
In thousands of kilowatt hours	278,000	270,700	603,900	614,255	600,255
Total SSH plants	58	49	39	33	27
FPC licensed SSH plants	6	6	14	15	14
			(*c*) Vermont		
Total SSH, in megawatts	109.335	106.735	109.142	107.383	107.708
In thousands of kilowatt hours	452,200	436,100	446,900	439,700	440,900
FPC licensed SSH, in megawatts	13.920	17.92	28.045	56.005	55.305
In thousands of kilowatt hours	60,000	85,000	121,000	261,100	258,100
Total SSH plants	61	55	53	47	47
FPC licensed SSH plants	2	3	10	19	18
			(*d*) Massachusetts		
Total SSH, in megawatts	145.133	137.899	135.001	129.348	139.245
In thousands of kilowatt hours	620,530	606,790	601,615	575,903	580,001
FPC licensed SSH, in megawatts	30.896	67.496	71.476	73.413	90.319
In thousands of kilowatt hours	161,200	447,200	386,925	392.225	431.816
Total SSH plants	75	67	62	54	49
FPC licensed SSH plants	5	10	11	13	18

TABLE 1.—*Continued*

(1)	(2)	(3)	(4)	(5)	(6)
			(*e*) Rhode Island		
Total SSH, in megawatts	4.317	3.125	2.860	2.860	1.5
In thousands of kilowatt hours	10,000	8,180	7,680	7,680	4,000
FPC licensed SSH, in megawatts	0	0	0	0	0
In thousands of kilowatt hours	0	0	0	0	0
Total SSH plants	8	5	4	4	1
FPC licensed SSH plants	0	0	0	0	0
			(*f*) Connecticut		
Total SSH, in megawatts	68.560[c]	74.135	63.415	61.344	61.220
In thousands of kilowatt hours	181,800[c]	205,600	174,500	172,570	172,570
FPC licensed SSH, in megawatts	0	0	2.2	2.2	2.2
In thousands of kilowatt hours	0	0	11,000	11,000	11,000
Total SSH plants	29[c]	21	19	16	16
FPC licensed SSH plants	0	0	2	0	0
			(*g*) New England		
Total hydropower, in megawatts	1,515.697[c]	1,497.283	1,491.130	1,510.983	1,506.462
In thousands of kilowatt hours	5,864,730[c]	5,959,270	5,934,851	6,086,513	6,046,791
Total SSH, in megawatts	827.970[c]	810.979	767.300	755.453	749.732
In thousands of kilowatt hours	3,910,730[c]	3,952,380	3,843,851	3,797,135	3,766,580
Total SSH plants	322[c]	277	255	230	208
Total LSH,[d] in megawatts	687.727[c]	686.304	723.830	755.330	756.730
In thousands of kilowatt hours	1,954,000[c]	2,006,890	2,091,000	2,289,378	2,280,211
SSH average capacity factor[e]	0.539[c]	0.556	0.572	0.574	0.574
LSH average capacity factor	0.324[c]	0.334	0.330	0.346	0.343
			(*h*) United States		
Total hydropower, in megawatts	31,825.343[f]	40,230.291	45,826.491	53,404.326	57,034.720
In thousands of kilowatt hours	166,274,000[f]	201,918,565	223,312,412	256,780,606	271,124,113
Average capacity factor[e]	0.596[f]	0.573	0.556	0.549	0.543

[a]Based on reports made to FERC by private, public, and cooperative utilities and industrial establishments limited to 100 Kw or more through 1964. After 1964, all 100 Kw or less projects that are licensed are included. Definition of SSH is nameplate capacity of 25 Mw or less. Some

TABLE 1.—*Continued*

(1)	(2)	(3)	(4)	(5)	(6)

of the facilities have gross heads greater than 100 ft. Capacities of facilities in two states are split between the states. Data from Ref. 8.

[b]Estimate of annual energy production under average water conditions.

[c]Adjustment needed as FPC (1960) includes Rocky River (Connecticut) with 7 Mw pumped storage as well as 24 Mw conventional hydropower.

[d]Large-scale hydropower (LSH) has installed capacity greater than 25 Mw.

[e]Capacity factor is ratio of average output to theoretical maximum output.

[f]Adjusted for inclusion of pumped storage generation in FPC (1960) tables.

TABLE 2.—SSH Ownership Data in New England (8)

Variable (1)	1960 Number (2)	1960 Percent of total (3)	1976 Number (4)	1976 Percent of total (5)	Percent of reduction (6)
Number of SSH plants					
Private	151	47	104	50	31
Industrial	145	45	81	39	44
Municipal or state	25	8	23	11	8
Total	321	100	208	100	
Capacity of SSH plants (mw)					
Private	533	64	513	69	4
Industrial	265	32	205	27	23
Municipal or state	30	4	32	4	+7
Total	828	100	750	100	

issued every four years since 1960. Prior to that they were issued in 1953 and 1957. The information in the reports is compiled from reports to the FPC by private, cooperative, public, and industrial installations and appear to be the most consistent data base available.

Analysis

Hydropower in United States.—The installed conventional hydroelectric capacity of the United States has continued to increase since 1960. However, the FPC (1976) reports that the growth rate is declining while that of steam-electric facilities is increasing. In 1976 hydropower provided only 11% of the United States total generating capacity. At one time hydropower provided 33% of capacity. A major factor contributing to this decline has been a continual decrease in the cost of electricity production by nonhydroelectric sources up until the mid 1970s (6). Another factor contributing to the decline growth rate is that the construction costs of hydropower increase steadily as better sites are developed (in 1960, 19% of the potential sites in the United States were developed; in 1976, 33%).

While the installed capacity of hydropower in the United States has increased, the total number of plants has decreased from 1,685 in 1960 to 1,426 in 1976

(8). The FPC (9) states that the decline is due to additional development of already developed sites and retirement of smaller, inefficient plants. Note in Table 1 that the average capacity factors of plants in the United States has steadily declined from 0.596 in 1960 to 0.543 in 1976. This reflects the trend toward the use of hydropower plants for peaking power production.

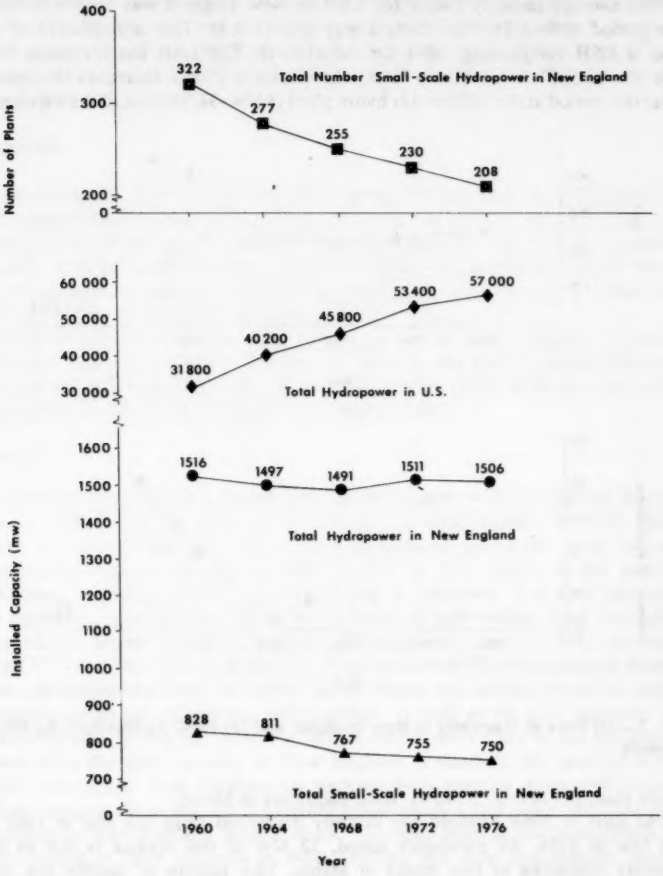

FIG. 1.—Number and Installed Capacity of Hydropower in United States and New England

Hydropower in New England.—The total installed capacity of hydropower in New England has remained relatively constant at 1,500 Mw because of offsetting increases in the development of large-scale hydropower (LSH) and decreases in SSH. About 30% of the total New England potential is developed. The average

capacity factor for all hydro plants in New England has increased slightly from 0.44–0.46 in the period 1960–1976. This increase is also seen when LSH and SSH plants are examined alone (considered later). This increase is probably indicative of the retirement of inefficient plants rather than a decrease in the use of plants for peak power production.

The average capacity factor for LSH in New England was approx 0.33 for the period 1960–1976. For SSH, it was approx 0.55. This is indicative of the use of LSH for peaking, SSH for run-of-river. The LSH has increased from 688 Mw in 1960 to 756 Mw in 1976. The change is due to increases in capacity over this period at the Millinocket hydro plant (8 Mw–31.5 Mw) and the Ripogenus

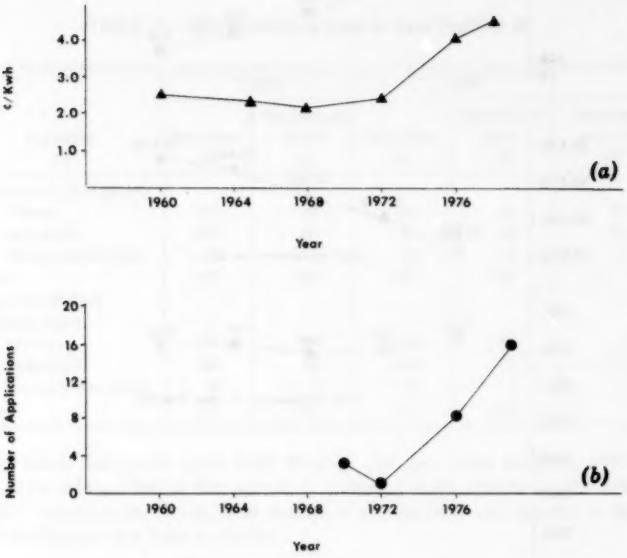

FIG. 2.—(*a*) Price of Electricity in New England; and (*b*) FERC Applications for Minor Projects

hydro plant (24 Mw–37.53 Mw). Both plants are in Maine.

The SSH in New England has steadily decreased from 828 Mw in 1960 to 750 Mw in 1976. As previously noted, 32 Mw of this decline is due to the capacity upgrading of two plants in Maine. This pattern of decline has also occurred in each of the states except Connecticut and Massachusetts, where there was one intervening year when capacity increased. Since the rate of decline of the total number of SSH plants is greater than that of the SSH installed capacity (see Fig. 1) and the average capacity factors of SSH are increasing, the smaller, less efficient plants are being retired. In 1960 the average plant size was 2.6 Mw and the average capacity factor was 0.54. In 1976, the comparative figures were 3.6 Mw and 0.57.

Costs of Electricity.—As shown in Fig. 2, the cost of electricity in New England steadily decreased from 1960–1968 and then began to increase. While perhaps coincidental, it is interesting to note that the rate of retirement of SSH plants in New England decreased after 1968 (see Fig. 1). This could have been the beginning of the recognition of the possible value of SSH in New England's and the nation's energy supply. "Official" recognition of the possible importance of SSH in the nation's energy future occurred in President Carter's April 20, 1977 comprehensive energy plan. At that time, the United States Army Corps of Engineers was directed to undertake a 90-day study of both large-scale and small-scale hydropower (7).

Ownership

As shown in Table 2, the ownership pattern of SSH in New England did not change considerably in the period 1960–1976. Throughout the period approximately 65% of the total installed SSH capacity was privately owned, i.e., utility owned, 30% industrially owned, and 5% municipally or state owned. Based on the number of plants owned by each group, the largest capacity plants are owned by utilities and then by municipalities or states.

Both in terms of number of plants and total installed capacity, industrial owners retired the greatest amount of SSH in the period 1960–1976 (even considering that approx 32 Mw of the industrially retired SSH was due to the upgrading of two plants in Maine from SSH to LSH).

Licensing

Between 1960 and 1976 the number of SSH plants in New England licensed by the FPC increased from 14 (or 4% of the total number of SSH plants) to 91 (or 44%). Nationally the number of licensed plants (all sizes) has also increased: from approx 20% in 1960 to 45% in 1976. Much of the licensing has been of plants already constructed and in operation. It is also interesting to note that, as shown in Fig. 2, the number of applications from throughout the United States for minor projects (capacity less than 1.5 Mw) decreased until 1972 and then sharply increased. These data are difficult to interpret because the applications are from the entire United States and include those for already constructed plants, relicenses, and hearings, as well as for new capacity. The available data do indicate, however, that in recent years many of the applications have been for new capacity in New England. Therefore, the interest in new SSH capacity in New England (at perhaps both existing dams and potential sites) seems to have started to increase significantly a few years after the sharp increase in New England electric costs. This also leads to the expectation that the decline in SSH capacity in New England will stop and actually start to increase.

Summary and Conclusions

Until recently, New England has followed the national trend of decreased interest in both LSH and SSH and of retiring small, inefficient plants. In New England it appears that LSH is used for peak-power production and SSH for run-of-river production.

As expected, the interest in and the development of LSH and SSH in both New England and the United States is inversely related to the costs of alternatives for producing electricity. It follows, then, that with the cost of fossil fuels continually increasing, interest in SSH will continue. Due to the economic sensitivity of SSH development (1,5), it is expected that most developers of SSH will attempt to use hydropower for peak-power production. This will undoubtedly cause controversies between developers, environmentalists, and other interest groups (see Ref. 10).

Industrial use of SSH has declined the most, and based on applications to FERC for preliminary permits and licenses it appears that industrial users are continuing to show little interest in SSH compared to other types of potential developers. The major disincentives for industrial developers of SSH might be the short payback periods required on major projects by industrial developers (10 yr or less) (1) and the difficulties they sometimes have obtaining backup power from utilities (similar to problems using cogeneration) (2). If this trend of industrial retirement and lack of interest continues, the mix of ownership of SSH facilities in New England shown in Table 2 will change. The data from Corso (1979) in a personal communication indicate that municipalities and rural electric cooperatives are very interested in SSH.

The licensing of already existing projects has increased in recent years. This may be due to greater enforcement by FERC or a desire by hydropower operators to protect their sites as interest in SSH increases, or both.

Finally, based on the recent increase in applications for major and minor projects, there is a significant increase in interest in SSH both in New England and elsewhere. The survey results of the New England River Basins Commission (4) indicate that there is a potential of 1,000 Mw of SSH at existing, nongenerating dams in New England based solely on hydraulic and hydrologic practicability. If this interest is to be maintained and some of this potential obtained, obstacles to development (such as the burdensome licensing process) will have to be overcome and incentives further emphasized (such as the value of renewable energy resources) (4). Several studies are currently underway to recommend development strategies, e.g., those of Franklin Pierce Law Center and Dartmouth College, United States Army Corps of Engineers Institute for Water Resources, and New England River Basins Commission, and it is hoped their results will be seriously considered by policymakers.

Acknowledgments

This work was supported by the United States Department of Energy, Contract No. EY-78-5-02-4943 through a subcontract to the Franklin Pierce Law Center, Concord, New Hampshire.

Appendix.—References

1. Amlin, J. S., "Economic and Technical Determinants of Small-Scale Hydropower Development in New England," thesis presented to Thayer School of Engineering, Dartmouth College, at Hanover, N.H., in 1979, in partial fulfillment of the requirements for the degree of Master of Science.
2. Dallaire, G., "Conservation Energy: Vast, Untapped New Energy Source for the U.S.," *Civil Engineering*, ASCE, Vol. 49, No. 12, Dec., 1979, pp. 77–88.

3. "Electric Utility Industry in New England, Statistical Tables, 1978," Electric Council of New England, Bedford, Mass., 1978.
4. "Hydropower: A National Energy Resource," Presented at the March 11–16, 1979, Engineering Foundation Conference, held at Easton, Md.
5. Kirshen, P. H., and Amlin, J. S., "Computer Model for Small-Scale Hydropower Policy Analysis," *Journal of the Water Resources Planning and Management Division*, ASCE, Vol. 107, No. WR1, Proc. Paper 16093, Mar., 1981, pp. 61–76.
6. "A Blueprint for Energy Action," New England Energy Congress, New England Congressional Caucus and Tufts University, Boston, Mass., May, 1979.
7. "Estimate of National Hydroelectric Power Potential at Existing Dams," United States Army Corps of Engineers, Institute for Water Resources, Ft. Belvoir, Va., July, 1977.
8. "Hydroelectric Power Resources of the United States, Developed and Undeveloped," United States Federal Power Commission, Washington, D.C., 1960, 1964, 1968, 1972, 1976.
9. "Hydroelectric Plant Construction Cost and Annual Production Expenses, 19th Annual Supplement, 1976," United States Federal Power Commission, Washington, D.C., Sept., 1977.
10. Wheeler, R. M., "A Pattern Recognition Approach to the Assessment of Conflict Potential in Small-Scale Hydropower Development," thesis presented to Thayer School of Engineering, Dartmouth College, at Hanover, N.H., in June, 1980, in partial fulfillment of the requirements for the degree of Master of Science.

OPTIMIZATION OF PUMP TURBINES

By Joachim Raabe[1]

INTRODUCTION

Pumped storage plants are a means of converting low-cost base-load energy into valuable peak-load power.

Equipment used to operate these power stations may be distinguished according to two categories, namely the binary set (comprising the pump turbine and the motor generator set), and the ternary set. The latter has been undergoing constant development in Switzerland and Germany since the beginning of the present century. It extends to a centrifugal pump, turbine, and motor generator set, all of which are arranged alongside a shaft. The turbine and pump can be designed as separate units adapted to the specific function they are required to perform.

Maintaining the same sense of rotation on all units, as applied to both pump and turbine function, it is possible, in addition, to minimize the period of transition between these two operational functions.

Greater compactness on the ternary set is effected by means of the so-called isogyre design.

Taking into account electricity rates, a 1% efficiency loss, occurring on an hydraulic motor system, signifies loss of revenue exceeding the cost of the entire set of machines, including installation. This is why West Germany, Switzerland, and Austria prefer to continue using the ternary set, distinguished as it is by a high degree of efficiency, and accompanied by features of easy handling.

A disadvantage, however, of the ternary set, when compared with the binary set is the extra cost involved in installing a second hydraulic machine along with its pertinent shutoff devices and manifold system, as well as the amount of additional space required for installation. This, of course, tends to weigh heavily in favor of the binary set, which is restricted to the pump turbine and motor generator set, especially in times of spiraling wage costs and growing capital expenditure. It is true that, when turbining, less efficiency is obtained from a pump turbine than a turbine specifically adapted to its function on optimum lines. Nevertheless, this is regarded with less significance on a system of electricity

[1]Full Prof. and Head of Chair and Lab. for Hydr. Machinery and Equipment, Technical Univ., Munich, Federal Republic of Germany.

Note.—Discussion open until October 1, 1981. To extend the closing date one month, a written request must be filed with the Manager of Technical and Professional Publications, ASCE. Manuscript was submitted for review for possible publication on April 22, 1980. This paper is part of the Journal of the Energy Division, Proceedings of the American Society of Civil Engineers, ©ASCE, Vol. 107, No. EY1, May, 1981. ISSN 0190-8294/81/0001-0041/$01.00.

interlinking network that is constantly expanding, owing to the increase in the supply of power tending to lessen the difference in cost between the base and peak load. In addition, modern hydraulic research makes it possible to obtain virtually optimum efficiency on pump turbines applying both modes of operation (pumping and turbining).

The design of pump turbines is based on the fact that a pump impeller can also be made to function as a turbine runner, even though it would be somewhat less efficient than a well-built turbine runner specially designed for the purpose. According to experience, a pump impeller engineered on optimum lines would reveal an outside diameter 40% greater than that of a turbine runner. Even so, it is possible, on principle, to replace the pump and turbine of the ternary

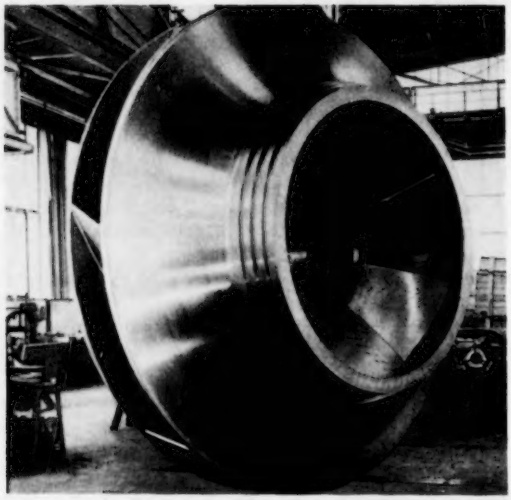

FIG. 1.—Impeller of Pump Turbine Designed for Roenkhausen Facility

set in pumped storage plants by one reversible pump turbine (binary set) (10,18,19,21,22).

The first pump turbines (operating with relatively low capacity) were installed during the early 1930s at the German Baldeney (2-MW) and Pedreira (4-MW) facilities. The idea of the pump turbine was not revived until after World War II in the United States, where the first pump turbine installed on a larger scale was at the Flat Iron Facility in 1950. With the two Taum Sauk pump turbine sets [head-780 ft (240 m)] put into service in 1964, the United States achieved a spectacular breakthrough in penetrating the 250-MW limit (14,15). A new dimension has since been attained on the sector of United States pump turbine development in the form of the four 392-MW sets now in operation at the Racoon Facility, along with the six 457-MW Bath County sets scheduled for service in 1979.

European countries whose hydromechanical industries were able to point to satisfactory results from the use of ternary sets installed at pumped storage plants, e.g., Italy, Germany, Austria, and France, were slow to follow the United States example, especially after having experienced some difficulty on their first large-scale pump turbines at the point of transition from turbine to pump operation (2,13).

The following are a few of the milestones recorded in the field of pump turbine development in Germany: In 1965, the first large-scale pump turbine were commissioned to be built for the Roenkhausen Facility (see Fig. 1) by Swiss manufacturers (4,8,10). Another order came from the Vianden pumped

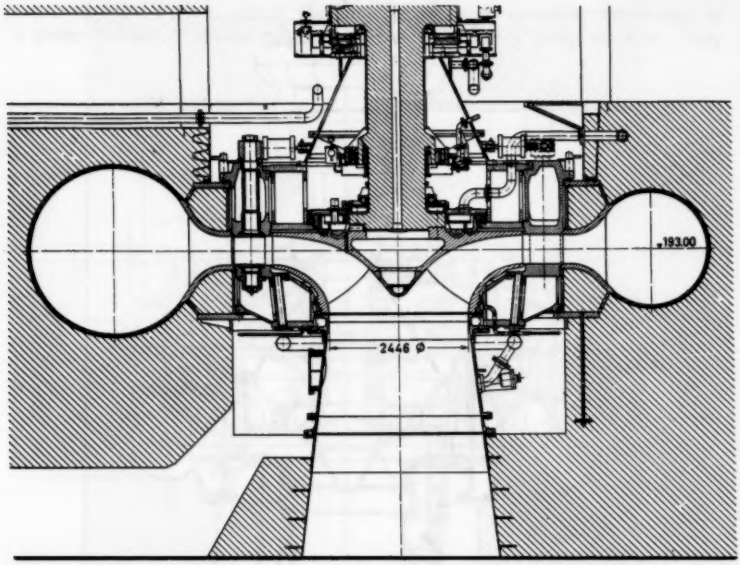

FIG. 2.—Binary Set Installed at Vianden 2 Pumped Storage Plant

storage plant in 1967 (already equipped with nine 100-MW ternary sets) for an additional 200-MW pump turbine Vianden 2 (see Fig. 2) (24,28). The guide vanes on this set are operated by individual servomotors, and the motor generator set is also capable of speeding up the water-filled turbine into pumping action from the stationary phase with closed valve. In 1971, two 75-MW pump turbines were purchased for the Langenprozelten Facility (see Fig. 3), a power station serving to generate single-phase traction power. For the purpose of speeding up the pump turbine into pumping action, provision is made in this case for a 27-MW Francis turbine designed on simple lines to function as a starting turbine (5,26). In 1974, the 250-MW Rodund 2 pump turbine (see Fig. 4) (6) was ordered from Germany to complement existing ternary sets in service at

the Austrian Luenersee and Rodund 1 pumped storage plants. The head in this case amounts to 1,140 ft (350 m).

Quite a number of papers have already been written on the subject of pump turbines of which only a brief selection can be cited here (1,2,3,5,7,9,11,12,23,25–28). Normally such treatises are concerned with the distinguishing features of a certain plant. This being the case, there appears to be some necessity of

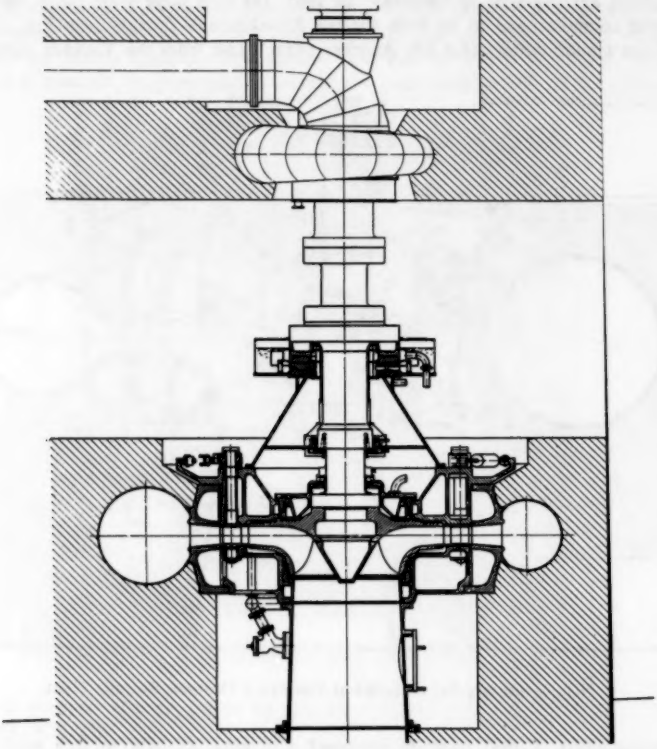

FIG. 3.—Binary Set Installed at Langenprozelten Pumped Storage Plant

approaching the subject of pump turbine design from a more general theoretical angle based on practical results.

The principal objective of this paper is to draw attention to a decisive factor, namely that of the costs arising from excavation work and mechanical losses occurring during the period of operation.

The key to the optimum design of the impeller (the actual centerpiece of a pump turbine) is a new process applied to computing the type number of

a semi-axial pump turbine. The type number is functionally related to the empirical loss coefficients (aerodynamics also being drawn upon for purposes of analogy), cavitation factors, operating characteristics, such as flow rate and head, as well as known geometrical dimensions of the impeller and diffuser. Also capable of computation are data applicable to speed coefficient and discharge ratio dependent on speed ratio. These figures provide useful information for compromises that may be necessary with regard to the needs of the electric power grid, taking into account the specific features of the hydraulic storage cycle.

Optimum Outside Diameter of Impeller on Pump Turbines in Terms of Efficiency

Let us begin by considering the impeller losses. In principle, the design of a pump turbine is always required to proceed from a pump impeller. Only

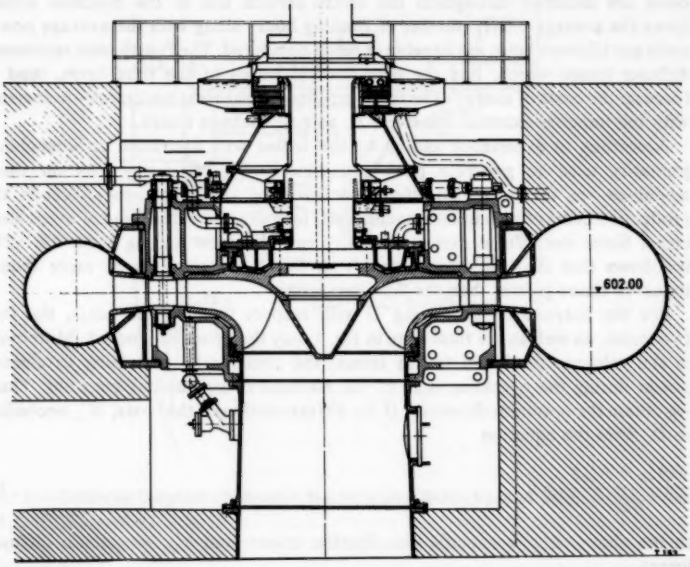

FIG. 4.—Binary Set Installed at Rodund 2 Pumped Storage Plant

a pump impeller which, owing to the backward bent vanes, reveals nonstalling relative flow and thus too, high efficiency, η_p, when pumping, is capable of functioning as a turbine achieving quite a satisfactory degree of efficiency, η_T, even in the case of reversed flow. Generally speaking, η_T is, in fact, greater than η_p. Bearing in mind the growing shortage of power, there is a need to increase the η_p in the process of pumping, also as a basis for stepping up the η_T as applied to the turbine action.

The resulting costs, K_r, of a centrifugal pump (or pump turbine) can be

approximated in the following way as a function of the impeller outside diameter, D:

$$K_r = k_1 \cdot D^m + k_2 \cdot D^3 + k_3 \cdot D^{23/5} + k_4 \cdot D^{-2} + k_5 \quad \ldots\ldots\ldots\ldots\ldots\ldots (1)$$

The first term of Eq. 1, having $m = 2.2 \ldots 2.4$, indicates the costs of manufacture composed of processing costs (proportional D^2) and material costs (proportional D^3). The second term combines the building and excavation costs for a large semi-axial machine having an extensive head and negative suction head. For example, on the pump turbines newly installed at the Austrian Kuehtai Facility, which registers a head of 1,460 ft (450 m), the suction head is at −144 ft (−48 m). This being the case, it was essential to locate the power station in a pit having a depth of some 330 ft (100 m). The third term is used to indicate disc friction losses occurring to the outer surfaces of the shrouds of the impeller. These losses necessitate an increase in power consumption so that additional costs are incurred throughout the entire service life of the machine which, given the average yearly number of running hours along with the average power costs per kilowatt hour, are capable of being computed. The fourth term represents diffuser losses which, like the disc friction losses of the third term, tend to force up the costs of energy. The final term describes losses not directly associated with the impeller external diameter, D, as e.g., leakage losses.

According to experience gained by the writer with hydraulic turbomachines primarily used to generate peak-load power, 1% efficiency loss on these machines—in terms of the life expectancy of the machines—exceeds the production costs of a complete machine set, including its percentage of excavation costs. Since centrifugal pumps normally reveal losses ranging from 8%–12%, it follows that the last three terms from Eq. 1 are going to be more than 8 times–12 times greater than the first two terms.

For the purpose of optimizing D with respect to minimum costs, the first two terms, as well as the final term in Eq. 1 may therefore be ignored. Moreover, in the relevant third and fourth terms, the cost factor pertaining to electric power during the operating time of the machine is assumed as constant. Thus, we obtain the optimum diameter, D, by differentiation of the costs, K_r, according to D, from the equation

$$\frac{d(h'_{vR} + h'_{vD})}{dD} = 0 \quad \ldots\ldots\ldots\ldots\ldots\ldots\ldots\ldots\ldots\ldots (2)$$

In the above, h'_{vR} = specific disc friction losses; and h'_{vD} = specific diffuser losses.

On the basis of test results using rotary discs (16,20), and applying the designations contained in Fig. 5, the specific disc friction losses, h'_{vR} are computed as follows from the geometrical dimensions and operating data:

$$h'_{vR} = 0.256 \cdot 10^{-2} \cdot \nu^{1/5} \cdot \left[1 + 1.4\left(\frac{f}{D} - 0.01\right)\right]$$

$$\cdot \left(1 + 5\frac{\Delta b}{D}\right) \cdot \omega^{14/5} \cdot \frac{D^{23/5}}{(gHQ)} \quad \ldots\ldots\ldots\ldots\ldots\ldots\ldots\ldots (3)$$

in which ν = kinematic viscosity of the fluid; f = average clearance between

the impeller shrouds and housing; Δb = resulting wall thickness of both shrouds at the outside diameter; ω = angular velocity; g = gravity acceleration; H = head; and Q = flow rate in the design point.

The following applies to specific diffuser losses, h'_{vD}, based on the assumption of nonswirl impeller influx and employing the designations contained in Fig. 5

$$h'_{vD} = \left(\frac{D_2}{D_3}\right)^2 \left(\frac{2gH}{\eta_u \omega^2}\right)\left(\frac{\zeta_D}{\cos^2 \alpha_3}\right) \cdot D^{-2} \quad \ldots\ldots\ldots\ldots\ldots\ldots (4)$$

In the above, $D_2 = D$ = outside diameter of the impeller; D_3 = inlet diameter of the vaned diffuser; ζ_D = diffuser loss factor; α_3 = angle between the diffuser vane skeleton structure and periphery at the diffuser inlet; and η_u = peripheral efficiency, including flow losses inside the diffuser, impeller, and suction pipe.

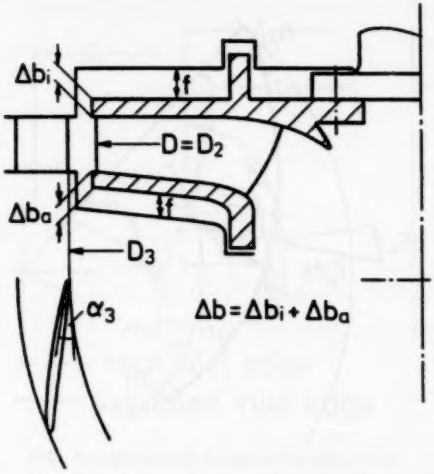

FIG. 5.—Sectional Diagram of Impeller, Housing, and Guide Vanes Applying Quantities Δb, f, D_2/D_3, and α_3

The following introduces further the nondimensional type number, n_q

$$n_q = \frac{\omega \cdot Q^{1/2}}{(gH)^{3/4}} \quad \ldots\ldots\ldots\ldots\ldots\ldots\ldots\ldots\ldots\ldots\ldots\ldots\ldots\ldots (5)$$

By expressing the angular velocity, ω, in Eqs. 3 and 4 by n_q, according to Eq. 5, and afterwards carrying out the differentiation according to Eq. 2, employing values h'_{vR} and h'_{vD} from Eqs. 3 and 4, we arrive at the following relationship applicable to the optimum outside impeller diameter, D_{op}:

$$d = D_{op} = \frac{C \cdot Q^{17/33}}{[\nu (gH)^8]^{1/33}} \quad \ldots\ldots\ldots\ldots\ldots\ldots\ldots\ldots\ldots\ldots\ldots\ldots\ldots (6)$$

In the above, C represents a nondimensional parameter which in turn, is dependent on nondimensional operating data and geometrical relationships:

$$C = \left\{ \frac{340 \cdot \dfrac{\zeta_D}{\eta_u^2 \cdot \cos^2 \alpha_3} \left(\dfrac{D_2}{D_3}\right)^2}{\left[1 + 1.4\left(\dfrac{f}{D} - 0.01\right)\right]\left(1 + 5\dfrac{\Delta b}{D}\right)} \right\}^{5/33} \cdot n_q^{-8/11} \quad \ldots\ldots\ldots\ldots (7)$$

It should be noted that f/D, $\Delta b/D$, and D_2/D_3 are given quantities, even if they contain $D = D_2$. The same applies to ζ_D, η_u, and α_3, these likewise being given.

From Eqs. 6 and 7, it will be observed that D_{op} is largely dependent on the type number, n_q, which is defined in Eq. 5.

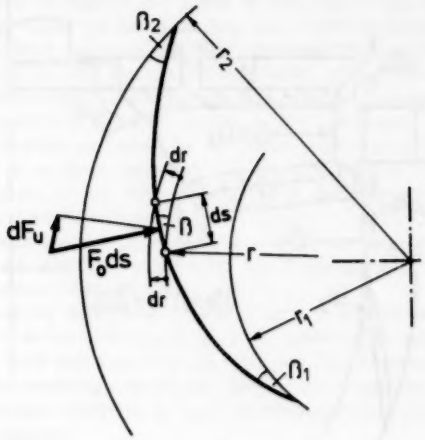

FIG. 6.—Simplified Layout of Impeller and One Vane

The type number itself, n_q, is likewise capable of being optimized as a function of geometrical data, loss, and cavitation coefficients. This is described in greater detail in the following section.

New Formula for Type Number of Semi-Axial Centrifugal Pump Impeller

Optimum Diameter of Impeller Eye in Respect to Internal Losses

Impeller Losses.—Further computation is based on the following assumptions (also compare to Fig. 6):

$$c_{m1} = c_{m2} = c_m \quad \ldots\ldots\ldots\ldots (8)$$

$$w_1 = w_2 = w \quad \ldots\ldots\ldots\ldots (9)$$

$$\beta_1 = \beta_2 = \beta \quad \ldots\ldots\ldots\ldots (10)$$

$$c_{u1} = 0 \quad \ldots\ldots\ldots\ldots\ldots\ldots\ldots\ldots\ldots\ldots\ldots\ldots\ldots\ldots\ldots\ldots\ldots\ldots \quad (11)$$

In the above, c = absolute speed; w = relative speed; β = angle between relative speed and circumference; c_u = circumferential component of c; and c_m = meridian component of c. The subscript 1 indicates the impeller inlet and the subscript 2 indicates the impeller outlet. All quantities are mean values ascertained between both the rim and the crown, and the vane pressure and the suction sides. The vanes are assumed to be perpendicularly arranged on the impeller shrouds.

The loss of output inside the impeller passage is computed from $P_r = w \cdot F_r$, in which F_r = resistance force inside the impeller passage parallel to w.

Along the vanes, a constant force per unit of length, F_o, is intended to act perpendicularly to the vane unit, as outlined in Fig. 6. The circumferential component of this force, which acts upon a vane unit of radial extension, dr,

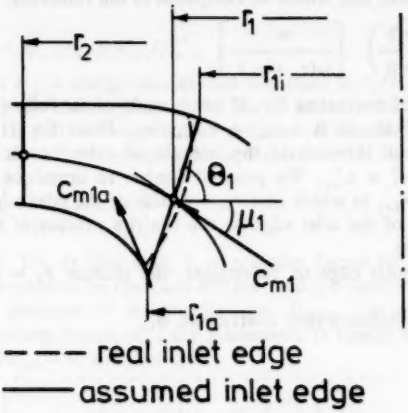

FIG. 7.—Actual and Assumed Impeller Inlet

is computed from $dF_u = F_o \cdot dr/\cos \mu$ and μ represents the mean angle between a mean meridian flow line and the radius. Thus, we obtain the peripheral input necessary for the propulsion of an impeller vane with angular velocity, ω:

$$P_u = \omega \int_1^2 r dF_u = \left(\frac{\omega}{2}\right)\left(\frac{F_o}{\cos \mu}\right)(r_2^2 - r_1^2) \quad \ldots\ldots\ldots\ldots\ldots\ldots\ldots \quad (12)$$

In the above, r = radius; r_2 = mean radius at the impeller outlet; and r_1 = mean radius at the impeller inlet.

Owing to the constancy of β, according to Eq. 10, the following applies approximately to the resulting force, F, perpendicular to the impeller vane: $F = F_o \cdot L \approx F_o \cdot (r_2 - r_1)/(\cos \mu \cdot \sin \beta)$. The value L signifies the mean vane length.

The resistance force, F_r, inside the vane passage can be split up into the component F_{rv}, originating from the opposite vane surfaces, and the component

F_{rsh}, from the shroud surfaces. Variables F_{rv} and F_{rsh} should be related to each other in proportion to their respective wetted surfaces. Afterwards, it is possible to represent F_r in the form $F_r = F_{rv} + F_{rsh} = \Omega \cdot F_{rv}$, in which Ω, with constant β (Eq. 10), is determined approximately

$$\Omega = 1 + \pi \sin\beta \frac{(r_1 + r_2)}{(z b_M)} \quad \ldots\ldots\ldots\ldots\ldots\ldots\ldots\ldots\ldots\ldots \quad (13)$$

In which, z = number of vanes; and b_M = mean width of the impeller passage. If, on the analogy of the airfoil wing theory, we were to introduce a gliding angle, ϵ

$$\epsilon = \frac{F_{rv}}{F} \quad \ldots\ldots\ldots\ldots\ldots\ldots\ldots\ldots\ldots\ldots\ldots\ldots\ldots\ldots \quad (14)$$

the specific impeller loss would be computed to the following:

$$h'_{vL} = \frac{P_r}{P_u} = \left(\frac{2\epsilon\Omega}{\sin\beta}\right) \cdot \left[\frac{w}{\omega(r_1 + r_2)}\right] \quad \ldots\ldots\ldots\ldots\ldots\ldots \quad (15)$$

For the purpose of converting Eq. 15 use is made of the following relationships. Observing Eqs. 8–10, $\sin\beta = c_m/w = c_{m1}/w_1$. From Eq. 11—by application of the Pythagorean theorem to the triangle of velocities at the inlet—there results $w_1^2 = \omega^2 r_1^2 + c_{m1}^2$. We proceed further to introduce the "hub to tip ratio" $N_1 = r_{1i}/r_{1a}$, in which case r_{1i} = radius of the inlet edge on the crown; and r_{1a} = radius of the inlet edge on the rim (i.e., radius of the impeller eye; compare to Fig. 7).

Assuming the inlet edge to be straight, the relation $r_1 = (r_{1a}/2)(1 + N_1)$ will apply.

In addition, we define a flow coefficient, ϕ_{1a}

$$\phi_{1a} = \frac{c_{m1a}}{(\omega r_{1a})} \quad \ldots\ldots\ldots\ldots\ldots\ldots\ldots\ldots\ldots\ldots\ldots\ldots\ldots\ldots \quad (16)$$

in which c_{m1a} = meridian velocity at the inlet edge on the rim. Thus, the specific impeller loss, h'_{vL}, can, following conversion of Eq. 15, eventually be represented as follows:

$$h'_{vL} = \epsilon\Omega \left(\frac{\omega r_{1a}}{c_{m1}}\right) \frac{\left[(1 + N_1)^2 + 4 \cdot \left(\frac{c_{m1}}{c_{m1a}}\right)^2 \phi_{1a}^2\right]}{\left[(1 + N_1)\left(1 + \frac{r_2}{r_1}\right)\right]} \quad \ldots\ldots\ldots\ldots \quad (17)$$

Diffuser Losses.—Observing Eq. 8, and $c_{m3} = (D_2/D_3)\, c_{m2}$, the specific diffuser loss, h'_{vD}, is computed as follows:

$$h'_{vD} = \left(\frac{\zeta_D}{\sin^2\alpha_3}\right) \cdot \left[\frac{c_{m1}^2}{(2gH)}\right] \cdot \left(\frac{D_2}{D_3}\right)^2 \quad \ldots\ldots\ldots\ldots\ldots\ldots \quad (18)$$

In the above, all characters have the same meaning as in Eq. 4.

Optimum Diameter of Impeller Eye in Respect to Internal Losses.—The variable

c_{m1} can be quoted (assisted by the continuity equation) as a function of the diameter of the impeller eye, D_{1a}. If a straight inlet edge is assumed in accordance with Fig. 7, along with c_{m1} being the mean meridian speed within the inlet area, then the continuity equation applicable to the impeller inlet will read

$$c_{m1} = \left(\frac{4}{\pi}\right)\left[\frac{(Q\cos\Theta_1)}{(1-N_1^2)\sin(\mu_1+\Theta_1)}\right] D_{1a}^{-2} \quad \ldots\ldots\ldots\ldots\ldots\ldots \quad (19)$$

In the above, Q = flow rate in the design point; Θ_1 = mean angle between the radius and the axial vane section within the area of the inlet edge; and μ_1 = angle between the radius and a mean meridian flow line at the inlet.

If we now proceed to insert c_{m1} from Eq. 19 into Eqs. 17 and 18, and also substitute r_{1a} in Eq. 17 by the expression $D_{1a}/2$, we shall, by adding Eqs. 17 and 18, obtain the resulting impeller and diffuser loss, h'_{vr}, as a function of the diameter of the impeller eye, D_{1a}. The variable h'_{vr} can be represented in the form:

$$h'_{vr} = h'_{vL} + h'_{vD} = K_1 \cdot D_{1a}^3 + K_2 \cdot D_{1a}^{-4} \quad \ldots\ldots\ldots\ldots\ldots\ldots\ldots\ldots \quad (20)$$

in which K_1 and K_2 = design-conditioned constants if r_2/r_1, N_1, c_{m1}/c_{m1a}, D_2/D_3, and ϕ_{1a} are assumed as given. As is known, the flow coefficient, ϕ_{1a}, defined in Eq. 16, is computed as a matter of convenience for reasons pertaining to cavitation, according to the equation:

$$\phi_{1a} = \tan\beta_{1a} = \left[\frac{\lambda}{2(1+\lambda+\zeta)}\right]^{1/2} \quad \ldots\ldots\ldots\ldots\ldots\ldots\ldots \quad (21)$$

(compare to Ref. 16). In this case, λ = pressure factor for the critical point with respect to cavitation on the vane surface, and ζ = suction pipe loss factor.

The optimum diameter of the impeller eye, $D_{1aop\eta}$, as regards efficiency, at which the resulting losses, h'_{vr}, are minimized, is finally obtained from the condition $dh'_{vr}/dD_{1a} = 0$, as follows:

$$D_{1aop\eta} + 1.156 \left\{\frac{\left(1+\frac{r_2}{r_1}\right)(1+N_1)\left(\frac{D_2}{D_3}\right)^2 \cdot \zeta_D}{\sin^2\alpha_3\left[(1+N_1)^2 + 4\cdot\left(\frac{c_{m1}}{c_{m1a}}\right)^2 \cdot \phi_{1a}^2\right] \epsilon\omega\Omega g H}\right\}^{1/7}$$

$$\cdot \left[\frac{Q\cos\Theta_1}{(1-N_1^2)\sin(\mu_1+\Theta_1)}\right]^{3/7} \quad \ldots\ldots\ldots\ldots\ldots\ldots\ldots \quad (22)$$

Optimum Diameter of Impeller Eye with Regard to Cavitation

The normal negative suction head, h_s, is computed to $h_s = B' - \text{NPSH}$, in which B' = barometric pressure head minus the critical pressure head; and NPSH = net positive suction head of the pump. In order to minimize excavation costs, i.e., the amount of h_s, the NPSH must be minimized. Proceeding from nonswirl influx (see Eq. 11), the following relationship applies to the NPSH, according to Ref. 17:

$$2g\cdot\text{NPSH} = \lambda u_{1a} + (1+\zeta+\lambda)\, c_{m1a}^2 \quad \ldots\ldots\ldots\ldots\ldots\ldots\ldots \quad (23)$$

In the above, $u_{1a} = \omega \cdot D_{1a}/2$. By means of this, the NPSH is obtained—after introducing c_{m1} from Eq. 19 into Eq. 23—(the relationship c_{m1}/c_{m1a} being given) as a function of the impeller inlet diameter, D_{1a}. The NPSH may be represented in the following form:

$$2g \cdot \text{NPSH} = K_3 \cdot D_{1a}^2 + K_4 \cdot D_{1a}^{-4} \quad \ldots \ldots \ldots \ldots \ldots \ldots \ldots \quad (24)$$

in which K_3 and K_4 = design-conditioned constants.

The optimum diameter of the impeller eye with regard to cavitation, $D_{1aop\text{NPSH}}$, at which the NPSH and thus, the excavation costs are also minimized, is then computed from the condition $d\text{NPSH}/d\,D_{1a} = 0$, to the following:

$$D_{1aop\text{NPSH}} = 2\left[\frac{2(1+\lambda+\zeta)}{\lambda}\right]^{1/6} \cdot \left[\frac{Q\cos\Theta_1 \cdot \left(\dfrac{c_{m1a}}{c_{m1}}\right)}{\omega\pi\,(1-N_1^2)\sin(\mu_1+\Theta_1)}\right]^{1/3} \quad \ldots \quad (25)$$

Optimum Type Number with Regard to Efficiency and Cavitation

By equating the diameters obtained from Eqs. 22 and 25, $D_{1aop\eta} = D_{1aop\text{NPSH}}$, we obtain the "natural optimum," $n_{qop\eta\text{NPSH}}$, of the type number, n_q, defined in Eq. 5. The variable $n_{qop\eta\text{NPSH}}$ is a function of the pump geometry (expressed by quantities Ω, r_2/r_1, Θ_1, μ_1, N_1, α_3), the velocity relation c_{m1}/c_{m1a}, loss factors (such as ζ_D, ϵ) and cavitation-conditioned quantities (such as λ, ζ, ϕ_{1a}):

$$n_{qop\eta\text{NPSH}} = 2.4 \left\{\frac{\sin^2\alpha_3\left[(1+N_1)^2 + 4\cdot\left(\dfrac{c_{m1}}{c_{m1a}}\right)^2\phi_{1a}^2\right]\epsilon\Omega}{\left(1+\dfrac{r_2}{r_1}\right)(1+N_1)\left(\dfrac{D_2}{D_3}\right)^2\zeta_D}\right\}^{3/4}$$

$$\cdot\left[\frac{(1-N_1^2)\sin(\mu_1+\Theta_1)}{\cos\Theta_1}\right]^{1/2} \cdot \left[2\left(1+\frac{1+\zeta}{\lambda}\right)\left(\frac{c_{m1a}}{c_{m1}}\right)^2\right]^{7/8} \quad \ldots \ldots \quad (26)$$

For the purpose of optimizing the impeller outside diameter in accordance with Eqs. 6 and 7, this optimum-type number is required to be introduced into the formula applicable to C (see Eq. 7).

An impeller designed on these lines represents a distinct optimum with regard to efficiency and costs of excavation.

Discharge Ratio as Function of Speed Ratio

Applying the customary speed coefficient

$$ku_2 = \frac{\omega r_2}{\sqrt{2gH}} \quad \ldots \ldots \ldots \ldots \ldots \ldots \ldots \ldots \ldots \ldots \quad (27)$$

(compare to Ref. 16), we proceed to defining the speed ratio thus:

$$\kappa = \frac{ku_{2p}}{ku_{2T}} \quad \ldots \ldots \ldots \ldots \ldots \ldots \ldots \ldots \ldots \ldots \quad (28)$$

In the above, ku_{2p} = speed coefficient applied to the process of pumping; and ku_{2T} = speed coefficient pertaining to turbining.

The discharge ratio must also be defined

$$q = \frac{Q_p}{Q_T} = \frac{\Phi_{2p} \cdot c_{m2p}}{\Phi_{2T} \cdot c_{m2T}} = \frac{\Phi_{2p} \cdot \phi_{2p}}{\Phi_{2T} \cdot \phi_{2T}} \cdot \kappa \cdot \chi \quad \ldots\ldots\ldots\ldots\ldots\ldots\ldots\ldots \quad (29)$$

In the above, Q = flow rate (discharge); Φ_2 = contraction factor at the pressure edge; c_{m2} = meridian speed at that point; $\phi_2 = c_{m2}/u_2$, in which $u_2 = \omega \cdot r_2$ = peripheral speed at the impeller outside diameter; and $\chi = H_p/H_T$ = head ratio. Index p denotes the pumping process; and T refers to the turbining operation.

From the triangles of velocities at the pressure edge (subscript 2), it is possible to read off the following relationships applicable to the meridian speeds, c_{m2p}

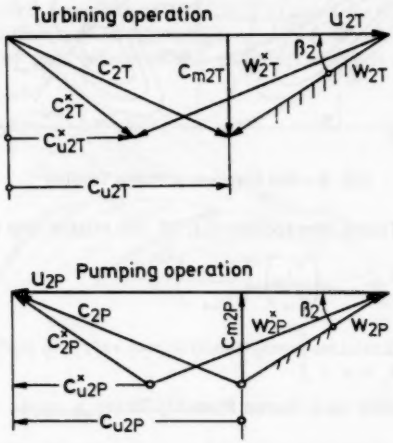

FIG. 8.—Impeller Outlet Triangle during Pumping Operation (P) and Inlet Triangle during Turbining Operation (T)

(pumping process) and c_{m2T} (turbining process), in accordance with Fig. 8:

$$c_{m2p} = [u_{2p} - (1 + p_p^*)\, c_{u2p}^*] \tan \beta_2 \quad \ldots\ldots\ldots\ldots\ldots\ldots\ldots\ldots \quad (30)$$

$$c_{m2T} = [u_{2T} - (1 + p_T^*)\, c_{u2T}^*] \tan \beta_2 \quad \ldots\ldots\ldots\ldots\ldots\ldots\ldots\ldots \quad (31)$$

In the above, β_2 = vane angle at the pressure edge; p^* = slip factor at that point; and c_{u2}^* = peripheral component of the absolute speed at the pressure edge (variable p/T = pumping/turbining process).

By means of this data, in conjunction with Euler's fundamental equation governing turbomachinery ($c_{u1} = 0$ applying in accordance with Eq. 11), it is possible to quote the discharge ratio, q, as a function of the speed ratio, κ, as follows:

$$q = \frac{\Phi_{2p}}{\Phi_{2T}} \cdot \kappa \cdot \chi^{1/2} \frac{\left[1 - \dfrac{(1 + p_p^*)}{(2ku_{2p}^2 \eta_{up})}\right]}{\left[1 - \dfrac{(1 + p_T^*)\kappa^2 \eta_{uT}}{(2ku_{2p}^2)}\right]} \quad \ldots\ldots\ldots\ldots\ldots\ldots\ldots\ldots (32)$$

In the above, η_u = peripheral efficiency (hydraulic efficiency) in the turbining (subscript T) and pumping (subscript p) state. The variable ku_{2p} may be computed from the known relationship between the type number, n_q, and the speed

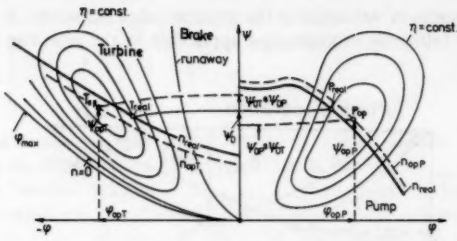

FIG. 9.—Hill Diagram of Pump Turbine

coefficient, ku_{2p}. Taking into account Eq. 19, this relationship reads as follows:

$$ku_{2p} = \pi^{-1/3} \cdot 2^{-1/2} \cdot \phi_{1a}^{-1/3} \cdot \left(\frac{r_2}{r_{1a}}\right) \cdot \left(\frac{c_{m1a}}{c_{m1}}\right)^{1/3} \cdot \left[\frac{\cos \Theta_1}{(1 - N_1^2) \sin (\Theta_1 + \mu_1)}\right]^{1/3} \cdot n_q^{2/3} \quad \ldots\ldots\ldots\ldots\ldots\ldots\ldots\ldots (33)$$

The optimum value for n_q is known from Eq. 26 ($n_{qop\eta NPSH}$).

Example for Computing Optimum Values of Impeller Diameter, Type Number, and Discharge Ratio as Compared with Corresponding Quantities of Actual Pump Turbine

As an example, let us study a pump turbine with the following data:

1. Impeller Geometry: $r_2/r_{1a} = 1.69$; $N_1 = 0.6$; $f/D = 0.01$; $\Delta b/D = 0.02$; $\beta_2 = 27°$; $\alpha_3 = 20°$; number of vanes $z = 7$; $D_2/D_3 = 0.94$; $b_M/(r_1 + r_2) = 0.2$; $\Theta_1 = 60°$; and $\mu_1 = 70°$. Thus, from Eq. 13, $\Omega = 2.019$ is obtained. Assuming the inlet edge to be straight, $r_2/r_1 = 2(r_2/r_{1a})/(1 + N_1) = 2.113$ will apply.

2. Operational-Conditioned Characteristic Quantities: $\eta_{up} = 0.92$; $\eta_{uT} = 0.96$; $\zeta_D = 0.19$; $\epsilon = 0.01$; $\zeta = 0.05$; $\lambda = 0.25$; $\Phi_{2p} = 0.9$; $\Phi_{2T} = 1.0$; $p_p^* = 0.2$; $p_T^* = 0.2$; $\nu = 14 \cdot 10^{-6}$ sq ft/sec; $(1.3 \cdot 10^{-6}$ m^2/s); and $c_{m1a}/c_{m1} = 1.2$.

3. Main Operating Data of Pump Turbine: $H_p = 1{,}130$ ft (346 m); $H_T = 1{,}100$ ft (336 m); $Q_p = 2{,}400$ cu ft/sec (67.2 m^3/s); $Q_T = 3{,}210$ cu ft/sec (90 m^3/s); and $\chi = H_p/H_T = 1.030$.

The data listed in "impeller geometry" and "main operating data of pump turbine" agree with those on the Austrian Rodund 2 pump turbine as far as the latter were available on simple lines. This pump turbine has a rotational speed of $n = 375$ rpm in both modes of operation, the outside diameter of the impeller measuring $D = 14.26$ ft (4.35 m).

Results.—By means of these figures, we obtain $\phi_{1a} = 0.310$ from Eq. 21, and thus the vane angle of the inlet edge on the rim $\beta_{1a} = \arctan \phi_{1a} = 17.2°$.

From Eq. 26, we obtain $n_{qop\eta NPSH} = 0.728$; thus from Eq. 7, $C = 2.365$; from Eq. 6, $D_{op} = 14.23$ ft (4.34 m). From Eq. 33, we obtain $ku_{2P} = 1.044$. The variables D_{op}, $n_{qop\eta NPSH}$, and ku_{2p} agree well with the actual values of the Rodund 2 pump turbine, which amount to $D = 14.26$ ft (4.35 m); $n_q = 0.724$; and $ku_{2p} = 1.037$.

From Eq. 17, we compute $h'_{vL} = 0.044$, and from Eq. 18, $h'_{vD} = 0.036$. These values require a peripheral efficiency $\eta_{up} = 1 - h'_{vL} - h'_{vR} = 0.92$, which agrees with the assumed $\eta_{up} = 0.92$.

The actual speed ratio in accordance with Eq. 28 reads $\kappa = 0.985$. Thus,

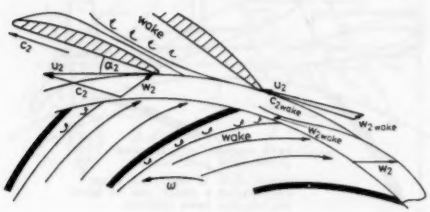

FIG. 10.—Effect of Wakes Behind Runner Vanes on Inlet Zone of Gate

from Eq. 32, we obtain $q = 0.738$, which agrees well with the actual value, $q = 0.747$.

Special Operational Features of Pump Turbines

Compromises Resulting from Hill Diagram and Practical Requirements.—Outlined in Fig. 9 is the so-called hill diagram (the curves with identical efficiency appear to be contours of a hill) plotted for a pump turbine in both modes of operation in the Ψ-ϕ plane. The variable Ψ indicates the pressure coefficient, $\Psi = 2gH/(\omega_o r_2)^2$; and ϕ, indicates the flow coefficient, $\phi = c_{m2}/(\omega_o r_2) = Q/(A_2 \omega_o r_2)$. [The value ω_o = angular velocity (design point); and A_2 = cross-sectional area at the impeller pressure edge.]

Evidently applicable to the optimum points in pumping and turbining modes of operation, according to Fig. 10, are the relationships

$$\Psi_{opP} < \Psi_{opT} \quad \ldots \quad (34)$$

$$\phi_{opP} < \phi_{opT} \quad \ldots \quad (35)$$

i.e., the optimum point of the turbine zone is located further away from the

origin of coordinates than the optimum point of the pump zone. Compared with the pump zone, the turbine section in the Ψ-ϕ diagram is more closely limited by the runaway parabola (where torque is zero) and the parabola of maximum discharge (this is the envelope of the curves with identical torque or identical rotational speed). From Fig. 9 it will be gathered that the curves of constant machine speed, n, cross through the efficiency hills over a greater length in the turbine zone than in the pump zone. This means a deviation from the optimum point, maintaining constant rotational speed, when pumping involves a greater drop in efficiency than when turbining.

In addition, by deviating from the optimum point when pumping, maintaining constant rotational speed, the machine lands in an operating zone in which it is highly sensitive to cavitation. This would necessitate increasing the negative suction head.

On a facility purely designed as a pumped storage plant, the pressure coefficient, Ψ_o, belonging to the average level difference between the head and tailrace level, is normally the same in the pumping and turbining modes of operation.

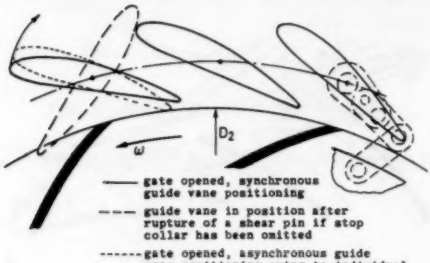
D2
ω
gate opened, synchronous guide vane positioning
guide vane in position after rupture of a shear pin if stop collar has been omitted
gate opened, asynchronous guide vane positioning owing to individual servomotors

FIG. 11.—Different Positions of Guide Vanes

If, as is usually the case, provision is made for the same adapted rotational speed, n_{real}, for both modes of operation, then the aforementioned circumstance calls for two courses of action to be taken (compare to Fig. 9): (1) It is necessary for selection of the constant rotational speed, n_{real}, to be lower in the pumping mode and higher in the turbining mode than the applicable optimum speed; and (2) owing to the same pressure coefficient, $\Psi_o = \Psi_{oT} = \Psi_{oP}$, in both modes of operation, the actual turbine operation point, T_{real}, must be transferred into the partial-load region (compare to Fig. 9), where efficiency is lower, and swirl occurs inside the suction pipe. This is mainly necessary in order to warrant optimum conditions as regards cavitation when pumping.

From Fig. 9 it will also be noted that, even in the case of a two-speed motor generator set (rarely used), which permits optimum rotational speeds n_{opP}/n_{opT} in both modes of operation, both optimum points, P_{op} and T_{op}, are not attained if the level difference (and thus too, the pressure coefficient, Ψ_o) is the same in pumping and turbining modes of service.

The discharge ratio, q, must (aside from the hydraulic optimum value) be determined with due consideration to the average duration of the base- and

peak-load period in the course of a working cycle. Furthermore, attention is required to be paid to balancing the water quantities in the turbining and pumping modes of operation, also taking into account the processes of inflow and outflow during the storage cycle.

Maximum turbine efficiency is attained only at the commencement of turbining in the storage cycle, owing to the presence of the maximum level difference and thus too, the highest pressure coefficient, Ψ (compare to Fig. 9). Maximum output will then be yielded.

Sources of Trouble and Remedies

Normal Pumping.—In the course of pumping, wakes occur on the impeller outlet (compare to Fig. 10). This produces a periodically highly-varying angle of attack, the guide vanes (functioning here as diffuser vanes) are flowed against.

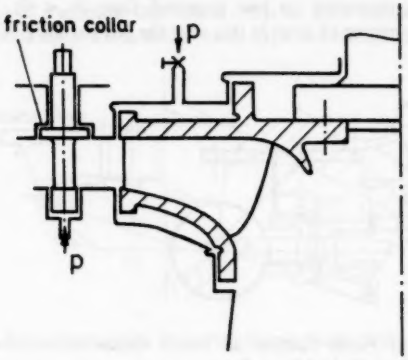

FIG. 12.—Friction Collar for Guide Vanes; Double-Sealed Impeller Crown, Acted Upon by Compressed Water

If a wake passes a guide vane, then the unfavorable angle of attack generates a stall at the rear of the vane (compare to Fig. 10).

As a result of this, the vane channel is temporarily blocked. At the same time, a torque, subject to periodic change, acts upon the guide vane in the opening direction.

If this causes rupture to a safety member (provision for which is usually made on gates actuated using a central servomotor), then the guide vane may strike against the adjacent vane (as depicted in Fig. 11), with its end projecting into the impeller. This causes destruction to the vane ends and possibly to the coupling bolts as well.

Such damage can be prevented by arranging for each of the guide vanes to be actuated by an individual servomotor, these motors being subjected to synchronous control.

The individual servomotor must provide a torque sufficient to drive a vane even in case the vane is temporarily in an asynchronous position (29).

In the course of pumping, care should be taken not to displace the gate. It will be best to block the guide vanes. If, e.g., the upper vane pin is provided with a friction collar (compare to Fig. 12), this collar can be pressed against the housing (by pressure applied to the front side of the lower vane pin) so as to block the vane.

Employing short upper vane pins (corresponding to Fig. 13), whose means of drive is immerged into the head cover, it is possible to prevent dangerous torsional vibrations from level, pins and vane (compare to Ref. 23).

Abnormal Operating Conditions.—The transitional operating conditions specified in the following and capable of occurring following load rejection while turbining or failure of the pump drive, might possibly involve extremely-varying forces and momenta acting on the guide vanes and thus too, heavy vibrations of the machine shaft and cover (compare to Refs. 2 and 10).

1. Slight opening of gate when pumping at full rotational speed.
2. Pump brake operation on low reversed flow ($\phi < 0$), lower rotational speed, and slight opening of gate; in this case the jet, partially deflected outwards

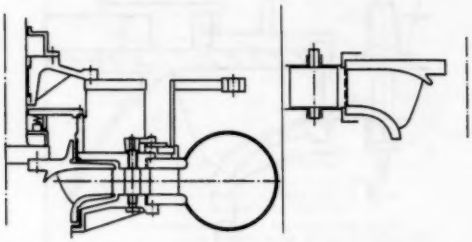

FIG. 13.—Section of Pump Turbine on Which Guide Vane Drive Mechanism is Immerged into Hollow, Ribbed Head Cover

by the runner vanes, exercises a fluctuating closing moment on the guide vanes (see Fig. 14).

3. Centripetal turbine operation with extensive reversed flow ($\phi < 0$), and reversed (negative) sense of rotation.
4. Runaway of turbine, ($\phi < 0$); when accelerating a radial machine up to the point of runaway, the flow will be throttled owing to centrifugal forces, this causing water hammer. The runaway, whose operating point on the Ψ-ϕ diagram (Fig. 9) is located on the runaway parabola, $\Psi_{ra} = \text{const.} \cdot \phi^2_{ra}$, is a dangerous condition owing to a high rotational speed being present without normal speed control.

While occurrence of the operating conditions described under 1–4 of the preceding may be "stationary" in a case of emergency, the following two conditions occur only temporarily in the transitional process.

1. Turbine brake operation above the runaway speed with reversed flow ($\phi < 0$); this zone, located on the Ψ-ϕ diagram (Fig. 9) between the runaway

parabola and ordinate, is passed through when the flow rate is reduced due to closure of the gate, while the speed is almost equal owing to the inertia of the rotating parts.

2. Reversed pumping ($\phi > 0$), with reversed (negative) sense of rotation; this condition occurs, proceeding from the turbining process, when water hammer is caused due to closure of the gate, and the rotational speed decreases only slowly, owing to inertia. Fig. 15 indicates, e.g., the water hammer characteristics in the event of the load being switched off at a point of time, t, in the turbining mode of operation and the gate continuing to close. Registered in Fig. 15 are the conditions at the upper and lower end of the pressure pipe (O_{t+nT_L} or U_{t+nT_L}), as well as on the pump turbine (T_{t+nT_L}, Br_{t+nT_L}, P_{rt+nT_L}), this being done at the times indicated in the index $t + nT_L$ ($n = 0, 1, 2 \ldots$). The variable $T_L = L/a$ = transit time of the pressure waves in the pipeline (L = pipe length between O and U; a = sonic speed).

Commencement of Pumping Operation.—Up to 80% of the full load input is required to speed up a water-filled radial type centrifugal pump with closed valve.

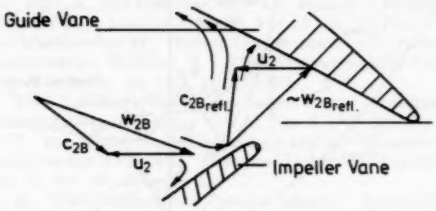

FIG. 14.—Flow Phenomena Occurring during Pump Brake Operation

Thus, speeding up into pumping action on the pump turbine presents a problem. The technical challenge and objective in this case is to attain as short a start-up time as possible, employing the smallest auxiliary set possible. To arrive at this solution numerous methods have already been devised, a few of which are mentioned in the following.

The pump turbine can be accelerated by the main motor generator set directly, provided that this is capable of functioning as an asynchronous motor. Owing, however, to the low permissible motor temperature (80° C), this necessitates the use of short-circuited full iron pole pieces as, e.g., at the Vianden 2 Facility (compare to Ref. 10).

On radial pump turbines with extensive head, the required start-up power has, in most cases, so far been reduced by filling the impeller with air. However, this solution extends the start-up time and transfers the ensuing problems to the subsequent filling process.

During the process of filling, the turbulent, vortex-affected two-phase mixture with its compressible air pockets may stimulate dangerous machine-shaft vibrations with frequencies below the synchronous rotational speed. These vibrations may be influenced by the design of the impeller seals, as well as by the virtual

mass of fluid linked with the vibrating impeller. Such problems need to be carefully examined with regard to each individual machine and solved by applying model tests.

Carrying out the process of filling from the suction pipe may, for one thing, force up the impeller temporarily besides causing some inlet shock to occur.

The upward-force effect can be prevented if (as at the Taum Sauk Facility) compressed water is briefly allowed to act on the double-sealed crown in accordance with Fig. 9, thus pressing the impeller downwards (compare to Ref. 14).

The inlet shock can be avoided if, by means of a jet, a simulated vortex is briefly produced in the draft tube mouth. No inlet shock occurs when filling from the gate owing to the speed coefficient normally incorporating the value $ku_2 = 1$.

Usually, both methods of filling are combined. The air pockets in the center of the suction pipe and at the top of the spiral housing must at all events be removed carefully and quickly since these may produce shaft vibration, as well as cause the drive power to fluctuate.

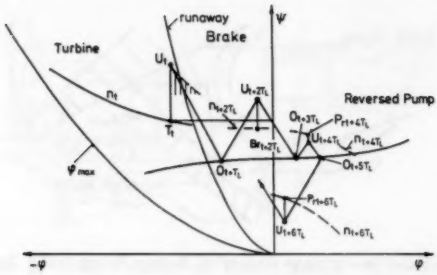

FIG. 15.—Water Hammer Characteristics

As a means of preventing faults from occurring, the following recommendations should be observed: Gates, cover, bearings, and shaft should be constructed as solid, stiff designs. Opening of the air-exhaust valves and gate must proceed in accordance with appropriate principles of timing. The vent valve must be arranged to correspond to the purpose it is to fulfill. Appropriately-designed damping type labyrinth seals are required to be provided at the impeller shrouds, as successfully applied in Europe.

Conclusions

The design of a pump turbine is required to be based on an impeller outside diameter that minimizes losses resulting from disc friction and the diffuser in the course of pumping. This diameter can be computed as a function of the given head, flow rate, and type number.

A new process applied to computing the type number contributes, in addition, to reducing internal losses and costs of excavation to a minimum. The optimum

type number is functionally related to geometrical data as well as to loss and cavitation coefficients.

The computed results are in quite close keeping with values encountered in actual practice on a modern pump turbine.

In addition, the design of pump turbines must take into account specific features related to the operation of the set.

Appendix I.—References

1. Abraham, K. H., "Construction Progress at the Waldeck II Plant," *Water Power*, London, England, Vol. 25, No. 12, Dec., 1973, pp. 464–466.
2. Boussuges, P., Megnint, L., and Amblard, H., "Turbines Pompes de Hautes Chutes," *La Houille Blanche*, Paris, France, Vol. 32, No. 7/8, 1977, pp. 647–655.
3. Casacci, S., et al., "Contribution a l'Etude des Vibrations des Organes de Vannage des Turbines-Pompes," *La Houille Blanche*, Paris, France, Vol. 32, No. 7/8, 1977, pp. 629–645.
4. Gersdorff, V. B., and Lottes, G., "Das Pumpspeicherwerk Roenkhausen," *Elektrizitätswirtschaft*, Frankfurt am Main, West Germany, Vol. 66, No. 24, 1967, pp. 725–734.
5. Gruener, J., "Das Pumpspeicherwerk Langenprozelten. Maschinen, Elektrische Einrichtungen und Stahlwasserbau," *Elektrizitätswirtschaft*, Frankfurt am Main, West Germany, Vol. 74, No. 24, 1975, pp. 868–877.
6. Innerhofer, G., Eder, A., and Gstettner, R., "The Rodund II Pumped Storage Scheme in Austria," *Water Power*, London, England, Vol. 25, No. 11, Nov., 1973, pp. 413–427.
7. Jaeger, H., and Muehloecker, H., "Entwurf und Bemessung der Hauptmaschinensaetze des Pumpspeicherwerkes Waldeck II," *Elektrizitätswirtschaft*, Frankfurt am Main, West Germany, Vol. 7, No. 24, 1971, pp. 685–691.
8. Kraft, W., "Das Krafthaus des Pumpspeicherwerkes Roenkhausen," *Siemens-Zeitschrift*, Erlangen, West Germany, Vol. 42, No. 6, 1968, pp. 475–486.
9. Landsberger, R., and Doelz, H., "Die Kraftwerksgruppe Edersee; Die Entwicklung des Pumpspeicherwerkes Waldeck II," *Energiewirtschaftliche Tagesfragen*, Essen, West Germany, Vol. 22, No. 10, 1972, pp. 515–525.
10. Meier, W., et al., "Pumpturbinen und Speicherpumpen," *Special Publication*, Escher Wyss Mitteilung, Zürich, Switzerland, 1971.
11. Meyer, J., *Kraft aus Wasser*, Staempfli und Cie AG, Bern, Switzerland, 1975, pp. 97–98.
12. Pfisterer, E., "Die Hornbergstufe der Schluchsee AG," *Wasserwirtschaft*, Stuttgart, Germany, Vol. 63, No. 1, 1973, pp. 12–21.
13. Plichon, J., et al., "Le Probleme des Pompes-Turbines vu par le Maitre d'Oeuvre," *La Houille Blanche*, Paris, France, Vol. 32, No. 7/8, 1977, pp. 575–582.
14. Raabe, J., "Studienreise Wasserkraft durch USA und Mexico," *Energie*, Muenchen, Germany, Vol. 17, No. 7, 1965, pp. 277–285.
15. Raabe, J., "Wasserkraftmaschinen, Jahresuebersicht," *Brennstoff-Waerme-Kraft*, Duesseldorf, West Germany, Vol. 18, No. 4, 1966, pp. 183–188.
16. Raabe, J., *Hydraulische Maschinen und Anlagen: Vol. 1, Grundlagen der Hydraulischen Stroemungsmaschinen*, VDI-Verlag, Duesseldorf, West Germany, 1968, pp. 37, 132–137.
17. Raabe, J., *Hydraulische Maschinen und Anlagen: Vol. 2, Wasserturbinen*, VDI-Verlag, Duesseldorf, West Germany, 1969, pp. 21–112.
18. Raabe, J., *Hydraulische Maschinen und Anlagen: Vol. 3, Pumpen*, VDI-Verlag, Duesseldorf, West Germany, 1970, pp. 88–104.
19. Raabe, J., *Hydraulische Maschinen und Anlagen: Vol. 4, Wasserkraftanlagen*, VDI-Verlag, Duesseldorf, West Germany, 1970, pp. 1–7, 89–111.
20. Raabe, J., *Gidravliceskyje Mashinyje i Ustanovskyi*, Energia, Moskva, Russia, 1974, (translation of Refs. 16–19 into Russian).
21. Raabe, J., "Hydraulic Turbines," *Special Lectures*, Indian Institute of Technology, Madras, India, Jan., 1975.
22. Raabe, J., "Maquinas Hidraulicas," Departamento de Engenharia Mecanica de Escola Politecnica da Universidade de Sao Paulo, Brasil, Aug., 1975, 3 Vols., (in English).
23. Raabe, J., "Chairman's Survey about Session Flow Effect on Structures," *Proceedings*

of the Joint Symposium on Design and Operation, ASCE, ASME, IAHR, Vol. 3, 1978, pp. 161–163.
24. Voith, J. M., "Pumpspeicherwerke," *Special Publication,* Voith, Heidenheim, West Germany.
25. Voith, J. M., "Storage Pumps and Spherical Valves in the Saeckingen Pumped Storage Plant," *Special Issue,* Voith, Heidenheim, West Germany.
26. Voith, J. M., "Probebetrieb Langenprozelten Maschine 2 Beendet," *Voith Information,* Geschaeftsbereich Wasserturbinen und Pumpen, No. 3, 1974.
27. Voith, J. M., "Francisturbine Waldeck II, Erfolgreiche Inbetriebsetzung," *Voith Information,* Geschaeftsbereich Wasserturbinen und Pumpen, No. 3, 1974.
28. Wehinkel, L., "Der Endausbau des Pumpspeicherwerkes Vianden," *Special Publication,* Rheinisch Westfaelische Elektrizitaetswerke, Essen, West Germany, 1965.
29. Grein, H., and Bachmann, P., "Hydraulic Torque on Misaligned Guide Vanes," *Water Power and Dam Construction,* London, England, Vol. 28, No. 2, Feb., 1976, pp. 37–40.

Appendix II.—Notation

The following symbols are used in this paper:

a = sonic speed;
b = width of impeller;
c = absolute speed;
D = outside diameter, diameter;
F = force;
g = gravity acceleration;
H = head;
h' = specific loss;
K = cost;
ku = speed coefficient;
N_1 = D_{1i}/D_{1a}, "hub/tip ratio";
n = rotational speed;
n_q = type number;
P = power;
p^* = slip factor;
Q = flow rate;
q = discharge ratio;
r = radius;
u = peripheral speed;
w = relative speed;
z = number of vanes;
α = gate vane angle;
β = impeller vane angle;
ϵ = gliding angle;
ζ = suction pipe loss number;
ζ_D = diffuser loss number;
η = efficiency;
η_u = hydraulic (peripheral) efficiency;
Θ = angle of axial vane section with radius;
κ = ku_{2P}/ku_{2T} = speed ratio;
λ = pressure number of critical point with respect to cavitation;

μ = angle of meridional speed with radius;
ν = kinematic viscosity;
ρ = density of fluid;
Φ = contraction number;
ϕ = flow coefficient = $c_m/(r\omega)$;
χ = H_P/H_T = head ratio;
Ψ = head coefficient = $2gH/(r_2\omega_o)^2$;
Ω = factor defined in Eq. 13; and
ω = angular speed.

Subscripts

a = belonging to rim;
D = diffuser;
i = belonging to hub (crown);
L = impeller;
M = mean;
m = meridional;
op = optimum;
P = pumping operation;
R = disc friction;
r = resistance, resulting;
sh = shrouds;
T = turbining operation;
u = peripheral;
v = vane;
1 = impeller inlet;
2 = impeller outlet;
3 = diffuser inlet; and
η = with respect to efficiency.

River Thermal Standards Costs in the Upper Midwest

By Thomas E. Croley II,[1] M. ASCE, Arthur R. Giaquinta,[2] and Robert A. Woodhouse[3]

Introduction

Electrical energy demand in the United States may more than double before the year 2000 (14). To meet this increasing energy requirement, power plants of large capacity presently are being planned or installed by many utilities. Table 1 summarizes existing and proposed power capacities along the Missouri and Upper Mississippi Rivers in the Mid-Continent Area Power Pool (MAPP) geographical area. Waste heat rejection from the generating units is achieved by the transfer of heat to the atmosphere by means of a cooling tower, spray canal, cooling pond, river, or other large body of water.

Once-through cooling has the lowest water consumption of any evaporative cooling system (although water use is greatest, virtually all is returned to the river). A summary of water consumptions of different cooling systems is given by the Environmental Protection Agency (6). However, the use of cooling water in a once-through mode from the Missouri and Mississippi Rivers has come under sharp scrutiny in recent years because of possible environmental ramifications. All states through which the rivers pass have adopted river temperature standards, which are enforced by Federal and state agencies. The U.S. Environmental Protection Agency has mandated that thermal discharges into natural rivers from power plants placed into service after January 1, 1970 (or 1974 depending on the size of the plant) will not be permitted after July 1, 1983 (6).

For existing plants, stringent standards sometimes require operation of the plant at a derated output level to maintain river temperatures within the allowable

[1]Assoc. Prof. and Research Engr., Dept. of Civ. Engrg., Iowa Inst. of Hydr. Research, Univ. of Iowa, Iowa City, Iowa 52242.

[2]Adj. Asst. Prof. and Research Engr., Dept. of Mech. Engrg., Iowa Inst. of Hydr. Research, Univ. of Iowa, Iowa City, Iowa 52242.

[3]Water Research Engr., Bechtel, Inc., San Francisco, Calif.

Note.—Discussion open until Oct. 1, 1981. To extend the closing date one month, a written request must be filed with the Manager of Technical and Professional Publications, ASCE. Manuscript was submitted for review for possible publication on May 13, 1980. This paper is part of the Journal of the Energy Division, Proceedings of the American Society of Civil Engineers, ©ASCE, Vol. 107, No. EY1, May, 1981. ISSN 0190-8294/81/0001-0065/$01.00.

limit. Thus, energy penalties and power production costs increase. If backfitting of a power plant with a closed-cycle cooling system is required to avoid this problem, the power plant will operate at less efficient energy conversion rates, and fuel and water consumption will increase. For proposed power plants (those which the utilities have committed to construction as well as those future plants which have been sited) similar comments can be made except outfitting economics (as opposed to backfitting economics) apply and planned capacity may be affected. For once-through cooling systems, fuel consumption and cooling-related power-generation costs are heavily dependent upon the thermal standards, since standards limit the amount of heat discharged to the river, increasing energy and efficiency penalties.

Studies of power-plant cooling systems (4,7) and investigations of the cooling potential of the Missouri and Mississippi Rivers (8,13,15) have revealed large water consumptions for cooling and large expenses borne by utilities in meeting river temperature standards at selected locations. These increases in water consumption and power-plant cooling costs are, of course, passed on to the consumer and are borne by society, both directly and indirectly. The importance

TABLE 1.—Existing and Proposed Total Plant Capacities along Missouri and Upper Mississippi Rivers, in megawatts

River and type of cooling (1)	Existing (1977)		Proposed (Through 1987)	
	Fossil (2)	Nuclear (3)	Fossil (4)	Nuclear (5)
Mississippi:				
Once-through	2,902	50	500	0
Wet cooling tower	1,770	1,692	2,750	1,100
Spray canal	0	1,600	0	0
Missouri:				
Once-through	2,453	1,311	2,321	0
Wet cooling tower	0	0	0	0

of the conservation of water, energy, and capital makes it clear that environmental thermal standards must be considered carefully. It is now evident in many areas that existing river temperature standards may over-protect environmental concerns at the expense of added water losses and energy usage. There exists a need then for the adjustment of these standards to effect society's desired balance between environmental protection and cooling-related energy-production impacts.

The purpose of this study is to evaluate the marginal (incremental) changes in cooling-related water consumption (evaporative water loss) and power-plant cooling expenses which result from unit changes in river temperature standards along the Upper Mississippi and Missouri Rivers in the MAPP geographical area. All existing and proposed (through 1987) plants located along the river reaches are assumed to be in operation. A number of hypothetical river thermal standards are considered including the extreme cases of free discharge (no thermal standards) and no discharge. The costs of existing and more restrictive thermal standards are assessed by computing the marginal increases in expense and

water consumption over the free-discharge case. Less restrictive standards also are examined for their probable impact in the MAPP region.

Background

Related regional studies were made by Giusti and Meyer (11) and Hu, et al. (12). Of course, specific site trade-offs involving thermal standards have little meaning since environmental impacts are created by (and affect) all power-plant cooling along the entire river, and standards cannot be set on a site-to-site basis, although variations are often allowed when downstream environmental impacts are demonstrated to be minimal.

Research efforts which supplied useful inputs to the present study include several projects at the Iowa Institute of Hydraulic Research (IIHR) in the areas of thermal regimes of the Mississippi and Missouri Rivers (8,13): (1) Optimization of dry-wet cooling towers (1,4,5); (2) economics of back-fitting power plants with closed-cycle cooling systems (3,7); and (3) a study of optimum mechanical-draft wet cooling towers to supplement once-through cooling at selected Missouri River sites (9).

The computational scheme to assess the cost of thermal standards required the use of models previously developed at IIHR. The Iowa Thermal Regime Model (ITRM) examines the steady-state thermal regime along the study reaches of the Missouri and Mississippi Rivers. A modified version of the model is used to locate regions where the river temperatures exceed allowable limits for any prescribed set of thermal standards, and to assess river evaporation for heat loadings consequent with those thermal standards.

The second model, referred to as the Backfitting Model, evaluates cooling-related costs of backfitting existing power plants (identified by the ITRM as requiring auxiliary cooling for a set of thermal standards) with mechanical-draft wet cooling towers. The third model, referred to as the Outfitting Model, computes cooling-related costs of outfitting proposed power plants (identified by the ITRM as requiring auxiliary cooling for a set of thermal standards) with combined once-through and wet tower cooling systems.

Iowa Thermal Regime Model (ITRM).—The steady-state ITRM presented by Paily, et al. (13), was used to determine the temperature profiles corresponding to average flow and weather conditions along the Mississippi and Missouri Rivers in the MAPP geographical area. The model is based on a numerical solution of the one-dimensional convection-diffusion equation which predicts the longitudinal distribution of the cross-sectional average temperature along a river. The total river reach of interest is divided into a convenient number of subreaches. Each subreach is further divided into a finite-difference grid defined by a number of meshpoints, and temperature distributions are computed for each subreach separately. The solutions for adjacent subreaches are linked by the common conditions at the junction joints connecting them. Each subreach of the river can have multiple thermal inputs and tributary inflows. The formulation allows for changes in the channel characteristics, river flow rate, and weather data along the river. The model is one-dimensional and assumes complete mixing of the heated effluent with the river. This definition of river temperature does not necessarily conform to state and Federal regulations which sometimes specify mixing zone limitations. A modified version of the thermal regime model was

used to compute the heat assimilation capacity (product of allowable temperature rise and river flow rate) at various locations along the river corresponding to various flow conditions. The modifications involved redefining the ranges of validity of the evaporation equations used in the model as detailed elsewhere (10). Evaporation rates are computed for the "natural" case in which no man-made heat sources are considered and for cases where thermal effluents from existing and proposed power plants are included. Net evaporation rates due to the presence of the heat loads are computed by subtracting the natural evaporation rate from the evaporation rate with thermal discharges. The model does not include sublimation from ice and assumes zero evaporation when water temperatures drop below freezing.

Outfitting and Backfitting Models.—The economics of power-plant cooling is dependent mainly on the turbine-condenser subsystem characteristics and on the size and type of cooling system. Two basic types of turbines are considered to be representative in outfitting and backfitting and their characteristics are given elsewhere (7). One turbine type is a high-pressure back-end loaded unit of contemporary design, while the other is a low-pressure back-end loaded unit representing some of the older plants. Cooling characteristics curves may be determined for any specified size and type of turbine-cooling system by using an appropriate model. The size of a once-through cooling system is primarily determined by the design condenser flow rate and by the design condenser temperature rise. The cooling characteristics curve is determined by the size of the system and by the actual heat-assimilation capacity of the stream. For mechanical-draft wet cooling towers, the size of the cooling system is specified by the dimensions of the tower and the design meteorological conditions chosen at the site. The cooling characteristics may then be determined from the basic thermodynamic models described by the first writer, et al. (5). Condenser sizing, capacity loss, fuel consumption, makeup water, energy loss, and other quantities may be obtained from operation points on the cooling characteristic curves corresponding to applicable meterological and stream conditions.

Power-plant cooling costs are composed of capital costs which include the costs of cooling system structures, condensers, pump and pipe systems, and replacement capacity, and operating costs which consist of the costs of fuel, makeup water, water treatment, maintenance, and replacement energy. These costs are determined from unit costs provided by MAPP (10) and from cost relations described by the first writer, et al. (2). The total annual cost is computed by adding the operating cost to the product of the capital cost and the "fixed-charge rate." The fixed-charge rate reflects the annual cost of raising the required capital and includes such factors as interest on debt, required return on the stockholders' equity, depreciation of equipment, property and income tax rates, etc.

Additional factors to consider in the economic assessment of backfitting an existing unit are: (1) The cost of installing the cooling tower, including materials, labor, site acquisition, and site preparation; (2) the plant downtime for system changeover; (3) the provision of additional generating capacity to replace the power consumed by the cooling system; and (4) the additional cost of power generation due to limitations imposed by the use of a closed-cycle system. The first three of these quantities are capital costs and the last is an operating cost incurred over the remaining lifetime of the plant. Procedures for their

determination are contained in Refs. 3 and 7. Once these costs have been fixed, the total cost may be computed by using the fixed-charge-rate method.

Application

There are 20 existing power plants, with a total of 48 units which utilize the Mississippi River for once-through cooling in the MAPP area. In addition, there are two proposed power plants, each with one unit, and five additional units at existing power plants for which the cooling system type has been specified. Along the Missouri River in the MAPP region, 10 power plants with a total of 24 units utilize the river for once-through cooling. The locations and cooling system details of existing and proposed power plants are given in Ref. 10. Besides power plants, other industries and municipalities located along the river impose additional thermal loads on the rivers. The industrial and municipal effluents are small compared to those of power plants and generally are not

TABLE 2.—Unit Costs, in 1977 Dollars[a]

Description (1)	Cost (2)
Wet towers (mechanical-draft)	\$21/tower-unit
Condenser	\$12/sq ft of surface area
Replacement capacity	\$400/kW
Land	\$5,000/acre
Makeup water	\$1.8/1000 gal
Water treatment	\$0.15/1000 gal
Fuel:	
Nuclear	\$0.001/kWh
Fossil	\$0.004/kWh
Maintenance of wet towers (mechanical draft)	\$300/yr/cell
Replacement energy	\$0.02/kWh

[a]Assumed to be spatially uniform in the region of study.
Note: 1 sq ft = 0.093 m^2; 1 acre = 4,047 m^2; 1 gal = 0.00378 m^3.

large enough to produce any significant effect on the temperature profiles or evaporation rates so they are not included in the present study.

The necessary unit costs required in the outfitting and backfitting economic determinations were provided by MAPP. They are listed in Table 2 in terms of 1977 dollars and are valid only for the MAPP region. All power plants are assumed to operate at an 80% capacity factor. Power plant costs are approximated herein by multiplying operating cost components of the full-throttle costs by 0.8 before computing the equivalent annual cost with the fixed-charge-rate method. Fixed-charge rates of 17.90% and 14.75% were used in the economic analysis of existing and proposed power plants, respectively (6). All existing power plants are assumed to have a remaining life of 20 yr and proposed power plants are assumed to have an operation horizon of 35 yr.

The flow chart shown in Fig. 1 outlines the computational procedures used to compute cooling-related costs of power production and water consumption

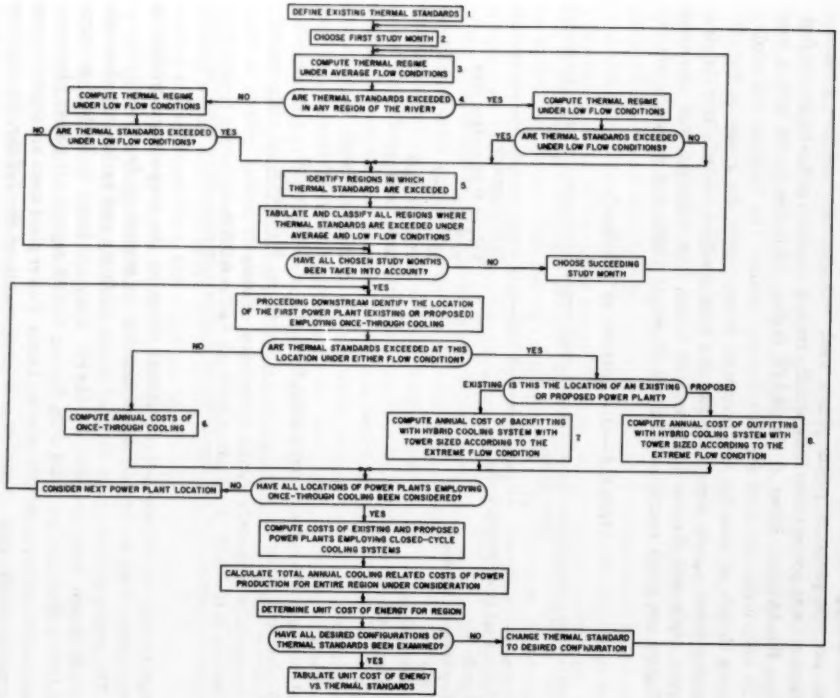
DEFINE EXISTING THERMAL STANDARDS 1
CHOOSE FIRST STUDY MONTH 2
COMPUTE THERMAL REGIME UNDER AVERAGE FLOW CONDITIONS 3
ARE THERMAL STANDARDS EXCEEDED IN ANY REGION OF THE RIVER? 4
NO
YES
COMPUTE THERMAL REGIME UNDER LOW FLOW CONDITIONS
ARE THERMAL STANDARDS EXCEEDED UNDER LOW FLOW CONDITIONS?
NO
YES
COMPUTE THERMAL REGIME UNDER LOW FLOW CONDITIONS
ARE THERMAL STANDARDS EXCEEDED UNDER LOW FLOW CONDITIONS?
YES
NO
IDENTIFY REGIONS IN WHICH THERMAL STANDARDS ARE EXCEEDED 5
TABULATE AND CLASSIFY ALL REGIONS WHERE THERMAL STANDARDS ARE EXCEEDED UNDER AVERAGE AND LOW FLOW CONDITIONS
HAVE ALL CHOSEN STUDY MONTHS BEEN TAKEN INTO ACCOUNT?
NO
CHOOSE SUCCEEDING STUDY MONTH
YES
PROCEEDING DOWNSTREAM IDENTIFY THE LOCATION OF THE FIRST POWER PLANT (EXISTING OR PROPOSED) EMPLOYING ONCE-THROUGH COOLING
ARE THERMAL STANDARDS EXCEEDED AT THIS LOCATION UNDER EITHER FLOW CONDITION?
NO
YES
EXISTING
IS THIS THE LOCATION OF AN EXISTING OR PROPOSED POWER PLANT?
PROPOSED
COMPUTE ANNUAL COSTS OF ONCE-THROUGH COOLING 6
COMPUTE ANNUAL COST OF BACKFITTING WITH HYBRID COOLING SYSTEM WITH TOWER SIZED ACCORDING TO THE EXTREME FLOW CONDITION 7
COMPUTE ANNUAL COST OF OUTFITTING WITH HYBRID COOLING SYSTEM WITH TOWER SIZED ACCORDING TO THE EXTREME FLOW CONDITION 8
CONSIDER NEXT POWER PLANT LOCATION
NO
HAVE ALL LOCATIONS OF POWER PLANTS EMPLOYING ONCE-THROUGH COOLING BEEN CONSIDERED?
YES
COMPUTE COSTS OF EXISTING AND PROPOSED POWER PLANTS EMPLOYING CLOSED-CYCLE COOLING SYSTEMS
CALCULATE TOTAL ANNUAL COOLING RELATED COSTS OF POWER PRODUCTION FOR ENTIRE REGION UNDER CONSIDERATION
DETERMINE UNIT COST OF ENERGY FOR REGION
HAVE ALL DESIRED CONFIGURATIONS OF THERMAL STANDARDS BEEN EXAMINED?
NO
CHANGE THERMAL STANDARD TO DESIRED CONFIGURATION
YES
TABULATE UNIT COST OF ENERGY VS THERMAL STANDARDS

FIG. 1.—Computational Flow Chart

for changing thermal standards. Major steps in the flow chart are indexed to the following clarifying remarks.

1. Data on existing thermal standards along the Upper Mississippi and Missouri Rivers were obtained from publications of various state government agencies applicable to the MAPP region. The allowable temperature rise "above the natural" presented in these thermal standards is assumed to refer to the temperature excess above the "natural thermal regime" of the river (temperature distribution that would exist along the river if all man-made heat sources were absent).

2. The months of February, May, August, and November are assumed to represent the four seasons of the year and, thus, characterize the meteorologic and hydrologic conditions that prevail over the whole year.

3. The river temperature profile is calculated separately for thermal discharges from existing and existing plus proposed power plants. When unspecified, it was assumed that proposed power plants utilize once-through cooling and operate with overall efficiencies of 36% and 32%, in-plant heat losses of 15% and 5%, and a condenser temperature rise of 18° F (10° C) and 25° F (13.9° C) for fossil and nuclear plants, respectively, in accordance with past IIHR experience.

4. Cases in which thermal standards are exceeded are identified corresponding to the thermal regime computation using average flow conditions.

5. Regions where thermal standards are exceeded under low flow (7-day, 10-yr low flow conditions) or average flow conditions are identified. Note that thermal standards exceedance under average flow conditions does not necessarily indicate that thermal standards are exceeded during low flow conditions. Because of the different rates of temperature decay for the two flow conditions, cumulative upstream effects on river temperature differ.

6. Capital and operating costs of once-through cooling systems are based on the assumption that the unit is operating at low turbine back pressures.

7. All of the power plants considered in this study are, or will be, located along major rivers; therefore, hybrid cooling systems were adopted for those cases in which the river heat-assimilation capacities were found to be inadequate to assume the entire waste-heat load when the plant is operated in the once-through cooling mode. It is recognized that few, if any, hybrid cooling systems have been utilized to date. However, rapidly increasing fuel costs and the results of other recent studies suggest that hybrid cooling systems will become steadily more attractive. These systems enable one to utilize the available heat-assimilation capacity of the river, with the result that smaller cooling-tower systems are required. Moreover, during major parts of the year it may not be necessary to operate the towers at all, which can result in further significant savings of replacement energy and maintenance costs. Hybrid cooling systems consist of once-through and mechanical draft wet cooling tower combinations. Hybrid systems are designed to meet thermal regulations at the 7-day, 10-yr low flow conditions and are operated to provide the least cooling required to meet thermal regulations under average flow conditions. Hybrid cooling-system costs were calculated in the following manner: The capital costs were assumed to vary linearly between the costs incurred for once-through cooling and those for full closed-cycle cooling with the wet cooling towers. The hybrid cooling-system capital costs were then calculated from the following equation.

$$C_H = C_O + \frac{(C_W - C_O)(Q_R - Q_C)}{Q_R} \quad \ldots \ldots \ldots

TABLE 3.—Regional Cost Comparisons of Different Thermal Standards

Thermal standard (1)	Total Costs		Incremental "Cost" of Standard above Free-Discharge	
	Annual 10^6 dollars (2)	Mils per kilowatt-hour (3)	Annual 10^6 dollars (4)	Mils per kilowatt-hour (5)
	(*a*) Mississippi River			
Free discharge	754.8	8.71	—	—
Existing	908.7	10.49	153.9	1.78
2° F decrement	912.6	10.53	157.8	1.82
3° F decrement	918.8	10.60	164.0	1.89
4° F decrement	939.3	10.84	184.5	2.13
No discharge	1,003.0	11.58	248.2	2.87
	(*b*) Missouri River			
Free discharge	427.8	10.03	—	—
Existing	447.0	10.48	19.2	0.45
2° F decrement	464.0	10.88	36.2	0.85
3° F decrement	475.1	11.14	47.3	1.11
4° F decrement	511.9	12.00	84.1	1.97
No discharge	551.5	12.93	123.7	2.90

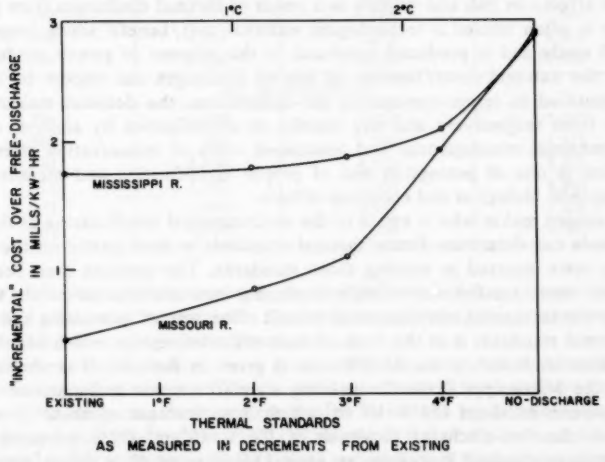

FIG. 2.—Incremental Cost Trade-Offs

a higher turbine back pressure and must also supply the required energy to run the fans and pumps of the cooling tower. These energy losses represent the amount of energy that must be purchased from other utilities. Energy losses were computed only for the existing and no-discharge cases. The amount of annual energy loss that occurs at the existing thermal standard for the power plants along the Mississippi River is 1.13×10^9 kWh or 129 MW. The total annual energy loss which would occur at the no-discharge thermal standard is 2.14×10^9 kWh or 244 MW. For power plants located along the Missouri River, there is no energy loss due to closed-cycle cooling at the existing standard because all of the existing plants use once-through cooling. The total annual energy loss which would occur at the no-discharge thermal standard is 1.04×10^9 kWh or 119 MW.

The increased evaporative water loss due to river temperature rise by thermal effluents in once-through cooling or due to heat transfer by evaporation in a wet cooling tower is also a cost that should be considered. A presentation of the details of evaporative water loss due to power generation along the aesthetics, etc. in comparison with benefits that can be measured in economic terms. Impacts of thermal discharges on streams can be measured in terms of temperature distributions, dissolved oxygen content, eutrophication, etc., and biological data can be used to determine tolerance levels for various species of fish. Combinations of these two data sources will result in cause-effect relationships whereby certain maximum temperatures or temperature increases can be related to the number of fish adversely affected. However, the value of preserving fish and wildlife cannot easily be quantified in dollar terms. As a result, the value of preserving the aquatic-life environment takes on a qualitative character in the determination of the costs and benefits of energy production.

The effects on fish and wildlife as a result of thermal discharges from power plants is often termed a technological external cost/benefit which cannot be priced easily and is produced incidental to the purpose of power production. Since the external costs/benefits of heated discharges can seldom be valued or quantified in terms appropriate for comparison, the decision maker must weigh them subjectively and rely heavily on identification by analysts of the environmental consequences and associated costs of conservation. Here the question is one of perception and of proper identification and measurement of long-term biological and economic effects.

A decision maker who is aware of the environmental ramifications of thermal standards can determine future thermal standards at least partly on the basis of the costs incurred in meeting those standards. The question then becomes not how much are fish and wildlife worth, but how much is the public willing to pay for increasing environmental benefit. One way of presenting the costs of thermal standards is in the form of trade-off relationships which Mississippi and Missouri Rivers in the MAPP area is given in Ref. 10. It is shown that along the Mississippi River the existing standards result in an annual water consumption of about 129×10^6 m^3 which is an increase of about 23×10^6 m^3 over the free-discharge condition of 106×10^6 m^3 (22% increase). The no-discharge standard represents an annual increase of 42×10^6 m^3 over the free-discharge condition (40% increase) and an annual increase of 19×10^6 m^3 over the existing thermal standard (15% increase). Water consumption for the 2° F (1.1° C), 3° F (1.7° C) and the 4° F (2.2° C) decrement standards is

not significantly larger than that for the existing standard since there is no substantial increase in the number of plants requiring backfitting with wet towers at these standards.

Since all power plants on the Missouri River use the once-through cooling mode at existing thermal standards, the annual water consumption of about 61×10^6 m^3 for the existing thermal standard is the same as that for the free-discharge standard. The no-discharge thermal standard represents an annual increase of about 6×10^6 m^3 over the existing or free-discharge condition (10% increase). There is no significant increase in water consumption at the 2° F (1.1° C) and 3° F (1.7° C) decrement thermal standards. However, at the 4° F (2.2° C) decrement standard, thermal exceedances occur under average

TABLE 4.—Permissible Plant Capacities—Fossil—at Different Standards, in megawatts

Location, river mile (1)	Existing (2)	2° F (1.1° C) increment (3)	4° F (2.2° C) increment (4)
	(*a*) Mississippi River		
1,150	337	481	625
1,113	356	504	654
1,076	396	562	684
1,039	457	647	757
1,001	514	729	908
964	541	768	1,037
700	3,407	4,532	6,800
599	3,372	5,201	7,500
500	4,984	7,252	9,552
399	5,928	8,592	11,302
	(*b*) Missouri River		
1,736	408	1,225	2,042
1,649	259	784	1,318
1,543	3,068	4,123	5,181
1,314	4,782	6,863	8,945
1,252	1,349	1,931	2,534
492	4,876	7,208	9,500

flow at a number of plants, causing them to adopt hybrid cooling systems thereby increasing total water consumption by about 1×10^6 m^3 (2% increase) because of the additional cooling tower operation.

To this point computations have been made for several thermal standards more restrictive than existing. (The free-discharge standard was considered merely as a basis for computing the incremental cost.) To address hypothetical standards more relaxed than existing, the 2° F (1.1° C) and 4° F (2.2° C) increment thermal standards, which represent a 2° F (1.1° C) and 4° F (2.2° C) increase above the existing allowable temperature rise are examined. Along the Mississippi River, the former standard would refer to an allowable temperature rise of 7° F (3.9° C) and the latter to a 9° F (5° C) allowable temperature rise. Since no exceedances

occur at the existing standards under average flow conditions and few occur at the low-flow conditions, no significant changes in costs may be expected at standards more relaxed than existing. It is evident, however, that there would be considerably more heat assimilation capacity in the river at the relaxed standards.

The real benefit of relaxed standards is, therefore, the ability to size larger future "permissible" plants at specified locations. However, for once-through-cooled plants there would be no substantial savings in cost in mills per kilowatt-hour as a result of greater installed capacity. Locations of permissible plants under investigation along the Mississippi River are the same as those identified previously by Paily, et al. (13). Permissible plant capacities (assuming 100% capacity factor) at these locations for the existing and the 2° F (1.1° C) and 4° F (2.2° C) increment thermal standards under average flow conditions are obtained through the sequential use of the ITRM. Existing and proposed power plants are assumed to operate at the 80% capacity factor. The computations are based on the assumption that the permissible plants are fossil units operating with an overall efficiency of 36% and in-plant losses of 15%. The permissible power plant capacities are listed in Table 4.

Concluding Remarks

Environmental objective functions are difficult to define due to the noncommensurable nature of the benefits derived from fish and wildlife preservation, depict the costs of meeting various thermal regulations.

Determining future thermal standards will be a difficult problem for decision makers. However, if the costs of providing different levels of environmental protection are considered along with a complete analysis of the benefits that would accompany different thermal criteria, the task of setting new regulations becomes a cost-benefit problem. The trade-off relations of this study can be used to assess the costs of maintaining the existing thermal standards or adopting more restrictive thermal standards.

Acknowledgments

This study was funded jointly by MAPP and the United States Department of the Interior, Office of Water Research and Technology under public law 88-379 as amended, made available through the Iowa State Water Resources Research Institute. The computer time was provided by the Graduate College of The University of Iowa. The cooperation of the MAPP-member utilities and the MAPP Coordination Center in providing power plant data, and the technical assistance of M. P. Cherian are gratefully acknowledged.

Appendix.—References

1. Cheng, M. S., Croley, T. E. II, and Patel, V. C., "Analysis of Different Types of Dry-Wet Cooling Towers," *IIHR Report No. 191*, Iowa Institute of Hydraulic Research, The University of Iowa, Iowa City, Iowa, 1976.
2. Croley, T. E. II, Giaquinta, A. R., Lee, R. M.-H., and Hsu, T. D., "Optimum Combinations of Cooling Alternatives for Steam-Electric Power Plants," *IIHR Report*

No. 212, Iowa Institute of Hydraulic Research, The University of Iowa, Iowa City, Iowa, 1978.

3. Croley, T. E. II, Giaquinta, A. R., and Patel, V. C., "Wet Cooling Tower Backfitting Economics," *Journal of the Power Division,* ASCE, Vol. 104, No. PO2, pp. 115–130, 1978.
4. Croley, T. E. II, Patel, V. C., and Cheng, M.-S., "Economics of Dry-Wet Cooling Towers," *Journal of the Power Division,* ASCE, Vol. 102, No. PO2, pp. 147–163, 1976.
5. Croley, T. E. II, Patel, V. C., and Cheng, M.-S., "Thermodynamic Models of Dry-Wet Cooling Towers," *Journal of the Power Division,* ASCE, Vol. 102, No. PO1, 1976, pp. 1–19.
6. "Development Document for Effluent Limitations and Guidelines and New Source Performance Standards for the Steam Electric Power Generating Point Source Category," United States Environmental Protection Agency, Washington, D.C., 1974.
7. Giaquinta, A. R., Croley, T. E. II, Patel, V. C., Melville, J. G., Cheng, M.-S., and Uzuner, A. S., "Economic Assessment of Backfitting Power Plants with Closed-Cycle Cooling Systems," *EPA Report No. EPA-600/2-76-050,* NTIS, Springfield, Va., 1976.
8. Giaquinta, A. R., and Keng, T. C. "Thermal Regimes of the Mississippi and Missouri Rivers Downstream from the Southern Iowa Border," *IIHR Report No. 211,* Iowa Institute of Hydraulic Research, The University of Iowa, Iowa City, Iowa, 1978.
9. Giaquinta, A. R., Croley, T. E. II, and Hsu, T. D., "Hybrid Cooling System Thermodynamics and Economics," *Journal of the Energy Division,* ASCE, Vol. 106, No. EY1, 1980, pp. 89–107.
10. Giaquinta, A. R., Woodhouse, R. A., and Cherian, M. P., "Utility-Borne Costs of Thermal Standards for the Mississippi and Missouri Rivers in the MAPP Geographical Area," *IIHR Report No. 223,* Iowa Institute of Hydraulic Research, The University of Iowa, Iowa City, Iowa, 1979.
11. Giusti, E. V., and Meyer, E. L., "Water Consumption by Nuclear Power Plants and Some Hydrological Implications," U.S. Department of the Interior, *Geological Survey Circular 745,* 1977.
12. Hu, M. C., Pavlenco, G. F., and Englesson, G. A., "Water Consumption and Costs for Various Steam Electric Power Plant Cooling Systems," EPA, Office of Research and Development, Research Triangle Park, N.C., 1978.
13. Paily, P. P., Su, T. Y., Giaquinta, A. R., and Kennedy, J. F., "The Thermal Regimes of the Upper Mississippi and Missouri Rivers," *IIHR Report No. 182,* Iowa Institute of Hydraulic Research, The University of Iowa, Iowa City, Iowa, 1976.
14. Searle, Milton, "Energy Supplies: A Look Ahead," *EPRI Journal,* Electric Power Research Institute, Palo Alto, Calif., 1978.
15. Su, T.-Y., "Thermal Regimes of Upper Mississippi and Missouri Rivers and Hybrid Once-Through-Wet Tower Cooling Systems for Power Plants," dissertation presented to the University of Iowa, at Iowa City, Iowa, in 1978, in partial fulfillment of the requirements for the degree of Doctor of Philosophy.

LOUVERED OFFSHORE INTAKE FOR DIVERTING FISH

By Yusuf G. Mussalli,[1] M. ASCE, Edward P. Taft,[2] Johannes Larsen,[3] and J. M. Toennies[4]

INTRODUCTION

The impingement of fish at cooling-water intakes has become a major concern in power-plant operation due to the potential impact which fish losses may have on the fisheries resources of an area. As a result, extensive research is being directed toward developing methods for diverting or collecting fish within takes or preventing their passage into intake structures.

For offshore intake structures connected to an onshore screenwell by tunnels or pipelines, efforts have been concentrated on the guidance or collection of entrapped fish within the screenwell. Another possible solution could be to initially prevent the presence of fish in the screenwell area by diverting them to a bypass within the offshore intake.

This paper examines investigation of wide-spaced louvers designed to divert fish within an offshore intake to bypass which lead to a submerged jet pump for discharge at a remote location. The studies described in this paper were conducted for Niagara Mohawk Power Corporation in an effort to develop a system for bypassing fish within the offshore intake structure of the proposed Nine Mile Point Nuclear Station—Unit 2 to be constructed on Lake Ontario.

REVIEW OF LITERATURE

A limited amount of research has been conducted on the design of offshore submerged intake structures for the prevention of fish entrapment. A small number of studies have been conducted to determine whether modifications to the conventional velocity cap intake might lower the number of adult and juvenile fish entrained in offshore intakes. Schuler and Larson (2) found that by extending the cap out from the vertical intake shaft, more uniform approach

[1]Consultant, Hydr. Div., Stone & Webster Engrg. Corp., P.O. Box 2325, Boston, Mass. 02107.

[2]Sr. Ecologist, Environmental Engrg. Div., Stone & Webster Engrg. Corp., P.O. Box 2325, Boston, Mass. 02107.

[3]Lead Engr., Alden Research Labs., Worcester Polytechnic Inst., Holden, Mass.

[4]Dir., Environmental Affairs, Niagara Mohawk Power Corp., Syracuse, N.Y.

Note.—Discussion open until October 1, 1981. To extend the closing date one month, a written request must be filed with the Manager of Technical and Professional Publications, ASCE. Manuscript was submitted for review for possible publication on June 10, 1980. This paper is part of the Journal of the Energy Division, Proceedings of the American Society of Civil Engineers, ©ASCE, Vol. 107, No. EY1, May, 1981. ISSN 0190-8294/81/0001-0079/$01.00.

velocities were achieved, resulting in reductions in fish entrapment.

Other changes in offshore intake designs have also been experimented with, examples are porous dikes and subterranean infiltration systems (1). The porous dike is costly, and problems of clogging and fish entrapment have not, as yet, been satisfactorily resolved. Also, when an adequate aquifer exists for an infiltration system, experience indicates that the maximum capacity of a single well may be limited to a maximum of 20,000 gal/min (80 m^3/min) thus restricting this concept to makeup intakes.

Another concept, the use of slotted wedge-wire screens and perforated pipes, requires an ambient current of approximately 1.0 fps (0.3 m/s) to aid in the self-cleaning of the screen or a backwash system, or both (1). This concept has also been limited to makeup intakes for small flow rates.

Behavioral barriers, such as air bubbles, hanging chains, and water jets have been shown to be only partially successful in diverting fish under specific hydraulic and environmental parameters (3).

Preliminary Laboratory Studies

The concept of utilizing wide-space louvers in an offshore intake arose as an extrapolation of screenwell diversion studies with louvers spaced 1 in. (25.4 mm) apart, angled 25° to the flow, and tested at approach velocities of 1.0 fps–1.5 fps (0.3 m/s–0.46 m/s) (4). Since such close spacings between louvers would be impractical at an offshore intake due to the potential for clogging with debris and ice, it was conceptualized that wider spacings, combined with high approach velocities, might act to establish the hydraulic conditions necessary to guide fish away from the main water flow and into a bypass located within the offshore intake structure.

Prior to testing in a large scale model, it was decided to conduct studies in a small-scale model in order to evaluate the potential of the wide-spaced louver concept. All tests were conducted with Coho salmon.

The small scale model used in this study is shown in Fig. 1. The test flume was 3 ft (0.91 m) deep, 3 ft (0.91 m) wide, and 58 ft (17.7 m) long and was capped with Plexiglas to a depth of 1 ft (0.30 m) to obtain the desired flow velocities. An array of 15 L-shaped louver vanes were placed at an angle of 6° to the flow and led to a 6-in. (150 mm) wide bypass downstream. The approach velocity was 3.5 fps (1.66 m/s) and the bypass velocity was 2.0 fps (0.61 m/s). The design criteria were based on achieving an approach velocity as high as possible within the flow limitations of the flume, a velocity through the louvers of about 0.5 fps (0.15 m/s), and a louver spacing of 1.0 ft (0.30 m) to minimize clogging.

The first series of tests conducted showed that most of the fish introduced into the system passed through the last three louvers (13, 14, and 15 in Fig. 1) rather than being guided to the bypass. It was apparent that, due to the nature of the louver system, hydraulic conditions had been established which caused a disproportionately large percentage of the total flow to enter the last few louvers. This, in turn, created high velocities which the fish could not avoid. For this reason, a 0.5 in. (12.7 mm) perforated plate was placed over these louvers to induce more flow into the upstream portion of the louver array, thereby causing a more even distribution of flow along the entire system.

In subsequent testing, a large percentage of the fish, which were introduced into the test area via four tubes inserted in the Plexiglas cap, entered the bypass successfully.

The average efficiency of the system under full light conditions was 80%. Generally, when fish were introduced into the flume, they avoided the louvers by swimming immediately to the wall on the bypass side and then passed downstream along the wall into the bypass. Those fish which entered the louvers did so within the first few louver vanes. It was evident that these fish were unable to quickly orient to the flow.

When fish were introduced to a fully darkened flume, the average efficiency dropped to 66%, suggesting that a favorable reaction to the louvers depended, at least partially, on the ability of the fish to perceive them visually.

Under both light and dark conditions, fish were never impinged on the 0.5 in. (12.7 mm) perforated plate covering the last few louvers. This suggests that the improved efficiency of the system with this arrangement was due to a better flow distribution rather than a physical screening of the fish in this critical area.

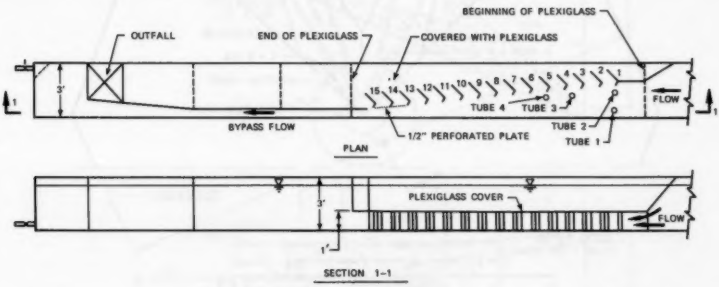

FIG. 1.—Simulated Offshore Intake Diversion Scheme, 3-ft Test Flume (1 ft = 0.305 m)

Due to the limitations of the small-scale test flume model it did not afford conclusive evidence that a wide-spaced louver system at an offshore intake might alleviate fish entrapment problems. However, it was felt that the concept had potential. Accordingly, plans were made to test the system in 1:9 and 1:1 scale models where efforts could be made to optimize the hydraulic characteristics of the system and where its biological efficiency could be better evaluated.

Description of Possible Prototype Offshore Intake

It was stipulated that any intake system evaluated or developed for fish diversion should be suitable for either once-through cooling, closed-loop cooling, or possible backfit to existing intake systems. In addition to this requirement of adaptability, the following criteria were also established: (1) Capability to minimize clogging with debris or ice; (2) must be practicable to construct; and (3) must require minimum maintenance.

To accomodate these criteria, the clear openings were set at a 10-in. (0.25

m) minimum, a distance equal to the spacing of the trash bars at the face of the intake and similar to that used in other existing intakes on Lake Ontario. Bars and louvers would be electrically heated and a flow-reversal capability would be incorporated in the design to backflush any accumulation of frazil or anchor ice. The intake structure could be prefabricated onshore and then sunk and secured in place. The wide-spaced louvers could be removed, if required, through slots in the roof of the structure. A jet pump would be used to induce the suction flow of the offshore bypass since it is the only type of pump that has no moving parts and does not require maintenance.

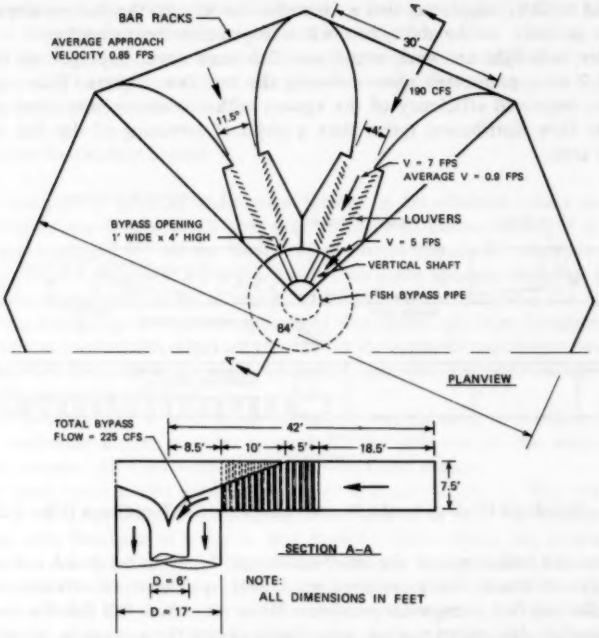

FIG. 2.—Octagonal Intake Structure with Wide-Spaced Louvers (1 ft = 0.305 m; 1 cfs = 0.028 m^3/s)

Two basic designs for the intake structure were considered for model testing. The first, as shown in Fig. 2, is an octagonal structure with a diameter of 84 ft (25.6 m). Flow would enter an intake segment through a 30 ft (9.15 m) wide by 7.5 ft (2.29 m) high opening at an average approach velocity of 0.85 fps (0.26 m/s). The flow would accelerate gradually up to approx 7 fps (2.13 m/s) at the beginning of the louver section. This 7 fps (2.13 m/s) component of flow would be maintained straight into a bypass opening which is 1 ft (0.30 m) wide by 4 ft (1.22 m) high and would represent 15% of the total intake

flow. The cooling water flow would pass through the 15 ft (4.57 m) long louver array at an average velocity of 0.9 fps (0.27 m/s).

The fish bypass pipe would be concentric with the main shaft and would return the fish back to the lake. The total design flow of this structure would be 1,500 cfs (42 m^3/s), or 190 cfs (5.32 m^3/s) per segment.

A second design, representing a self-contained module, was later developed for one segment connecting to a main shaft, as shown in Fig. 3. Structure dimensions were based on the water requirements for a closed-loop cooling system. However, the intake concept could also be incorporated into a once-

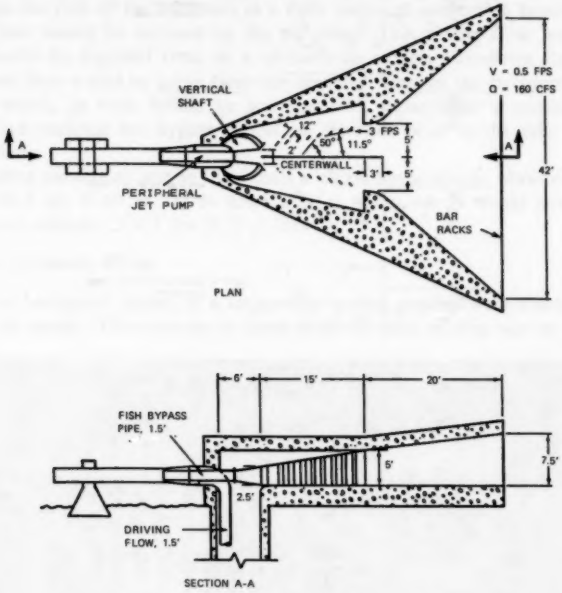

FIG. 3.—Intake Structure Segment Module: Conceptual Design (1 ft = 0.305 m; 1 in. = 25.4 mm; 1 cfs = 0.028 m^3/s)

through cooling system by connecting several segment modules to an intake shaft.

The intake module would be a triangular-shaped segment, having a velocity cap, a converging section, a wide-spaced louver array through which the cooling water would pass, and a fish bypass. This structure would be located so that the highest elevation was at least 12 ft (3.66 m) below the low water lake surface, as required by the United States Army Corps of Engineers and the United States Coast Guard regulations for navigational hazards. The opening to the lake would be 7.5 ft (2.29 m) high × 42 ft (12.81 m) wide and would be protected by 2-in. (50-mm) diam vertical bars having 10-in. (25-m) clear

spacings between them. The opening would be sized for a maximum average approach velocity of 0.5 fps (0.15 m/s) and would face away from the lake shore in order to minimize the possibility of shore line pack ice drifting into and blocking the opening.

From the inlet opening, the structure would converge at approximately a 45° angle to a width of 10 ft (3.05 m). Similarly, the roof would slope down to a height of 5 ft (1.52 m). The 15 ft (4.58 m) long wide-spaced louver arrays

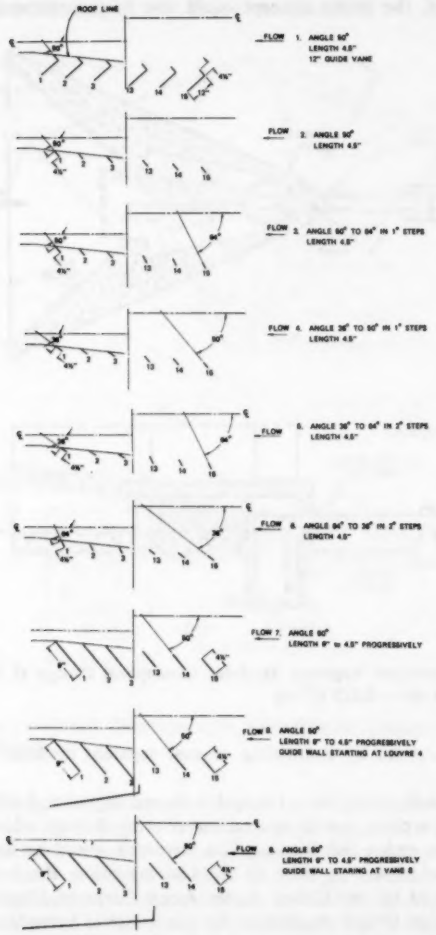
ROOF LINE
FLOW
1. ANGLE 90°
LENGTH 4.5"
12" GUIDE VANE
2. ANGLE 90°
LENGTH 4.5"
3. ANGLE 90° TO 84° IN 1° STEPS
LENGTH 4.5"
4. ANGLE 36° TO 90° IN 1° STEPS
LENGTH 4.5"
5. ANGLE 36° TO 84° IN 2° STEPS
LENGTH 4.5"
6. ANGLE 84° TO 36° IN 2° STEPS
LENGTH 4.5"
7. ANGLE 90°
LENGTH 9" to 4.5" PROGRESSIVELY
8. ANGLE 90°
LENGTH 9" TO 4.5" PROGRESSIVELY
GUIDE WALL STARTING AT LOUVRE 4
9. ANGLE 90°
LENGTH 9" TO 4.5" PROGRESSIVELY
GUIDE WALL STARING AT VANE 8

FIG. 4.—Test Configurations, 1:9 Segment Intake Model (1 in. = 25.4 mm)

would begin at this section on both sides and would be angled in the horizontal at 11.5° to the flow to a 2 ft (0.61 m) wide × 2.5 ft (0.76 m) high bypass opening. The roof would slope down to a height of 2.5 ft (0.76 m). A center wall would be incorporated between the louver arrays to enhance fish guidance.

The louvers would be arranged with a 10-in. (0.25-m) clear spacing between them. The louver slats would be set at a 50° angle to the center line of the intake. The service and makeup water flow would pass through these louvers and down the offshore intake shaft located behind the bypass opening. Fish would guide along the louvers and enter the bypass opening which would converge into a suction pipe and then into an offshore jet pump. This pump would be located at the rear of the structure in a fully enclosed removable housing. The bypass flow would be induced by the jet pump. The driving flow for the jet pump would be supplied from in a closed-loop system blowdown flow. The blowdown flow would be taken from the discharge lines of the circulating water pumps, which, in turn, would be supplied with water from a cooling tower basin. Fish entering the bypass would be returned back to the lake through the jet pump.

A limiting parameter was in this study a maximum available blowdown flow rate of 24.5 cfs (0.69 m^3/s) to drive the jet pump which would correspond to a bypass velocity of 4.5 fps (1.37 m/s).

1:9 Scale Hydraulic Model

Prior to biological testing in a large-scale model, studies were conducted in a 1:9 scale model. The purpose of these hydrodynamic studies was to evaluate

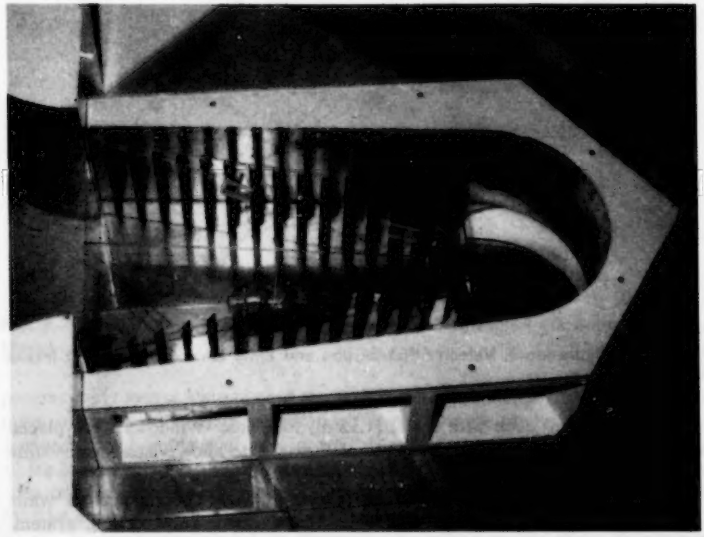

FIG. 5.—1:9 Scale Model of Segment Module

hydraulically both prototype design concepts: the octagonal structure and the segment module. The major objectives were to observe the flow distribution along the louvers for various louver geometries, louver array angles, and location of the backwall of the structure.

The 1:9 scale model was adopted because of its flexibility in allowing rapid model alterations, thereby permitting an evaluation of different geomeric configurations prior to testing in a 1:1 scale model. In this way, reasonable design criteria for the 1:1 scale model were established.

Model Description.—One intake segment was modeled. The test section was rectangular in shape and was situated in a head tank. The triangular test section

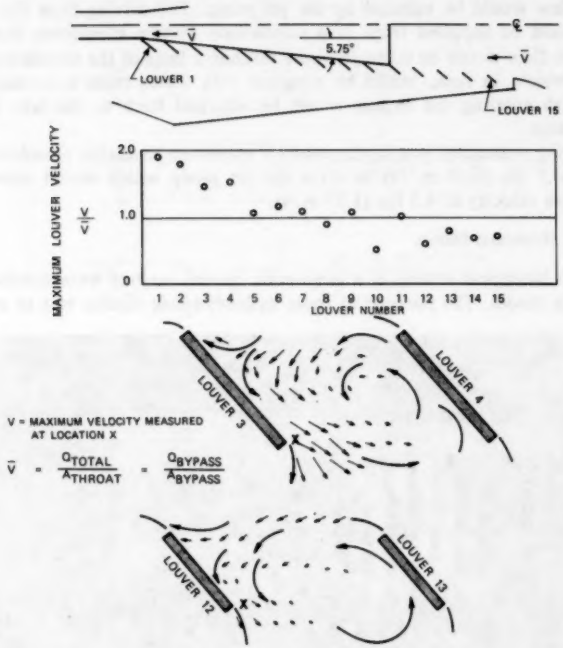

FIG. 6.—Configuration 7, Velocity Distribution and Flow Lines 1:9 Segment Intake Model

was 10 in. (0.25 m) deep with a 5 ft (1.52 m) long side. Windows were placed in the side walls, and the top was made of Plexiglas to allow visual observation of flow patterns.

The octagonal model was based on a once-through cooling system while separately the segment module was based on a closed-loop cooling system. The design criteria were established on the basis of approach velocities and the velocity through the louvers, as shown in Figs. 2 and 3. These criteria

resulted in louver angles of 5.75° and 11.5° for the octagonal and segment module models, respectively. Since the intake study was geared for a closed-loop system, the segment module was developed further than the octagonal model.

In the octagonal structure model, nine different louver configurations were tested as shown in Fig. 4. Configuration 1 was L-shaped with 4.5 in. (115 mm) long slats and 12 in. (300 mm)-long guide vanes oriented at an angle of 50 deg to the structure centerline. In configurations 2 through 6, the slats were 4.5 in. (115 mm) long, but the angle between the louver slat and the center line of the segment was varied between 64° and 36°. Configuration 7 had

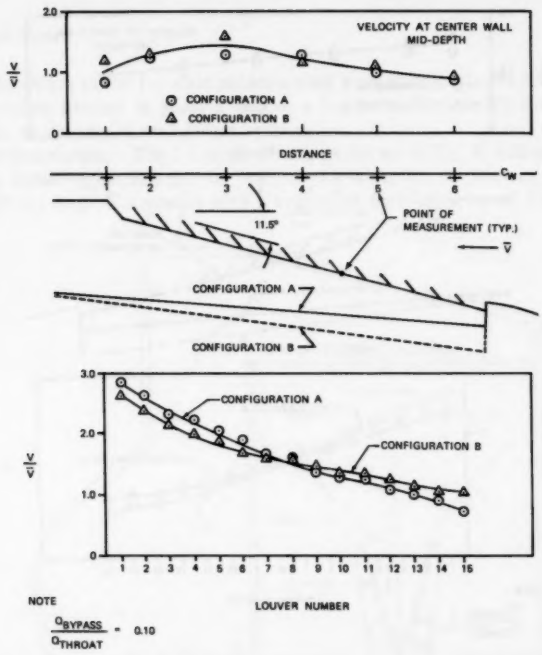

FIG. 7.—Configuration 7, Intake Module Velocity Distribution 1:9 Segment Intake Model

progressively longer slats toward the downstream end ranging from 4.5 in. (115 mm) to 9 in. (229 mm). Configurations 8 and 9 were similar to configuration 7 except that a guide wall was located downstream of the louvers. The angle of the louver array to the flow direction was 5.75°.

In the segment module model, only louver configuration 7 was tested (Fig. 5). The angle of the louver array to the flow direction was 11.5°. The location of the backwall was varied to determine its effect on the flow distribution along the louvers.

Test Results and Analysis.—Louver configuration 7, which had progressively longer louvers toward the downstream end, was chosen for preliminary testing with fish in the 1:1 scale model. This was based on the characteristics that high velocities were confined to a region less than 2 in. (50 mm) wide and that large eddies were created at the longer downstream slats with the position of the maximum velocity being located at a greater distance from the leading edge of the louver than the other louver configurations (Fig. 6).

The large eddies, resulting in a velocity gradient at the face of the louvers, were judged desirable for diverting fish away from the louvers. The small region

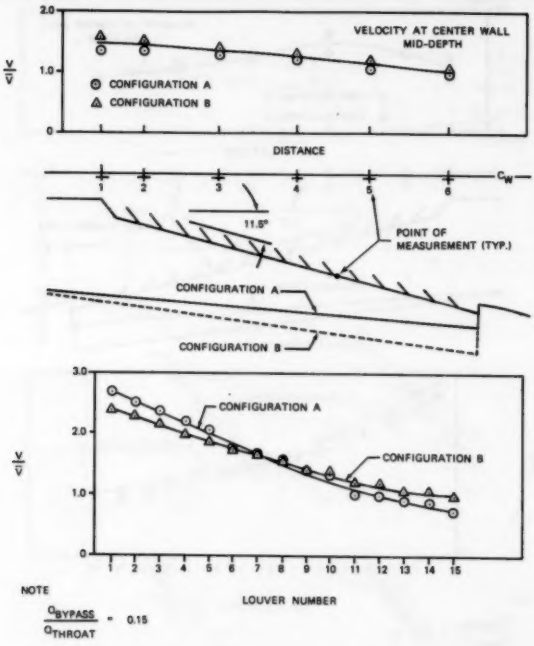

FIG. 8.—Velocity Distribution, 1:9 Segment Module

of high velocity together with the position of the maximum velocity being further away from the face of the louver would enable the fish to react prior to reaching the vicinity of high velocities.

Louver configuration 7 was used in the segment module model. The resulting maximum velocities were lower and the distribution was slightly better than in the octagonal structure. This could be due to the greater louver array angle of 11.5° with the flow direction.

The velocity distribution at the center wall is shown in Figs. 7 and 8 for bypass flows of 10% and 15%, respectively, of the total intake flow. The 10%

bypass flow corresponds to an approach to bypass velocity ratio of 1:1 and the 15% flow to a 1:1.5 ratio. The velocity gradually increases towards the bypass under the 15% bypass flow condition in contrast to the sudden decrease in velocity at the bypass under the 10% bypass flow condition. The gradual increase, based on past louver studies, is preferred for guiding fish to a bypass, because fish are known to avoid areas of sudden increase or decrease in velocity.

Moving the backwall further away from the louvers resulted in a slightly improve velocity distribution along the louver face, as shown in Figs. 7 and 8. This configuration, however, was not tested in the 1:1 scale model with fish.

1:1 Scale Model

The objectives of the 1:1 scale model testing were to evaluate the effectiveness of wide-space louvers in guiding fish to a bypass and to verify the 1:9 scale hydraulic model results on a larger scale.

Model Description.—The 1:1 scale model, as shown in Fig. 9, was constructed inside a basin approximately 60 ft (18.3 m) wide, 70 ft (21.3 m) long, and 6 ft (1.83 m) deep. Six pumps with a combined flow capacity of 130 cfs (3.64

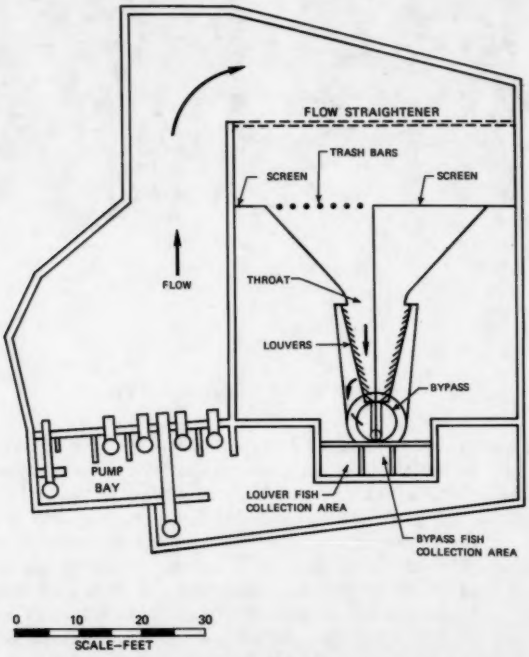

FIG. 9.—1:1 Scale Intake Segment Module

m^3/s) were installed to circulate water through the intake model.

Since the intake structure was symmetric around the center wall, only half the structure was modeled. Fig. 10 shows the louver and bypass arrangement. Since the maximum depth of the test basin was 6 ft (1.83 m) and at least 1-ft (0.013-m) submergence was needed above the inlet to prevent vortices, the maximum height of the model inlet was restricted to 4 ft (1.22 m).

Hydraulic Evaluation.—Approach section and bypass entrance velocities were documented for each test. These velocity distributions were found to be fairly uniform. In addition, the velocity distribution within the area bounded by the louvers, approach section, center wall, and bypass was fully documented. Fig. 11 shows the mid-depth velocity distribution, normalized to the approach velocity,

FIG. 10.—Intake Structure Louvers and Bypass

at approach and bypass velocities of 3.15 fps and 4.74 fps (0.96 m/s–1.44 m/s), respectively. Under these conditions, velocities along the louver array and center wall increased gradually and then suddenly decreased in the vicinity of the bypass, as shown in Fig. 12. It was concluded that a larger bypass to approach velocity ratio of about 2.0 would be needed to maintain the gradually increasing velocity gradient into the bypass, in order to enhance better fish guidance.

Biological Testing.—Testing of the 1:1 scale louver system began in late October 1974. Testing with alewives was conducted in the fall of 1974, and the summer, fall, and winter of 1975. Testing with rainbow smelt was conducted in May 1975. These two species were selected for this study on the basis of their abundance in impingement samples at Lake Ontario power-plant intakes.

Fish were introduced in the large upstream portion of the model basin between the flow straighteners and the retaining screen shown in Fig. 9. The 12 ft (3.66 m) × 45 ft (13.73 m) area was sufficiently large to permit the fish to behave in a normal manner and to react naturally to the intake structure. Fish entering the structure passed either through the louvers or into the bypass and were collected in separate holding areas. The water temperature, time of day, intake velocity (measured at the beginning of the louver section), bypass velocity, number of fish which passed through the louvers, number of fish which entered the bypass, and the time of each event were recorded for each test. Diversion efficiency was calculated on the basis of the number of fish bypassed divided by the total number of fish which entered the intake model.

Test Results and Analysis.—The results of the biological test program are given in Table 1. Tests were conducted at louver section approach velocities of approximately 2 fps, 3 fps, and 4 fps (0.5 m/s, 0.9 m/s, and 1.2 m/s) and bypass velocities ranging from 2.25 fps–4.8 fps (0.69 m/s–1.5 m/s). Water temperature ranged from 39° F–85° F (3.9° C–29.4° C). A total of 45 tests were conducted from October 1974–December 1975.

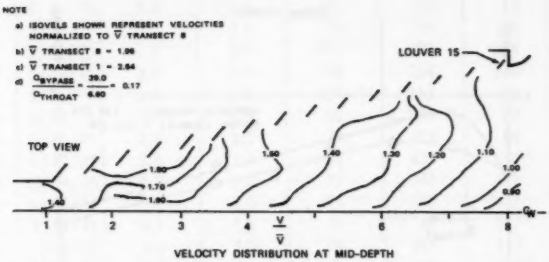

FIG. 11.—Normalized Velocity Distribution, 1:1 Segment Intake Model

The results were analyzed by a least-squares analysis of covariance. The independent variables analyzed included the number of fish in a test, water temperature, approach velocity, and the ratio of approach to bypass velocity. Since the tests were conducted in three distinct time periods, testing period was also included as a variable. The initial period of testing occurred in the fall of 1974 when eight tests were performed with alewives and four tests were performed with smelt. The third period of testing was conducted in the fall of 1975 when ten tests were performed with alewives.

The number of tests conducted with smelt were insignificant and therefore not included in the analysis. However, the mean efficiency for the four smelt tests were 22% with a 95% confidence interval of ±8%.

Results of 41 alewife tests showed that louver diversion efficiency ranged from 8%–80% with a mean of approx 50%. A first analysis of the data indicated that testing period, approach velocity, and the ratio of approach to bypass velocity were the most important independent variables influencing efficiency. The remaining variables were tested and eliminated from the statistical model on the basis of the criterion that $P < 0.05$. The final analysis showed that

test period ($P = 0.00$), approach velocity ($P = 0.0008$) and approach-to-bypass velocity ration ($P = 0.0011$) were highly significant.

Due to the wide variability in diversion efficiency both between and among test periods, the results are difficult to interpret. However, it might be concluded that generally poor efficiency might be expected with this louver system under the physical and hydraulic conditions evaluated. The analysis indicates that some difference in the behavior of fish tested in the three periods was important in determining efficiency. However, the cause of this difference could not be

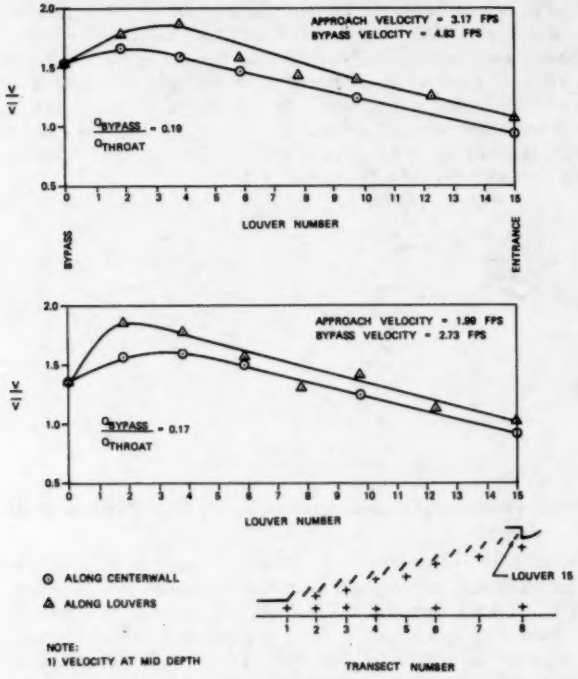

FIG. 12.—Normalized Velocity Gradient, 1:1 Intake Segment Module (1 fps = 0.305 m/s)

determined within the scope of the study. The average diversion efficiency for all alewife tests was 48% with a 95% confidence interval of ±14.5%. In order to determine the range of efficiencies which might be expected to occur within an offshore, louvered intake at Nine Mile Point—Unit 2, actual velocity conditions which would exist at this site was applied to the predictive least-squares equation developed from the study data. It was found that the efficiency value ranged from 90.9% to a minimum value of 23.2% depending on velocity, water temperature, and fish species.

TABLE 1.—Data Summary—Offshore Intake Segment Model

Test species (1)	Date (2)	Approach velocity, in feet per second (3)	Bypass velocity, in feet per second (4)	Water temperature, in degrees Fahrenheit (5)	Fish through louvers (6)	Fish through bypass (7)	Efficiency, as a percentage (8)
Alewife	10/30/74	2.0	2.3	50	169	318	65
Alewife	10/31/74	2.0	2.5	52	130	286	69
Alewife	11/14/74	2.0	2.5	48	33	110	77
Alewife	11/15/74	2.9	3.5	48	74	111	60
Alewife	11/18/74	2.9	3.7	42	57	228	80
Alewife	11/20/74	4.0	4.8	42	210	355	63
Alewife	11/29/74	2.9	3.5	41	101	400	80
Alewife	11/21/74	3.0	4.0	42	180	280	61
Smelt	5/13/75	3.3	3.3	64	109	14	11
Smelt	5/14/75	4.0	5.0	67	66	26	28
Smelt	5/15/75	2.1	3.0	65	233	97	29
Smelt	5/16/75	4.0	5.0	65	53	12	19
Alewife	5/21/75	3.0	3.5	75	88	34	28
Alewife	5/22/75	3.0	3.5	72	93	254	73
Alewife	5/23/75	3.0	3.5	78	254	149	37
Alewife	5/24/75	3.1	3.6	81	333	101	23
Alewife	6/25/75	3.0	3.5	81	383	86	18
Alewife	6/26/75	2.0	2.5	78	332	60	15
Alewife	6/27/75	2.0	2.5	75	434	35	8
Alewife	6/29/75	4.0	5.0	77	366	178	33
Alewife	6/30/75	4.0	5.0	75	285	155	35
Alewife	7/08/75	3.1	5.1	79	88	317	78
Alewife	7/09/75	3.0	5.0	79	285	152	35
Alewife	7/10/75	3.0	5.0	78	170	410	71
Alewife	7/11/75	3.0	5.0	78	122	165	58
Alewife	7/13/74	1.5	2.3	77	118	108	48
Alewife	7/14/75	1.5	2.3	77	428	53	11
Alewife	7/15/74	1.5	2.3	77	340	39	10
Alewife	7/16/75	4.0	6.0	77	204	221	52
Alewife	7/17/75	4.0	6.0	79	197	243	55
Alewife	7/18/75	4.0	6.0	85	199	283	59
Alewife	7/19/75	4.0	6.0	84	162	326	67
Alewife	7/20/75	3.0	5.0	82	156	214	58
Alewife	7/21/75	3.0	5.0	81	143	211	60
Alewife	7/22/75	3.0	5.0	83	150	226	60
Alewife	11/04/75	3.0	5.0	55	200	217	52
Alewife	11/06/75	3.0	5.0	51	187	131	41
Alewife	11/12/75	4.0	6.0	51	144	245	63
Alewife	11/13/75	4.0	6.0	51	231	145	39
Alewife	11/19/75	4.0	6.0	45	276	188	41
Alewife	11/20/75	4.0	6.0	49	266	174	40
Alewife	11/24/75	3.0	5.0	41	297	119	29
Alewife	11/25/75	3.0	5.0	42	237	167	41
Alewife	12/02/75	3.0	5.0	40	73	86	54
Alewife	12/03/75	3.0	5.0	39	234	85	27

Conclusion

The concept of louvered offshore intake is unique and requires further development prior to being considered a practical solution for fish protection. The study is presented to report on the developmental work accomplished to date and to provide a guide for researchers in this field.

The conclusions of this study are as follows:

1. The fish diversion efficiencies varied, ranging from about 91%–23%.
2. Louver orientation and shape affect the flow and velocity distribution along the louvers. This in turn affects the fish diversion efficiencies. A gradually increasing velocity gradient into the bypass is needed to enhance better fish guidance.

This concept was not incorporated at the Nine Mile Point Station—Unit 2. Instead, a highly effective screenwell fish-diversion system had been developed which will be used to minimize impingement. This system will utilize angled traveling screens which will divert fish to a bypass for return to Lake Ontario via a jet pump and transport pipeline. Studies with this system have shown it to be very effective in diverting and transporting fish with low resultant mortality (3,4).

Appendix.—References

1. Mussalli, Y. G., Taft, E. P., and Hofmann, P., "Biological and Engineering Considerations in the Fine Screening of Small Organisms from Cooling Water Intakes," *Proceedings of the Workshop on Larval Exclusion Systems for Power Plant Cooling Water Intakes*, R. K. Sharman and J. B. Palmer, eds., *NUREG/CP-002, ANL/ES-66*, Argonne National Laboratories, Argonne, Ill., Feb., 1978, pp. 197–123.
2. Schuller, V. J., and Larson, L. E., "Improved Fish Protection at Intake Systems," *Journal of the Environmental Engineering Division*, ASCE, Vol. 101, No. EE6, Proc. Paper 11756, Dec., 1975, pp. 897–910.
3. "Studies to Alleviate Fish Entrapment at Power Plant Cooling Water Intakes—Final Report," Stone & Webster Engineering Corporation, prepared for Niagara Mohawk Power Corporation and Rochester Gas & Electric Corporation, 1976.
4. Taft, E. P. and Mussalli, Y. G. "Angled Screens and Louvers for Diverting Fish at Power Plants," *Journal of the Hydraulics Division*, ASCE, Vol. 104, No. HY5, Proc. Paper 13731, May, 1978, pp. 623–634.

METHANE GAS UTILIZATION FROM LANDFILL SITE

By Anthony J. Crutcher,[1] Frank A. Rovers,[2] and Edward A. McBean[3]

INTRODUCTION

With increasing concern being given to future energy availability, attention is now focusing on nonconventional sources. A nonconventional energy resource that has historically been wasted, and in some cases creates a potential hazard (e.g., Refs. 3, 5, 6), is landfill-generated methane gas.

The objectives of a recently completed study conducted for Environment Canada were to develop landfill gas extraction technology, to effectively use low energy gas utilization technology, and to project the economics of landfill gas extraction and utilization (4). To this end, a gas extraction and greenhouse utilization system was installed at the St. Thomas Sanitary Collection Services Limited Landfill Site in southern Ontario. It is the intent of this paper to describe the important details of the study and to indicate the operational experience gained over the winter of 1979.

GAS RECOVERY SYSTEM

The section of the St. Thomas landfill site investigated was in operation from approximately 1967 to site closure in 1978. This 9.7-hectare section has an average depth of refuse of approx 12 m. The landfill site received primarily domestic and industrial solid waste. No segregation or recycling was performed at the site. Liquid and hazardous wastes were excluded, although sludge from the local sewage treatment plant was accepted for disposal. The site was operated primarily as a sanitary landfill, using the cell method of operation. Little daily cover was placed except when required to prevent blowing debris. Presently there is approx 0.3 m of final clay till cover soil.

A gas recovery and utilization system was installed in the fall of 1978. The

[1]Assoc. Partner, Conestoga-Rovers and Assocs., 651 Colby Drive, Waterloo, Ontario N2V 1B4, Canada.

[2]Sr. Partner, Conestoga-Rovers and Assocs., 651 Colby Drive, Waterloo, Ontario N2V 1B4, Canada.

[3]Assoc. Prof., Dept. of Civ. Engrg., Univ. of Waterloo, Waterloo, Ontario N2L 3G1, Canada.

Note.—Discussion open until October 1, 1981. To extend the closing date one month, a written request must be filed with the Manager of Technical and Professional Publications, ASCE. Manuscript was submitted for review for possible publication on November 21, 1980. This paper is part of the Journal of the Energy Division, Proceedings of the American Society of Civil Engineers, ©ASCE, Vol. 107, No. EY1, May, 1981. ISSN 0190-8294/81/0001-0095/$01.00.

gas recovery and utilization system consists primarily of a gas extraction well, a pumping house to contain the gas pump, meters, etc., and a greenhouse facility. The system is depicted schematically in Fig. 1. The system extracts the gas from the gas production well and either pumps the gas to the furnace (inside

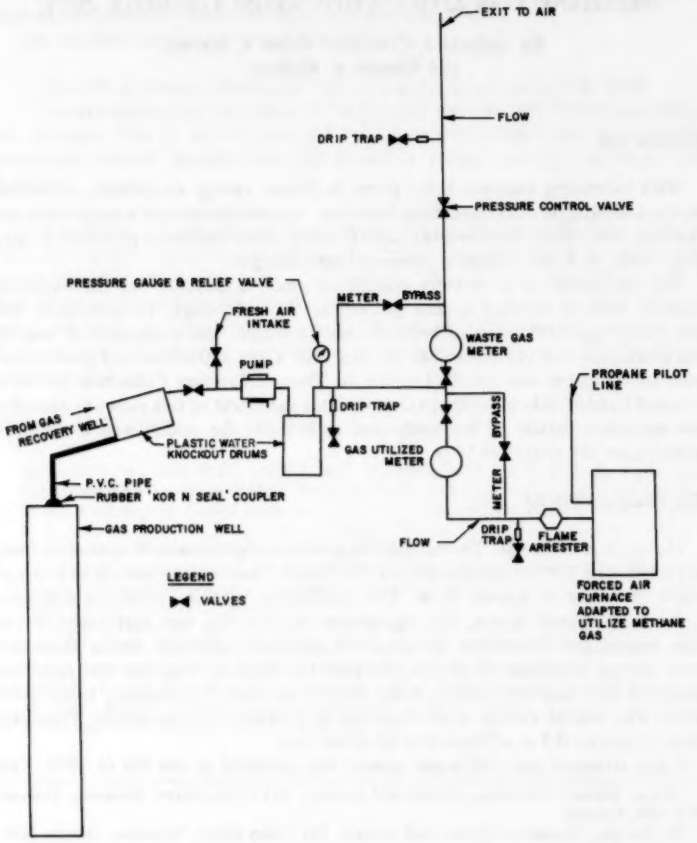

FIG. 1.—Schematic of Installed Gas Utilization System

the greenhouse) or wastes the gas to the atmosphere. More specific details on the elements of the system are described below.

The gas recovery well installation detail is shown in Fig. 2. The well consists of a 9-m diam augered borehole, logged as 0.3 m of cover soil, 8.5 m of refuse, and 0.9 m of native clay till soil. A 15.2-cm diam PVC (polyvinyl chloride) pipe with an attached 2.4-m section of stainless steel well screen was placed

in the center of the augered hole. The hole was then backfilled with pea gravel. It is estimated that the gas well is located in waste deposited during 1972–1973.

The top of the gas production well was enclosed with a 2.3-m section of 0.9-m diam concrete tile and a concrete plug poured at the surface. A precast concrete cap was placed and sealed on top of the concrete tile.

Two water knock-out drums were installed in the recovery system. The first drum was installed prior to the gas pump on the negative pressure side. The

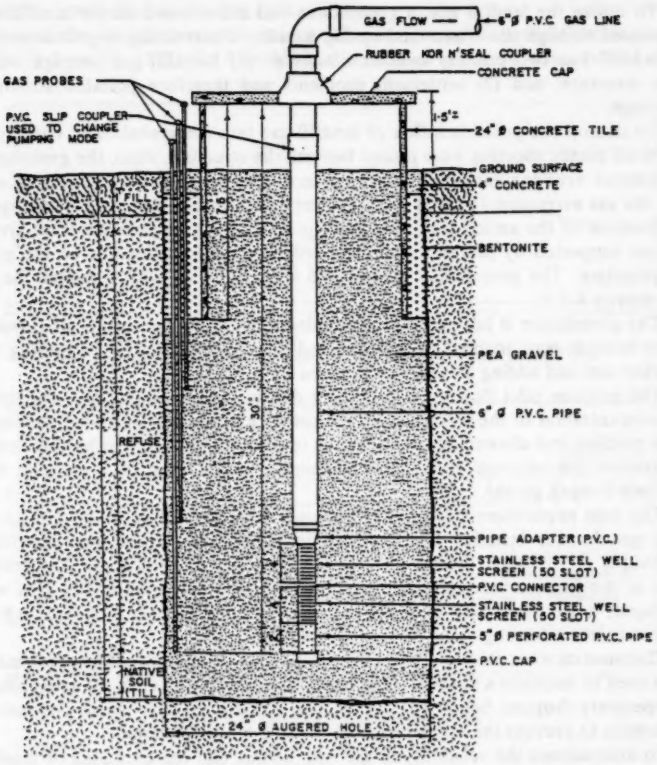

FIG. 2.—Gas Production Well Installation Detail

second water knock-out drum was installed immediately after the gas pump on the positive pressure side of the pump. In addition, several drip taps were installed in the system.

The pressure within the distribution line was controlled by a pressure control valve. This pressure was set manually using a pressure gage. A pressure relief valve was installed as a safety measure. Two gas meters were installed to measure

the waste gas volume and the utilized gas volume.

The gas extraction and recovery system was initially put into daily operation in January 1979. From January 30, 1979–June 29, 1979, the gas extraction system was operated continuously. During this time the pumping was interrupted only briefly for routine maintenance and adjustments.

Gas Utilization System

To utilize the landfill gas, a greenhouse was constructed on the landfill and operated through the winter and spring months. Constructing a greenhouse on a landfill has two primary concerns, namely: (1) Landfill gas seepage within the structure; and (2) settlement problems and therefore possible structural damage.

To control the possible influx of landfill gas into the greenhouse, two layers of 6-mil plastic sheeting were placed beneath the structure. Also, the greenhouse is located near the gas production well to allow the negative pressure created by the gas extraction to assist in preventing gas intrusion into the greenhouse.

Because of the anticipated settlement problems, a fiberglass panelled greenhouse supported by prefabricated steel arches was determined to be the most appropriate. The greenhouse measures 6.4 m × 7.3 m with a central height of approx 3.2 m.

The greenhouse is heated by a conventional domestic gas forced air furnace. The furnace was adapted to run on landfill-generated gas by increasing the orifice size and adding an external propane pilot flame.

The propane pilot flame was necessary due to possible significant variations in concentration of the landfill gas. The use of a propane pilot flame alleviated this problem and allowed interruption-free operation. It is noteworthy that during operation, the propane pilot flame consumed approx 9 kg of a propane in a 2-week–3-week period.

The heat requirements for the greenhouse were calculated to be 116 kJ/h. The gas furnace installed was designed to operate on natural gas, providing an output of 169 kJ/h. Because of the lower quality of landfill gas, the orifice size of the furnace was enlarged (0.25 cm–0.36 cm). After the orifice size was changed, a gas flow rate of 0.123 m^3/min into the furnace resulted, which converts into a heating value of approx 139 kJ/h.

Thermostats were used to control the greenhouse temperature. The gas furnace was used to maintain a constant temperature of approx 21° C. If the greenhouse temperature dropped below 10° C a backup electric furnace would commence operation to prevent the temperature decreasing below freezing.

To demonstrate the reliability of the heat source and the exclusion of landfill gas from within the greenhouse, bedding plants and tomatoes were grown over the 1979 winter period.

Experience Gained

Landfill methane gas concentrations were measured on site. The variation in gas concentrations and pressures throughout the landfill site is covered elsewhere (1) wherein a drawdown zone was identified. Of primary interest herein, however, is just the variability of methane concentrations in the gas

delivery to the greenhouse. The methane concentrations as a function of time are shown in Fig. 3; a relatively stable supply of methane gas is apparent.

Fig. 4 presents a plot of recorded temperatures. Examination of the figure reveals that during the colder months the greenhouse temperature varied only slightly from the thermostat setting of 21° C.

As the weather moderated in spring and sunlight intensity became stronger, daytime greenhouse temperatures frequently rose to values in the high 20s and low 30s. The higher temperatures were common in the month of June but were somewhat controlled by cooling fans.

The standby electric furnace operated only once during the period from January 30, 1979–June 28, 1979. On March 13, the propane gas tank used to fuel the

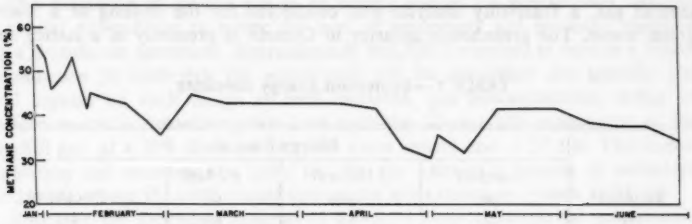

FIG. 3.—Methane Concentration in Gas Line as Function of Time

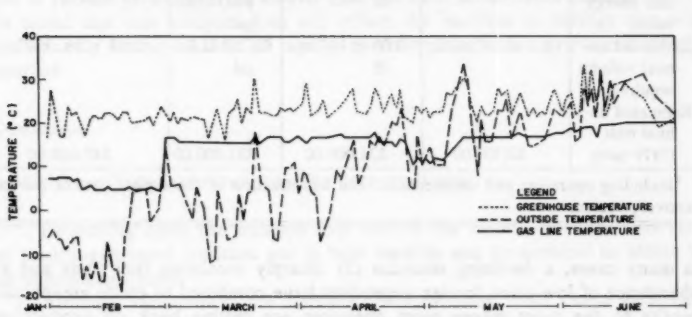

FIG. 4.—Temperatures Versus Time

pilot flame ran out of fuel. With no pilot flame the furnace could not operate and therefore the standby furnace was automatically activated to maintain the greenhouse temperature above freezing.

The furnace operated on methane having variable concentrations with no difficulty. As recorded in Fig. 3, the methane varied from a low concentration of 33% to a high of 55%.

A test was conducted to determine at what level the furnace would not sustain a flame. The test consisted of diluting the landfill gas with nitrogen, and thus reducing the percent volume of methane. The results of this test indicated that

the lower limit of methane combustibility for the installed system was 25% methane.

The total amount of gas utilized to heat the greenhouse for the period January 30, 1979–June 28, 1979 was measured as 13,000 m^3. The gas wasted to the air for the same period was measured as 240,000 m^3.

A steady growth was achieved by the tomato plants in the greenhouse. The first ripe tomato was obtained on May 23, 1979. During June and July tomato production was continuous.

Economic Analysis

As an example of the economic viability of extracting and utilizing unprocessed landfill gas, a feasibility analysis was conducted for the heating of a 1-acre green house. The greenhouse industry in Ontario is presently in a static, and

TABLE 1.—Equivalent Energy Amounts

Variable (1)	Energy Source: Landfill gas (2)	Natural gas (3)	#2 fuel oil (4)	Electricity (5)
Approximate unit energy value	500 Btu/cu ft	1,000 Btu/cu ft	142,000 Btu/U.S. gal	3,412 Btu/kWh
Estimated annual volume required	18.1×10^6 cu ft	9.05×10^6 cu ft	63,750 U.S. gal	2.65×10^6 kWh
Estimated annual cost (1979 rate)	$8,100.00	$24,000.00	$33,000.00	$45,600.00

*Including operation and maintenance, and amortization of the capital cost of the gas recovery system.

in many cases, a declining situation (2). Sharply escalating fuel costs and an abundance of low-price foreign vegetables have combined to erode greenhouse profits to the point where most operators are cutting back on production. Seventy-five percent of the increase in production costs between 1973 and 1975 have been attributed to rising fuel prices.

Historically the greenhouse industry in Ontario has been closely associated with the fruit and vegetable industry. In many cases the greenhouses are used to supplement field crops. For this reason most Ontario greenhouses are located in three main vegetable-growing areas of Ontario.

The use of landfill gas, however, would limit the greenhouse locations to landfill sites that are both properly constructed and large enough to produce reliable, useful amounts of gas. This would tend to decentralize greenhouse construction and would require that the greenhouse be economically viable in its own right and not be just a part of a large farm system.

The total, installed and ready-to-use cost of a one acre greenhouse is approx

$445,000 (4). This cost includes greenhouse structure and covering material and the support systems including boiler, air heating, backup heating, cooling and ventilating, electrical and control, service building and utilities, irrigation and fertilization facilities, drainage system, and sterilization.

The annual energy consumption for a greenhouse in southern Ontario is 241,000 L of #2 fuel oil/acre. The equivalent amounts of landfill gas, natural gas, and electricity are as recorded in Table 1.

The estimated average annual cost is calculated based on unit rates of March 1979. The per unit rates for natural gas and electricity both decrease with increasing consumption. An attempt was made to reflect this variable rate structure by proportioning the average annual energy requirements over the 12 months of the year according to estimated seasonal requirements.

The extraction of landfill gas as an energy source for greenhouses requires a capital expenditure to cover the cost of equipment not normally required by a greenhouse operation. Approximately $62,000 is required to service a 1-acre greenhouse (4) (although the actual cost will be somewhat site specific and will depend on such things as well locations, gas concentrations, radius of influence, etc.). Amortizing this cost over the 20-year life expectancy of the landfill gas, at a 10% discount rate, the extra annual cost is $7,100. The annual operating and maintenance costs for the gas extraction system is estimated as $1,000, giving the total annual cost of the gas extraction system as $8,100.

Based on the preceding analysis of a typical 1-acre commercial greenhouse, annual energy cost savings of at least $16,000/yr can be expected when landfill gas is chosen as a fuel over natural gas, the next lowest cost fuel. It should be noted that this analysis does not reflect the increase in savings that will undoubtedly accrue because of rapidly escalating costs of conventional energy sources.

Conclusions

Major conclusions derived from the case study are:

1. Depending upon the location and size of the landfill site, the recovery of landfill-generated methane gas is both feasible and economical to utilize in an unprocessed state.
2. Although variations in the methane concentrations occur, these variations can be designed for in the gas train assembly.
3. As energy costs escalate, the demand for alternative energy sources will continue, further increasing the economic viability of landfill gas extraction and utilization.

Acknowledgments

The assistance of St. Thomas Sanitary Collection Service Ltd. and especially Bob McCaig and Don McCaig is greatly appreciated. In addition, thanks are extended to Cyril McCaig, for without his help in operating the system and tending the plants, the success of the project would not have been possible. The study was funded in part by Environment Canada with Hans Mooij as

scientific authority who provided encouragement and direction throughout the study.

Appendix.—References

1. Crutcher, A. J., McBean, E. A., and Rovers, F. A., "Statistical Analyses of Landfill-Generated Methane Gas," submitted to *Water, Air and Soil Pollution*.
2. "Feasibility Analysis of the Utilization of Moderator Heat for Agricultural and Aquacultural Purposes," Conestoga-Rovers and Associates, report to the Ontario Ministry of Energy, Government of Ontario, Canada, Dec., 1977.
3. First, N. W., Viles, F. J., and Levin, S., "Control of Toxic and Explosive Hazards in Buildings Erected on Landfills," *Public Health Reports*, Vol. 81, No. 5, May, 1966.
4. "Gas Recovery and Uitilization from a Municipal Waste Disposal Site," Conestoga-Rovers and Associates, report to Environment Canada, Ottawa, Ontario, Canada, July, 1979.
5. McFarlane, I. C., "Gas Explosion Hazards in Sanitary Landfills and Garbage Dumps," *Public Works*, May, 1970, pp. 76–78.
6. Nosanov, M. E., and White, R. L., "Gas Control and Beneficial Use of Completed Landfills," *Public Works*, Nov., 1975, pp. 62–64.

EFFECTS OF CLAMPS ON FATIGUE OF ACSR CONDUCTORS

By George E. Ramey,[1] M. ASCE and John S. Townsend,[2] A. M. ASCE

INTRODUCTION

Aeolian vibration of electrical conductors is a major problem in the design of transmission power lines. Transverse oscillatory motion of low amplitude, short wave length, and relatively high frequency are some of the basic characteristics of this wind-induced vibration phenomenon (6,10). Bending stresses resulting from the vibrations cause cyclic variations in the longitudinal stresses of the conductor strands. In the central portion of the span, these dynamic stresses present little difficulty; however, at conductor support points this is not the case. At suspension clamps, the superposition of static stresses caused by conductor bending curvature, tensile load, and local clamp bearing load can constitute a major fatigue problem should the dynamic stresses due to aeolian vibration become large.

Many techniques for reducing aeolian vibrations and minimizing fatigue failures are employed by the electric utility industry. Some attempt to reduce the vibrations to acceptable levels while others, through improvement of suspension systems, attempt to reduce local line stresses at conductor suspension locations. These are reflected in the numerous suspension clamp hardware designs on the market today. Theoretical considerations and engineering judgment indicate that some of these designs are superior to others. However, the transmission line designer would like a more quantitative evaluation of the superiority or inferiority of these clamps. An evaluation of the relative fatigue mitigating merits of three such clamps was the objective of the research being reported herein (3,9).

THEORETICAL CONSIDERATIONS

Thorough analyses of aeolian vibrations and the fatigue of overhead transmission lines are available (10), and the interested reader should go to the literature for detailed considerations of these topics. To assist in understanding and interpreting the experimental results of this investigation, brief summary consid-

[1]Assoc. Prof. of Civ. Engrg., Auburn Univ., Auburn, Ala. 36849.
[2]Research Engr., Bethea/National Corp., Birmingham, Ala.

Note.—Discussion open until October 1, 1981. To extend the closing date one month, a written request must be filed with the Manager of Technical and Professional Publications, ASCE. Manuscript was submitted for review for possible publication on July 22, 1980. This paper is part of the Journal of the Energy Division, Proceedings of the American Society of Civil Engineers, ©ASCE, Vol. 107, No. EY1, May, 1981. ISSN 0190-8294/81/0001-0103/$01.00.

erations of the major factors operative in the fatigue of aluminum conductor steel-reinforced (ACSR) conductors are presented.

Conductor Nominal Stresses.—ACSR conductor fatigue is an extremely complex mechanism due to the complex stress and fretting conditions existing at clamp locations (7,8,9,10). Stresses occurring in the central portion of a conductor span result from: (1) Bending of the conductor into vibrating loops—S_{db}; (2) stringing tension in the conductor—S_t; (3) additional tension in the conductor caused by the increased length of the curved form of the vibrating loop—S_{dt}; and (4) static bending stresses due to the conductor weight—S_{sb}. The S_{sb} stresses are very small within the span and can be neglected, as can the S_{dt} stresses.

The stresses at suspension clamp locations consist of the aforementioned four (except that S_{sb} is no longer small) plus bearing stresses due to cable tension/slope angle and keeper clamping pressure. These bearing stresses are sufficient to cause plastic flow of the strands and therefore indentations and longitudinal stress concentrations at the clamp location. Additionally, they increase the normal forces between adjacent strands, and thus increase surface tractions, stresses, and fretting at the clamps. This severe environment can often create conductor fatigue problems at the clamp locations.

Static stresses due to stringing tension (S_t) can be estimated by using a standard transformation of areas method while assuming the aluminum to be linearly elastic and the strands to be straight and in pure axial tension. This yields

$$S_t = \frac{T}{n A_s + A_a} \quad \ldots\ldots\ldots\ldots\ldots\ldots\ldots\ldots\ldots\ldots\ldots\ldots\ldots\ldots\ldots\ldots\ldots\ldots (1)$$

in which T = tension in the conductor; A_s = total area of steel; A_a = total area of aluminum; and n = modulus of elasticity for steel/modulus of elasticity for aluminum.

An expression for static bending stress (S_{sb}) due to the conductor sag was developed by Poffenberger and Swart (2). In that derivation, the expression for moment at the clamp is obtained from the differential equation of bending assuming fixity at the suspension clamp and that planes remain plane. The moment at the clamp is given as

$$M_{sb} = \left(\frac{L_s}{2p} - \frac{EI}{T}\right) w \quad \ldots\ldots\ldots\ldots\ldots\ldots\ldots\ldots\ldots\ldots\ldots\ldots\ldots\ldots\ldots\ldots\ldots\ldots (2)$$

and the resulting bending stress is

$$S_{sb} = \frac{M_{sb}\, c}{\dfrac{EI}{E_o}} \quad \ldots\ldots\ldots\ldots\ldots\ldots\ldots\ldots\ldots\ldots\ldots\ldots\ldots\ldots\ldots\ldots\ldots\ldots (3)$$

in which w = weight of the conductor per unit length; L_s = length of span; T = tension in conductor; EI = composite flexural rigidity of the conductor; $p = (T/EI)^{1/2}$; c = distance from neutral axis to point in question; EI/E_o = equivalent moment of inertia in terms of material in question; and E_o = modulus of elasticity of material in question (E_o of aluminum taken as 10,000 ksi or 68,950 MPa). The assumption of clamp fixity is valid for the common occurrence of symmetric wave patterns in adjacent spans.

Equation 3 is commonly used in the literature, and it is interesting to note that this equation does not consider the physical geometry of the conductor suspension clamp in any manner. Sandberg (4) states that the major cause of fatigue failures is the suspension clamp and the geometry of the clamp is an important parameter in fatigue performance. It would appear logical that this should be the case, since local clamp geometry and attachments should affect local stresses in the conductor which in turn should affect fatigue performance.

As a conductor passes over a suspension clamp, it is forced around the clamp such that the curvature of the conductor matches that of the clamp. Thus

$$y'' = \frac{1}{R} \quad \ldots\ldots\ldots\ldots\ldots\ldots\ldots\ldots\ldots\ldots\ldots\ldots\ldots\ldots\ldots\ldots\ldots\ldots\ldots\ldots\ldots\ldots (4)$$

in which R = the radius of curvature of the clamp. Therefore the static bending moment in the conductor at the clamp is

$$M_{sb} = EIY'' = \frac{EI}{R} \quad \ldots\ldots\ldots\ldots\ldots\ldots\ldots\ldots\ldots\ldots\ldots\ldots\ldots\ldots\ldots\ldots\ldots\ldots\ldots\ldots\ldots\ldots (5)$$

$$\text{Therefore } S_{sb} = \frac{M_{sb}\, c}{\frac{EI}{E_o}} \quad \ldots\ldots\ldots\ldots\ldots\ldots\ldots\ldots\ldots\ldots\ldots\ldots\ldots\ldots\ldots\ldots\ldots\ldots\ldots\ldots\ldots\ldots (6)$$

or upon substituting Eq. 5 into Eq. 6, the strand stresses are as stated by Sandberg (4), i.e.:

$$S_{sb} = \frac{E_o\, c}{R} \quad \ldots\ldots\ldots\ldots\ldots\ldots\ldots\ldots\ldots\ldots\ldots\ldots\ldots\ldots\ldots\ldots\ldots\ldots\ldots\ldots\ldots\ldots (7)$$

The stresses given by Eq. 7 for common clamp radii of curvature, are much larger than those predicted by Eq. 3. Table 1 shows this for the three different clamp radii and conductor tested in this investigation. The high stresses predicted by Eq. 7 are based on assuming a linear σ-ϵ relationship. Obviously these stresses

TABLE 1.—1033.5 kcmil 45/7 ACSR Nominal Static Bending Stresses for Conditions in this Study

Suspension clamp (1)	Static Bending Stresses, S_{sb}	
	Using Eq. 3, in pounds per square inch (2)	Using Eq. 7, in pounds per square inch (3)
Short-radius: (R = 6 in.)	1,495	126,330
Medium-radius: (R = 11.2 in.)	1,495	67,680
Long-radius: (R = 24 in.)	1,495	31,580

Note: 1 in. = 2.54 cm and 1 psi = 6.89 kPa.

do not actually exist, but rather plastic deformations occur in the strands at the associated plastic stress levels.

Experimental test specimens show permanent bending deformations at clamp locations when they are "cut-down." These bending plastic deformations are felt to be evidence that the strains associated with Eq. 7, i.e.:

$$\epsilon_{sb} = \frac{S_{sb}}{E_o} = \frac{c}{R} \quad \ldots\ldots\ldots\ldots\ldots\ldots\ldots\ldots\ldots\ldots\ldots\ldots\ldots\ldots\ldots\ldots (8)$$

and the corresponding stresses, which one can evaluate from the material σ-ϵ curve, are probably more accurate than those predicted by Eq. 3.

As indicated earlier, at suspension clamp locations, bearing stresses due to line tension-slope angle and clamp keeper forces cause longitudinal stress concentrations. Thus, at clamp locations, the sum of the nominal longitudinal stresses should be multiplied by a stress concentration factor k_1. However, experimental results indicate that strand breaks occur in the strand fretting region (immediately in front of the clamp) rather than the strand crimped region (where clamp is in contact with the conductor). Therefore an attempt to quantify k_1 will not be pursued.

The dynamic stresses S_{dt} and S_{db} are more difficult to assess than the static stresses. The S_{dt} stress is felt to be small relative to the other stresses and is usually neglected. Nominal S_{db} stresses are typically formulated in terms of vibration amplitudes, i.e., bending amplitude (Y_b) or midloop amplitude (y_{max}). Bending amplitude is defined as the total peak-to-peak amplitude measured relative to the suspension clamp at the 3-1/2 in. (8.89 cm) point. Midloop amplitude is the maximum displacement at an antinode measured from the static equilibrium position of the conductor.

From Ref. 10, the S_{db} equation in terms of Y_b is

$$S_{db} = \frac{\dfrac{c\,E_o\,p^2}{2}}{e^{(-3.5p)} - 1 + 3.5p}\,Y_b \quad \ldots\ldots\ldots\ldots\ldots\ldots\ldots\ldots\ldots\ldots\ldots\ldots (9)$$

and in terms of y_{max} is

$$S_{db} = 2\pi\,c\,E_o \left(\frac{m}{EI}\right)^{1/2} f(y_{max}) \quad \ldots\ldots\ldots\ldots\ldots\ldots\ldots\ldots\ldots\ldots\ldots\ldots (10)$$

in which m = the conductor mass density per unit length; f = the vibration frequency, in hertz; and the other variables are as defined earlier.

As in the static bending case, the assumption that planes remain plane is incorporated in the derivations of Eqs. 9 and 10, and is a source of error in those equations. Probably an even greater source of error is the omission of the effect of fretting on the dynamic stresses and fatigue resistance properties of the conductor. Equations 9 and 10 give drastically different stresses for a given vibration condition. However, they are valuable for calculating relative stresses and do exhibit a reasonable correlation between nominal S_{db} stresses and conductor fatigue damage (10).

ASCR Conductor Flexural Rigidity.—In order to use the stress equations presented in the previous section, a value for the flexural rigidity of the conductor

must be available. Two assumptions commonly made in evaluating this rigidity are: (1) The conductor acts as a group of individual and independent strands with no friction between the strands; or (2) the conductor acts as a solid bar with all the strands acting as a unit. In actuality the rigidity lies somewhere in between these two and probably much close to the first. In normal practice friction between strands is recognized, but it is not felt to be sufficient to prevent relative slip between strands. Thus, rigidity is calculated using the sum of each strand per the first assumption. Numerical values of the flexural rigidity were calculated for both assumptions for comparative purposes and the results are presented in Table 2.

When the slip *EI* is used in the conductor bending stress equations of the previous section, then the corresponding "*c*" values in those equations should be taken as an individual strand radii. Dynamic bending stresses, using Eq. 10, were calculated using both rigidities for comparative purposes and these results are also presented in Table 2. As can be seen from this table the assumption regarding strand slip has a tremendous effect on conductor flexural rigidity, but a greatly dampened effect on conductor bending stresses.

TABLE 2.—1033.5 kcmil 45/7 ACSR Flexural Rigidity

Behavioral assumptions (1)	Flexural rigidity *EI*, in pound-square inches[a] (2)	Dynamic bending stress,[b] S_{db}, using Eq. 10, in pounds per square inch (3)
No strand slip	790,360	5,424
No friction/strand slip	12,740	5,338

[a] $E = 10{,}000{,}000$ psi.
[b] For y_{max} value of 0.19 in.
Note: 1 lb = 4.45 N; 1 in. = 2.54 cm; 1 psi = 6.89 kPa.

Conductor Fatigue.—The fatigue fracture of an individual strand within an ACSR conductor is the result of a large number of high level stress reversals which exhaust the inherent ductility of the aluminum (5). When enough aluminum strands break, the electrical resistance and resulting heat build up become sufficiently large to anneal the steel core and precipitate a catastrophic failure of the line (10).

The process of fatigue fracture can be divided into two fundamental steps, i.e., crack formation and crack growth (6). The formation or "crack nucleation" step is a highly localized and somewhat random process. It begins at the surface of the material and is governed by stress concentrations. These stress risers can take the form of inherent imperfections in the material surface or damage done to the surface by its working environment. In ACSR conductors, the damage caused by the presence of the suspension clamp (including its affect on fretting), is by far the dominant factor in crack formation. If sufficiently high, the stress risers cause highly localized plastic deformations which ultimately lead to a local failure (crack).

The second fundamental step in the fatigue process is crack growth or propagation which is much less random than "crack nucleation." In this case,

the location of the stress riser is fixed and it is simply a matter of the crack working its way through the material. The mechanism for crack growth has been established as the repeated plastic deformation caused by stress concentrations at the crack tips (1).

Fretting is a very important parameter in the fatigue of ACSR conductors. Researchers have found that all fatigue strand breaks and cracks occur at fret marks. This phenomenon has been estimated to reduce the fatigue strength of conductor strands by a factor of two relative to unfretted fatigue strengths (10).

Experimental Parameters and Testing

Amplitude and cycles of vibration, conductor type/size/stranding, and suspension clamp hardware are the variables felt to contribute most significantly

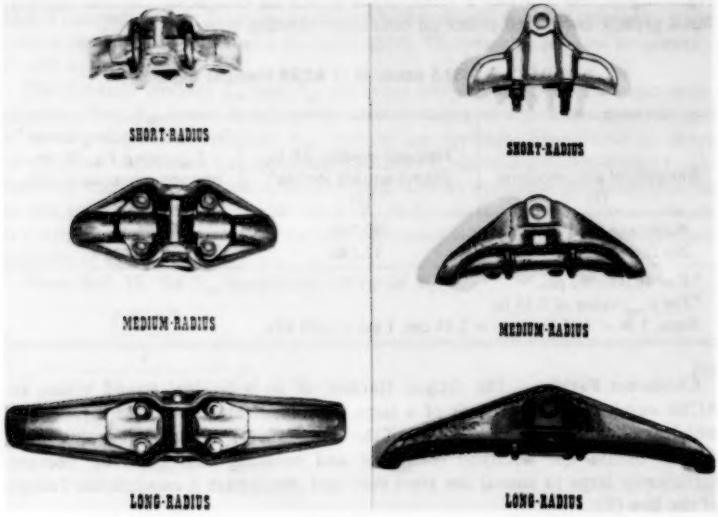

FIG. 1.—Photographs of Suspension Clamps Tested

to the fatigue performance of overhead conductors. Only suspension clamp hardware was varied in this study. This isolated the effect of this parameter and allowed an evaluation of its importance in the fatigue process.

Suspension Clamps Tested.—As previously indicated, three different suspension clamp hardwares were tested. All were cast aluminum but of considerably different radius of curvature (of the clamp groove). The clamps are referred to herein as the: (1) Short-radius (R = 6 in. or 15.24 cm) clamps; (2) medium-radius (R = 11.2 in. or 28.45 cm) clamps; and (3) long-radius (R = 24 in. or 60.96 cm) clamps. Figure 1 shows photographs of the clamps used and Fig. 2 presents

drawings showing some of the basic clamp dimensions. For each radius clamp, the size used was the one recommended for a conductor diameter corresponding

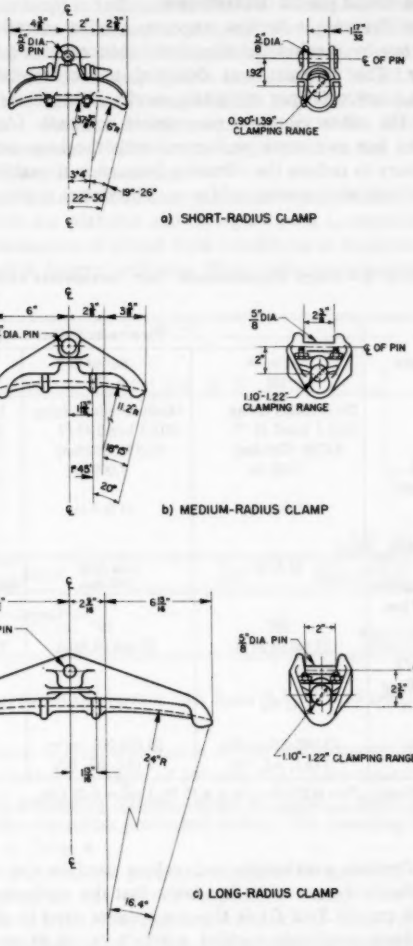

FIG. 2.—Line Drawings of Suspension Clamps Tested (1 in. = 2.54 cm)

to that of 1033.5 kcmil 45/7 ACSR. The short-radius clamp was designed to support conductors of diameters ranging from 0.90 in.–1.39 in. (2.29 cm–3.53 cm), whereas the medium and long-radius clamps were designed for a range

of 1.10 in.–1.22 in. (2.79 cm–3.10 cm). The closer fit between clamp and conductor for the medium and long-radius clamps results in a more uniform distribution of the clamp bearing forces. This in turn reduces conductor cross-sectional distortions and strand plastic deformations.

Experimental Program.—In this program, aeolian vibrations were simulated in the laboratory by mechanical vibrations induced at a natural frequency of the conductor. The program was designed to accomplish the objective of evaluating the relative fatigue mitigating merits of the three suspension clamps while holding the other vibration parameters constant. (An exception to this occurred in the last two tests performed with the long-radius clamp when it became necessary to reduce the vibrating frequency to stabilize the equipment.) Three identical tests were conducted for each hardware to give statistical credence to the results.

TABLE 3.—Major Experimental Test Parameters and Values

Test parameters (1)	Parameter Values		
	Series A (2)	Series B (3)	Series C (4)
Test clamp	Short-radius clamp	Medium-radius clamp	Long-radius clamp
Conductor	1033.5 kcmil 45/7 ACSR (Ortolan)	1033.5 kcmil 45/7 ACSR (Ortolan)	1033.5 kcmil 45/7 ACSR (Ortolan)
Conductor tension	7,000 lb	7,000 lb	7,000 lb
Length of conductor "Test Span"	33 ft-3 in.	33 ft-3 in.	33 ft-3 in.
Torque applied to keeper bolts of test clamp	45 ft-lb	45 ft-lb	45 ft-lb
Conductor slope exiting back side of test clamp	10°	10°	10°
Vibration double amplitude at 3-1/2 in. location/midloop	27 mil/0.38 in.	27 mil/0.38 in.	35 mil/0.38 in. (Test C1) 35 mil/0.42 in. (Test C2 and C3)
Vibration frequency	42 Hz	42 Hz	42 Hz (Test C1) 35 Hz (Test C2 & C3)
Duration of test run	20,000,000 cycles	20,000,000 cycles	20,000,000 cycles
Number of tests	3 (A1, A2, A3)	3 (B1, B2, B3)	3 (C1, C2, C3)

Note: 1 in. = 2.54-cm; 1 ft = 0.305 m; 1 lb = 4.45 N; 1 psi = 6.89 kPa.

The major vibration parameters and values used in the testing are shown in Table 3. It should be noted in that table that the midloop double amplitude of 0.38 in. (0.96 cm) in Test C1 is the same value used in the A and B series tests. This midloop amplitude yielded a 3-1/2 in. (8.89 cm) location double amplitude of 35 mil (0.89 mm) which is larger than the 27 mil (0.69 mm) of the A and B series tests. This was the result of the long-radius clamp having its bottom and top last points of contact more widely separated (with the top point being located back toward the clamp center line from the bottom point). Since in the field a given wind velocity or power input would cause the same midloop amplitude independent of the clamp, it was felt that maintaining a

constant laboratory midloop amplitude represented the fairest comparative test. Additionally, equipment overheating and ensuing vibration stability problems, necessitated a reduction in vibration frequency for tests C2 and C3 to 35 Hz (and one less vibration loop) as indicated in Table 3. To maintain the comparative nature of the tests, it was necessary to employ the higher midloop amplitude of 0.42 in. (1.07 cm) at this reduced frequency (and increased loop length) to maintain the 3-1/2 in. (8.89 cm) double amplitude of 35 mil (0.89 mm) of test C1. Thus, the three tests conducted with the long-radius support hardware were all executed at a vibration double amplitude of 35 mil (0.89 mm) at the 3-1/2 in. (8.89 cm) location. These in turn correspond to the same windfield as simulated in the A and B series tests.

The vibration amplitude and frequency values used (see Table 3) were selected after consultation with the Alabama and Georgia Power Companies. The values are felt to be representative of actual field conditions at locations where lines are experiencing aeolian fatigue problems. The conductor tension value of 7,000

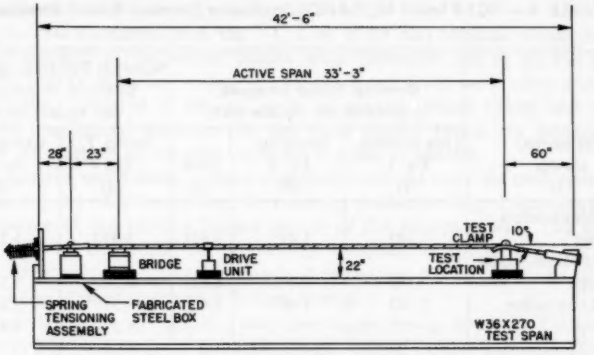

FIG. 3.—General Layout of Laboratory Test Span (1 in. = 2.54 cm, 1 ft = 3.05 m)

lb (31,150 N) is realistic and representative of line winter conditions. The keeper bolt torque and conductor sag angle of 10° (see Fig. 3) are typical field values.

The experimental parameter values shown in Table 3 were translated into stresses by use of the equations presented earlier. The resulting nominal strand stresses are shown in Table 4.

In summary, the experimental program consisted of mounting a 1033.5 kcmil 45/7 ACSR conductor in one of the suspension clamps and tensioning the conductor to 7,000 lb (31,150 N) to simulate winter conditions. The test specimen was vibrated at a frequency of 42 Hz and a midloop amplitude of 0.38 in. (0.96 cm) (with the exceptions indicated herein) for 20,000,000 cycles. Upon terminating the vibrations, the conductor was opened up for visual inspection of strand breakage.

Experimental Testing.—The experimental testing was conducted in an indoor laboratory of controlled environment. A steel beam was used for the vibration bed with the test conductor anchored to the bed at each end by steel box

assemblies as shown in Fig. 3. The spring tensioning system at the end was used to maintain the 7,000 lb (31,150 N) load (24.2% UTS) on the conductor.

At the "test location" end of the span was a steel box which supported the suspension "test clamp," which in turn supported the test conductor. Threaded rods bolted to the box were adjusted to a snug fit under the bottom of the "test clamp" after the conductor was tensioned to prevent articulation of the clamp and thereby fixed its position during the test. This fixed-clamp condition is not realistic of actual field connections; however, the fixity accomplishes acceleration of the fatigue process and is representative of field conditions when vibrations are symmetrical with respect to the suspension clamp. Also, results obtained from such a restrained condition are directly applicable to field lines since 3-1/2 in. (8.89 cm) amplitude values measured in the field are the conductor displacements relative to the clamp.

An electromagnetic vibrator was used to simulate the aeolian vibrations. The electromagnetic drive unit was mounted on the vibration bed and the conductor

TABLE 4.—1033.5 kcmil 45/7 ACSR Conductor Nominal Strand Stresses

Test series/clamp (1)	Nominal Static Stresses, in pounds per square inch			Nominal Dynamic Bending Stresses, in pounds per square inch	
	Line tension, Eq. 1 (2)	Bending, Eq. 3 (3)	Total (4)	Using Y_b, Eq. 9 (5)	Using y_{max}, Eq. 10 (6)
"A" Short-radius clamp	7,143	1,495	8,638	3,370	5,338
"B" Medium-radius clamp	7,143	1,495	8,638	3,370	5,338
"C" Long-radius clamp	7,143	1,495	8,638	4,370[a]	5,338[a]
				4,370[b]	4,917[b]

[a]Test C1.
[b]Test C2 and C3.
Note: 1 psi = 6.89 kPa.

was vibrated at resonance. The vibrator driving force was applied to the conductor through a "safety/breakaway" dowel. An open-loop vibration system consisting of a high stability oscillator, a power amplifier, and an electromagnetic vibrator were used to maintain the resonant vibrations at constant frequency and amplitude. With periodic checking and manual adjustments (approximately every 6 h) this system provided stable vibration control. It should be noted that for the first two tests (A1 and B1), the laboratory was not well insulated (this was later corrected) and temperature changes caused changes in resonance which in turn caused the vibration amplitude to drift down. The amplitudes were adjusted manually, but the net effect was that test A1 and B1 were subjected to a little less severe vibration conditions.

Upon completion of a test run (20,000,000 cycles), the vibration system was shut down and the conductor line tension released. A section of the conductor, centered on the "test clamp," was then cut out and visually examined for

fatigue damage. This examination disclosed the number and location (cross-sectional and longitudinal) of the strand breaks and cracks.

Experimental Results and Data Analysis

Experimental Data.—The primary experimental data consisted of the number of strand breaks and their locations for each test using the short, medium and long-radius suspension clamps. The total number of strand breaks and number occurring in each layer is shown summarized in Table 5. Upon completion of a test, all strand breaks were located by a visual inspection of the conductor. A strand failure location chart for each test is shown in Fig. 4. The chart summarizes the number and location of breaks and the suspension clamp used. The broken strands are shown as solid shaded circles and the cracked strands are shown as partially shaded circles (the propagation of a crack is indicated by the shaded portion). The sections shown are as viewed from the 3-1/2 in. (8.89 cm) location with the clamp keeper located directly at the top of the cross section and the clamp groove at the bottom.

Longitudinal distances from the 3-1/2 in. (8.89 cm) location (from the last point of contact) to the strand breaks were measured and in all but a few cases the breaks occurred within 1/2 in. (1.27 cm) from each other and were approximately centered at the last point of contact. Mean values and ranges for these longitudinal distances for the three clamps tested are presented in Table 6. An analysis of the data collected is given as follows.

Data Analysis and Results.—Since suspension clamps were the only parameter varied during the vibration testing, the resulting conductor fatigue damages should be indicative of the relative fatigue merits of the clamps tested. The data of Table 5 can be condensed for convenient comparative purposes as shown in Table 7. The values in this table clearly demonstrate the effectiveness of using longer radius clamps to mitigate fatigue damage.

The number of outer, middle, and inner layer breaks listed in Table 5 and located in Fig. 4 appear to indicate certain critical strand locations. For the three tests performed with the medium-radius clamp, failure locations in the outside layer were limited to strands along the bottom of the conductor where it rests in the clamp groove. The bottom location was also critical in the short-radius clamp tests; however, for this clamp, some outer strand failures at the top of the conductor cross section were also recorded. No outer strand failures occurred in the conductors supported with the long-radius clamp.

The majority of the strand breaks for all tests occurred in the conductor middle layers. These failures tended to be in the areas vertically above the clamp groove or below the clamp keeper. Broken strands in the inner layers also tended to occur vertically above the clamp groove or below the keeper. These breaks were greatest in number for conductors supported by the short-radius clamp. Inspection of Fig. 4 reveals that almost no strand failures occurred on the sides of the conductor. This is as expected since bending stresses, stress concentration factors, and fretting are all at minimal levels on the conductor sides.

The results of the visual inspection listed in the "Comments" column of Table 5 are conclusive in a couple of respects. First, since only one cracked strand was observed (Test A3), it appears that once a crack grows to a visible

TABLE 5.—Summary of Results of Visual Inspection for Strand Breaks

Test series (1)	Clamp (2)	Test number (3)	Strand Breaks				Comments (8)
			Outer (4)	Middle (5)	Inner (6)	Total (7)	
A	Short-radius	A1[a]	3	2	0	5	No cracks observed, abundant fret dust.
		A2	3	8	4	15	No cracks observed, abundant fret dust.
		A3	4	7	1	12	One crack (2/3 through) inner layer strand, abundant fret dust.
B	Medium-radius	B1[a]	1	1	0	2	No cracks observed, abundant fret dust.
		B2	1	6	0	7	No cracks observed, abundant fret dust.
		B3	2	4	2	8	No cracks observed, abundant fret dust.
C	Long-radius	C1	0	0	0	0	No cracks observed, abundant fret dust.
		C2	0	0	0	0	No cracks observed, abundant fret dust.
		C3	0	3	0	3	No cracks observed, abundant fret dust.

[a]Test specimen subjected to little less severe vibration amplitude due to stability problem.

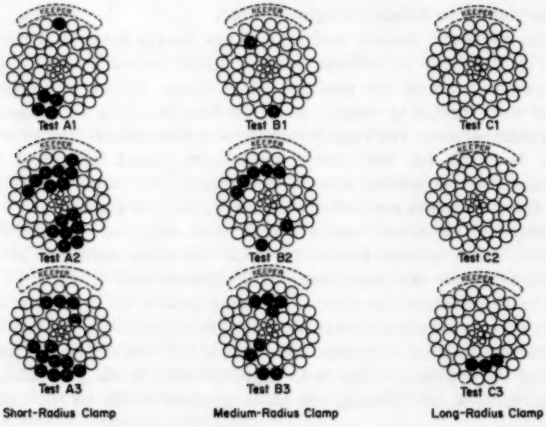

FIG. 4.—Strand Failure Location Chart

TABLE 6.—Longitudinal Locations of Strand Breaks

Suspension clamp (1)	Strand Break Location From 3-1/2 in. Point: Mean Value, in inches (Range, in inches)			
	Test 1 (2)	Test 2 (3)	Test 3 (4)	Average of all breaks (5)
Short-radius	3.65 (3.50–4.00)	3.58 (3.38–4.00)	3.70 (3.50–4.00)	3.64
Medium-radius	3.81 (3.62–4.00)	3.12 (2.00–4.00)	3.55 (3.38–3.88)	3.40
Long-radius	No breaks	No breaks	3.50 (3.38–3.62)	3.50

Note: 1 in. = 2.54 cm.

TABLE 7.—Comparative Results of Accelerated Fatigue Tests of 1033.5 kcmil 45/7 ACSR Conductor under Fixed Simulated Wind Power Input

Clamp (1)	Number of Strand Breaks			
	Test 1 (2)	Test 2 (3)	Test 3 (4)	Average (5)
Short-radius	5	15	13	11
Medium-radius	2	7	8	6
Long-radius	0	0	3	1

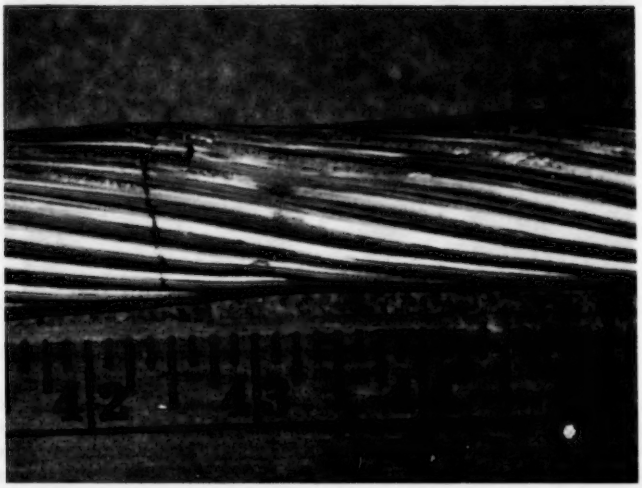

FIG. 5.—Conductor Deformations at Suspension Clamp Location

size, its rate of propagation is very fast. Secondly, the abundance of fret dust in the region of the suspension clamp is indicative of considerable fretting at the clamps. This fretting was probably a major factor in the fatigue damage sustained by the conductors.

FIG. 6.—Photograph of Strand Fret Mark

FIG. 7.—Photograph of Strand Break

The longitudinal location of strand break data of Table 6 indicates that breaks typically occur very close to the last point of contact. This is a region of reduced strand bearing stress (relative to that at the clamp), but where relative strand slip and thus fretting are possible. This implies that fretting is probably a much more important parameter in the fatigue process than is local strand crimping

due to excessive bearing stresses. During visual inspections of the test specimens, it was observed that many outer, middle, and inner strands immediately below the clamp keeper and above the groove were badly crimped (some almost 1/3 way through the cross section) indicating local regions of high bearing stress and plastic flow. Yet, not a single strand break occurred at these locations. Figure 5 shows a photograph of some outer strand local bearing deformations at the clamp location.

The detailed visual inspection performed at the end of each test revealed that without exception, every strand break nucleated at a strand outside fret mark and propagated from the oustide in. This is consistent with the fact that fretting and alternating stresses are higher at the strand outer fibers. Figures 6 and 7 shows photographs of fret marks and strand breaks at fret marks. These photographs are typical of all strand breaks occurring during this study.

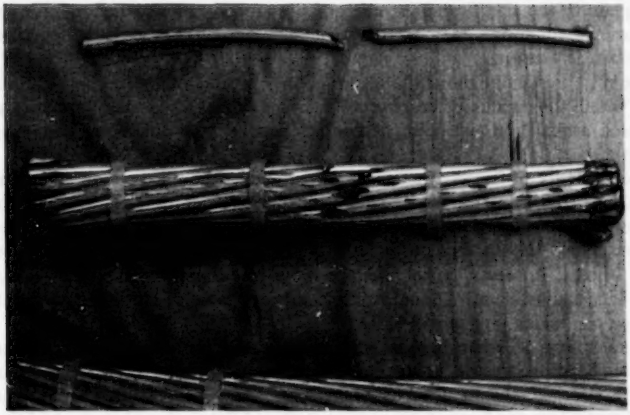

FIG. 8.—Photograph of Damage Inner Layer of 1033.5 kcmil 45/7 ACSR Conductor

Figure 8 is a photograph of a section of conductor removed from the suspension clamp with its inner layer exposed. Note the longitudinal location of the inner strand breaks relative to the "shiny" local strand indentations caused by the clamp bearing stresses, and the blackened fret marks which occur in front of the clamp.

Conclusions

The experimental results of this investigation indicates that suspension clamp hardware is a major factor in ACSR conductor aeolian fatigue, and that long-radius clamps can substantially mitigate this fatigue damage.

Based on theoretical considerations, the long-radius clamp should provide the least damaging stress environment of the three clamps tested. Static bending stresses should be smaller using this clamp as indicated by Eq. 7. Also, dynamic

bending stress ranges should be smaller due to local shifting of the section of maximum moment during vibration (due to the longitudinal separation of the top and bottom last points of contacts). Local bearing stresses should be smaller for the long-radius clamp because of the longitudinal separation of cable tension and clamp keeper pressures, and because of the larger bearing surface of the clamp. This reduced local bearing stresses should result in reduced strand crimping and longitudinal stress concentrations, and reduced levels of fretting. It appears that strand crimping is not a major factor in the fatigue damage of ACSR conductors; however, it is felt that the reduced fretting does have a significant positive effect on fatigue performance.

From the limited testing conducted herein, it is not possible to say which of the factors mentioned had the greatest effect on the fatigue performance of the test conductor. However, their net effect was a significant reduction in aeolian fatigue damage when using the long-radius clamp. Attempts to isolate and quantify the significance of each of the aforementioned factors along with the associated design features of the clamp hardware should be pursued in other research efforts.

The zone vertically above the clamp groove and below the keeper is a critical zone within the conductor cross section. Longitudinal locations of strand breaks centered around the last point of contact between the conductor and support clamp.

The existence of fretting was very evident, and without exception every strand break occurred at a fret mark. Thus it appears that fretting is the single most important parameter in fixing strand break locations. It is also a major parameter in determining the number of cycles at a given amplitude/stress level to cause these breaks. It seems logical that the reduced bearing stresses present when using long-radius clamps should result in a lower level of fretting and therefore prolong conductor fatigue life.

In summary, whether because of reduced static bending stresses, reduced dynamic bending stresses, or less severe fretting environment because of reduced bearing stresses, the long-radius suspension clamp used in this study caused significantly less conductor fatigue damage than did the other clamps. Additionally, the medium-radius clamp yielded approximately half as many strand breaks as occurred when using the short-radius clamp. Whereas the aforementioned results and conclusions are only directly applicable to the conductor, line tension, and clamp support condition (no articulation allowed) used in this investigation, engineering inferences and extrapolations can and should be made for cases where direct test results are not available.

Acknowledgments

The writers are grateful to the Alabama Power Company for their furnishing of the conductors and hardwares used in this investigation.

Appendix.—References

1. Grosskreutz, J. C., and Shaw, G. G., "Microstructures at the Tips of Growing Fatigue Cracks in Aluminum Alloys," *American Society for Testing and Materials Meeting Paper*, Atlantic City, N.J., June–July, 1966.

2. Poffenberger, J. C., and Swart, R. L., "Differential Displacement and Dynamic Conductor Strain," *Institute of Electrical and Electronics Engineers Meeting Paper,* New York, N.Y., Jan.–Feb., 1965.
3. Ramey, G. E., "Results of Accelerated Conductor Fatigue Tests Utilizing a Long-Radius Suspension Clamp," Report to Bethea/National Company, Aug., 1977.
4. Sandberg, S., "A New Transmission-Line Suspension Clamp," *American Institute of Electronics Engineers Fall General Meeting Paper,* Cincinnati, Ohio, Oct., 1949.
5. Sandor, B. I., *Fundamentals of Cyclic Stress and Strain,* The University of Wisconsin Press, Madison, Wisc., 1972, p. 89–90.
6. Silva, J. M., "An Experimental Evaluation on the Effect of Amplitude Reduction on the Fatigue Life of Overhead Transmission Lines Subjected to Aeolian Vibration," thesis presented to Auburn University, at Auburn, Ala., in 1976, in partial fulfillment of the requirements for the degree of Master of Science.
7. Siter, R. B., Strange, W. F., and Komenda, R., "The Effects of Galloping and Static Stresses on Conductor Fatigue," *Institute of Electrical and Electronics Engineers Summer Power Meeting Paper,* Chicago, Ill., June, 1968.
8. Sturm, R. G., "Vibration of Cables and Dampers—I," *Electrical Engineering,* Vol. 55, May, 1936, pp. 445–465.
9. Townsend, J. S., "An Experimental Investigation of the Comparative Effects of Two Support Hardwares on the Fatigue Life of 1033.5 kcmil 45/7 ACSR Conductors," thesis presented to Auburn University, at Auburn, Ala., in 1977, in partial fulfillment of the requirements for the degree of Master of Science.
10. "Transmission Line Reference Book: Wind-Induced Conductor Motion," Electric Power Research Institute, 1979.

OPTIMIZATION OF INTERGRATED ENERGY SYSTEMS[a]

By Theodore A. Shugar,[1] A. M. ASCE, Michael D. Jackson,[2] and Steven J. Anderson[3]

INTRODUCTION

This paper presents a quantitative approach for defining an optimal mix of energy conversion systems for supplying the energy demand requirements of medium to large industrial facilities. Fergy coion technologies studied include those for both renewable and nonrenewable sources. The former include solar-based, wind-based, and refuse derived fuel-based energy conversion technologies. The latter include conventional oil-fired and coal-fired technologies as well as fluidized-bed combustion and cogeneration technologies. Commercially supplied grid energy is included in the competition.

In contrast with most energy engineering economic studies, this method focuses on integrated energy conversion systems rather than on any one kind of energy conversion system. Integrated systems that are sought are defined as those mixes of energy conversion systems that are capable of supplying the energy demand and have the least, life-cycle cost. The central motivation of this study is that a least-cost mix of all feasible energy resources may be more economical than a least-cost system that is derived from one technology exclusively.

A mathematical model is derived and examined that defines optimal integrated energy systems within the framework of linear and nonlinear mathematical programming statements. A variety of participating energy conversion systems are synthesized with physical and economic input-output submodels. Key performance and cost parameters are examined for individual systems. Energy-related characteristics of industrial facilities that are specific to the mathematical model are defined. The division of total energy demand into energy-use sectors for space and hot water heating, process steam, and electricity is presented and reviewed. Application of the integrated energy system optimization model is demonstrated by employing it to match the combined energy resources of

[a]Presented at the February 5–7, 1980, ASME/ASCE Energy-Sources Technology Conference and Exhibition, held in New Orleans, La.

[1]Research Struct. Engr., Civ. Engrg. Lab., Naval Construction Battalion Center, Port Hueneme, Calif. 93043.

[2]Project Mgr., Acurex Corp., Mountain View, Calif. 94042.

[3]Project Engr., Acurex Corp., Mountain View, Calif. 94042.

Note.—Discussion open until October 1, 1981. To extend the closing date one month, a written request must be filed with the Manager of Technical and Professional Publications, ASCE. Manuscript was submitted for review for possible publication on March 12, 1980. This paper is part of the Journal of the Energy Division, Proceedings of the American Society of Civil Engineers, ©ASCE, Vol. 107, No. EY1, May, 1981. ISSN 0190-8294/81/0001-0121/$01.00.

a set of admissible technologies to the energy requirements of 10 medium and large Naval industrial facilities.

This paper will be of interest to engineers who need to be familiar with the issues surrounding the planning of future industrial energy supply and the complexity of their resolution. The complete report, of which this paper is a summary, is found in Ref. 1.

Applicable Optimization Theory

The central component of the present engineering economic analysis is the optimization scheme by which quantitative selections of least-cost systems are made. The optimization scheme in this study selects that mix of admissible energy conversion systems that possess the least, life-cycle cost while simultaneously satisfying a set of constraints. As it presently exists, the optimization scheme is cast as one in nonlinear programming. In explicating the nonlinear programming statement it is useful to begin with the linear programming statement that preceded it.

Linear Programming Formulation.—The optimization model originally began as a linear programming model as given in Ref. 6. The objective function was linear in the unknowns, and the constraints were linear inequalities in the unknowns.

The linear programming statement is as follows:

$$\text{Minimize:}\quad f(\mathbf{x},\mathbf{y}) = \sum_{i=1}^{N} c_i x_i + c_o \sum_{k=1}^{T} y_k \Delta t_k \quad \ldots\ldots (1)$$

$$\text{Subject to:}\quad \sum_{i=1}^{N} a_i(t_k)\, x_i + y_k \geq D_k \quad \text{for all} \quad k \quad \ldots\ldots (2)$$

$$\sum_{k=1}^{T} y_k \leq L_{\max} \quad \ldots\ldots (3)$$

$$\sum_{i=1}^{N} s_i x_i \leq A_{\max} \quad \ldots\ldots (4)$$

$$y_k \geq 0 \quad \text{for all} \quad k \quad \ldots\ldots (5)$$

$$x_i \geq 0, \quad \text{for all} \quad i \quad \ldots\ldots (6)$$

in which f = total uniform annual cost of the mix of energy conversion systems plus the total annual cost for commercial energy necessary to supplement facility energy demand; x_i = unknown number of units of energy conversion system, i; c_i = life-cycle, uniform annual cost of one unit of energy conversion system, i; N = total number of energy conversion systems being considered; c_o = uniform annual cost of one unit of energy which is purchased commercially by an industrial facility; y_k = unknown number of commercial energy units purchased by facility during the kth time increment; Δt_k = time increment size. It may be an hourly, daily, weekly, or monthly increment; T = total number of time increments which must equate to one year's time; $a_i(t_k)$ = performance coefficient for energy conversion system, i, at time, t_k; D_k =

facility demand for energy at time, t_k; L_{max} = maximum allowable annual amount of purchased commercial energy; s_i = real estate area required for siting one unit of energy conversion system, i; and A_{max} = maximum real estate area available for siting integrated energy conversion systems.

The optimal solution sought is that pair of vectors $(\mathbf{x}, \mathbf{y})$ which minimizes the value of the objective function, $f(\mathbf{x}, \mathbf{y})$, in Eq. 1, while at the same time satisfying constraint Inequalities 2–6.

The primary constraint is imposed by Inequality 2 which requires that the total amount of energy produced and purchased either equal or exceed the predicted demand for energy during the kth time interval. Notice that there is one inequality for every time interval, and that this constitutes a set of T inequalities. The first term on the left-hand side represents the energy produced by all energy conversion systems during the kth time interval. Some of these systems are renewable energy systems (wind, solar, etc.) for which energy output is independent of demand D_k. It is therefore possible that during some intervals the demand may be exceeded by supply. Other systems may be nonrenewable systems in which energy output can be modulated accordingly to demand. The second term represents the amount of energy purchased commerically during the kth interval y_k. It is supplementary energy whenever $\Sigma_{i=1}^{N} a_i(t_k) x_i < D_k$. Under these circumstances Inequality 2 becomes an equality, and the demand constraint is therefore active. Further, the non-negativity of y_k (Inequality 5) provides for a no-sell-back policy when an overproduction of energy occurs.

Inequality 3 requires that the sum of purchased commercial energy not exceed a prescribed maximum value L_{max}. This has been designated as a "crunch" constraint because of the rather traumatic impact its imposition may have on a given industrial facility. Inequality 4 requires that the total area necessary to site the optimal mix of energy conversion systems not exceed the maximum available area, A_{max}, allocated to such development. The final set of constraints are feasible set constraints. The non-negativity of x_i, specified by Inequality 6, merely insures against an obvious nonsensical result.

Using a linear programming model for optimizing the mix of integrated energy conversion systems has the following advantages:

1. It is relatively simple, and thus can be easily understood by a nontechnical decision maker.
2. It would not be difficult to analyze the effect that changes in any part of the problem would have on the solution and the total cost.
3. Computer programs that will solve the problem are well-understood and easily available.
4. A linear model is much quicker and easier to solve than a corresponding, but more general, constrained nonlinear problem.

However, the linear programming model also has the following disadvantages:

1. Since T can be very large (if Δt_k = 1 h, T = 8,760), the standard methods of solution can be time consuming and expensive.
2. The real problem is certainly nonlinear. This is due to many factors such as economies of scale, inflation, and changing energy demand.

The following reformulation removes the first disadvantage.

Piecewise Linear Programming Formulation.—The demand constraint, Inequality 2, is assumed active and therefore can be written as

$$y_k = D_k - \sum_{i=1}^{N} a_i(t_k)\, x_i \quad \text{for all} \quad k \quad \ldots\ldots\ldots\ldots\ldots\ldots\ldots\ldots (7)$$

Substituting this expression in Eq. 1 results in a new linear program which is stated as:

$$\text{Minimize:} \quad f(\mathbf{x}) = \sum_{i=1}^{N} c_i x_i + c_o \sum_{k=1}^{T} \left[D_k - \sum_{i=1}^{N} a_i(t_k)\, x_i \right] \Delta t_k \quad \ldots\ldots\ldots (8)$$

$$\text{Subject to:} \quad \sum_{i=1}^{N} s_i x_i \le A_{\max} \ldots\ldots\ldots\ldots\ldots\ldots\ldots\ldots\ldots\ldots (9)$$

$$x_i \ge 0 \quad \text{for all} \quad i \ldots\ldots\ldots\ldots\ldots\ldots\ldots\ldots\ldots\ldots\ldots\ldots (10)$$

Most of the constraint inequalities in the original statement have been eliminated by this substitution. The demand constraint, crunch constraint, and set constraint on y_k are to be satisfied implicitly in the computer program though they no longer appear explicitly in the new linear program statement. During iteration to the optimal point these constraints are to be satisfied in the following manner.

Inequality 6 is satisfied by monitoring the expression in brackets of Eq. 8. When this expression becomes negative it is reset to zero before computation continues. Therefore, when energy in excess of demand occurs, demand is satisfied but the excess energy is discarded computationally. Otherwise the demand constraint is satisfied through a purchase of commercial energy; that is, a sufficient, supplementary amount of energy is assigned to y_k. This amount is recorded for each time interval.

To satisfy the crunch constraint, Inequality 3, another monitoring process is proposed. During the computation, and if and when the running sum of the y_k exceeds the allowable maximum amount, $L_{\max}$, the value of c_o is assigned to be artificially high. In effect, the price of commercial energy is penalized so that it is not competitive with the cost of energy from any of the energy conversion systems studied. The solution scheme is then forced to opt for the alternative energy conversion systems while seeking to meet the demand.

The programming problem has been transformed into one with substantially the same objective function but with only the real estate area and non-negativity set constraints on x_i remaining. It comes at the expense of monitoring the objective function and the running sum of y_k as the program iterates. Since the second term in Eq. 8 remains linear in the x_i and the coefficients y_k and c_o can now abruptly change in value, the objective function is piecewise linear.

Ref. 2 stated the foregoing manipulations more concisely with the aid of the max function $y_k^+ = \max(0, y_k)$ or

$$y_k^+ = \max\left(0, D_k - \sum_{i=1}^{N} a_i(t_k)\, x_i\right) \quad \text{for all} \quad k \ldots\ldots\ldots\ldots\ldots\ldots (11)$$

Substitute y_k^+ for y_k in both Eq. 1 and Inequality 3 and the linear programming statement becomes:

$$\text{Minimize: } f(\mathbf{x}) = \sum_{i=1}^{N} c_i x_i + c_o \sum_{k=1}^{T} \max\left(0, D_k - \sum_{i=1}^{N} a_i(t_k)\, x_i\right) \quad (12)$$

$$\text{Subject to: } \sum_{k=1}^{T} \max\left(0, D_k - \sum_{i=1}^{N} a_i(t_k)\, x_i\right) - L_{\max} \le 0 \quad (13)$$

$$\sum_{i=1}^{N} s_i x_i - A_{\max} \le 0 \quad (14)$$

$$-x_i \le 0 \quad \text{for all } i \quad (15)$$

Though the objective function remains (piecewise) linear and the constraints remain linear, this statement is now in a standard form for nonlinear programming, and is usually written as: minimize $f(\mathbf{x})$, subject to $\mathbf{g}(\mathbf{x}) \le \mathbf{0}$, in which $f(\mathbf{x})$ is defined by Eq. 12, $\mathbf{g}(\mathbf{x})$ incorporates Inequalities 13, 14, and 15.

Further, this problem is solved using a standard approach to constrained nonlinear programming problems—the gradient projection method. Ref. 5 gives the necessary background on these methods. The gradient projection method is mathematically sound if the problem is still convex. It is convex if there are no local optimums that the program might converge to which are different from the true, global optimum. This has been shown to be the case in Ref. 2 for the problem at hand.

Nonlinear Programming Formulation.—This reformulation of the programming statement is motivated by the second disadvantage previously mentioned. The economy-of-scale phenomenon possessed by many energy conversion systems suitable for industrial facilities cannot be ignored in the analysis. Capital costs of these systems are not always linearly proportional to their size.

Economy of scale formulae of the form

$$I = CQ^n(x_i) \quad (16)$$

are used in this study. The capital or investment cost I is in dollars; C = a capital cost factor, in dollars per system unit size; Q = the system size and is a simple algebraic function of the independent variables, x_i; and n = an economy-of-scale exponent which varies between 0 and 1. Both C and n are determined, where possible, from cost data available in the literature. A value of 1 is assigned to n for those systems possessing no economy-of-scale effect.

The concept of economy of scale introduces nonlinearity in the following way. The uniform annual cost coefficient, c_i, expresses the annualized, life-cycle costs of energy conversion systems and is given by

$$c_i(x_i) = \frac{1}{b_n} CQ^n(x_i) + C_{\text{om}} + \frac{b_e}{b_n} C_f \quad (17)$$

in which C_{om} and C_f = the expected annual operation and maintenance cost and the expected annual fuel cost, respectively. The constants, b_n and b_e, are standard economic discounting terms which account for the time value of money and the differential inflation rates of fuels, respectively. Eq. 17 shows that the cost coefficients in Eq. 12 are functions of the independent variables x_i, and therefore, the objective function is nonlinear in the unknown x_i.

In summary, it has been shown that the piecewise linear programming approach manages to simplify the original linear programming problem by reducing the number of constraints and thereby simplifying its solution. It manages this in a way that does not alter the meaning of the original programming problem. Introduction of the economy-of-scale effect renders the formulation nonlinear. Further, the nonlinearity does not alter the convexity property possessed by the objective function as long as $n \leq 1$ in Eq. 17. A global optimum solution therefore exists. A suitable solution method for the constrained nonlinear programming problem presented is provided by the gradient projection method.

Description of Energy Conversion Systems Studied

The conventional and alternative energy conversion systems included in this study are listed in Table 1. A brief description and review of these systems is given in the following. Each system is represented by an input-output (I/O) model which is necessarily simplified but which provides a uniform mechanism for inclusion of many different systems and promotes a basis for equal evaluation.

The basic form of the system I/O models is shown in Fig. 1. Values for the indicated parameters distinguish one system I/O model from another. Cost parameters are those data necessary to calculate a life-cycle, uniform annual cost which is discounted at 10% over a 25-yr economic period. A base year of 1985 has been assumed for the 25-yr period.

Ref. 3 contains the basic Navy guidelines used for computing economic analysis parameters in this study. Navy policy assumes that the cost of money is 10% above and beyond any rise or fall in inflation. It assumes the government's ability to print money, sell or not sell bonds, etc., and annually collect taxes guarantees keeping pace with the national inflation rate. Differential inflation rates for fuels required to operate systems are included to calculate that portion of the life-cycle cost due to operation and maintenance. Long term differential inflation rate values used in this study are shown in Table 2. These values escalate the annual energy costs of fuels (see C_f term in Eq. 17) over and above the rate attributed to national inflation. Capital costs are computed by Eq. 16.

Performance parameters are those data that characterize the physical properties of the energy conversion system. Efficiency is the average ratio of output energy to input energy. The load factor accounts for all manner of down-time; it is the ratio of time during which the conversion system is operating to the maximum time the system could have been operating. The area factor is the amount of area (real estate) required per unit energy conversion system.

Primary input data consists of the current iteration value of system size x_i. The type and form of other input data depends on the system, but must always include some quantity of input energy to drive the energy conversion system. For nonrenewable energy systems, the input energy is in the form of required fuel. For renewable energy systems, input energy is in the form of insolation, wind velocity, etc. Input energy data for renewable systems are predicted from historical records.

Required output data consists of values for uniform annual costs that are the cost coefficients, c_i, of the objective function in Eq. 12. Energy production capability of the current configuration (size) is required to define the product

$a_i x_i$ in Inequality 13. Likewise, the land-area requirements are necessary output data for defining the product $s_i x_i$ in Inequality 14.

Conventional Oil-fired (or Natural Gas-fired) Energy Sources.—The economic analysis procedure separates energy demand into three end-use categories: (1) Heating; (2) process steam; and (3) electricity. Various combinations of energy systems within each energy-use sector compete on an economic basis with

TABLE 1.—Energy Conversion Systems Studied

Energy use (1)	Energy system (2)
Heating	Refuse derived fuel (RDF)
	Fluidized-bed combustion (FBC)
	Conventional coal combustion (CCC)
	Solar thermal
	Oil-fired boilers
Process steam	RDF
	FBC
	CCC
	Cogeneration
	Oil-fired boilers
Electricity	RDF
	FBC
	CCC
	Cogeneration
	Solar photovoltaic
	5-kW wind-turbine generator
	200-kW wind-turbine generator
	1,500-kW wind-turbine generator
	Commercial

TABLE 2.—Energy Cost Escalation Rates

Fuel (1)	Differential inflation rate, as a percentage (2)
Coal	5
Fuel oil	8
Natural gas and LPG	8
Electricity:	
New England states	7
Pacific coast	7
All other states	6

conventional systems to meet demand at minimum cost. The demand for conventional energy usually equals the portion of the total demand not met by alternative sources.

For the heating and process steam sectors, it is assumed that existing systems would be replaced with new, modern boilers fired on fuel oil. (It is believed that these systems could equally be assumed to be fired on natural gas since

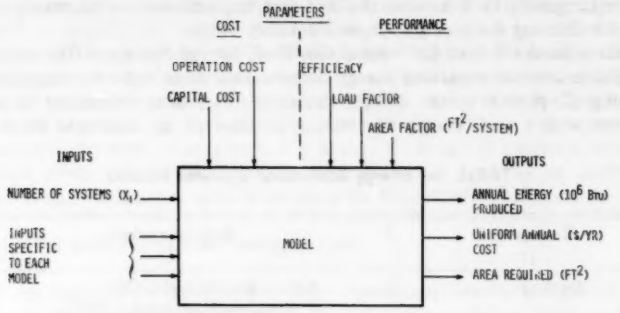

FIG. 1.—Energy Conversion System Input/Output Model

life-cycle costs and performance characteristics are about the same for both technologies.) Also, it was assumed that the demand was decentralized and therefore many smaller size units were required as compared to one large central plant. Thus, no cost for distribution systems is included. Average costs were then estimated for heating and process steam systems. Boiler efficiency (ratio of heat output to British thermal unit content of fuel input) was taken to be 80%.

For both heating and process steam systems, boilers were sized to meet the maximum peak demand remaining after alternative energy systems contributed to the heating or process steam sectors. Because of demand variations, this often meant that only 50% of the boiler capacity (ratio of actual energy produced to potential energy produced) was required. However, in situations where the demand was satisfied mostly by oil-fired systems much higher capacity factors were obtained.

In the electrical sector, demand not met by alternative systems is purchased from local utility companies. Electricity was assumed to be available in unlimited supply and no penalty was charged for consumption during peak demand periods. Actually, demand charges and time of day use will result in higher costs depending on individual utility rate schedules, but these costs were neglected.

Solar Thermal.—Solar thermal systems can be used to supply energy in all three end-use categories; however, this study only modeled a solar thermal system for supplying domestic hot water or space heating, or both. The system included flat plate collectors, thermal storage for 1 or 2 days, heat exchangers, and associated process controls. Costs were estimated based on installed collector square footage and constant fixed costs for heat exchangers and controls. No economies of scale were included.

System performance was predicted using an empirical technique known as the *f*-chart method. This method requires only average monthly insolation and temperature data to estimate system output. Collector efficiency and system heat losses are also included. The technique provides an approximate value for the fraction of total monthly load supplied by the solar system. Since storage was included, a constant daily output was then estimated based on the monthly figure.

Solar Photovoltaic.—A photovoltaic system was chosen over solar thermal systems for the electrical sector because of higher system efficiencies. The system modeled included concentrating parabolic trough collectors, dc to ac inverter, and associated wiring and protection systems. Also, the system was conceptualized to include circulating water to cool the photovoltaic cells. Electrical storage was not included in the system.

An overall system efficiency of 10% was assumed. Costs were estimated based solely on square footage of installed collectors. System performance was calculated based on actual hourly insolation data using collector efficiency curves.

Wind-Turbine Generators.—Three different size wind-turbine generators were modeled to convert wind power into electricity: (1) 5-kW; (2) 200-kW; and (3) 1,500-kW. Each of these systems included a rotor, turbine, tower, inverter, controls, wiring, protection systems, and foundations. Electrical storage was not included.

The analysis procedure was free to choose the optimum number of units in any size or combination of sizes. Costs were estimated on a per unit basis with no economies of scale assumed for multiunits. The costs for all components, materials, and installation were included.

Performance was modeled based on hourly wind velocity profiles and the conversion efficiency characteristics of each system. In general the larger units are more efficient and have correspondingly lower costs per produced kilowatt.

Refuse Derived Fuel (RDF).—This study modeled RDF systems to meet demands in the heating, process steam, and electrical sectors. Of the variety of possible systems, incineration in a waterwalled combustion chamber was chosen as the basis for all three systems. Further, only solid municipal garbage, either available on site or from nearby sources, was considered. Typically, municipal refuse consists of 70%–90% combustibles and on the average has an energy content of 4,500 Btu/lb.

The RDF systems in all three sectors included costs for transportation, shredding, air classification, storage, and incinerator as well as clean up devices such as cyclone and electrostatic precipitators. In addition, the RDF models included processing of the noncombustibles using a magnetic system to separate out ferrous metals and included a credit of 40% of operating cost for these recovered materials.

Overall efficiency (ratio of British thermal unit output to British thermal unit refuse input) for RDF heating and steam systems was 55%. A 23% efficiency was used for the electrical system. Also, because of material handling difficulties and refuse composition variations, an average 80% load factor was assumed for all three systems. No economies of scale were used on any of these systems.

Conventional Coal Combustion.—Aside from more advanced coal combustion techniques, this study also modeled a more conventional stoker-fired system for each demand sector. This system was selected over suspension firing because of its operating flexibility and because industrial size boilers tend to be smaller than is economical for suspension firing. The steam/hot water systems were conceptualized to include the boiler and associated equipment, pollution control equipment, and coal and ash handling equipment. The electrical system added a condensing turbine-generator and associated controls and protection systems.

The efficiency for the steam/hot water system was taken at 85%. This was reduced by an additional 10% to account for distribution losses. The efficiency

for the electrical system was assumed to be 36%. For all three systems, a 90% load factor was assumed. Costs for each system were itemized based on equipment and varied slightly depending on the sulfur content of the coal. The exponent for econimies of scale was 0.75.

Fluidized Bed Combustion (FBC).—An atmospheric FBC system was modeled for all three demand sectors. The steam and heating systems were the same and included the fluid bed, material handling equipment, limestone regenerator, and particulate clean-up systems. A turbine-generator and associate controls were added to the electrical system.

Costs for these system were itemized based on current experience and projections. Cost data were widely scattered and relatively conservative capital

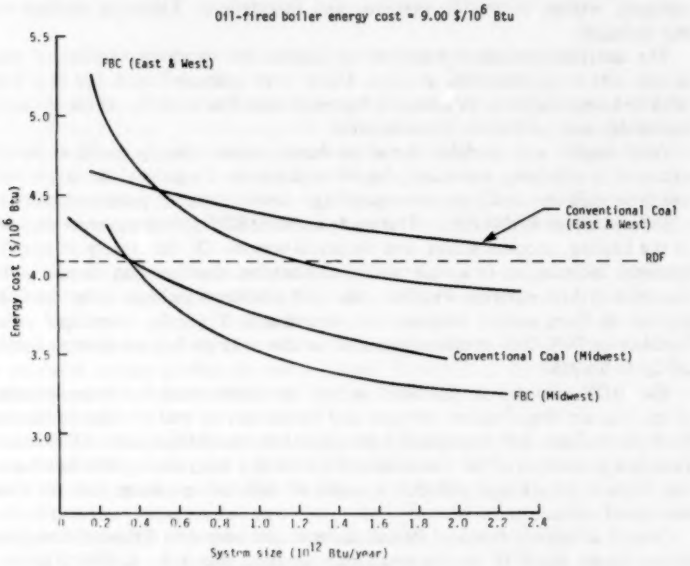

FIG. 2.—Conversion System Energy Costs in Heating Demand Sector

estimates of $3,600,000/megawatt and $3,900/1,000,000 British thermal units/yr were chosen for the electrical and thermal systems, respectively.

System efficiencies were 37% for the electrical model and 85% for the thermal model. Load factors were taken at 90%. Based on existing data, economies of scale were considerably higher than other systems, having an exponent of 0.65.

Cogeneration.—A steam topping cogeneration system fired on coal was modeled. The system consisted of four primary components: (1) Coal-fired stoker boiler; (2) coal and ash handling equipment; (3) pollution control equipment; and (4) an extraction turbine and generator. The system was conceptualized

to use 1,000 psig, 900° F-system and to provide steam at 150 psig for process use.

Capital costs included all major equipment, controls, and installation. In addition, as for the conventional coal model, costs varied slightly with sulfur content of the fuel. System performance was calculated based on estimated steam and electrical efficiencies (ratio of steam or electrical output to heating value of coal input). These values were 70% and 10%, respectively. A 90% load factor was assumed. The exponent for economies of scale was determined at 0.80.

Comparison of Economies of Scale.—Figs. 2 and 3 compare the effects of economies of scale for four of the aforementioned systems in the heating and process steam sectors, respectively. The energy costs are normalized on the energy that can potentially be produced by a given system and include the

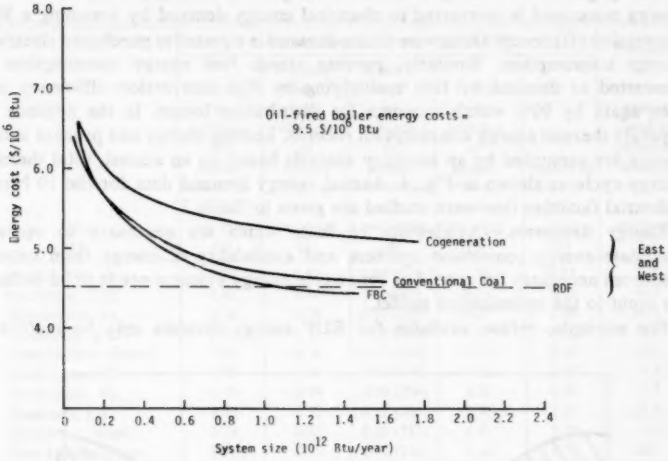

FIG. 3.—Conversion System Energy Costs in Process Steam Demand Sector

effects of assumed load factors. These energy cost curves were generated from Eq. 17 and the corresponding I/O models. Fig. 2 also shows the sensitivity of fuel prices and sulfur content on the cost of fluidized-bed and conventional coal systems.

As indicated in these figures, fluidized-bed systems are more economical at large sized compared to RDF or conventional coal systems. At smaller sizes, RDF systems become more cost effective. The influence of these trends are illustrated later when the results of application of the optimization model are considered.

Industrial Facility Energy Characteristics

The purpose of this section is to describe the energy-related characteristics

of industrial facilities that are required for use with the optimization model. These characteristics involve three general data catagories: (1) Energy requirements; (2) energy resources; and (3) fuel and commercial utility rates.

Energy Requirements.—Energy requirements at each industrial facility is disaggregated into three end-use categories: (1) Heating; (2) process steam; and (3) electricity. This information is generated from historical consumption data and projected as future demand requirements. In this regard it is tacitly assumed that conservation measures will be just sufficient to offset any growth and that energy demand will remain constant throughout the 25-yr economic time frame of this analysis. Calculated energy demand data refers to delivered or end-use energy and therefore is not always simply equated to past consumption. Recorded fuel consumption (natural gas, fuel oil, coal, and electricity) is converted to demand in each of the three end-use categories. Where an industrial facility currently generates some portion of its required electricity on site, the fuel energy consumed is converted to electrical energy demand by assuming a 30% conversion efficiency. Otherwise future demand is equated to purchased electrical energy consumption. Similarly, process steam fuel energy consumption is converted to demand by first multiplying by 80% conversion efficiency and then again by 90% which accounts for distribution losses. In the absence of separate thermal energy consumption records, heating energy and process steam energy are separated by an auxiliary analysis based on an annual, total thermal energy cycle as shown in Fig. 4. Annual energy demand data for the 10 Naval industrial facilities that were studied are given in Table 3.

Energy Resources.—Availability of fuels which are necessary to operate candidate energy conversion systems, and availability of energy from natural resources necessary for candidate renewable energy systems needs to be defined for input to the optimization model.

For example, refuse available for RDF energy systems may be restricted

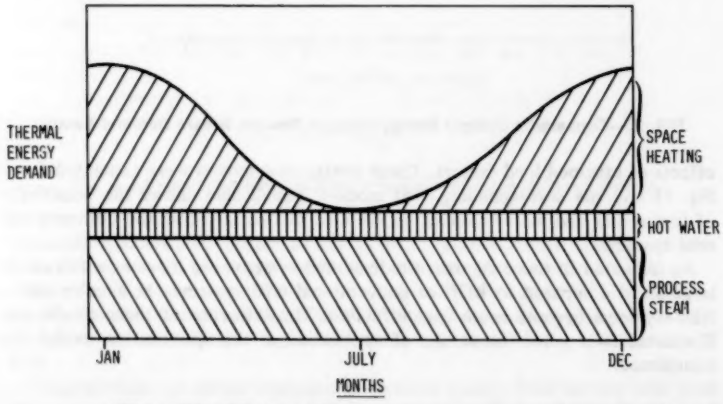

FIG. 4.—Total Thermal Energy Demand Resolution

to that which is produced by the industrial facility itself or it may also include that which is supplied by surrounding sources. Coal availability is realistically restricted by the capacity of rail, truck, and barge transportation networks. A more significant factor for coal-based energy may be the air quality standards that govern locally or nation-wide as shown in Table 4 and given in Ref. 4. Some industrial facilities may reside within designated nonattainment regions wherein no coal combustion may be employed.

Insolation and historical wind data is generally available in sufficient quantity and accuracy for integrated energy system analysis. Meteorological data tapes list hourly total insolation on a horizontal surface, hourly average wind velocities, and hourly ambient temperatures. This information is available for sites throughout the United States for various years.

TABLE 3.—Industrial Facility Energy Requirements

Site (1)	Annual Energy Demand (FY 1976)					Fraction of process steam used to generate electricity, as a percentage (7)
	Heating, in trillions of British thermal units per year (2)	Process steam, in trillions of British thermal units per year (3)	Electricity,[a] in trillions of British thermal units per year (4)	Total, in trillions of British thermal units per year (5)	Steam to electricity ratio (6)	
Norfolk, Va.	2.24	1.73	1.79 (524)[a]	5.76	0.97	7.2
San Diego, Calif.	0.92	1.69	1.93(565)	4.54	0.88	0.0
Philadelphia, Pa.	2.74	0.78	0.75 (205)	4.27	1.04	16.4
Charleston, S.C.	0.54	1.12	1.04 (301)	2.68	1.10	2.3
Pearl Harbor, Hawaii	0.63	0.58	1.13 (330)	2.34	0.51	0.0
Great Lakes, Ill.	1.58	1.04	0.39 (116)	3.01	2.67	2.13
Portsmouth, Va.	0.89	0.74	0.70 (206)	2.33	1.06	27.7
Pensacola, Fla.	0.39	1.32	0.55 (163)	2.26	2.40	22.8
Bremerton, Wash.	0.74	0.67	0.52 (153)	1.43	1.29	7.6
New London, Conn.	0.88	0.70	0.40 (116)	1.98	1.75	22.1

[a]Values in parenthesis are expressed in thousands of megawatt hours per year.

Energy resource data that are applicable to the 10 Naval industrial facilities studied are presented in Table 5.

Unit energy costs are the costs that an industrial facility must pay for fuel-energy as a consumer. The fuel-energy purchased is for supplying the demand for energy by conventional or status quo conversion methods. In this study conventional energy costs for heating and process steam were based upon decentralized boilers fired with fuel oil. Natural gas-fired boiler systems are assumed to possess similar fuel costs. Since the economic analysis has a beginning or base year of 1985, present unit fuel costs must be converted to their 1985 value. The specific fuel and commercial energy costs used in this study are given in Table 6.

Application of Optimization Model

A presentation and analysis of the results for each of the 10 industrial facilities

described would require considerable space. Further, the optimization model was developed primarily to provide information on the future application potential of energy conversion systems in a global or aggregate sense. The approach was based on the belief that when the results from many individual facilities are summed, definite application trends would emerge. Thus, the results of

TABLE 4.—Current Federal Stationary Source Standards

Pollutant (1)	Proposed standard (2)
SO_x	1.2 lb/10^6 Btu coal burned
Particulates	0.03 lb/10^6 Btu
NO_x	0.50 lb/10^6 Btu—Subbituminous coal
	0.60 lb/10^6 Btu—Bituminous coal

TABLE 5.—Fuel and Natural Energy Resources Available at Industrial Facilities

Site (1)	Refuse, in tons per day (2)	Air quality attainment status, (yes/no) (3)	Daily average insolation flat surface, in British thermal units per square foot (4)	Average wind velocity, in miles per hour (5)	Land area, in millions of square feet (6)
Norfolk, Va.	120	Yes	1,339[a]	8.71	13.89
San Diego, Calif.	190	No (NO_x, particulates)	1,338	5.74	6.53
Philadelphia, Pa.	50	Yes	1,339[a]	9.33	1.84
Charleston, S.C.	70[b]	No (NO_x, particulates)	1,516	8.14	22.18
Pearl Harbor, Hawaii	70[b]	Yes	1,778	11.12	Unlimited
Great Lakes, Ill.	41	Yes	1,329	9.33	2.68
Portsmouth, Va.	54	Yes	1,339[a]	8.71	6.53
Pensacola, Fla.	190	Yes	1,678	9.02	19.57
Bremerton, Wash.	68	Yes	1,117	9.44	8.70
New London, Conn.	30[b]	No (particulates)	1,243	9.25	2.70

[a]Based on insolation in Sterling, Va.
[b]Estimate.

the model application for the 10 Naval industrial facilities studied are presented and examined in aggregate form.

Aggregate Results and Analysis.—For each energy sector the aggregate mix of alternative and conventional energy systems that yield the lowest total energy cost at each facility is shown in Table 7. The status quo energy supply systems

that were presumed for each energy sector are also included for purposes of comparison and estimation of savings. Data for the status quo systems are enclosed in parenthesis.

Definition of optimal integrated systems was a basic objective of the study. Because they are presented here in aggregate form, it should first be stated that for all facilities analyzed no single conversion technology was selected exclusively by the model when coal conversion systems were not excluded as candidates. Integrated systems were always more cost-effective in supplying energy demand at industrial facilities. The relative penetration of optimal energy conversion systems is given for each energy sector under the heading, "fraction of demand met." These percentages sum to 100% in each sector. The energy represented by the percentage is given in the adjacent column. The annual

TABLE 6.—Unit Energy Costs[a]

Site (1)	Fuel oil cost, in dollars per million British thermal units (2)	Electricity cost, in dollars per megawatt hour (3)	Coal	
			Cost, in dollars per million British thermal units (4)	Sulfur content (5)
Norfolk, Va.	2.89	43.51	1.58	High
San Diego, Calif.	2.87	63.23	1.60	Low
Philadelphia, Pa.	2.89	52.28	1.58	High
Charleston, S.C.	2.97	43.83	1.58	High
Pearl Harbor, Hawaii	4.40	55.67	—	—
Great Lakes, Ill.	2.97	40.32	1.33	High
Portsmouth, Va.	2.89	63.91	1.58	High
Pensacola, Fla.	2.89	44.95	1.60	Low
Bremerton, Wash.	2.89	24.57	1.60	Low
New London, Conn.	2.89	52.58	1.58	High

[a]All costs are for 1985 expressed in real 1977 dollars.
[b]It is assumed that coal cannot be economically delivered to Hawaii.

energy delivered by the integrated system sums to the figure given for the status quo system. Two necessary prerequisites to economic comparibility are satisfied; the integrated system supplies the same amount of energy and has the same duration (25-yr economic life) as the status quo system.

The annual savings are computed by subtracting the annual costs for the integrated optimal system from the annual costs of the status quo system. The aggregate annual savings achieved by optimal integrated systems amounts to $97,500,000.

It is seen that potential savings derived from optimal integrated energy systems require extraordinary capital investment levels, an aggregate $323,500,000 in this study. However, the results indicate that for limited investment strategies, the best policy is to invest in on-site generation within the electrical energy sector rather than investing in either of the other two energy sectors. This

is primarily due to the high average energy cost of commercial electricity ($30.92/1,000,000 Btu) relative to that for FBC electrical systems ($9.54/1,000,000 Btu). Despite the high level of required investment that is indicated by the optimal integrated solution, an attractive payback period of 3.3 yr (323.5/97.5) can be calculated. Payback period calculations are often dismissed as oversimplifications of complex economic issues. But a 3.3-yr payback relative to a 25-yr

TABLE 7.—Aggregate Results for 10 Naval Industrial Facilities

Energy sector (1)	Optimal integrated system (2)	Fraction of demand, met, as a percentage (3)	Delivered energy, in billions of British thermal units per year (4)	Initial capital costs, in millions of dollars (5)	Total annual costs, in millions of dollars (6)	Average[a] energy costs, in dollars per million British thermal units (7)	Oil-consumed, in thousands of barrels per year (8)
Heating	RDF	1.10	126.6	2.33	0.56	4.08	—
	FBC	43.29	4,997.0	51.22	29.56	3.88	—
	Solar thermal	0.53	61.4	5.25	0.69	10.99	—
	Oil-fired boilers	55.08	6,358.0	32.76	58.07	9.13	1,419.0
	(Oil-fired boilers alone)	(100.0)	(11,543.0)	(44.12)	(101.17)	(8.76)	(2,577.0)
Steam	RDF	1.07	111.0	2.07	0.50	4.53	—
	FBC	25.14	2,604.0	24.15	12.11	3.98	—
	Cogeneration	26.39	2,733.0	46.03	19.96	5.40	—
	Oil-fired boilers	47.40	4,910.0	21.03	48.08	9.79	1,201.4
	(Oil-fired boilers alone)	(100.0)	(10,358.0)	(33.13)	(98.49)	(9.51)	(2,551.0)
Electricity	RDF	2.63	240.9	11.79	2.55	10.60	—
	FBC	42.27	3,866.0	81.91	44.42	9.54	—
	Cogeneration	6.11	558.6	—[b]	—[b]	—[b]	—
	1,500-kW wind	3.21	293.4	45.00	8.33	27.86	—
	Commercial	45.78	4,187.1	—	129.44	30.92	—
	(Commercial alone)	(100.0)	(9,146.0)	—	(252.15)	(27.57)	—
Total optimum mix		100.0	31,047.0	323.5	354.27		2,620.4
(Total commercial/oil alone)		(100.0)	(31,047.0)	(77.3)	(451.81)		(5,128.0)

Savings = $97,500,000/yr
Oil saved = 2,507,000 barrels/yr[c]

[a]Average life-cycle energy costs (Eq. 17) weighted on energy delivered at each industrial facility.
[b]Cogeneration costs included in steam sector.
[c]Data does not include potential oil savings by electrical utilities.

economic life is nonetheless an indicator of substantial, potential savings to be realized from investment in optimal integrated energy conversion systems.

Another attractive feature of optimal integrated energy conversion systems is that they represent a surprisingly high level of self-sufficiency from fuel-oil and commercial electricity. It can be observed in the heating energy sector that oil-fired conversion systems cannot be entirely displaced. In the aggregate,

45% of demand is satisfied by alternative energy conversion systems. In the steam energy sector this percentage increases to 53%, and in the electrical energy sector 54% of the energy can be supplied by on-site generation systems which require no fuel oil. Overall the optimal integrated energy systems, which are based upon least cost, produce a self-sufficiency level from oil of approx 50%.

A greater self-sufficiency level can only be obtained at the expense of increased (less than optimal) cost. This is because no artificial constraints were placed on consumption of fuel oil ($L_{max} = \infty$, see Inequality 13) while computing the data shown in Table 7. Yet the least cost solution represented approx a 50% level of self-sufficiency. However, coal combustion conversion systems were precluded from competition in four of the 10 industrial facilities analyzed. At these four facilities, the optimal integrated system degenerated to oil-fired technology almost exclusively. Thus, the level of self-sufficiency is heavily dependent on whether or not coal combustion is to be permitted in the future.

Optimal Energy Conversion Systems.—The various converison systems shown in Table 7 are the "winning" systems in the economic competition of the 10 industrial facilities studied. The optimization model selects these systems while iterating to a minimum cost solution for supplying the demand. The decision process requires the computer because the economic competitiveness of these systems depends on many factors (see Eq. 17, for example). System energy costs often vary with system size (see Figs. 2 and 3) and system size remains unknown during the solution process and is only finally defined after convergence is achieved. Other factors include energy demand size, variation in the demand with time, difference in demand size among the three energy sectors, availability of fuel, and fuel price. These are all site-specific factors and identification of optimal systems depends heavily in the accuracy of supporting input data.

The energy costs of FBC and RDF systems were very close in all three energy sectors and the optimal mix depended on refuse and coal availability, coal prices, and demand characteristics. In general, FBC systems were more cost-effective in the midwest or at large demands, but RDF systems almost always participated in one or another energy sector and always used all available refuse. Coal systems were excluded from competition at four industrial facility sites for reasons of either nonattainment or prohibitive coal delivery costs. At these sites, RDF was more effective in reducing total facility energy cost when participating in the electrical energy sector rather than when participating in either the heating or steam sector. RDF participation is invariably minor due to the availability of only small amounts of refuse.

The energy cost of FBC systems is less than the energy cost of cogeneration systems in the steam sector. But cogeneration generally participates more in the supply of steam because of free electricity by-product is created in the electricity sector for which cogeneration is credited. The credit arises because the optimization model seeks to minimize total facility energy cost instead of the energy cost within any one sector. Thus, cogeneration systems are effectively perceived by the model to be more economical than FBC systems.

There were two industrial facility sites where cogeneration did not participate in the optimal integrated system. These two sites, Great Lakes and Pensacola, are characterized by a relatively large ratio of steam energy demand to electrical energy demand (see Table 3). The cogeneration system in this study was modeled to yield 5.8 units of energy in the steam sector for each unit of energy supplied

in the electrical sector. Furthermore, its economy of scale is smaller than that for the FBC systems. The FBC systems benefit more from larger energy demands and are also a cheaper form of energy in the steam sector (see Figs. 2 and 3). In certain energy demand cases, these advantages offset the credits cogeneration systems receive for what is essentially a free electrical energy by-product. The results of this study demonstrated that this is the case when the ratio of steam energy to electrical energy demand is 2.4 or more.

Conventional oil-fired boilers or commercial electricity purchases always supplied a portion of the demand in the optimal integrated solutions. The actual penetration depended upon demand variation with time, cost, and whether or not coal was excluded. In all cases where coal was not excluded, these sytems participated as peaking units thereby reducing the size and the cost of competing alternative systems which participated as baseload systems. When coal was excluded, the status quo systems prevailed.

Only in Hawaii were solar thermal conversion systems and wind-turbine generators cost-effective. Their participation in the optimal integrated systems (as shown in Table 7) was due solely to the analysis of Pearl Harbor. They were not found to be cost-effective in the continental United States. It was found that for solar thermal systems to be competitive in the heating sector of large industrial facilities, solar radiation had to equal or exceed an average of 489 langleys/day. Likewise, in the electrical sector, wind-turbine generators were competitive only when the average wind speed equaled or exceeded 13 mph.

Summary and Conclusions

A methodology has been presented that determines the least, life-cycle cost energy supply system for medium to large industrial facilities. An industrial facility's energy needs are viewed as being comprised of three energy-use sectors: (1) Space and hot water heating; (2) process steam; and (3) electricity. Within each sector, renewable and nonrenewable energy conversion systems compete for participation in an optimal least-cost integrated system that is sufficient to meet the total energy demand, and other constraints as well, for a given industrial facility.

Implicit in the methodology is the possibility of optimal solutions composed of only a single energy conversion technology instead of an integrated system composed of more than one technology. However, application of the methodology to 10 medium and large Naval industrial facilities scattered throughout the United States has demonstrated that least, life-cycle cost systems are associated with integrated combinations of energy conversion systems. These systems require substantial investment levels, but computed simple payback periods are very attractive. Furthermore, the optimal integrated energy systems are consistent with a surprisingly high degree of self-sufficiency from fuel oil.

Energy conversion technologies that are most prominent in the optimal solution for medium to large industrial facilities include integrated systems of coal-based energy, and conventional oil-fired energy systems with smaller amounts of energy supplied by refuse-derived fuel. More specifically, for heating energy demands, a combination of fluidized-bed coal combustion, refuse-derived fuel, and oil-fired technologies are optimal. Process steam energy demands are best supplied by

a combination of fluidized-bed coal combustion, coal-fired cogeneration, and oil-fired technologies. The oil-fired sytems participate in a peaking capacity role for both the heating and process steam demand sectors whenever coal combustion is permitted. Electrical energy demand is best supplied by a combination of fluidized-bed coal combustion, coal-fired cogeneration, and commercially supplied grid energy. Commercial grid energy serves as a peaking source in the optimal integrated solution.

Where air quality regulations preclude the combustion of coal, oil-fired technology will continue to supply most all of the heating and process steam energy demands. Likewise, electrical demand will be met by commercial purchases of grid energy with small amounts displaced by on-site refuse-derived fuel-based energy.

For nine of the 10 medium and large Naval industrial facilities studied, plant-size facility applications of solar-and wind-based energy are not economically competitive.

Acknowledgments

This work was sponsored by the Naval Material Command and carried out under the Naval Shore Facilities Energy Research and Development Program.

Appendix.—References

1. "Application Potential of Energy Systems at Navy Sites," *Civil Engineering Laboratory Contract Report CR 80.006*, Vol. I and Vol. II, Acurex Corporation, Mountain View, Calif., Jan., 1980 (AD #A081383 and A081384).
2. Cooper, C., and Stear, E. B., "Analysis of Algorithms Used in CEL Report Optimization Model for Integrated Alternate Energy Systems," Department of Electrical Engineering, University of California, Santa Barbara, Calif. (Final Report, N62583/78 M R245, July, 1978).
3. *Economic Analysis Handbook*, NAVFAC P-442, Department of the Navy, Naval Facilities Engineering Command, Alexandria, Va.
4. *Federal Register*, Vol. 44, No. 113, June 11, 1979.
5. Luenberger, D. G., *Introduction to Linear and Nonlinear Programming*, Addison-Wesley Publishing Co., Inc., Reading, Mass., 1973.
6. Shugar, T. A., Shoemaker, N. F., and Eaton, M. L., "Optimization Model for Integrated Alternative Energy Systems," *Technical Memorandum No. 51-78-03*, Civil Engineering Laboratory, Port Hueneme, Calif., Nov., 1977.

EQUIPMENT QUALIFICATION: SPECIAL CONSIDERATIONS

By Anil K. Kar,[1] M. ASCE

INTRODUCTION

Nuclear power plant facilities have numerous safety-related equipment. These are needed for the safe-shutdown of the reactor. The safety requirements call for the verification of functional operability of the equipment. This functional operability is sought to be demonstrated not only for self weight and load generated as a result of operation, but also for significant vibratory loads, unusually high or low temperature, pressure, humidity, radiation, etc. The aspect of equipment qualification, which involves the consideration of effects due to earthquakes, is traditionally referred to as seismic qualification.

It has been a common practice in the past to consider only the earthquake motions among all the possible vibratory motions. Some of these vibratory motions, which can often be more severe than the seismic motions, are those due to the safety relief valve discharge (SRV) and the loss-of-coolant accident (LOCA). There are several possible types of valve discharges, e.g., one valve, 19 valves, etc. Similarly, there are several loss-of-coolant accidents, e.g., small break, intermediate break, large break, etc. The vibratory motions due to the SRV discharge and LOCA are characteristic of the boiling water reactors (BWR's).

As it has been mentioned earlier, not all the possible vibratory motions have been considered in the past. This has brought into question the qualification of many equipment, systems and subsystems. Similar to the neglecting of some of the vibratory motions in both test and analysis, concurrent mechanical, pressure and thermal loads have also been disregarded in the qualification of equipment by test. The paper deals with the application of vibratory and concurrent loads. Equipment qualification in general has been covered in Ref. 3; the requirements for qualification have been covered in Ref. 2.

An area of shortcoming in the qualification of equipment has been the failure to apply the three components of vibratory motion. It has been assumed that all equipment possess axes of symmetry, and the responses of the equipment in two horizontal directions are independent. It is shown in the paper that

[1]Chf. Exec., Engrg. Services International, Calcutta, India.

Note.—Discussion open until October 1, 1981. To extend the closing date one month, a written request must be filed with the Manager of Technical and Professional Publications, ASCE. Manuscript was submitted for review for possible publication on June 17, 1980. This paper is part of the Journal of the Energy Division, Proceedings of the American Society of Civil Engineers, ©ASCE, Vol. 107, No. EY1, April, 1981. ISSN 0190-8294/81/0001-0141/$01.00.

the assumption of independence of response can in many cases be untenable.

In the qualification by test, the test response spectra (TRS) have been shown to arbitrarily envelop the required response spectra (RRS). This disregard for the characteristics of the test input motion has led to arbitrarily conservative tests in some cases.

Concurrent Loadings

The attempted qualification of equipment has been for vibratory motions due to earthquake. Vibratory motions may develop during a LOCA as well as an SRV actuation. The attendant accelerations or displacements will require qualification of equipment for such effects of vibration. This is specially true for equipment in the containment or reactor building. In some instances, the loads due to the SRV or LOCA conditions will be higher than the traditionally considered dead load, live load and seismic load. Consideration of fatigue under numerous events of the SRV loadings can be important.

In the qualification of equipment by the method of analysis, all concurrent loadings are easily considered. However, in the case of qualification by test all concurrent loadings are not generally considered simultaneously. This can make the qualifications by test and analysis not fully consistent with each other.

In a test, it may be difficult to duplicate the design temperature, pressure and vibratory loads simultaneously. The same can be said of nozzle loads. Generally, the qualification for temperature, pressure, etc. are performed in the process of qualification for aging. In the tests for vibratory loadings, the only loads considered are electrical loads, where applicable, self weight of the equipment and the vibratory loadings. The normal operating pressures are not considered. Since the actual in-plant environment may have simultaneous temperature, pressure and vibratory loadings, the present method of qualification may not, in the opinion of the writer, constitute adequate qualification. It is important that proper attention be given to improve the method of qualification by test, so that nozzle loads, temperature and pressure loadings can be imposed on the test specimen simultaneously with the vibratory motions. In this connection, the following is to be noted in subsection 6.1.5 Loading, of *IEEE Std 344-1975* (1) Sec. 6 Testing:

> Seismic qualification tests of Class 1E equipment shall be performed with the equipment subjected to normal operating conditions. These shall include electrical loads, mechanical loads, thermal loads, pressure, etc., which adversely affect the Class 1E function. These may be simulated but should be shown to be equal to or greater than those expected in normal service. If not included as part of this test, the absence of the loading shall be justified.

IEEE Std 344 (1) recommends the consideration of operating condition loads concurrently with the vibratory motions due to seismic loads. Ref. 1 was prepared specifically for qualification of equipment for seismic loads. It would be logical to suggest that other concurrent vibratory loads, e.g., loads due to SRV actuation and LOCA shall be considered along with the vibratory motion due to earthquakes. Since the safety relief valve actuation can occur much more often than the

operating basis earthquake (OBE) and safe shutdown earthquake (SSE), the SRV loadings are also to be considered separately from the earthquake loads. This is primarily for determining the fatigue resistance of equipment to low stress cycles.

IEEE Std 344 (1) mentions the normal operating conditions. The writer sees no reason why other possible concurrent loadings, e.g., those for accident conditions, shall not be considered along with earthquake and SRV loadings for the qualification of equipment, when such loads may occur simultaneously.

The writer finds that it may not be too difficult to simulate the in-plant environment in many cases. The vibratory motions due to earthquake, SRV discharge and LOCA can be combined, where necessary. This is being done today for BWR plants. The temperature and pressure can be duplicated, even if approximately, during the test for vibratory motions. Even though it may be very difficult, nozzle loads can be simulated in some cases. Thus, there exists no reason why the qualification of equipment shall not be attempted for all concurrent loadings, including temperature, pressure, vibratory motions due to SRV actuation, LOCA, etc.

Three Components of Earthquake

The vibratory motions due to earthquake, SRV discharge and LOCA can be considered to have components along the three axes of the Cartesian coordinate system. The physical characteristics of the structure or equipment can lead to responses not only along these three coordinate directions, but also to rotary or rocking responses.

The effects of the three components of the vibratory motion are approximately considered in an analysis. The specifications on equipment qualifications generally call for the application of the three components of the vibratory motion. However, as it is considered difficult to apply the three vibratory motions simultaneously, *IEEE Std 344* (1) permits single or biaxial tests, if the tests are designed to conservatively reflect the seismic event at the equipment mounting locations, or if the equipment being tested can be shown to respond independently in each of the three orthogonal directions, or otherwise withstand the seismic event at its mounting location.

It should be clearly evident that a single or a biaxial test can almost never duplicate the effects of the three components of vibratory motion, unless of course the applied motion in the single or biaxial directions is significantly higher than the otherwise required test motion. In practice today, biaxial input motion is most frequently used in the qualification of equipment by test. It is to be noted here that many equipment show moderate to significant responses in torsional modes.

Let Fig. 1 be a "so-called" symmetrical equipment or cabinet. In the United States, this is almost invariably tested by applying biaxial motion. It is apparent that the corner elements of the equipment are subjected to the effects of the applied vertical and one horizontal motion. If, however, a vertical and two horizontal vibratory motions were applied, the corner elements would respond to all the three motions. This can be true of not only the corner elements, but also of many other elements of the piece of equipment.

Fig. 2 shows the transmissibility of motion due to a test motion in the side to side direction of a typical cabinet. It is seen that even though the test motion has been applied along only one horizontal axis, namely, the side-to-side direction, the responses in the frequency ranges of interest are about the same in the two orthogonal horizontal directions.

Fig. 3 shows the developed view of another cabinet. Also shown are the response spectrum curves developed for motions in two orthogonal horizontal

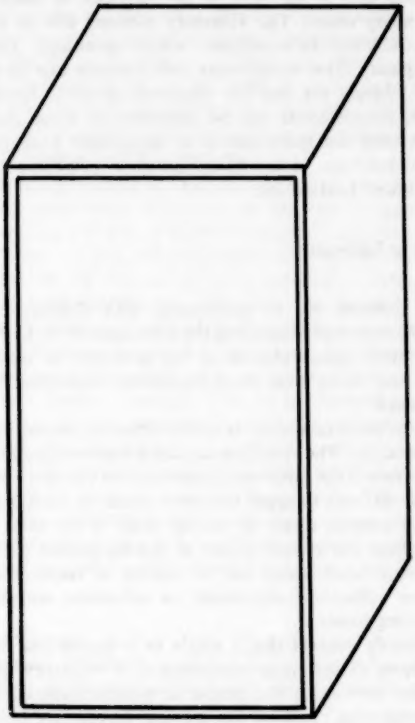

FIG. 1.—General Piece of Equipment: Cabinet

directions for test motion in the vertical and front to back directions. It is to be noted that the horizontal component of the test motion has been only in the front-back-front direction.

For the cabinet in Fig. 1 it is seen that the response in an element may not be independent of applied forces in some of the other directions. From Figs. 2 and 3 it has been observed that the responses in the horizontal directions can be coupled. Similar observations can be made of many other devices on

which at present a biaxial test motion is applied.

One way to approximate the multidirectional vibratory motion would be to locate equipment with their geometric axes at angles to the direction of motion applied to the test table. Components of the applied single axis or biaxial motions to the table would be effective in directions parallel to the axes of the equipment. This may, however, have the shortcomings of inadequate consideration of the gravity loads. The TRS's, generated for motion in the component directions, should envelop the RRS's. Since the motions, effectively applied along the

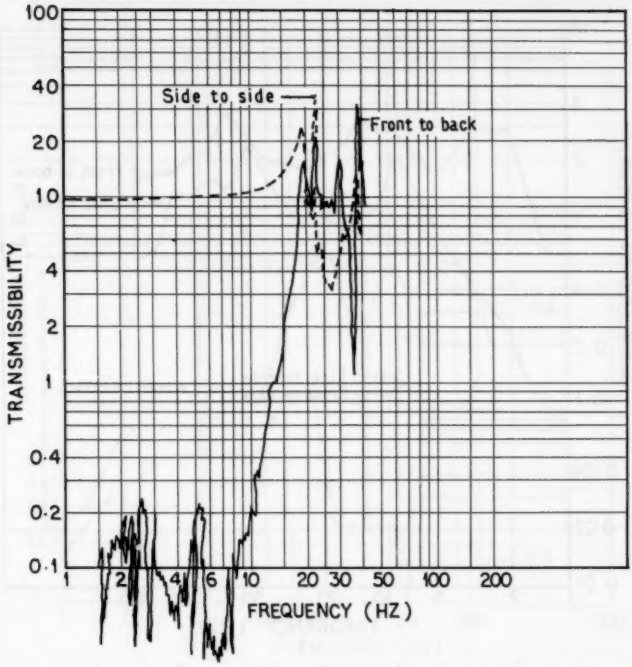

FIG. 2.—Side-to-Side Test of Cabinet: Transmissibility Plots

different axes of the equipment, are in phase, it will be necessary to repeat this test by rotating the equipment through 90° or 180°, as the case may be. Another way to approximate the three components of the vibratory motion would be to use the vertical RRS in conjunction with a horizontal RRS, obtained from the square root of the sum of the squares (SRSS) of the two horizontal RRS's. The test is performed for the vertical RRS and this new horizontal RRS. The test is repeated by rotating the equipment through 90°. If the applied vertical and horizontal motions are phase coherent, then tests are to be repeated for 180° out-of-phase motions.

TRS FROM VIBRATORY MOTION

For any test involving vibratory motions, it is necessary that the test response spectrum (TRS) curve, generated from an analysis of the test motion, envelops the specified or required response spectrum (RRS) curve. *IEEE Std 344* (1) states that the proof test seismic simulation waveforms should:

1. Produce a TRS which closely envelops the RRS or the applicable portions thereof using single or multiple frequency as required, to provide a conservative

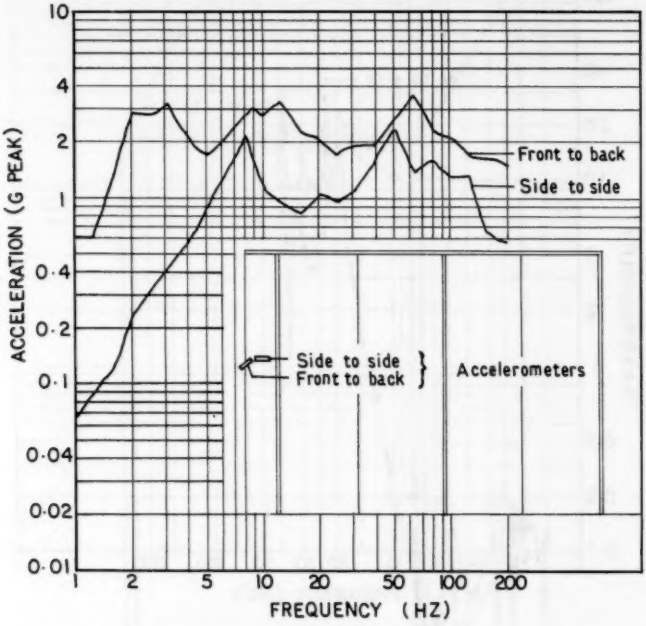

FIG. 3.—Front-to-Back/Vertical Test of Cabinet: Response Spectra

(but not overly conservative) test table motion.

2. Not include frequencies above the ZPA asymptote.

The ZPA is defined as the zero period acceleration, which is the acceleration that is not amplified beyond the input acceleration.

There are very good reasons why the TRS should closely envelop the RRS, and why the test motion should not include frequencies above the ZPA asymptote.

If the TRS is lower than the RRS, then (generally speaking) the test motion does not conservatively represent the design vibratory motion. At very small frequencies, however, the TRS may not envelop the RRS. This is because

it is difficult to attain large accelerations at small frequencies. This may not be of any concern because these small frequencies, say below 3 Hz, are less than the fundamental period of the equipment. Similarly, there may be problems of shaker control at high frequencies. This may be manifested during tests involving vibratory motions due to the SRV actuation. The TRS should closely envelop the RRS. Otherwise, the test motion may be too conservative. This may lead to an overdesign of the equipment.

Every physical system has the quality of filtering vibratory motions. The

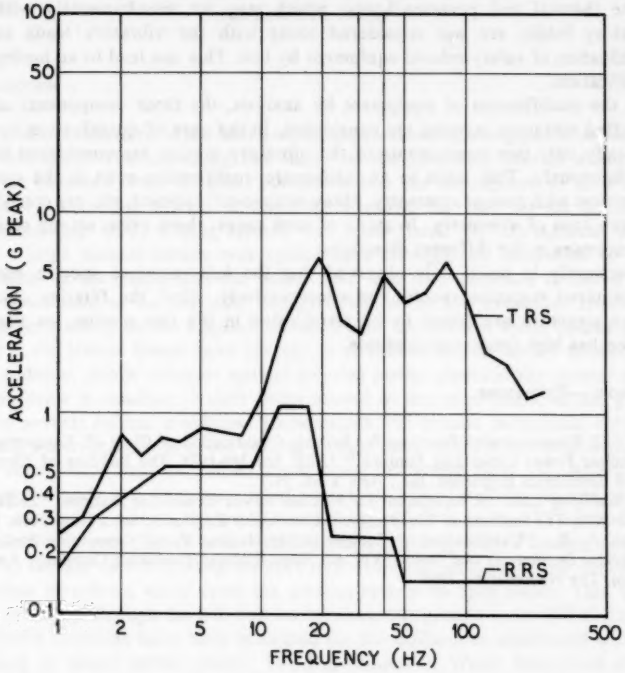

FIG. 4.—Example of TRS Enveloping an RRS Too Conservatively

ZPA asymptote of the floor or required response spectra indicates that the vibratory motions at the frequencies of the asymptote have been filtered without any magnification. Thus, application of any test motion, with frequency contents higher than that at the onset of the ZPA asymptote, is tantamount to disregarding the filtering effects of the structural or soil-structure system. Unfortunately, however, it is a frequent experience that the TRS envelops the RRS too conservatively. Fig. 4 is such an example. The test motion for equipment, with undetermined natural frequencies or with multiple frequencies, will generally be random in nature. It is to be noted here that the frequencies of internal

components of equipment are not monitored. It is suggested that for random motion, the ZPA of the TRS should not be more than one-fourth of the peak acceleration of the RRS for 1% damping, not more than one-third of the peak acceleration of the RRS for 2% damping, and not more than 1/2.6 of the peak acceleration of the RRS for 3% damping. The basis for this recommendation can be found in the attainable response to random input motion.

Conclusions

The thermal and pressure loads, which may act simultaneously with the vibratory loads, are not considered along with the vibratory leads in the qualification of safety-related equipment by test. This can lead to an inadequate qualification.

In the qualification of equipment by analysis, the three components of the specified vibratory motions are considered. In the case of qualification by test, generally only two components of the vibratory motion are considered to act simultaneously. This leads to an inadequate qualification even in the case of equipment with axes of symmetry. Many equipment, cabinets, etc. are considered to have axes of symmetry. In many of such cases, there exists strong coupling of responses in the different directions.

Frequently in tests, it is observed that the test response spectra envelop the required response spectra too conservatively. Also, the filtering qualities of the structure are found to be disregarded in the test motion, as the test motion has high frequency contents.

Appendix.—References

1. "IEEE Recommended Practices for Seismic Qualification of Class 1E Equipment for Nuclear Power Generating Stations," *IEEE Std 344-1975*, The Institute of Electrical and Electronics Engineers, Inc., New York, N.Y.
2. "Qualifying Class 1E Equipment for Nuclear Power Generating Stations," *IEEE Std 323-1974*, The Institute of Electrical and Electronics Engineers, Inc., New York, N.Y.
3. Kar, A. K., "Qualification of Equipment for Nuclear Power Generating Stations," *Nuclear Engineering and Design*, Vol. 60, North-Holland Publishing Company, Amsterdam, The Netherlands, 1980.

DOMESTIC WATER SUPPLIES FOR POWER PLANT COOLING

By Gideon Sinai,[1] M. ASCE, Willaim A. Jury,[2] and Lewis H. Stolzy[3]

INTRODUCTION

Only about one third of the heat generated in a steam power plant is converted into electricity. The remaining two thirds of the generated heat is waste and must be removed from the plant condenser into the atmosphere or to a body of water. A cooling system is therefore required for this. In the past, the "once-through" (OT) cooling method was widely used. By this method, water from a large natural source was cycled once through the condenser to cool the steam in the plant, and the waste heat was thus disposed to the water. This was found to be the most energy-efficient method available. However, recent restrictions on the disposal of waste heat into natural water bodies (P.L. 316a) in the United States have limited the continued use of the OT method.

In addition, public pressure against locating power plants in the coastal areas of California is resulting in their being moved to unsettled inland areas, giving rise to several further problems. These plants will require substantial volumes of fresh water, regardless of the cooling method used, and will therefore compete with other users for the limited fresh water resources (9,11,15). Alternative cooling methods also have associated problems. "Dry" systems do not require large volumes of water, but are not as energy efficient as the OT method and consume large quantities of generated electricity (2). Evaporative cooling methods such as the use of wet cooling towers suffer from the problem of the deposition of saline blowdown water from the cooling system to open fields. This water may percolate through the soil and contaminate the ground water (10,15,16,23).

Several solutions have been proposed for the difficulties associated with the building of inland power plants. The Department of Water Resources of the

[1]Lect. of Soil and Water Engrg., Faculty of Agricultural Engrg., Technion—Israel Inst. of Tech., Haifa, Israel.

[2]Assoc. Professor of Soil Physics, Dept. of Soil and Environmental Sci., Univ. of California, Riverside, Calif. 92521.

[3]Prof. of Soil Physics, Dept. of Soil and Environmental Sci., Univ. of California, Riverside, Calif. 92521.

Note.—Discussion open until October 1, 1981. To extend the closing date one month, a written request must be filed with the Manager of Technical and Professional Publication, ASCE. Manuscript was submitted for review for possible publication on June 17, 1981. This paper is part of the Journal of the Energy Division, Proceedings of the American Society of Civil Engineers, ©ASCE, Vol. 107, No. EY1, May, 1981. ISSN 0190-8294/81/0001-0149/$01.00.

State of California, and others, are considering the use of agricultural waste water and brackish waters as a coolant (20,21,22). Although this solution alleviates the competition for fresh water, it has other attendant problems which are discussed by Jury et al. (15). The United States Environmental Protection Agency (EPA) has proposed the use of evaporation ponds to prevent the contamination of ground water by the saline blowdown water. However this has proven to be expensive, and an alternative method of cooling water disposal by use of controlled irrigation of adjacent fields has been suggested (14,15,16).

An alternative approach to power plant cooling, the "once-through conveyor" (OTC) method, is proposed here. The method utilizes water from large domestic networks close to the site of the power plant. The water is siphoned from the domestic system, passed once through the power plant condenser and then returned, slightly warmed, to the system downstream of the intake point (Fig. 1).

The OTC method is similar to the conventional OT method. However it has several advantages which are detailed in the following text. In the southwestern United States, principally California, there are large water supply and aqueduct

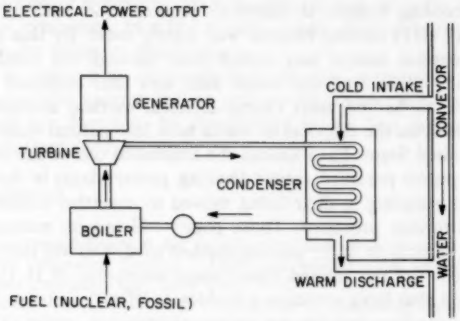

FIG. 1.—Schematic Diagram of Proposed OTC Cooling Method

networks that are highly suitable for application of the proposed OTC method. The method discussed herein is shown to be a feasible source of cooling water sufficient to meet anticipated expansion of electrical generating facilities in the western United States, which has no adverse environmental impact other than an insignificant water consumption and salinity increase in the domestic water supply.

Description of Proposed Cooling Method (OTC)

The principal elements of the system are shown in Fig. 1. Cold water is withdrawn from a conveyor, which may be a canal, a pipe, or any other part of a water supply network. The water is passed through the power plant condenser, where it acts as a coolant, and is then returned, slightly heated, to the same conveyor downstream of the intake point. The OTC method differs from the conventional OT method in that it uses water from domestic supply networks

and returns the water to the same network. Obviously, the effect of the cooling process on this water must be very carefully monitored, and the water source and recipient are therefore integral components in the overall design process.

The excess heat is carried into the aqueduct where it is dissipated by several different mechanisms, depending on the form of the aqueduct. For example, if the section of the aqueduct downstream of the water return point is a canal, then most of the heat will be transferred to the atmosphere by convection and evaporation carrying off latent heat. Thus is this case, there is some associated excess water consumption. Alternatively, if the heated water passes into a buried pipe, or network of pipes, or even into a tunnel, then the heat will dissipate slowly, mainly by conduction through the soil, and there is very little water consumed.

It can be seen therefore that analysis of the OTC method is dependent on the form of the aqueduct downstream of the heated water return point. For

FIG. 2.—Schematic Representation of Six Types of OTC Methods

example, if we consider the California State Water Project, several locations could be chosen for the intake and disposal points along the aqueduct. The networks, in the Central Valley consist mainly of a canal section (see Fig. 2) and also have several irrigation networks using water diverted from the aqueduct. The southern section of the aqueduct has some tunnel section reservoirs, and even a network, operated by the Metropolitan Water District of Southern California (MWD), to distribute water to the urban areas of Los Angeles and San Diego. We have therefore classified an aqueduct into six different possible forms: open canals, tunnels, buried pipes, water reservoirs and lakes, irrigation networks, and urban networks. Each of these different types of conveyors requires different design considerations with regard to power plant siting, heat dissipation mechanism, and environmental impact assessment. We have also

classified the general OTC method into six groups, corresponding to the six forms of water conveyors. These are shown schematically in Fig. 3.

Fig. 3 shows the California state project divided into segments in which each of the six OTC groups may be applied. If for example, a plant is located in the Central Valley so that the heated water will be returned into the irrigation water that is diverted from the main canal, then the heat will be dissipated through the irrigation network. This case is therefore designated as OTC-Irr network. If on the other hand, the power plant is located in the Central Valley

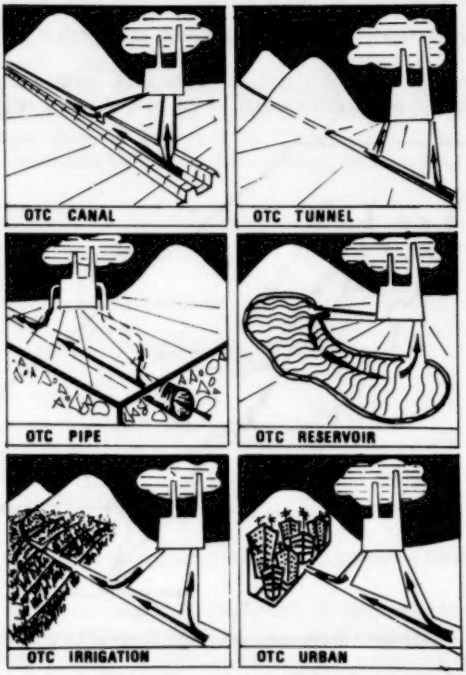

FIG. 3.—Division of California Aqueduct into Segments in which Different OTC Types May Be Applied

close to the California Aqueduct, then the heated water is returned into the canal reaches of the aqueduct. Therefore, in this case, the cooling system is designed as OTC-Canal.

Design Aspects in Applying OTC Method

In designing cooling systems for power plants there arises a conflict between the desire to minimize construction and operation costs, and the desire to prevent

any pollution or other hazards associated with cooling systems. Most states in the United States have restrictions against thermal or salinity pollution from power plants, although the degree of these restrictions varies from state to state. Most of these restrictions were imposed to prevent pollution from commonly used cooling systems, principally the conventional OT method. The regulations and rules that will be developed for the anticipated use of the OTC method are obviously not yet known, and therefore, a fully developed design concept cannot yet be proposed. However, an estimation of the environmental aspect of the OTC method, is presented in the next section of this paper. The design process for the OTC cooling system will have the following elements:

1. Determination of the electrical output capacity, heat rejection requirements at full load, projected capacity factor, and typical varied load operation of the power plant.
2. Collection and compilation of data on possible water sources for the cooling system, including flow characteristics and temperature regime of the water in the conveyors and climatic data for the site and downstream along the aqueduct.
3. Calculation and estimation of the thermal capacity of the conveyor which depends on, among other aspects, the type of OTC system being used.
4. Meeting the heat rejection requirements, determined in item 1, with the thermal capacity of the conveyor calculated in item 3.
5. Consideration of the environmental restrictions which may be imposed in the future; e.g., limitations on the maximum allowable increase in the temperature of the water.
6. Economic evaluation of the alternatives developed in items 4 and 5 in order to select the optimal system.

When planning a new power plant, the utility company is required to file a "Notice of Intention" (NOI) to the public authorities for consideration, public hearing, and approval. Regulations regarding submission of an NOI require the checking of different siting alternatives. This means that for every site that is considered, the same prescribed planning procedure must be followed. An optimal solution for a cooling system at one location may not necessarily correspond with the overall optimum siting for the power plant since there are many site-specific aspects considered in the planning process. Detailed consideration of the planning procedure for an OTC cooling system is beyond the scope of this paper. However, further details can be found in a paper by Sinai et al. (18). A brief review of some of the aspects involved in the planning process follows.

Determination of Power Plant Characteristics and Power Utility Management.—Power utility companies constantly survey and monitor their distribution areas in order to estimate future demand for electric power. The electrical load demand for a given region does not have a steady value. It fluctuates with the hour of the day, the day of the week, and even the month of the year. The utility company attempts to optimize the utilization of its generation facilities in order to meet this demand.

The demand figures for a specific region are usually expressed in a load-duration curve (Fig. 4). This curve shows the electrical load demanded, and the duration of each demand event. Maximum load usually has the minimum duration. The

generation plants are usually divided into three basic categories: viz. base load units, cycling load units, and peaking load units.

Analysis of the most economical combination of units suggests the following specifications: (1) Meeting the base load by units operating almost continuously at maximum capacity, using the least expensive fuel (these are usually fossil-fueled or nuclear power plants); (2) meeting the cycling load by units that operate for most of the time, but at a loading that varies with the demand; (3) meeting the peak load by units that operate only for the short peak-demand periods. These are usually gas turbine or hydroelectric plants, which have a short response time and relatively low operation costs, and are therefore economically viable even at a capacity factor of 0.05 or less.

Thus, we see that the cooling requirements for base load units will be of a steady nature, whereas those for cycling and peaking units will be more transient. In fact the cooling requirements for peaking units will be relatively small and the OTC system will therefore be most suitable for base load and cycling units.

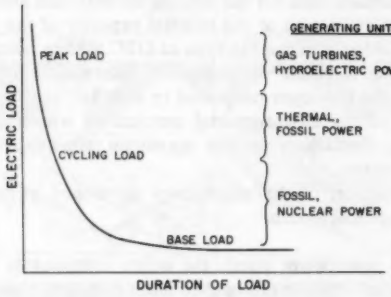

FIG. 4.—Generating Units Used to Meet Different Loads Defined by Electric Load Demand Curve

The operating efficiency of a power plant ranges from about 32% (nuclear) to as high as 38% (fossil), and thus for a 1,000 MW nominal electrical output capacity, between 1,600 MW and 2,100 MW of excess heat must be rejected by the cooling system. Open cycle cooling systems are typically designed to have up to a 10° C–15° C temperature difference between water entering and passing out of the condenser. These specifications may vary, but they are adequate for initial planning. Thus the siting of the power plant, its capacity, its capacity factor and operating characteristics, and its fuel type are sufficient parameters for initial design of the cooling system.

Estimating Thermal Capacity of Conveyor.—The thermal capacity of a given conveyor can be calculated using heat budget procedures. The concept of equilibrium or ambient temperature T_a is usually used. This is the temperature of the water under natural climatic conditions, without the influence of the power plant. When heat is added to the conveyor, the water temperature T will increase to a maximum at the heated water return point. Instead of dealing with the regime of the two temperatures T_a and T, it is useful to relate to

the difference $\Theta = T - T_a$ which is called "excess temperature" (Fig. 1). The excess heat injected into the conveyor will dissipate by various heat-exchange processes into the environment. This physical process was extensively studied in the 1960s and early 1970s for predicting thermal pollution of natural water bodies by warm water disposed from conventional OT cooling systems.

TABLE 1.—An Analysis of Heat Transfer and Water Consumption for Different Types of OTC Cooling Methods

Type of OTC (1)	Rate of heat dissipation along the conveyor (2)	Water losses through evaporation (3)	Models used in calculating water temperature distribution along the conveyor[a] (4)
Canal	very fast, mostly by evaporation and convection	high	$\theta(x) = \theta_o \exp\{[1 - (Q + 4KdDb^2/\rho C_p Q^2)^{0.5}]\, Qx/2dbD\}$
Pipe	very slow, mostly by conduction through the soil to the atmosphere	none	$\theta_s(x) = \theta_{os} \exp[-2\pi kx/Q\rho C_p \ln(2h - R/R)]$
Tunnel[b]	very slow, mostly through conduction to the ground, depending on the temperature differences	none	$\theta_{gr}(x) = \theta_{ogr} \exp[-2\pi kx/Q\rho C_p \ln(R_{gr}/R)]$; $\theta_{gr}(x) = T_w - T_{gr}$, $\theta_{ogr} = T_o - T_{gr}$
Reservoir	fast, mostly by evaporation and convection	high	As in OTC Canal but with other shape factors
Irrigation	fast, depending on type of irrigation method	moderate for sprinkler; high for surface irrigation	$\theta_s(x) = \theta_{os} \exp\{-2\pi kx/Q\rho C_p [\ln(2h - R/R) + \Sigma_{i=1}^{N} \ln((iL)^2 + (2h - R)^2/(iL)^2 + R^2)]\}$ in which $\theta_s(x) = T_w - T_s$; $\theta_{os} = T_o - T_s$
Urban[c]	moderate to fast, depending on branches and travel time	moderate	$\theta_s(x) = \theta_{os} \exp\{-2\pi kx/Q\rho C_p [\ln(2h - R/R) + \Sigma_{i=1}^{N} \ln((iL)^2 + (2h - R)^2/(iL)^2 + R^2)]\}$ in which $\theta_s(x) = T_w - T_s$; $\theta_{os} = T_o - T_s$

[a]Symbols are defined in Appendix II.

[b]It is assumed that the ground temperature remains unchanged ($T = T_{gr}$) at radial distance greater than Rgr from the tunnel center line.

[c]This equation is for $2N + 1$ parallel pipes; there are N on each side of the center pipe.

Several models describing the excess temperature, Θ, distribution along a conveyor and summarized in Table 1 have been published in previous papers (3,4,8,13,17,19). The temperature at the return point T_0 is the maximum temperature, and therefore the excess temperature θ is also a maximum at this point. From the return point, Θ decays downstream along the conveyor. The models shown in Table 1 for some of the OTC types are taken from models developed to describe similar situations. For example, the model shown for OTC Canal

is an expression developed by Brady (4) to describe excess temperature distribution $\Theta(x)$ from the heat injection point. The model shown for OTC-Irrigation and OTC-Urban Networks describes the case of parallel pipes buried under the surface with water flowing in the same direction in all of the pipes. It was developed by Kendrick and Havens (17) for a soil warming study.

In all of these models, steady flow of the water in the conveyor, constant flux of heat injected, and constant ambient temperature T_a have been assumed for the system. Simulation of more realistic cases for OTC-Canal will require complicated computer models such as in (3,8,13,19). Similarly, with OTC-Irrigation and OTC-Urban Networks, the geometry and flow regimes of the reaches in the network will greatly influence the computation, thus again necessitating computer simulation.

Qualitative estimations were calculated for the different OTC types from a detailed study of the heat exchange mechanisms (18). These estimations are given in Table 1 under the heading "Rate of Heat Dissipation Along the Conveyor."

Meeting the Heat Rejection Requirements with Thermal Capacity of Conveyor.—The thermal capacity of an aqueduct is directly proportional to the flow rate

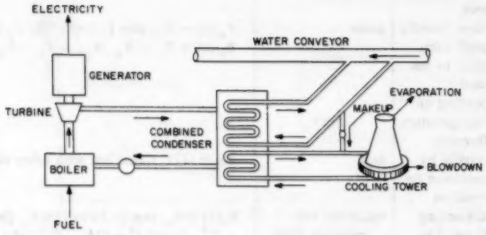

FIG. 5.—Schematic Diagram of Proposed Combined Condenser Method (OTC-TOWER)

of the water in the aqueduct. In many cases, the flow rate in aqueduct systems is governed by the local authorities in response to influences such as the storage situations, the demand for water, and the anticipated availability of natural water at the sources. Unlike the flow rate pattern in natural streams, the flow rate in aqueduct systems in the southwestern United States is not at its peak in the spring, nor at its minimum at the end of the summer. The seasonal peak in the demand for water for irrigation and public consumption is in the mid-summer and early fall periods (July–October). Thus the flow rate in the aqueduct networks of the southwestern United States is high during the summer, and therefore the thermal capacity of these conveyors is also high during the summer season.

The demand for electricity in the southwestern United States also peaks in the summer, due principally to the extensive use of air conditioning. Thus the peak demand for electricity conveniently coincides with the summer peak of the thermal capacity of the aqueduct systems. The large volumes of water flowing in the aqueducts can be used for cooling the generating units that operate at full capacity over this peak demand period. This enables substantial energy

conservation and reduced construction costs of the cooling facilities.

"Combined Condenser": Method for Increased Flexibility in Use of OTC Cooling Method.—The OTC method requires large volumes of water to cool the steam in the condenser. For example, it is estimated that about 617×10^6 m^3 of water are required annually to cool a 1,000-MW power plant. In some cases a power plant may be located near an aqueduct that has insufficient water for cooling the plant when it is operating at full capacity. In other cases an existing wet cooling system may need to be enlarged or even replaced. In both of these instances, it is proposed that the OTC method can be used in conjunction with another cooling method to meet the cooling requirements of the power plant.

TABLE 2.—Estimated Thermal Capacity of Water Supply Systems in Southwestern United States

Aqueduct system (1)	Length, in kilometers (2)	Annual Flow, in 10^6 cubic meters			THERMAL CAPACITY, in megawatts	
					Case I—Minimum	Case II—Maximum
		1977 and earlier (3)	1985 (4)	1995 (5)	Only one EPP on each aqueduct (6)	Combination of secondary networks, etc. (7)
All American:						
Imperial	130	3,423	unchanged	unchanged	5,550	12,000
Coachella	200	465	unchanged	unchanged	750	3,000
Central Valley Project	550	2,460	unchanged	unchanged	4,000	7,000
California Aqueduct:						
In San Joaquin Valley	688	1,972	3,225	4,721	5,750	15,000
In Tehachapi		1,156	1,722	2,610	(average)	5,000
Colorado Aqueduct	392	984	833	433	1,500 (or less)	2,500
Los Angeles Aqueduct	528	570	unchanged	unchanged	930	1,500
Gila Project	240	984	unchanged	unchanged	1,590	3,000
Salt River Project	128	1,625	unchanged	unchanged	2,630	5,000
Central Arizona Project	624	—	861	1,845	3,000 (in 1995)	7,000
Total for Southwestern U.S.					25,700	61,000

Note: Data on the aqueduct systems was compiled from Refs. 6, 7, 8, 12, 18, 19, 20, 22. The additional cooling requirements for California's power industry was estimated by ERCDC (5) to be 10,000 MW in the year 1985 and 26,000 MW in 1995.

A special "combined condenser" has been examined with Straughan and Larson (Ian Straughan and Lorry Larson, The Southern California Edison Co., Rosemead, Calif., personal communication). It will consist of two or more separate units receiving coolant from different sources and cooling the same steam from the steam cycle of a power plant.

Fig. 5 shows a schematic arrangement of the combined cooling system for

the case of a combination of cooling towers with an OTC system ("OTC-TOWER"). A similar combination could be set up with other cooling methods. The combined condenser can be constructed in the same way as an ordinary condenser, except that the OTC unit must be made from titanium alloy in order to prevent any contamination of the water in the aqueduct system. This is covered in more detail in the following section.

By way of illustration we consider the hypothetical case of a new 2,000-MW power plant to be sited in the low desert in Riverside County in California. The nearby Colorado Aqueduct had an annual flow of 984×10^6 m^3 in 1977. However this flow will be reduced to 433×10^6 m^3 in 1995 due to the construction

TABLE 3.—Overall Comparison of Cooling Methods for Thermal Power Plants

Cooling method (1)	Water Consumption for 1000-Megawatt Fossil Power Plant: In millions of cubic meters per year (2)	Water Consumption for 1000-Megawatt Fossil Power Plant: OT, as a percentage (3)	Unit Cost of Cooling[a]: In mils per kilowatt-hour (4)	Unit Cost of Cooling[a]: OT, as a percentage (5)	Conservation of Energy: Power plant efficiency, as a percentage (6)	Conservation of Energy: Energy losses, as a percentage of OT (7)	Environmental implications (8)
OTC[b]	22	100	0.118	100	37	—	Relatively none
OT	22	100	0.118	100	37	—	Thermal pollution of natural water bodies
Cooling ponds (CP)	44	200	0.17	150	35	6	Groundwater contamination (slight) Requires large areas
Spray ponds (SP)	42	191	0.18	160	35	6	Groundwater contamination (slight) Aerosal drift (moderate)
Wet towers (WT)	50	222	0.32	240	34	9	Groundwater contamination by disposing blowdown water A severe aerosol drift problem
Dry tower (DT)	3.6	16	0.50	480	26	43	Dust, noise

[a] As of 1975 United States prices.
[b] A proposed method, the figures are an estimation only.

of the Central Arizona Project (see Table 2). Since about 617×10^6 m^3 of water are required annually to cool a 1,000-MW plant by the OTC system, the Colorado Aqueduct could be utilized to meet the heat rejection requirements from a power plant of approx 1,350 MW until 1995, and thereafter only 700 MW. Another cooling system with an initial capacity of 650 MW, to be enlarged to 1,300 MW in 1995 could be constructed to operate in combination with the OTC system to meet the requirements for the proposed 2,000-MW plant. In this way substantial savings in fuel and construction and operating costs can be achieved (see Table 3).

ENVIRONMENTAL ASSESSMENT OF OTC METHOD

The quality of the water supplied to the customers is of prime importance both to the public as the user, and to the water resources authority which operates the distribution system. Several laws, restrictions, and regulations have been imposed to ensure maintenance of the necessary water quality. The possible effects of the OTC cooling method on the water quality in the aqueduct networks must obviously be carefully considered. Three main issues arise: (1) The risk of contamination of the water by toxic material while flowing through the condenser; (2) disturbance of normal biological activity in the water due to the excess heat disposed into the aqueduct; and (3) the possibility of oversalinization of the water in the aqueducts due to increased evaporation from the heated water. These issues are discussed in more detail in the following section.

Toxicity.—Investigation of the materials used to construct condensers showed that the copper alloy currently in use in closed-type cooling systems is a potential

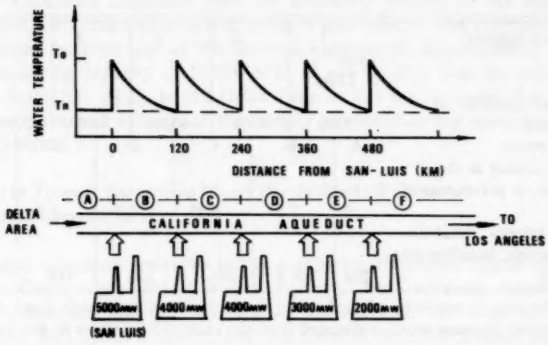

FIG. 6.—Schematic Diagram of Five Power Plants Located in Series along California Aqueduct

hazard to public health due to the possibility of contamination of the water by copper ions. However, the titanium alloy currently used in open-cycle cooling systems was found to be nontoxic. This titanium alloy has a high thermal conductivity and is therefore a suitable material for the tubes conducting the coolant in a condenser. Although it is twice as expensive as the copper alloy, it is suggested that the titanium condenser be used in applications of the OTC method (Straughan and Larson, personal communication). As an alternative, it may be possible to use a stainless steel alloy, which is considerably less expensive than titanium.

Heat Disposal.—The disposal of excess heat into natural water bodies is prohibited by P.L. 316a. This law is intended to protect the normal biological activity in the recipient water body at the point of heat injection. The law restricts the allowable elevation of the ambient temperature to about 1° C.

The OTC method disposes the excess heat into domestic aqueduct systems

in which the biological activity is not generally considered to be part of the natural ecosystem. Water flowing in an aqueduct network will finally be diverted either to irrigation of agricultural fields or for public use. In both cases, there is no major reason to keep the ambient temperature in the aqueduct system unchanged. The travel time and length of flow from a power plant located in the Central Valley along the California Aqueduct, to the customers in the Los Angeles area is sufficiently large so that there will be no change in the temperature of the water flowing from the taps in Los Angeles (18).

Thus the problem of pollution from heat disposal does not arise. No major degradation in wild life activity along the water supply systems is anticipated. However, this question should be re-examined more carefully.

Salinization.—Jury, et. al (15) have estimated that about 2.2% of the water withdrawn and passed through the condenser will be consumed through excess

TABLE 4.—Expected Increase in Salinity Along California Aqueduct Due to Situation Shown in Fig. 6

Power plant number	1 (San Luis)	2	3	4	5
Power plant capacity, in megawatts	5000	4000	4000	3000	2000
Aqueduct reach	A	B	C	D	E	F
Increased salinity in the aqueduct, in percentage of initial	0	2.25	4.55	6.9	9.3	11.76
Aqueduct salinity, (total dissolved solids, in milligrams per liter)	200	204.5	209	214	219	224

Note: The output capacity of each plant is progressively reduced along the length of the aqueduct, because water is diverted from the canal for irrigation in the San Joaquin Valley and the thermal capacity of the canal is therfore reduced in the lower reaches.

The spacing between the power plants was determined on the basis of Brady's model (1975) for heat dissipation along the aqueduct. It was calculated that the excess temperature, θ, would decrease from 10° C to 1° C (which is effectively zero) over a length of 93 km. Thus the 120-km spacing allows for a 30% safety factor.

evaporation due to the heating of the water when an evaporative cooling tower is used. Although we will use this number in our calculations, it is likely to overestimate water loss in an aqueduct system. The latter system would have water losses more closely corresponding to evaporation ponds or OT cooling systems which consume less water than the evaporative cooling tower (15). Thus for a 1,000-MW plant requiring 617×10^6 m^3 of water annually for cooling, 13.9×10^6 m^3 will be consumed through evaporation.

The increased salinity due to this evaporation is given by the following expression:

$$C_0 = \frac{C_i}{(1 + \alpha)} \quad \ldots\ldots\ldots\

in which C_0 = the salinity of the water in the aqueduct downstream from the section in which the excess evaporation takes place; C_i = the salinity of th water upstream from the power plant; and α = the ratio of water consumed by evaporation to water withdrawn by the cooling system. Jury, et al. (15) used a value for α of 0.022 for the conventional OT method. If we assume the same value for the OTC method then we get a salinity increase C_0/C_i factor of 1.0225. Thus, if all the water in an aqueduct is used for cooling, then there will be a 2.25% increase in the salinity of the water, which may be considered as negligible. The 2.2% water-loss estimate is conservative.

For example, if a 5,000-MW power plant were constructed in the San Joaquin Valley using the water in the California Aqueduct for cooling by the OTC method, it would cause an elevation in the salinity of the water in the aqueduct from about 200 mg/L total dissolved solids (TDS) in the Delta Area to about 204.5 mg/L in the Los Angeles area. This can hardly be monitored and is unlikely to be considered as contamination.

If we consider an extreme example of five power plants located in series along the California Aqueduct then the increased salinity in the aqueduct is only 11.76%. This example is shown in Fig. 6 and Table 4. The example assumes the maximum possible use of the thermal capacity of the aqueduct, enabling a total generating capacity of 18,000 MW. It can be seen that the salinity only increases from 200 mg/L in the Delta Area to 224 mg/L in the Los Angeles area. Thus increased salinity of the supply networks is not anticipated to be a major problem.

Estimation of Thermal Capacity of Major Water Supply Systems in Southwestern United States

The major aqueduct networks in the southwestern United States are the All American Canal, the Central Valley Project, the California Aqueduct, the Colorado Aqueduct, and the Los Angeles Aqueduct in California, and the Gila Project, the Salt River Project, and the Central Arizona Project in Arizona (see Fig. 7).

The length of conveying facilities and the annual flow data were collected from several sources, both published (1,6,7,12), and unpublished personal communication (R. Giles, Los Angeles Dept. of Water and Power; R. A. Marsden, Los Angeles Metropolitan Water District; B. Simpson, Nevada, United States Bureau of Reclamation), in order to evaluate the potential thermal capacity of these aqueduct networks (Table 2). In some cases there was no available data on the future flow in the aqueduct system. It was therefore assumed that the flow would remain unchanged until 1995 in these cases.

The thermal capacity of an aqueduct may be calculated in several different ways (18). A realistic assumption was made for purposes of calculation, that an annual average flow of 617×10^6 m^3 is required to pass through the condenser of a 1,000-MW power plant which is cooled by the OTC method. This is the same flow required for the conventional OT cooling method. On the basis of this assumption, two possible scenarios were calculated.

In the first case (Table 2, Case I—Minimum) it was assumed that only one power plant will be located along each of the aqueduct systems. This is representative of the situation in which heat disposal into the aqueduct systems

will be strictly controlled and limited. In this case it was calculated that a total capacity of 25,700 MW of new electrical generating facilities could be cooled using the aqueduct networks of the southwestern United States. About 73% of this capacity is located in California and the remainder is in Arizona, close enough to cool power plants also serving southern California.

In the second case a more liberal policy towards disposal of excess heat into the aqueduct networks was assumed (Table 2, Case II—Maximum). The maximum thermal capacity of each aqueduct system was calculated, based on the siting of power plants in series at selected intervals along the aqueducts (as was done in the example shown in Fig. 6). In addition, combined condenser

FIG. 7.—Aqueduct Networks in Southwestern United States

systems were considered to increase the flexibility in utilizing the water resources, and the use of secondary distribution networks such as irrigation and urban systems for cooling was also considered. An efficiency factor of 60% was applied assuming that not all of the capacity could be utilized. On this basis it was calculated that a total of 61,000 MW additional generating capacity could be cooled by the water supply systems in the southwestern United States. Again, most of this capacity is in California, or close to its border.

Only 10,000 MW additional generating capacity is predicted for the area for 1985 and 26,500 MW for 1995. Thus it can be seen that even if the conservative policy assumed in Case I is adopted, the thermal capacity of the major aqueduct networks in the southwestern United States is adequate to meet the expected need for cooling.

Comparison of Proposed OTC Method with Other Cooling Methods

The OTC method is similar in several aspects to the conventional OT method. In both methods there is a withdrawal of a large volume of water which is passed once through the condenser. They are both open-cycle systems which are considerably cheaper to construct than closed-cycle cooling systems such as cooling towers and ponds. They require very little storage facilities and the only energy required is that needed to pump the water through the condenser.

A general comparison of the major types of cooling methods is shown in Table 3. Most of the data in this table are from Jury, et al. (16) where the methods are covered in more detail. The factors compared are water consumption, water withdrawal, unit cost of cooling, energy conservation, and environmental effects.

It can be seen from the table that the OT and OTC methods are the cheapest and least energy consumptive of the cooling methods. However, they both withdraw large volumes of water which may be a disadvantage in desert areas where such volumes are unavailable. Apart from the dry tower cooling system, the OT can OTC methods are also the least water consumptive of the methods. The OT method has some adverse environmental implications due to thermal pollution of the natural water bodies used as a source and recipient for the coolant. However this problem does not arise with the OTC method.

Conclusions

There is an increasing tendency in California to move power plants from the coastal zone to inland sites. This shift has attendant problems in the cooling process since the ocean is no longer available as an unlimited source of coolant. The OTC cooling method, which utilizes water from existing domestic supply networks, has been proposed in response to these problems.

The OTC method is the cheapest to construct and operate, the least water consumptive of all wet methods, and the most energy efficient. In addition, it has less adverse environmental implications that the conventional OT method.

The thermal capacity of existing water supply networks in California and Arizona is well in excess of the anticipated needs for additional electricity generation in the near future. It is therefore suggested that new power plants should be sited along these existing large aqueducts in order to utilize their thermal capacity for cooling.

Although no major adverse environmental implications are anticipated in applying the OTC method, it is recommended that continued investigations into the environmental implications of the proposed system should be carried out.

Acknowledgment

The authors would like to thank the Southern California Edison Co. for financial assistance on this project. Thanks are also extended to Ian Straughan and Lorrey Larson, both from R&D Department at Southern California Edison, for their inspiring review of this work.

Appendix I.—References

1. "Annual Report Appendix for the Fiscal Year 76/77," The Metropolitan Water District of Southern California, Los Angeles, Calif., 1977.
2. "A Survey of Alternative Methods for Cooling Condenser Discharge Water," Dynatech, *EPA Report 16130DHS*, Environmental Protection Agency, Washington, D.C., 1969.
3. Bowles, D. S., Fread, D. L., and Grenney, W. J., "Coupled Dynamic Stream-Flow-Temperature Models," *Journal of the Hydraulic Division*, ASCE, Vol. 103, No. HY5, Proc. Paper 12929, May, 1977, pp. 515–530.
4. Brady, D. K., "Design of Impoundments and Lakes for Cooling," *Water Management by the Electric Power Industry, Water Resources Symposium No. 8*, E. F. Gloyna, ed., University of Texas, Austin, Tex., 1975.
5. "California Energy Trends and Choices, Vol. II: Electricity Forecasting and Planning," *1977 Biennial Report*, California State Energy Commission, ERCDC, State of California, Sacramento, Calif., 1977.
6. "California State Water Project in 1976 and California State Water Project in 1977," *Bulletin Nos. 132-76, 132-77*, Department of Water Resources, State of California, Sacramento, Calif., 1977, and 1978.
7. "California State Water Project, Vol. II. Conveyance Facilities," *Bulletin No. 200, II.*, Department of Water Resources, State of California, Sacramento, Calif., 1974.
8. Harleman, D. R. F., Brocard, D. N., and Najarian, T. O., "A Predictive Model for Transient Temperature Distributions in Unsteady Flows," *Report No. 175*, Ralph M. Parsons Laboratory for Water Resources and Hydrodynamics, Massachusetts Institute of Technology, Cambridge, Mass., 1973.
9. Harte, J., and El-Gasseir, M., "Energy and Water," *Science*, Vol. 199, 1978, pp. 623–634.
10. Holburt, M. B., and Ginler, B. J., "Legal Aspects of Salinity Caused by Cooling Towers," *Cooling Towers*, a Civil Engineering Publication Technical Manual, American Institute of Civil Engineering, 1972, pp. 54–58.
11. Huston, R. J., "An Overview of Water Requirements for Electric Power Generation," *Water Management by the Electric Power Industry, Water Resources Symposium No. 8*, E. F. Gloyna, ed., University of Texas, Austin, Tex., 1975.
12. Humlum, J., "Water Development and Water Planning in the Southwestern United States," *Publication No. 4*, Institute of Economics and Applied Geography, University of Aarhus, 8000 Aarhus C, Denmark, 1969.
13. Jobson, H. E., "The Dissipation of Excess Heat from Water Systems," *Journal of the Power Division*, ASCE, Vol. 99, No. PO1, Proc. Paper No. 9702, May, 1973, pp. 89–103.
14. Jury, W. A., Frenkel, H., Flühler, H., Devitt, D., and Stolzy, L. H., "Use of Saline Irrigation Waters and Minimal Leaching for Crop Production," *Hilgardia*, Vol. 46, No. 5, 1978, pp. 169–192.
15. Jury, W. A., Sinai, G., and Stolzy, L. H., "Future Sources of Cooling Water for Power Plants in the Western United States," *Water Resources Bulletin*, Vol. 15, No. 5, Oct., 1979, pp. 1444–1458.
16. Jury, W. A., Vaux, H. J., and Stolzy, L. H., "Reuse of Power Plant Cooling Water for Irrigation," *Water Resources Bulletin*, Vol. 16, No. 5, Oct., 1980, pp. 830–836.
17. Kendrick, J. H., and Havens, J. A., "Heat Transfer Models for a Subsurface, Water Pipe, Soil Warming System," *Journal of Environmental Quality*, Vol. 2, No. 2, 1973, pp. 188–196.
18. Sinai, G., Jury, W. A., and Stolzy, L. H., "Heat Dissipation of Power Plant Effluent from Water Supply Networks," *Journal of the Energy Division*, ASCE (in preparation).
19. Sonnichsen, J. C., et al., "The Colheat River Simulation Model," *Report No. HEDL-TME 72-103*, Hanford Engineering Development Laboratory, Richland, Wash., 1972.
20. Stamets, L., "Power Plant Cooling Options for California," *Report No. AID-20A*, Energy Resources Conservation and Development Commission, State of California, 1977.
21. "Use of Brackish Ground Water Resources for Regional Energy Center Development, Tularosa Basin, New Mexico," *Preliminary Evaluation FEA/G-77/102*, Department

of Energy Los Alamos Science Laboratory, N.M., 1977.
22. "Water for Power Plant Cooling," *Bulletin No. 204,* Department of Water Resources, State of California, Sacramento, Calif., 1977.
23. "Water Quality Control Policy on the Use and Disposal of Inland Waters Used for Power Plant Cooling," California State Water Resources Control Board, Sacramento, Calif., 1975.

Appendix II.—Notation

The following symbols are used in this paper:

b = width of canal;
C = salt concentration in cooling water;
C_p = specific heat of water;
D = mixing coefficient;
d = average depth of water in canal;
h = depth of pipe below soil surface, measured to pipe center line;
K = surface heat exchange coefficient (water-atmosphere);
k = thermal conductivity of soil;
L = spacing between parallel buried pipes;
Q = flow rate of water through single conveyor;
R = external radius of pipe;
Rgr = radial distance from tunnel center at which ground temperature is practically unchanged;
T = temperature;
x = horizontal distance from the heat injection point along conveyor; coordinate;
α = ratio of water consumed by evaporation to water withdrawn by OT cooling system;
θ = excess temperature due to thermal load; and
ρ = water density.

Subscripts

gr = ground;
i = counter numbering from the center pipe;
o = at heat injection point;
n = ambient;
s = soil; and
w = water in the conveyor.

Occurrence and Prediction of Acid Drainages[a]

By Frank T. Caruccio,[1] Gwendelyn Geidel,[2] and Mike Pelletier[3]

Introduction

Acid Drainage Problem.—During earth moving operations (such as in coal strip mining, highway construction, foundation excavations, tunneling, etc.) rock strata, which up to this time were isolated from the atmosphere, are exposed to accelerated weathering processes and oxidizing conditions. Under these new weathering conditions the rocks disturbed become physically and chemically decomposed to various degrees. The products caused by weathering may affect the drainages with suspended sediment, highly dissolved solids contents, metal contamination and, in some cases, acidity. Acidic drainages, in addition to degrading the aqueous environment, have been known to decompose concrete structures and to dissolve and pit metallic structures in contact with these drainages.

Acid mine drainages, as the name defines, are highly acidic drainage that have pH's below 2.3, anion concentrations (usually sulfate) exceeding 10,000 mg/L, and acidities averaging 5,000 mg/L (as $CaCO_3$). They form when certain sulfide minerals are exposed to the atmosphere and allowed to oxidize. Commonly, the problem is associated with coal mines but it has also been reported in areas where pyrite (or marcasite) is uncovered during the land disturbance. In the presence of oxygen and water the sulfides oxidize to form a series of soluble hydrous iron sulfates that commonly appear as white and yellow crusts on the weathered rock or sediment surface. Natural waters flowing over these crusts dissolve the salts which hydrolyze to form acidic drainages with high concentrations of sulfate and ferrous iron. Subsequently, the ferrous iron may be oxidized to the ferric state, complexing with ferrous and ferric oxyhydroxides

[a]Presented at the October 27–31, 1980, ASCE National Convention, held at Hollywood, Fla. (Preprint 80-658).

[1]Assoc. Prof., Dept. of Geology, Environmental Hydrogeology Program, Univ. of South Carolina, Columbia, S.C. 29208.

[2]Dept. of Geology, Univ. of South Carolina, Columbia, S.C. 29208.

[3]South Carolina Water Resources Commission, Columbia, S.C. 29204.

Note.—Discussion open until October 1, 1981. To extend the closing date one month, a written request must be filed with the Manager of Technical and Professional Publications, ASCE. Manuscript was submitted for review for possible publication on September 16, 1980. This paper is part of the Journal of the Energy Division, Proceedings of the American Society of Civil Engineers, ©ASCE, Vol. 107, No. EY1, May, 1981. ISSN 0190-8294/81/0001-0167/$01.00.

which impart a deep red and yellow color that is characteristic of the acid drainage.

The chemical reactions explaining the oxidation of FeS_2 and the production of acidity (H^+) are given by the following equations (1):

$$2FeS_{2(s)} + 7O_2 + 2H_2O = 2Fe^{2+} + 4SO_4^{2-} + 4H^+ \quad \ldots\ldots\ldots\ldots\ldots\ldots (1)$$

$$Fe^{2+} + \frac{1}{4}O_2 + H^+ = Fe^{3+} + \frac{1}{2}H_2O \quad \ldots\ldots\ldots\ldots\ldots\ldots\ldots\ldots (2)$$

$$Fe^{3+} + 3H_2O = Fe(OH)_{3(s)} + 3H^+ \quad \ldots\ldots\ldots\ldots\ldots\ldots\ldots\ldots (3)$$

The stoichimetry of Eq. 1 shows that 1 mole of FeS_2 will produce 2 moles of H^+ (acidity). In turn, the Fe^{2+} generated by the reaction of Eq. 1 can readily oxidize into Fe^{3+} and produce an additional 3 moles of H^+ (Eq. 3). Singer and Stumm (7) report that iron oxidation, Eq. 2, is the rate limiting step of the reaction and proceeds slowly under sterile conditions. However, iron bacteria can enhance the ferrous iron oxidation and, therefore, serve as catalysts for Eq. 2.

Three bacteria have been isolated from the acid mine drainage geochemical regimes and identified as being responsible for the catalytic affect. They are: (1) *Thiobacillus thiooxidans*, a sulfur-oxidizing bacteria; (2) *thiobaccillus ferrooxidans*, a bacterium which oxidizes Fe^{2+} to Fe^{3+}; and (3) *ferrobaccillus ferrooxidans*, another sulfur-oxidizing bacteria (10). These bacteria are indigenous to aqueous environments with pH values that range from 2.8–3.2.

Factor Affecting Drainage Quality

General Relationships.—Whether a rock or sediment system produces acidic or alkaline drainages is dependent upon the presence of the acidity and alkalinity producing components within that system. If the amount of alkalinity generated exceeds the acidity, then the system remains neutral or basic. The catalyzing bacteria are inhibited and solubility of Fe^{2+} and Fe^{3+} is greatly reduced, which collectively inhibits the acid production reactions. On the other hand, if the acidity generated within any part of the geochemical system exceeds the alkalinity, the solubility of the FeS_2 is enhanced and the acid production is increased. In addition, the low pH of the system, which controls the distribution of the catalyzing bacteria, will augment the amount of Fe^{3+} in solution, which increases the acid load. Once the acid reaction begins, it becomes self-propagating, and all acid-producing mechanisms begin to interact in a synergistic manner.

The mineralogy of the geologic regime controls, to a large extent, the chemical quality of the water or drainage permeating through the system. Table 1 lists some of the more common minerals that may be found at a particular site and the anticipated acid or alkaline production capacity that each will have upon exposure to the atmosphere and water.

It is important to remember that the quality variations expressed in Table 1 are qualitative and that the chemical translation of the mineral from the solid to ionic phase in water is dependent upon a variety of solubility and kinetic restrictions which limit the amount of each quality component in the aqueous phase.

To evaluate the drainage quality variations that could be expected from

particular rock strata, each mineral component that may affect a change in drainage quality is identified and the rock's potential to produce acidity is balanced against the potential to produce alkalinity to determine the net resultant geochemistry. In general, the problem can be resolved by identifying and measuring the amount of sulfide and calcareous material present in the system, in as much as these two mineralogic constituents have the greatest chemical impact on the aqueous regime.

The presence of feldspars may enhance the alkalinity produced, and certainly, the clays and micas afford a high ion exchange capacity which may ameliorate the acid produced. Usually these effects are manifested on a regional basis. In those cases, however, where the potential impact of the land disturbance is directly affected by the weathering reactions, it is the exposure of calcareous material and sulfides that dominates the drainage quality characteristics.

Acidity (Sulfur Content).—One measure of the stratum's capability to produce acid is the sulfur content. However, sulfur in coal, associated strata and organic-rich rocks, may occur as organic sulfur, sulfate sulfur, and pyritic sulfur. Organic sulfur is the component that is organically bound and is generally not chemically reactive. Generally, organic sulfur contents of coals have consistent average values between 0.35%–0.5% (weight per weight basis) (4). With rocks, the total sulfur measures pyritic sulfur.

Sulfate sulfur commonly represents the weathering products of the disulfides, as outlined in Eq. 1. Samples of rock collected from Kentucky, Pennsylvania, and West Virginia, were shown to have low sulfate sulfur values. This constitutes a small percentage of the total sulfur that was measured and can be generally neglected (4).

Iron sulfides, however, are generally recognized to be the primary sources of acidity because of their ease of oxidation. It is often assumed that the amount of acidity produced can be related to the amount of pyrite present, that is, the higher the pyrite (or sulfur) content, the greater the potential of the sample

TABLE 1.—Some Common Minerals and Expected Acid or Alkaline Impact on Drainages

Mineral (1)	Reactions and projected water quality impacts (2)
Quartz	Inert; low specific conductance
Feldspars	Mildly reactive; some alkalinity
Clays, micas	Ion exchange; may serve as neutralizing agent
Calcareous material (calcium, magnesium carbonate), e.g., limestone, dolomite, marble	Soluble in water; produces alkalinity in proportion to partial pressure of carbon dioxide and solubility of mineral phase
Siderite (iron carbonate)	Slightly soluble; produces alkalinity initially but turns acidic with iron oxidation
Disulfides [includes sulfides of iron (Pyrite, Marcasite) and those of lead, copper, zinc, etc.]	Oxidize to a series of soluble hydrous sulfates which readily hydrolize to produce acidic, high sulfate and metal-rich drainages

to produce acid. However, Caruccio (2,3) showed that rocks with a paucity of carbonate produced acidities that varied more directly with the pyrite particle size. It was shown that coarse grained pyrites (greater than 50 μ) were the least reactive of the sedimentary forms and remained relatively stable when compared to the small pyrite particles (less than 0.25 μ) which rapidly decomposed upon exposure to the atmosphere. In terms of a sample's potential to produce acidity (all other parameters being equal) the samples with a predominance of fine grained (framboidal) pyrite generate orders of magnitude more acid than samples having coarse grained pyrite. Thus, by monitoring samples for total sulfur, which reflects to some degree the pyritic sulfur content, and noting the pyrite morphology, the rock's potential to produce acidity can be assessed. This holds true only if the geologic system is carbonate deficient.

Alkalinity (Calcareous Material Content).—The first writer (2), and the first writer and Geidel (5) have shown that the degree of acidity or the potential of a rock to produce acidity is also related to the calcareous material ($Ca\text{-}MgCO_3$) content of the rock. This component can produce alkalinity and a highly buffered and potentially neutralizing leachate. In addition, it raises the pH of the ground-water regime which effectively surpresses the iron bacteria microbial activity and reduces the catalysis of the oxidation of ferrous iron. Recent evidence suggests that the calcareous material can also inhibit the oxidation of pyrite which tends to stabilize the sulfide bearing rock.

However, unlike the acid-forming reactions (which have few rate limiting steps due to the high solubility of the oxidation products), alkaline production from calcareous material is constrained by the low solubility of the specific carbonate mineral in water (siderite excluded) (6). As a result, levels of alkalinity are limited by the partial pressure of carbon dioxide, the time of water contact and the solubility of the specific mineral or rock, e.g., calcite, dolomite, limestone.

Role of pH.—One additional factor plays an important role in this examination, and that is, the pH of the geochemical system before the land disturbance. The pH of the ground-water regime may be low (due to the carbonic acid reaction predominating in the absence of calcareous material) or high (due to the carbonate species present). In the former case, the iron catalyzing bacteria are viable and capable of accelerating the acid-producing pyrite oxidation reactions and leach the pyrite grains of their stabilizing carbonate; whereas in the latter case the bacteria are displaced, the reactions are not catalyzed and the pyrite stabilizing mechanism is preserved.

The three factors examined in the foregoing have been summarized into a conceptual model that interrelates all three factors and projects the drainage quality that may be expected under a variety of conditions (3).

In one hypothetical hydrogeochemical case, the strata contain primarily coarse grained pyrites which are relatively slow reacting and do not produce large amounts of acidity. In the same setting there is an abundance of calcareous material which causes the pH of the ground water to be above 6.4 (which deactivates the iron bacteria) and gives the water a highly alkaline, strongly buffered character. In this geologic setting, the minor amounts of acidity produced by the coarse grained pyrite are neutralized by the alkalinity, the acid reaction is not catalyzed and the pyrite stabilizing carbonates, if present, are preserved. Here, drainages could be expected to be chemically neutral and have low sulfate concentrations.

At the other extreme of a hypothetical geologic setting most of the pyrite is fine grained and rapidly oxidizes to produce abundant acidity. Here, in the absence of calcareous material, the pH of the ground water is low which supports the iron bacteria that can catalyze the acid reaction. The lack of calcareous material also produces low alkaline-lightly buffered ground waters (low specific conductance) that are easily degraded by the acidity produced. Drainages in this environment have high acidity, sulfate and specific conductance.

Neutral-high sulfate drainages are created when strongly alkaline ground waters come in contact with acid drainages. Such a geologic system has strata that produce highly acidic, high sulfate drainages but which are capped by material that can produce highly alkaline waters. In this environment the acid waters are neutralized by the alkaline waters to produce neutral, high sulfate type mine drainages.

Moderately acidic, moderate sulfate drainages may occur with degrees of mixing of the two geologic settings.

Assessment of Stratum's Capability to Produce Acidic Water

Mine Drainage Characterization.—As shown in the foregoing, the chemical quality of a drainage emanating from a land pertubation is determined primarily by the ground-water geochemistry, mode of pyrite distribution, occurrence of calcareous material, presence of iron bacteria and the manner in which all of these are allowed to interact by the nature of the land disturbance. Thus, the prediction of acid waters cannot be based exclusively upon rock analyses. At best, rock analyses provide a first approximation of the expected drainage quality and it is only when the strata of various chemistries are allowed to interact in a completed or restored site (which itself is constantly readjusted in terms of its hydrology, geochemistry, pore space gases, and surface revegetation) that the quality of drainage can begin to be assessed. Usually these adjustments take place over many years and the true nature of the drainage quality may not be immediately discerned.

The information presented in the following, in terms of the assessment of a stratum's capability to produce alkaline or acid drainage is best used as a guide for the placement of rock material to minimize the environmental impact of the land pertubation on the adjacent streams. Acid-producing material should be isolated from the near surface environment, whereas alkaline material should be utilized to enhance revegetation efforts. To extend rock analyses to the prediction of drainage quality without considering the kinetics of acid or alkaline release, the ground-water geochemistry, the chemistry of recipient streams, the quality of the rain, the arrangement of the material in the backfilled site (blending versus segregation), the hydrology of the site, the evolution of pore space gases, and the chemical loads (as opposed to concentrations) of the acid and alkaline leachates, ignores the multivariant nature of the acid drainage problem and will lead to erroneous conclusions.

Experimental Design.—The initial objective of this study was to ascertain, through laboratory experiments, the affect that various leaching solutions would have upon the quality of leachates from several dark gray shales. Historically, these rock types produce acidic drainages. Because each sample was expected to have a different chemical composition, the experimental design was modified

to include an ancillary study to see which parameter best predicts the quality of leachate expected from each sample.

Eleven samples of dark gray to black shales were collected from newly cut cores of several strip mines in Wharton Township in southwestern Pennsylvania. Four samples were collected from above the Brush Creek coal seam, four from above the Mahoning coal, and three from above the Lower Kittanning seam. The 11 shale samples were crushed to pass a 4-mm sieve and subsequently riffled into three representative portions of roughly equal size, giving three groups and a total of 33 samples. Each of these was then further riffled to produce two representative but unequal portions. The larger portion was used in the simulated weathering tests, and the smaller portion was used for whole rock analysis.

The small portions (10 g–20 g) of the samples were pulverized to pass 100 μ and analyzed for total sulfur (a measure of the pyrite content) and calcareous material contents. These two parameters, and the relative preponderance of

TABLE 2.—Chemistry of Synthesized Acid Rain, *R*, and Synthesized Acid Mine Drainage, *A*

Synthesized Acid Rain, *R*		Synthesized Acid Mine Drainage, *A*	
Component (1)	Concentration, in milligrams per liter (2)	Component (3)	Concentration, in milligrams per liter (4)
H^+	0.21	Fe^{+++}	210.0
Ca^{++}	1.08	Al^{+++}	15.0
Mg^{++}	0.15	Mg^{++}	51.0
Na^+	4.75	Mn^{++}	19.0
K^+	2.25	Ca^{++}	100.0
SO^-	8.45	Na^+	2.0
Cl^4	9.39	H^+	3.0
NO^-_3	6.50	SO^-	1,100.0
		Cl^4	110.0

one over the other, should identify the sample's acid or alkaline production potential.

The sulfur analyses were made by igniting a 100 mg portion in a LECO Combustion Furnace, entraining the gases and sulfur dioxide into a dilute HCl, starch, and KI solution and titrating the solution with KIO_3 to a predetermined endpoint. These results are expressed as sulfur percentages on a weight per weight basis (4).

The calcareous material content was analyzed by the hot digestion of 2.00 g of sample in an aliquot of 0.1 N HCl, cooling and back titrating to a predetermined endpoint with a standard base. The amount of titrant required to achieve the endpoint measures the amount of HCl consumed by the samples and is a measure of the neutralizing potential (NP) of the sample (8). These results are expressed as milligrams of $CaCO_3$ equiv per 1.0 g of sample.

The 33 larger portions of the samples (100 g–300 g) were placed in individual covered plastic chambers through which humidified air was constantly passed.

At weekly intervals the chambers were opened and one group of samples was covered with deionized water (*W*), the second group was covered with synthesized acid rain (*R*), and the third group with synthetic acid mine drainage (*A*). The composition of these solutions is shown in Table 2.

The leachate volume produced by the flushing was measured and analyzed for pH, specific conductance, acidity (hot mineral), alkalinity (cold titratable), and sulfate concentrations in accord with *Standard Methods* (9). Using the weight of the rock sample used in the weathering test and the leachate volume and quality, all results were converted to milligrams of acidity, alkalinity, or sulfate produced for each leaching per 100 g of sample. These values were plotted versus time to graphically depict acid or alkaline production trends with time.

By relating the measured chemical parameters to the chemical reactions previously mentioned, the chemistry of the leachates can be used to interpret the weathering responses of the rocks to the different leachants. As an example, the specific conductance of the leachate measures the ionic strength of the solution and reflects the rock sample's reactivity. Sulfate ion is derived primarily

TABLE 3.—Chemical Reactions and Associated Leachate Characteristics

Leachate Quality				
Specific conductance (1)	Sulfate (2)	Acidity (3)	Alkalinity (4)	Chemical Reactions (5)
low	absent	absent	absent	Sample is inert
high	absent	absent	high	Calcium, magnesium carbonate dissolution
high	high	high	absent	Pyrite oxidation in absence of carbonate
high	high	absent	present	Pyrite oxidation to produce acid and subsequently neutralized by alkalinity

from the oxidation of pyrite and can be used to measure the instability of the pyrite contained in the rock leached. The acidity and alkalinity of the leachate measure the balance between the acid and alkaline producing components found in the sample.

Table 3 outlines the relationships between leachate quality and the chemical reactions responsible for the ionic species.

Results and Analysis.—The 11 samples used in this study had varying sulfur and neutralization potential values and after being leached for 17 weeks were found to produce leachates that varied from alkaline to acid. Some of the samples had similar characteristic chemical responses and in order to facilitate the analysis four of the 11 samples, which were identified to be representative of the results obtained in this study, are presented.

The four samples are shown in Figs. 1–4. The dashed line in Figs. 1–4 represents the acidity of the synthesized acid mine drainage. The dashed lines appear to shift vertically when one figure is compared to another. This does not mean that different concentrations of acid were used in the study, rather these shifts

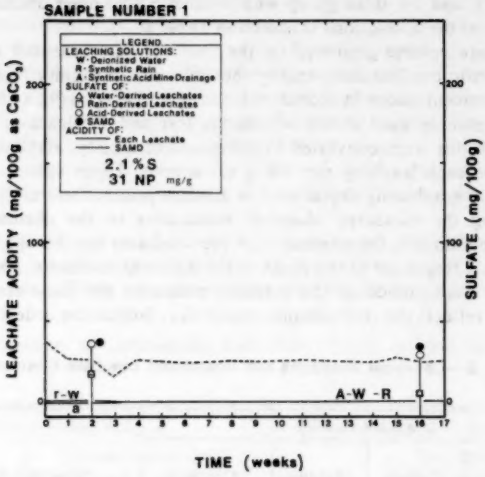

FIG. 1.—Plot of Leachate Acidity and Sulfate Content for Sample #1

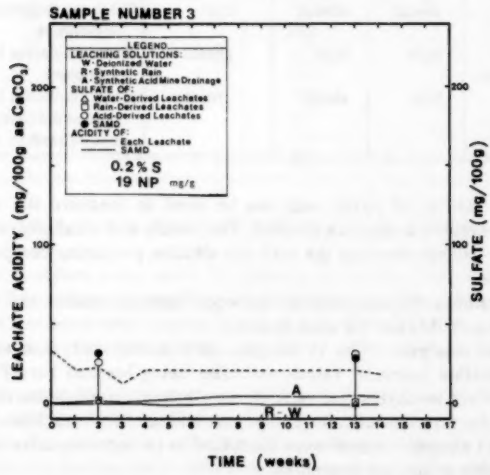

FIG. 2.—Plot of Leachate Acidity and Sulfate Content for Sample #3

represent an adjustment of acid levels to accomodate variations in sample size. Uniform aliquots of acid were used to leach all samples, consequently, large samples (greater than 250 g) would produce different leachate qualities than small samples (smaller than 150 g), even though the sample compositions were the same. There was a strong correlation between the specific conductance values and the sulfate content and both trends mimicked each other; as did the pH and the leachate acidity. For these reasons the pH and specific conductance values are not shown.

Sample #1 had a high sulfur content (2.1% S) and an NP of 31 mg of $CaCO_3$ equiv per 1 g. As Fig. 1 shows, this sample did not produce acidity, as reflected by the nonincrease in sulfate and the fact that all leachates were neutral. In fact this sample, because of the high NP, neutralized the acidity of both the acid rain and the acid mine drainage. Clearly the leachate from the sample

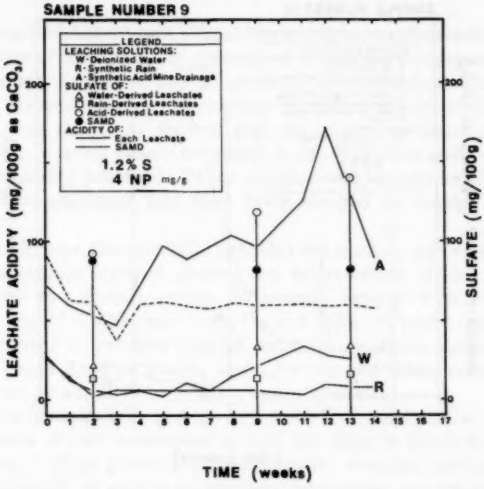

FIG. 3.—Plot of Leachate Acidity and Sulfate Content for Sample #9

leached with acid mine drainage was nonacid, indicating neutralization had taken place. Thus, although the potential of this sample to produce acid was high (2.1% S), the calcareous material present not only neutralized the acidity introduced, but, as shown by the nonincrease in sulfate, inhibited the oxidation of the pyrite.

Sample #3 had a lower sulfur content (0.2% S) and a lower NP (19 mg of $CaCO_3$ equiv per 1 g). The acidities of all leachates produced are lower than the levels of acid introduced into the system (Fig. 2). Here again, the acid added to the sample (A) is being neutralized, but significantly, minor amounts of acid begin to appear in the A leachate after about the fifth week. Minor increases in the sulfate (i.e., the sulfate content of the leachate exceeds the sulfate content of the leachant A) suggest that some of the calcareous material

has been removed from some pyrite sites but a large amount is still present to neutralize the acidity introduced.

Sample #9 had a low NP (4 mg of $CaCO_3$ equiv per 1 g) but a moderate sulfur content (1.2% S). As evident in Fig. 3, the amount of acidity produced after the third week exceeds the amount introduced by leachant A. Note too how the sulfate content increases with time, reflecting pyrite oxidation. This is true for both the deionized water and the synthesized acid rain. This sample also showed that deionized water was more reactive than the acid rain. Aside from the empirical results this sample is identified as an acid producer because it has a paucity of calcareous material (low NP) and a moderate amount of sulfur (pyrite).

Sample #10 had a high acid production potential (3.1% S) and some NP (13 mg of $CaCO_3$ equiv per 1 g). In Fig. 4, it is interesting to note that the

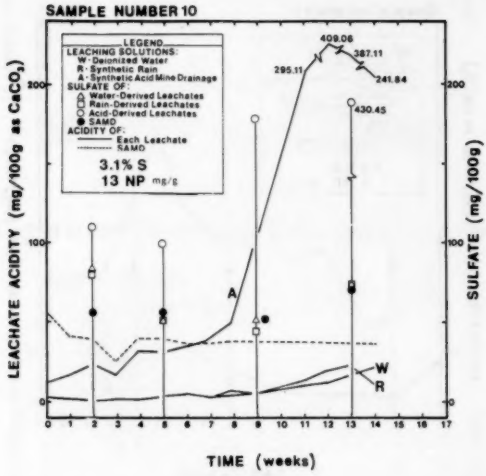

FIG. 4.—Plot of Leachate Acidity and Sulfate Content for Sample #10

sulfate contents of all leachates during the entire course of the experiment, were significantly high. Yet during the first 6 weeks the sample neutralized the acidity that was introduced into the system. After this time the amount of acidity produced exceeded the amount introduced. This may coincide with the total consumption of calcareous material during the neutralization process. In this case, though, the amount of calcareous material present was not sufficient to inhibit pyrite oxidation; it simply provided neutralization of the acidity produced.

Toward the end of the tests a reduction in the amount of acidity produced took place in the samples #9 and #10 that were leached with synthesized acid mine drainage (Figs. 3 and 4). Most probably this was due to a depletion of pyrite reaction sites on the surface of the grains. Unless the sample physically

decomposed, thereby making available new reaction surfaces, the samples will continue to produce less acid with time.

Although samples #9 and #10 had the capability to produce acid (as expressed by the high sulfur contents) the presence of calcareous material either inhibited the oxidation reaction (sample #9) or neutralized the acid (sample #10). To maintain these potentially acid samples in a nonacid producing state, requires their immersion in a nonacid aqueous medium. The experimental data showed that following a sustained acid bath, the samples, which hithertofore produced nonacid leachates, turned acid. Under field conditions, during burial or backfilling, these rock types should be segregated and capped with alkaline material to preserve the inhibitory calcium carbonate component and should not be blended with acidic material nor subjected to acid waters.

Conclusions

This study showed that the rock's capability to produce acidic leachates requires the consideration of both the sulfur content and the amount of calcareous material present in the sample. These two components were used in conjunction with leaching tests to assess a stratum's capability to produce acid or alkaline leachate. At the same time this study showed that the calcareous material present in samples serves, in some cases, to inhibit pyrite oxidation and, in others, to neutralize the acidity produced. Those samples with critical sulfur-calcareous material contents generated acid after being leached for some time with an acid solution.

Plots of the leachate characteristic, (whether the leachate was acid or alkaline) against the calcareous material content and sulfur values yielded a clustering of samples into two distinct groups. In general, samples with NP values of more than 15 mg of $CaCO_3$ equiv per 1 g and sulfur contents less than 0.5% S can be expected to produce alkaline leachates, whereas samples with NP values of less than 2 mg of $CaCO_3$ equiv per 1 g and sulfur contents greater than 1.5% S can be expected to produce acidic leachates.

However, for those samples that have critical calcareous material-sulfur ratios, a simple balance of one component against the other to produce a "net acid or base account" (8) to predict the acid potential, does not always yield valid results. The kinetics of acidity or alkalinity generation are not considered in this method. Furthermore, during the hot acid digestion, minerals other than calcium and magnesium carbonate are also degraded by the hot acid and appear in the NP column.

These short comings must be considered in attempting to predict the chemical weathering attributes of those samples with critical calcareous material—sulfur ratios. In this arena, a technique has been developed which utilizes a cold acid digestion and relates empirically derived weathering trends to whole rock analyses to produce tables that predict the potential leachate quality of a sample (patent pending). In general, the use of the NP—sulfur analysis (8) is satisfactory for the majority of the cases where the acid or alkaline production potential of a geologic unit is clearly defined. However, in those terranes that contain lightly buffered streams or where the geologic units have critical calcareous material—sulfur ratios and the acid or alkaline production potential is not as apparent, the more sophisticated, though time consuming, rock weathering

assessment technique previously described should be used.

On a long term basis this study showed that alkaline shale samples with carbonate-sulfur ratios falling near the acid boundary generated acid after being leached for some time with an acidic leachant. With the exception of sample #10, which showed a slight acid production toward the end of the tests, the results showed that the simulated acid rain had little affect on the acceleration of acid production from these samples. However, it is quite possible that had the acid rain leaching been continued through time, the sample responses would have been similar to those of the acid mine drainage.

APPENDIX.—REFERENCES

1. Barnes, H. L., and Romberger, S. B., "Chemical Aspects of Acid Mine Drainage," *Journal Water Pollution Control Federation*, Vol. 40, Part 1, 1968, pp. 371–384.
2. Caruccio, F. T., "An Evaluation of Factors Affecting Acid Mine Drainage Production and the Ground Water Interactions in Selected Areas of Western Pennsylvania," *Preprints of Papers Presented Before the 2nd Symposium on Coal Mine Drainage Research*, Bituminous Coal Research, May, 1968, pp. 107–151.
3. Caruccio, F. T., "Estimating the Acid Production of Coal Mine Refuse," *The Ecology of Resource Degradation and Renewal*, Blackwell Scientific Publ., London, England, 1975, pp. 197–205.
4. Caruccio, F. T., Ferm, J. C., Horne, J., Geidel, G., and Baganz, B., "Paleoenvironment of Coal and Its Relation to Drainage Quality," *EPA-600/7-77-067*, National Technical Information Service, 1977, pg. 108.
5. Caruccio, F. T., and Geidel, G., "Geochemical Factors Affecting Coal Mine Drainage Quality," *Reclamation of Drastically Disturbed Lands*, Chap. 8, American Society of Agronomy, 1978, pp. 129–148.
6. Geidel, G., "Alkaline and Acid Production Potentials of Overburden Material: The Rate of Release," *Reclamation Review*, Vol. 2, No. 3, Pergamon Press, Inc., New York, N.Y., 1980, pp. 101–107.
7. "Inorganic Sulfur Oxidation by Iron-oxidizing Bacteria," Water Pollution Control Research Series, *14010-DAY-06/71*, United States Environmental Protection Agency, Superintendent of Documents, Washington, D.C., 1971.
8. Singer, P. C., and Stumm, W., "Acid Mine Drainage: The Rate Determining Step," *Science*, Vol. 167.
9. Sobek, A. A., Schuller, W. A., Freeman, J. R., and Smith, R. M., "Field and Laboratory Methods Applicable to Overburdens and Minesoils," *EPA-600/2-78-054*, National Technical Information Service, Springfield, Va., 1978.
10. *Standard Methods For the Examination of Water and Waste Water*, 13th Ed., American Public Health Association, Washington, D.C.

DISCUSSION

Note.—This paper is part of the Journal of the Energy Division, Proceedings of the American Society of Civil Engineers, ©ASCE, Vol. 107, No. EY1, May, 1981. ISSN 0190-8294/81/0001-0181/$01.00.

Discussions

Discussions may be submitted on any Proceedings paper or technical note published in any *Journal* or on any paper presented at any Specialty Conference or other meeting, the *Proceedings* of which have been published by ASCE. Discussion of a paper/technical note is open to anyone who has significant comments or questions regarding the content of the paper/technical note. Discussions are accepted for a period of 4 months following the date of publication of a paper/technical note and they should be sent to the Manager of Technical and Professional Publications, ASCE, 345 East 47th Street, New York, N.Y. 10017. The discussion period may be extended by a written request from a discusser.

The original and three copies of the Discussion should be submitted on 8-1/2-in. (220-mm) by 11-in. (280-mm) white bond paper, typed double-spaced with wide margins. The length of a Discussion is restricted to two *Journal* pages (about four typewritten double-spaced pages of manuscript including figures and tables); the editors will delete matter extraneous to the subject under discussion. If a Discussion is over two pages long it will be returned for shortening. All Discussions will be reviewed by the editors and the Division's or Council's Publications Committees. In some cases, Discussions will be returned to discussers for rewriting, or they may be encouraged to submit a paper or technical note rather than a Discussion.

Standards for Discussions are the same as those for Proceedings Papers. A Discussion is subject to rejection if it contains matter readily found elsewhere, advocates special interests, is carelessly prepared, controverts established fact, is purely speculative, introduces personalities, or is foreign to the purposes of the Society. All Discussions should be written in the third person, and the discusser should use the term "the writer" when referring to himself. The author of the original paper/technical note is referred to as "the author."

Discussions have a specific format. The title of the original paper/technical note appears at the top of the first page with a superscript that corresponds to a footnote indicating the month, year, author(s), and number of the original paper/technical note. The discusser's full name should be indicated below the title (see Discussions herein as an example) together with his ASCE membership grade (if applicable).

The discusser's title, company affiliation, and business address should appear on the first page of the manuscript, along with the *Proceedings* paper number of the original paper/technical note, the date and name of the *Journal* in which it appeared, and the original author's name.

Note that the discusser's identification footnote should follow consecutively from the original paper/technical note. If the paper/technical note under discussion contained footnote numbers 1 and 2, the first Discussion would begin with footnote 3, and subsequent Discussions would continue in sequence.

Figures supplied by the discusser should be designated by letters, starting with A. This also applies separately to tables and references. In referring to a figure, table, or reference that appeared in the original paper/technical note use the same number used in the original.

It is suggested that potential discussers request a copy of the *ASCE Authors' Guide to the Publications of ASCE* for more detailed information on preparation and submission of manuscripts.

Hybrid Cooling System Thermodynamics and Economics[a]

Errata

The following corrections should be made to the original paper:

Page 89, paragraph 2, line 3: Should read "temperature rise and river flow rate." instead of "temperature rise and rive flow rate."
Page 96, paragraph 1, line 9: Should read "consideration in a detailed study." instead of "consideration in a detail study."
Page 96, paragraph 1, line 21: Should read "The extreme value of RHAC is the minimum value" instead of "The extreme values of RHAC is the minimum value"
Page 96, Fig. 2 and Fig. 3 should be exchanged
Page 98, line 5: Should read "most of the heated condenser effluent" instead of "must of the heated condenser effluent"
Page 103, line 14: Should read "and the optimum design of the Type 1" instead of "and optimum design of the Type 1"

Feasibility of Five Low-Head Hydro Projects[b]

Errata

The following corrections should be made in the original paper:

Page 57, paragraph 2, line 3: Should read "8 ft (2.4 m)–60 ft (18.3 m)" instead of "8 ft (2.4 m)–60 ft (28.3 m)"
Page 65, line 7: Entire line should be deleted.

[a]April, 1980, by Arthur R. Giaquinta, Thomas E. Croley II, and Tai-Dan Hsu (Proc. Paper 15319).

[b]April, 1980, by James V. Williamson and Anthony Wayne Pietz (Proc. Paper 15327).

Technical Papers

Original papers should be submitted in triplicate to the Manager of Technical and Professional Publications, ASCE, 345 East 47th Street, New York, N.Y. 10017. Authors must indicate the Technical Division or Council, Technical Committee, Subcommittee, and Task Committee (if any) to which the paper should be referred. Those who are planning to submit material will expedite the review and publication procedures by complying with the following basic requirements:

1. Titles must have a length not exceeding 50 characters and spaces.

2. The manuscript (an original ribbon copy and two duplicate copies) should be double-spaced on one side of 8-1/2-in. (220-mm) by 11-in. (280-mm) paper. Three copies of all figures and tables must be included.

3. Generally, the maximum length of a paper is 10,000 word-equivalents. As an *approximation*, each full manuscript page of text, tables or figures is the equivalent of 300 words. If a particular subject cannot be adequately presented within the 10,000-word limit, the paper should be accompanied by a rationale for the overlength. This will permit rapid review and approval by the Division or Council Publications and Executive Committees and the Society's Committee on Publications. Valuable contributions to the Society's publications are not intended to be discouraged by this procedure.

4. The author's full name, Society membership grade, and a footnote stating present employment must appear on the first page of the paper. Authors need not be Society members.

5. All mathematics must be typewritten and special symbols must be identified properly. The letter symbols used should be defined where they first appear, in figures, tables, or text, and arranged alphabetically in an appendix at the end of the paper titled Appendix.—Notation.

6. Standard definitions and symbols should be used. Reference should be made to the lists published by the American National Standards Institute and to the *Authors' Guide to the Publications of ASCE*.

7. Figures should be drawn in black ink, at a size that, with a 50% reduction, would have a published width in the *Journals* of from 3 in. (76 mm) to 4-1/2 in. (110 mm). The lettering must be legible at the reduced size. Photographs should be submitted as glossy prints. Explanations and descriptions must be placed in text rather than within the figure.

8. Tables should be typed (an original ribbon copy and two duplicates) on one side of 8-1/2-in. (220-mm) by 11-in. (280-mm) paper. An explanation of each table must appear in the text.

9. References cited in text should be arranged in alphabetical order in an appendix at the end of the paper, or preceding the Appendix.—Notation, as an Appendix.—References.

10. A list of key words and an information retrieval abstract of 175 words should be provided with each paper.

11. A summary of approximately 40 words must accompany the paper.

12. A set of conclusions must end the paper.

13. Dual units, i.e., U.S. Customary followed by SI (International System) units in parentheses, should be used throughout the paper.

14. A practical applications section should be included also, if appropriate.